COLORECTAL CANCER LIVER METASTASIS PROGRESSION AFTER PORTAL VEIN EMBOLIZATION

Eve B. Simoneau
Department of Surgery – Division of Experimental Surgery
McGill University, Montreal

December 2015

A thesis submitted to McGill University in partial fulfillment of the requirements of the Doctorate degree in Experimental Surgery

© Eve B Simoneau 2015

Contributions of Authors

This thesis consists of five manuscripts describing multiple and novel aspects related to colorectal liver metastasis progression after portal vein embolization. The first paper establishes the evidence of tumor growth after embolization in the largest series published to date, the second paper describes for the first time in the literature the impact of progression on long-term outcomes for these patients, the third paper highlights potential pathways and genes involved in metastatic progression in this context. The fourth paper consists of a multi-institutional collaboration and describes an association between histological growth patterns and colorectal liver metastasis progression and resistance to anti-angiogenic therapy. Finally the last paper describes a correlation between the histological growth patterns and metastatic progression in other clinical contexts, namely staged resections and portal vein embolization.

The prospective study related to the third manuscript was conducted under the approved protocol GEN-11-140 and all material related to the third, fourth and fifth manuscripts was supported by the protocol of the Liver Disease Biobank (McGill University Health Center).

A list of the manuscripts and contributions of authors is found below.

1. Simoneau E, Aljiffry M, Salman A, Abualhassan N, Cabrera T, Valenti D, El Baage A, Jamal M, Kavan P, Al-Abbad S, Chaudhury P, Hassanain M, Metrakos P. Portal vein embolization stimulates tumor growth in patients with colorectal liver metastases, HPB (Oxford), 2012 Jul;14(7):461-8
2. Eve Simoneau, Mazen Hassanain, Mohammed Shaheen, Murad Aljiffry, Nouran Molla, Prosanto Chaudhury, Shirin Anil, Alla Khashper, David Valenti, Peter Metrakos. Impact

of Tumor Progression Following Portal Vein Embolization for Colorectal Cancer Liver Metastasis. – *published in British Journal of Surgery*

3. Eve Simoneau, Jarred Chicoine, Sarita Negi, Ayat Salman, Anthoula Lazaris, Mazen Hassanain, Stephanie Petrillo, Lotfi Amri, David Valenti, Ramila Amre, Peter Metrakos. Next generation sequencing of progressive colorectal liver metastases after portal vein embolization. For submission

4. Eve Simoneau[*], Sophia Frentzas[*], Victoria L. Bridgeman[*], Peter B. Vermeulen, Andrew Wotherspoon, Zu-hua Gao, Jonathan Lachapelle, Gert Van den Eynden, Shane Foo, Frances Daley, Patrycja Gazinska, Tracy Berg, Zak Eltahir, Clare Peckitt, Laila Ritsma, Jacco Van Rheenen, Alla Khashper, Gina Brown, Hanna Nystrom, Malin Sund, Evelyne Loyer, Luc Dirix, David Cunningham, Peter Metrakos, & Andrew R. Reynolds. An invasive growth pattern that facilitates vessel co-option mediates resistance to anti-angiogenic therapy in liver metastases – *under revision, Nature Medicine*

5. Eve Simoneau, Peter Vermeulen, Gert Van den Eynden, Andrew Reynolds, Stephanie Petrillo, Anthoula Lazaris, Ayat Salman, David Valenti, Mazen Hassanain, Peter Metrakos. Colorectal liver metastasis progression after portal vein embolization is associated with the histological growth patterns. For submission

I collected the clinical data, analyzed the data, performed tumor volumetric analysis and radiological response assessment of the entire PVE database. I obtained IRB approval after writing the prospective study protocol and patient consent forms. I consented patients, collected and analyzed all tissue samples and data of patients in the prospective study and I followed the patients until the end of the study. I conceived the ideas behind the clinical studies and in the design of the prospective cohort study. I also analyzed the data resulting from the RNA Seq bioinformatic analyses. For the histological growth pattern projects, I contributed to the design of the clinical validation, I collected all clinical data and relevant histological sections related to the tissue analyzed; I compiled, graded and analyzed radiological response data, and performed statistical analyses with the raw data and interpreted the results.

Dr Peter Metrakos conceived the ideas behind this thesis, the clinical and experimental studies and he directed the RNA Seq study design as well as the histological growth pattern and portal vein embolization project. For the prospective study, he identified eligible patients, and helped procuring the intraoperative tissue samples. He reviewed all manuscripts as well as the thesis.

Dr Andrew Reynolds conceived the idea behind the histological growth pattern and resistance paper (fourth manuscript). He directed the project, analyzed and interpreted the data (resulting from the MUHC as well as other centers).

Dr Mazen Hassanain conceived the ideas behind all the clinical studies and provided significant assistance in data collection and analysis for the first paper, as well as data analysis for the other clinical paper. He provided assistance in generating the prospective study protocol for the RNA sequencing as well as consent forms. He reviewed all manuscripts (except fourth).

Dr Murad AlJiffry contributed significantly in the volumetric calculation and analysis of the patient database as well as review of the first two manuscripts.

Dr Nasser Abualhassan contributed to the data collection and volume calculation and analysis for the first paper.

Dr Tatiana Cabrera and Dr David Valenti contributed to supervising the volumetric analyses calculations as well as the procuring tissue samples prior to the embolization in the angio suite.

Dr Arwa El Baage, Dr Mohammad Jamal and Dr Saleh Al-Abbad contributed to clinical data collection of patients in the database for the first paper.

Dr Petr Kavan followed most of these patients and reviewed the first manuscript.

Dr Prosanto Chaudhury contributed in identifying eligible patients for the study and in providing intraoperative tissue samples. He also brought significant contribution in the review of the clinical abstracts and manuscripts (first two manuscripts).

Dr Nouran Molla provided all clinical and volumetric data of control patients in the second manuscript.

Dr Jarred Chicoine helped me in doing the RNA extraction for biopsy tissue samples for the RNA Seq and assisted in the analysis of the RNA sequencing data.

Dr Sarita Negi taught me and assisted in the validation part of the RNA-Seq paper (PCR validation).

Dr Anthoula Lazaris is the lab manager and provided significant input related to data analysis, validation methods, RNA Seq experimental design, and teaching of laboratory techniques. She also reviewed the third, fourth and fifth manuscripts.

Ms Ayat Salman supported for the ethics requirements regarding the prospective study and introduced the study to most of the patients. She also contributed to clinical data collection for the first paper.

Ms Stephanie Petrillo assisted in collecting intra-operative tissue through the biobank as well as helped in the validation part of the RNA Seq paper.

Dr Nicole Beauchemin reviewed the manuscript and provided valuable input into the data analysis resulting from the RNA Seq. She also provided significant support related to developing the animal model of partial hepatectomy (unpublished data).

Dr Ramila Amre and Dr Zu-hua Gao are pathologists who helped in scoring the histological tissue sections in the RNA Seq paper (Dr Amre) and in scoring pathological response used in the fourth paper (Dr Gao).

Dr Shirin Anil is an epidemiologist and assisted in the statistical analyses and predictive model of the second paper.

Dr Alla Khashper is a radiologist and contributed to the chemotherapy response assessment (morphological response) required in the fourth paper.

Dr Peter Vermeulen and Dr Gert Van den Eynden are pathologists from Antwerp (Belgium) and scored by consensus the histological growth patterns in the fourth and fifth papers.

Dr Sophia Frentzas is a medical oncologist from London UK who worked in collaboration in the histological growth pattern paper (fourth manuscript), she was responsible for the data of the London patient cohort as well as was involved directly in the experiments with mouse models in the paper.

Acknowledgements

This research is the product of four years of work at the Surgical research Laboratories at the Royal Victoria Hospital. First and foremost I would like to thank Dr Mazen Hassanain. This work would not have been possible without his unconditional support, since the very beginning of this project in 2010. I would like to express my gratitude to Dr Andrew Reynolds from London (UK) for his constant support, guidance, and scientific input; his leadership and enthusiasm were truly inspiring. I would also like to thank Dr Anthoula Lazaris, who guided me throughout experimental protocols, experimental organization and planning, grant writing, and laboratory techniques. Her patience and scientific expertise were critical for the completion of my work. I want to thank Ayat Salman for her cooperation, as she helped me through ethics board requirements, patient recruitment, follow-up and assisted with data collection. The expertise of Stephanie Petrillo in biobanking was critical to achieve all human tissue collection and her help were greatly appreciated all throughout my work. I thank my committee members (Dr Beauchemin, Dr Sladek and Dr Tchervenkov) for their valuable scientific inputs and discussions. I would also like to thank Ms Marie Monaghan for her support.

Finally I would like to express my gratitude for my supervisor and mentor Dr Peter Metrakos, for his continuous guidance throughout the years. Without his support and mentorship, the completion of this work would not be possible. I thank him for always encouraging my research, advising me in my career and allowing me to grow as a surgeon scientist.

Table of Contents

I. Tables

II. Figures

Abbreviations

CRC	colorectal cancer
CRCLM	colorectal cancer liver metastasis
LM	liver metastasis
FLR	future liver remnant
PVE	portal vein embolization
HGF	hepatocyte-growth factor
TGFβ	transforming growth factor beta
NK	natural killer
aFLR	adequate future liver remnant
NAFLD	non-alcoholic fatty liver disease
naFLR	non-adequate future liver remnant
RFA	radio-frequency ablation
MWA	microwave ablation
CT	computed tomography
MRI	magnetic resonance imaging
IL-6	Interleukin-6
TNF-alpha	Tumor necrosis factor alpha
EGF	Epidermal growth factor
HGF	Hepatocyte growth factor
TGF	Transforming growth factor
PH	Partial hepatectomy
NICD	Notch intracellular domain
STAT3	Signal transducer and activator of transcription 3
NFκB	nuclear factor kappa-light-chain-enhancer of activated B cells

MMP9	matrix metalloproteinase 9
FGF	Fibroblast growth factor
VEGF	Vascular endothelial growth factor
SCF	Stem cell factor
PDGF	Platelet-derived growth factor
HB-EGF	Heparin-Binding EGF-like Growth Factor
MMP2	matrix metalloproteinase 2
MAPK	Mitogen-activated protein kinases
PI3K	Phosphoinositide 3-kinase
ERK	extracellular signal-regulated kinases
AKT	Protein kinase B
AP-1	Activator protein 1
IGFBP1	Insulin-like growth factor binding protein 1
SOCS	suppressors of cytokine signalling
APC	Adenomatous polyposis coli
K-RAS	Kirsten Rat Sarcoma Viral Oncogene Homolog
SH2	Src homology 2
PMS1	Postmeiotic Segregation Increased 1
PMS2	Postmeiotic Segregation Increased 2
MLH1	MutL homolog 1
um	micrometer
MET	mesenchymal-epithelial transition
RNA-Seq	Ribonucleic acid sequencing

Abstract

Colorectal cancer constitutes a major disease burden in Western society and most patients will die with metastatic disease to the liver. Surgical resection of liver metastasis provides superior survival advantage compared to conservative treatment modalities such as systemic chemotherapy. Strategies aim towards increasing the number of patients eligible for surgical resection. Unfortunately, the majority of patients presents with unresectable disease. Preoperative portal vein embolization is a method that can be used to convert initially unresectable patients to a resectable state. In some patients, this procedure has been associated with tumor progression in the preoperative period. We present evidence that radiological tumor progression occurs in a large proportion of patients undergoing portal vein embolization, and that this affects the resectability rate of patients. Our results also show that tumor progression after portal vein embolization is closely associated to the extent of neoadjuvant chemotherapy response. Since tumor control in the preoperative setting is crucial to ensure resectabliity and superior outcomes, we aimed to investigate the response to neoadjuvant chemotherapy and we thus provided evidence that response to chemotherapy, in particular to anti-angiogenic therapy, is mediated by different histological growth patterns of the liver metastasis (desmoplastic and replacement). We also demonstrate that the histological patterns utilize different tumor vascularization processes which explain resistance to anti-angiogenic therapy. Finally we show that these distinct histological growth patterns seem to determine colorectal cancer liver metastasis progression observed after portal vein embolization.

Résumé

Le cancer colorectal constitue un fardeau majeur en terme de santé en Occident, et la majorité des patients décèderont d'un stade métastatique au foie. La résection des lésions métastatiques au foie permet un taux de survie supérieur comparativement aux traitements plus conservateurs comme la chimiothérapie. Les stratégies ont donc pour but d'augmenter le nombre de patients éligibles à la résection hépatique. Malheureusement, la majorité des patients se présentent avec une maladie hépatique non-résécable. L'embolisation portale en période préoperatoire est une méthode qui peut être utilisée pour convertir des patients d'un stade non résécable a un stade résécable. Chez certains patients, cette procédure a été associée avec une progression tumorale en période préoperatoire. Premièrement, nous présentons l'évidence de la présence de progression tumorale, déterminée par mesures radiologiques, et ce dans une large proportion des patients subissant une embolisation portale, ce qui se traduit par des consequences néfastes sur le taux de résection hépatique. Nos résultats démontrent également que la progression tumorale après l'embolisation est intimement reliée au niveau de réponse a la chimiothérapie néoadjuvante, Puisque le contrôle des tumeurs en période préoperatoire est crucial pour assurer la résécabilité des patients ainsi que des résultats oncologiques et à long-terme supérieurs, nous avons étudié la réponse tumorale à la chimiothérapie néoadjuvante. Nous avons donc démontré que la réponse à la chimiothérapie, particulièrement au traitement anti-angiogénique, est médiée par différent types histologiques de croissance tumorale (types desmoplatique et infiltrant). Nous avons également démontré que les types de croissance histologiques utilisent différents processus de vascularisation tumorale, expliquant la résistance à la thérapie anti-angiogénique. Finalement, nous démontrons que ces types de croissance histologiques distincts semblent également déterminer la progression des lésions métastatiques du cancer colorectal observés après l'embolisation portale.

Introduction

III. Rationale

Colorectal cancer (CRC) is the third most common cancer in North America, and is the third leading cause of cancer-related death(1). The American Cancer Society estimates that about 142 820 new cases of colon or rectal cancer will have emerged in 2013 in the USA. Combined, these will cause about 52 390 deaths(1). Approximately 50% of patients will be diagnosed with colorectal cancer cancer liver metastasis (CRCLM) during the course of their disease. Around 20–25% of patients will have synchronous liver metastases (LM) at presentation and a further 20–25% will develop metachronous LMs at a later date(2). Untreated, patients with CRCLM will survive for few months (3) and with chemotherapy a median survival of 20-24 months can be achieved(4-6). Liver resection is increasingly offering eligible patients an improved long-term survival and even potential cure. In fact resected CRCLM patients have an expected 5-year survival of 24-58%(2,7-19).

During last decade, selection criteria for the resectability of CRCLM have experienced a shift in paradigm from criteria related to the tumor burden, to criteria that focus on the amount of liver that is left behind after resection (the so-called future liver remnant (FLR)). Surgeons therefore consider patients resectable if an R0 resection (microscopic margin free of cancer) can be achieved, while leaving the patient with an adequate FLR to avoid post-operative liver dysfunction. One method that has been developed to improve the size of the FLR in the preoperative period is portal vein embolization (PVE). Preoperative portal vein embolization is a method that induces hypertrophy of the liver lobe contralateral to the embolization(20,21). It is performed when a greater disease burden or a misdistribution of lesions within the liver precludes surgical resection, because the predicted FLR would be too small to sustain normal hepatic function

in the post-operative period. Therefore, without this procedure, patients are considered to be unresectable, a category in which patients have a much lower overall survival. Since it may allow initially unresectable patients to become resectable(22,23), clinicians favored the use of this preoperative technique when indicated, for CRCLM patients with small FLR.

It was hypothesized and suggested in small case series (24-26) that PVE may not only stimulate the contralateral liver parenchyma to grow, but it may also stimulate tumor progression. Moreover, some other investigators evaluating long-term outcomes of PVE patients noticed incidentally that most of the patients who remained unresectable after the PVE had experienced disease progression after the procedure(25,27,28).

Faced with a promising strategy aimed to increase resectability that may in fact have a double-edge sword, clinicians need more evidence on preoperative tumor progression in order to plan more efficiently the perioperative course of these complex patients, reduce the drop-out rate to surgery and optimize patient stratification in order to improve their outcomes.

IV. Objectives

The initial objective of the study was to investigate post-PVE tumor progression in patients with colorectal liver metastasis. The project involved looking at different aspects of this clinical entity: outcomes and clinical predictors of progression after embolization, describing molecular pathways involved in progression after embolization, and correlation of histological growth patterns with colorectal cancer liver metastasis progression in the context of different clinical interventions, such as systemic therapy, staged resections and embolization. Hence the objectives were:

- To establish the evidence of post-PVE tumor progression and to determine the long-term impact of tumor progression in patients with colorectal liver metastasis
- To highlight molecular pathways related to tumor progression after portal vein embolization using high throughput technology in a clinical prospective cohort study
- To correlate histological growth patterns with colorectal cancer metastatic progression in the context of neoadjuvant treatment resistance
- To correlate histological growth patterns with colorectal cancer metastatic progression in the context of staged resections and portal vein embolization

Literature Review

V. Liver Anatomy

The liver is located in the right upper quadrant and is divided into 8 segments (so-called Couinaud segments), numbered I to VIII, each supplied by a triad (portal vein, hepatic artery and bile duct) and drained by hepatic venous system. According to this functional anatomy, the right liver consists of segments V to VIII, and the left liver consists of segments II, III and IV (a and b) respectively. Segment 1 (or caudate lobe) is considered separate, because of its supply from both right and left-sided branches. In addition to the segments, the liver is also divided into sectors: the right anterior, right posterior, left medial and left lateral sectors. Hence, segments VI and VII make the right posterior sector and segments V and VIII make the right anterior segments. Segment IV (a and b) make the left medial and segments II and III make the left lateral sector. (Figure 1) The liver is peculiar since it has dual blood supply: the portal vein (made by the confluence of the superior mesenteric and splenic veins) consists of 75-80% of the blood-flow and the hepatic artery (originating from the celiac trunk) makes the remaining 20-25%.

The arterial and portal venous supply further divide within liver lobes until they form capillaries and supply the liver lobules, where the hepatocytes are located. The hepatic sinusoids are the largest microvascular system of the liver and are made of several cell types, including the hepatocytes. Going from the vessel lumen to the hepatocytes, the following cells are also present: 1) the Kupffer's cells (liver macrophage, which performs a variety of immune-related functions such as phagocytosis of cellular debris, platelet aggregates and opsonized organisms as well as regulation of blood flow and interaction with hepatocytes); 2) endothelial cells (fenestrated endothelial cells that allow nutrients and lipid from the portal venous flow to the surface of hepatocytes); 3) Space of Disse (space

between sinusoids which contains different cell types related to immunity and nutrient transport. This space contains loose extracellular matrix and several cell types, such as the stellate cells (which produce hepatocyte-growth factor (HGF) and transforming growth factor beta (TGFβ)), T and B lymphocytes and natural killer (NK) cells).

VI. Surgical approaches

Surgical resections are based on tumor burden and location, keeping in mind the anatomical and functional anatomy described above (Couinaud classification). A right hepatectomy or a left hepatectomy consists of removing the functional right or left lobe of the liver respectively. An extended right hepatectomy (or right trisegmentectomy) corresponds to resection of the right lobe in addition to segment 4 resection; similarly an extended left (or left trisegmentectomy) corresponds to resection of the left lobe in addition to segments 5 and 8 resection (medial part of right lobe). The term “segmentectomy” (with defined anatomical segments removed) consists of removing a defined functional segment, and lastly, a wedge resection (a smaller, triangular-shaped portion of the liver for tumors located more in periphery) is considered to be a non-anatomical resection and does not constitute the removal of a complete segment. In general, a surgical resection can be performed if the following conditions are present for the liver remnant: portal venous and arterial supply, hepatic venous drainage, bile duct drainage and a liver parenchyma of sufficient quality and size.

Indications for surgery

Hepatic resection can be done because of 1) benign disease, 2) trauma, or 3) malignancy (most common one). Indications for surgery for benign disease would include symptomatic lesions causing pain or discomfort and caused by simple cysts, hemangiomas, adenomas,

or focal nodular hyperplasia(29-32). Sometimes, large hemangiomas or adenomas (>4-5cm) require resection even if asymptomatic(31). Regarding infectious causes, resection of pyogenic abscess can sometimes be required to achieve source control(33), but generally they are best treated with antibiotics and drainage. Amebic abscesses are resected if they are of large size with a risk of rupture or unresponsive to medical therapy(34). For trauma, hepatic resections are rare and usually associated with a high mortality (60%) (35); anatomical resection secondary to high-grade injury may carry a much lower morbidity and mortality risk only if performed by experienced hepatobiliary surgeons(36). Resections are usually reserved for devitalized liver portions and do not follow anatomic plane and are considered to be debridement procedures.

The most common indication for hepatic resection is malignancy. In large surgical series, hepatocellular carcinoma was the most common diagnosis in patients undergoing hepatectomy (37,38) and cholangiocarcinoma was the second most common cause in another large surgical case-series(39). Since the liver is the site of metastasis of multiple primary malignancies, it was shown in multiple series that resection of metastases, when indicated and with a limited disease, was beneficial to patients in terms of long-term outcomes and with a low morbidity and mortality(40-44). Therefore, resection of liver metastasis from colon cancer (commonest), breast cancer, sarcoma, genitourinary cancer, melanoma and neuroendocrine tumor were all described(45-48).

Historical perspective of liver resections for CRCLM

Wangesteen performed one of the first liver resections for cancer in 1951, for gastric cancer liver metastasis(49). Liver surgeons initially put more efforts on building expertise and techniques for liver transplantation, and they started to “cut” liver parenchyma to transplant liver lobes in children from adult donors, also prompted by organ shortage. Based on principles learnt from transplantation (vascular supply, venous drainage and

amount of liver parenchyma required) and based on the functional anatomical classification brought by Couinaud, hepatic resection emerged in the early 1980s and was followed by three decades of learning, advancements, innovations and positive impact for patients. Table 1 summarizes the major surgical series published between 1986 until recently. The perioperative mortality dramatically improved over time, being now at about 4% (Table 1). In the last decade, the reported 5-year survival after resection range between 36-58%(13-19). There is no randomized controlled trial on surgery vs. conservative or medical therapy (chemotherapy) since the first series already reported a dramatic benefit favoring surgery over chemotherapy only. In fact, chemotherapy only can offer at best a median survival of 26.0 months with the combination of anti-angiogenic targeted therapy(5). The combination of perioperative chemotherapy with surgery has also contributed to better long-term outcomes specifically in terms of disease-free survival(8). Unfortunately, the majority (80%) of patients fall into the category of unresectable disease, therefore efforts are directed towards developing strategies that can convert more patients into a resectable state.

VII. The adequate future liver remnant: a fundamental element in the management of colorectal liver metastasis

Patients with CRCLM who are amendable to an R0 liver resection (microscopic resection margin free of tumor) have expected 5-year survivals of 24-58%. These types of five-year outcomes plus the markedly decreased operative mortality from liver resection (to less than 5%) (2,7-19) have spurred a revolution in the surgical treatment of CRCLM during the last 10 to 15 years. The advancement of the chemotherapeutic regimes has also been pivotal in helping these improvements to occur. There has been a shift in the paradigm of how we determine the resectability of the patient with CRCLM. In the past

surgeons considered what they were removing: number of lesions, size of lesions, tumor volume. Hepatic surgeons were looking for surrogate markers of the biologic behavior of the particular cancer and patient considered for resection. Recently many centers are determining resectability by what is left behind rather than what is being removed; in other words surgeons proceed with hepatic resection if all metastases can be removed while leaving enough liver behind (the FLR) to ensure the survival of the patient. This approach to resectability makes the future liver remnant one of the most important factor as to how the patient is treated. Hence obtaining an adequate future liver remnant (aFLR) should be the initial goal for every CRCLM patient. It should be stressed that the FLR represents the quantity of functional liver left behind, which does not necessarily correlate with the volume of liver. In an era where CRCLM management is associated with wide spread use of neo-adjuvant chemotherapy and potential liver toxicity, where there is an increase prevalence of NAFLD (non-alcoholic fatty liver disease), older patients and more complex comorbidities, similar liver volumes do not necessarily translate to similar levels of liver function, as the quality of that FLR becomes crucial. Thus for equal liver volumes after resection, one patient may achieve an aFLR while another may have a non-adequate FLR (naFLR). Strategies of how to achieve this goal are reviewed in the next sections, and evidence that this treatment strategy provides the best possible outcomes for these patients is highlighted.

Presently, treatment options for patients with hepatic metastases fall into 3 main categories: 1) Patients that are resectable on presentation go to surgery with or without neo-adjuvant therapy. 2) Patients that are potentially resectable if the tumor burden could be downsized and/or the FLR increased in size with portal vein embolization and/or a staged resection strategy applied. 3) Patients who will never be resectable and will be treated with chemotherapy and local regional therapies.

Advances in chemotherapy and surgical techniques have expanded the horizons of what now is considered resectable disease. The extensive series of patients that have been resected and followed offer evidence that the resected patient with CRCLM is better off than the unresected patient therefore it would follow that one might think that conversion to resectability should be the aim for all patients when possible. Every time a patient is evaluated for a liver resection, a formal or informal assessment of the size of the future liver remnant (FLR) is made, since this remnant has to be of adequate size and function to support the patient post-operatively. Thus we should always be thinking about the adequate future liver remnant (aFLR).

Three options exist that may help the patient to achieve an aFLR (see Figure 1), which is especially important for borderline or initially unresectable disease due to greater disease burden or misdistribution of lesions: 1) decrease the size of the resection, 2) increase the size of the FLR or 3) improve the function of the FLR. For each of these options, several approaches exist and will be reviewed. In many instances a combination of these strategies will be the only way of achieving an aFLR and converting the patient to a resectable state.

i. Decreasing the size of the resection

The first option that aims to achieve an adequate future liver remnant is by reducing the size of the resection. This can be achieved by several methods: by the administration of neoadjuvant chemotherapy, by using local ablative therapy in combination with surgical resection or by performing non-anatomical resections to achieve an R0 resection with removing less liver parenchyma. Even if some evidence exists suggesting that the failure to achieve microscopically clear margins may not affect negatively long-term outcomes (50), recommendations still advise surgeons to consider patients for surgical resections only if negative margins are anticipated to be achieved.

Downsizing chemotherapy

Two decades ago, the introduction of the chemotherapeutic agent 5FU (5-fluorouracil, a pyrimidine analogue belonging to the antimetabolites family) for CRCLM has been shown to be superior to supportive therapy and has remained in all chemotherapy regimens since then(51). In the early 2000, the arrival of oxaliplatin (platinum-based antineoplastic agent) and irinotecan (topoisomerase I inhibitor), combined with 5FU and leucovorin to make FOLFOX and FOLFIRI respectively, demonstrated superiority to 5FU alone in terms of progression-free survival and overall survival(4,52-54) (Table 2). There was no regimen that showed superiority over the other when irinotecan-based and oxaliplatin-based regimen were compared, which now provides clinicians with options for patients, especially in cases where side effects or intolerance to a particular agent is manifested, or if resistance develops after the first-line(55,56). The addition of Bevacizumab, a recombinant humanized monoclonal antibody inhibiting vascular endothelial growth factor, showed for the most part to be non-superior to cytotoxic chemotherapy alone, in terms of overall survival(5,57). One randomized-controlled trial has shown longer progression-free survival.(58) Therefore its administration, in combination to the cytotoxic chemotherapy (FOLFOX or FOLFIRI) still varies, depending on centers and physician's preference.

Surgeons were now equipped with powerful cytotoxic agents and with a growing experience in surgical resections for CRCLM. The long-term outcomes for these stage IV patients, who used to be condemned to a survival of 6-9 months without treatment, reached a 5-year survival of close to 60% (13,14) in some large cohort studies. Adam et al showed that even for patients presenting with initially unresectable disease, those patients who were "downsized" by neoadjuvant chemotherapy (12.5%) and converted to a resectable state had significant long-term survival benefit(59). An important concept over the years that has also been raised especially in the medical oncology literature is response to

chemotherapy. Incorporating aspects of tumor biology within treatment strategies was thus becoming a predominant concern in the field of oncology. In 2004, a landmark study by Rene Adams et al highlighted an association between neoadjuvant chemotherapy response and long-term outcomes after hepatic resection for CRCLM. This study stated that CRCLM chemotherapy responders, assessed by changes in lesion size, had better survival when compared to non-responders (37 vs. 8%, $p<0.001$)(60). Despite the fact that the exact timing of perioperative chemotherapy for CRCLM is still controversial, studies proved the combination of downsizing chemotherapy with surgery to be effective in providing long-term outcomes.

Local ablative therapies

Considered non-surgical options, local ablative therapies can be used for patients who are not surgical candidates, and can also be used as adjunct to hepatectomy to achieve R0 resection while reducing the size of the resection. Hence depending on the size and location of the tumors, a resection can be performed with the use of intra-operative local therapy to treat an additional lesion, which would otherwise be requiring much more liver parenchyma to be removed. For CRCLM, the most commonly used procedures include radio-frequency ablation (RFA) and microwave ablation (MWA). Additional non-surgical options exist in the management of CRCLM but their use are reserved mainly for unresectable patients, hence beyond the scope of this review which discusses local therapy in the context of potentially CRCLM resectability.

For RFA in general, the morbidity rate (major complications) is relatively low (6-9%) and mortality ranges between 0-2%(61). RFA is the preferred option for smaller lesions (<3.0cm) and that are not in close contact to major vascular structures. Despite the fact that the use of RFA was described as an adjunct to macroscopically incomplete resections of liver metastasis, in several studies(14,62-65), no proper comparison was made to the

standard of care (systemic chemotherapy) for unresectable lesions and the evidence regarding its use in this specific context remains scarse. For larger lesions, microwave ablation is another option and has been described in the context of unresectable disease as an alternative to systemic chemotherapy. However there is no report mentioning the benefit of using MWA in combination to surgery for otherwise incomplete resection of CRCLM. One Asian study compared MWA to surgery and stated that similar long-term outcomes were achieved with both procedures(66). Nevertheless, more randomized controlled trials are needed to establish evidence of using microwave ablation in the context of resectable or potentially resectable disease.

Non anatomical resections

As the definition of resectability expanded its criteria and was evolving around the concept of an adequate future liver remnant while achieving negative margins, more nonanatomical resections were performed and was indeed reported to have similar long-term and oncologic outcomes(67-69). Despite the fact that some of the groups were slightly heterogenous, the nonanatomical resections being more often harbouring smaller disease burden than the anatomical resection groups, the encouraging results of these studies yielded another option for hepatic surgeons, allowing for safe resections while preserving enough liver remnant.

ii. Increasing the size of the future liver remnant

The second venue to achieve an adequate future liver remnant for the surgical management of CRCLM is by increasing the size of the FLR. This aspect is based solely on the regenerative capacity of the liver. The size of the future liver remnant can increase by

two methods that are clinically utilized: by performing staged resections or by a portal vein embolization. The description of these methods will be made in the following section.

Staged resections

A staged resection is done when two or more surgeries (hepatectomies) are required to clear the liver from all tumors (performing surgeries in "stages"). Most often, it will be considered when patients present with bilateral lesion, multinodular disease or larger size lesions, for which resection of all the affected segments could not be performed in one single operation as it would leave a remnant liver of insufficient size to sustain normal hepatic function. As an example, a typical common clinical scenario would be the following: a first surgical resection would be performed to clear one side of the liver from tumors, followed by a time interval to allow for regeneration of the contralateral side. Then, a second procedure would be performed to remove the remaining lesions, leaving a liver free of measurable disease. In most cases, to induce hypertrophy of the remnant liver prior to the second stage surgery, a portal vein embolization is performed (see below). Surgical case series describing the experience with staged resections reported similar outcomes when two consecutive resections were performed(70). The long-term outcomes of completed staged resections were also shown to be similar to the reported long-term outcomes of resected CRCLM, and failed staged resections (only first operation completed) did not have worst outcomes than conservative management (systemic chemotherapy)(71,72).

Portal vein embolization

Preoperative portal vein embolization (PVE) consists of embolizing (ie blocking) the portal venous flow supplying the side of the liver that is to be resected. The theory behind the use of PVE is that embolization of the portal vein subsequently induces a contralateral

hypertrophy of the non-embolized lobe. This is in the optic of resecting a patient who, without embolization, would have a remnant liver too small to sustain normal hepatic function post operatively. The indication for preoperative portal vein embolization is a small predicted future liver remnant: <20% for patients with normal liver function or <30% for patients with underlying liver disease with impaired ability to regenerate, such as non-alcoholic steatohepatitis(22). It is considered to be an adjunct procedure to major hepatectomy (extended right or left hepatectomies) or to achieve staged resections for bilobar disease(27). In observational studies, patients who received preoperative embolization had better survival and less postoperative liver failure after extended liver resections(20,21,23,73-75). The resectability rate was shown to increase from 46 to 79% in one study(76). Thus, PVE has many clinical benefits, such as being a low risk procedure, being associated with low rates of liver failure after major hepatectomy(77) and allowing some patients to become resectable. PVE is usually performed via percutaneous transhepatic access, and follow-up imaging using CT scan or MRI is recommended about 4 weeks after the procedure to assess the degree of hypertrophy(78,79).

iii. Improving the quality of the future liver remnant

In addition to the size, the function of the future liver remnant is also a critical component. In fact a poor quality liver, whether cirrhotic or steatotic, will have an impaired ability to regenerate and to recover from injury, hence after a partial hepatectomy. Multiple strategies therefore focus on this aspect: limiting the administration of neoadjuvant chemotherapy as well as several perioperative strategies that attempt to improve hepatic function and the thus the quality of the FLR. In an era where systemic chemotherapy is readily available and administered in the majority of the cases in patients presenting with CRCLM, side effects and complications related to the cytotoxic treatments inevitably were

described along and prompted clinicians to limit the number of cycles administered preoperatively. More precisely, irinotecan-based regimens have been more associated with cases of steatohepatitis(80-83), whereas oxaliplatin-based regimens have had more cases of sinusoidal obstruction syndrome reported(65,81,83-89). Some investigators have therefore suggested that neoadjuvant chemotherapy should be limited to no more than 4 to 6 cycles, with an interruption of 4 weeks or more between end of chemotherapy and surgery, to reduce complications related to chemotherapy-related liver injury(85,90,91). Novel strategies aiming to improve liver function post hepatectomy include the use of perioperative hyperinsulinemic-normoglycemic insulin clamp(92,93), which has been shown to be safe and effective in improve the quality of the liver remnant by improving glycogen content and reducing inflammation and apoptosis after major hepatectomy. Further research is needed to help in the application of these experimental findings to clinical practice.

VIII. Liver Regeneration

Since portal vein embolization stimulates the liver to regenerate, the following section will summarize the chronological events of this complex process. As previously mentioned, the liver is made of multiple cell types: hepatocytes (80% of the liver cells), the Kupffer cells, the stellate cells, immune cells and endothelial cells forming the hepatic sinusoids. Adult hepatocytes do not normally undergo cell division and normally stay in G0 phase(94,95), unless liver injury stimulates them to proliferate. The term liver “regeneration” was given to this process, although the injured, or removed liver parts (in the case of hepatectomy) do not grow back; instead the remaining hepatocytes undergo compensatory hypertrophy and proliferation. Many signaling pathways have been shown to be involved in

this process, and particularly several cytokines, such as IL-6 and TNF-alpha, and growth factors (such as EGF, HGF, TGF and insulin and glucagon) are known to be key players in liver regeneration. Nevertheless none of these factors have been shown to be absolutely indispensable for liver regeneration to occur; in other words, the complex interplay between different pathways allows for liver regeneration even if some factors are downregulated or knocked-down experimentally. Liver regeneration may be diminished but will occur to some degree.

Most of the evidence about liver regeneration mechanisms is derived form experimental studies with rodent models, specifically after partial hepatectomy (PH). Immediately following PH, 90-95% of hepatocytes start to proliferate and enter the cell cycle(94,96). Chronologically, many important early events occur in the first 24-48 hours after PH. Within minutes after hepatectomy, urokinase, HGF and EGF receptors and their ligands show increased levels. In parallel, intracellular signals within hepatocytes are seen with increased levels of beta-catenin, Notch NICD, STAT3 and NF**κ**B (between 5 and 60 minutes of PH). After 30 minutes, matrix metalloproteinase 9 (MMP9) has increased levels, and after the first hour, upregulation of TGFalpha, FGF1, FGF2, angiopoietin 1 and 2, VEGF, SCF, PDGF and amphiregulin (by the hepatocytes) is noted. Around the same time (one hour) stellate cells produce increased levels of TGFbeta-1 and HB-EGF; around the third hour, newly synthesized HGF is produced by the stellate cells. At 12 hours, MMP2 show increased levels and finally, DNA synthesis peaks at 24 hours post-PH in rats (6-12 hours later in mice(94)). The liver mass is mostly increased by 3 days, and is completely restored by 5-7 days(97).

Two main pathways exist that form the major elements of the liver regeneration cascade: a cytokine-dependant pathway and a growth factors-dependant pathway(96). Cytokine-dependant pathways are triggered by IL-6, which further mediate the activation of STAT3 and NF**κ**B as well as the MAPK and PI3K signaling pathways(98-101). Unless IL-6

is present in supraphysiological concentration; its presence has no direct mitogenic effect on hepatocytes(96). Another important cytokine, TNFα and its receptor activation were also shown to play a role in the proliferation of hepatocytes after PH(102). As for the growth factor-mediated pathways, HGF and TGFα were both demonstrated to have mitogenic properties in experimental studies with in vitro and in vivo models(95,96,103-108). The binding of HGF to its receptor Met activates several downstream pathways, notably PI3K, ERK, S6 kinase and AKT(108). Finally, an interplay between cytokine and growth factor-mediated pathway exist; for instance IL6-TNFα and HGF all promote various dimers of the AP-1 transcription factor, which itself is a major regulator of cellular growth response(109,110). IGFBP1 is another common factor common to both IL-6 and HGF and is one of the most abundant factors produced early in the regeneration cascade, modulating cell growth and replication through IGF pathways(111). The termination of liver regeneration is also a complex process, poorly understood and constitutes an area of active research. In spite of that, suppressors of cytokine signalling (SOCS) and TGFβ are both negative regulators involved in feedback mechanisms that promote termination of liver regeneration with their antiproliferative properties(112,113).

IX. Progression of colorectal liver metastasis

Colorectal cancer spreads primarily to the liver, and metastasis is the most common cause of death for these patients(114,115). Primary colon cancer is sporadic in about 70% of the cases, the remaining ones being hereditary(116). It is known to accumulate multiple genetic hits, and those can be divided into two genetic pathways alterations(117-119). First, the most common pathway is chromosomal instability, which accounts for 60% of all primary colon cancers. Included in this category are mutations of tumor suppressors APC and p53, proto-oncogene K-Ras, allelic loss of 18q and aneuploidy. Second, is the

pathways of microsatellite instability, which include alterations in DNA mismatch repair genes (SH2, PMS1,PMS2 and MLH1) and aberrations in SMAD4 and BRAF(117-119). In parallel to carcinogenesis and primary tumor formation, the metastatic cascade occurs(120,121) and consists of several critical steps necessary for distant organ invasion and appearance of secondary metastatic lesions(122-125).

Neovascularization (or angiogenesis) occurs in the primary tumor and can also become a route for disseminated cells to enter the circulatory system of patients, a process called intravasation(126). Similarly, lymphangiogenesis (formation of new lymphatic channels around the primary tumor) is an important process in the progression of CRC(127). Thus, after malignant cells escape the primary tumor, they undergo intravasation, a process that is thought to be secondary to certain MMPs, selectins and integrins, as well as a leaky tumor neovasculature(128). As the liver is the most common organ for distant metastasis, the route of the detached circulating tumor cells is via the porto-venous system, along with the neighboring lymphatic system. Most of the circulating cells then undergo apoptosis, due to mechanical stress when entering the blood vessels and immunological response against tumor cells(129,130). Once arrested in the host organ (liver in the case of CRCLM), tumor cells then have different potential fate: they may become small pre-angiogenic metastasis, larger vascularized metastasis, they may remain as dormant solitary cells (neither proliferating nor apoptotic), or dormant micrometastasis (in which apoptosis is in balance with proliferation resulting in stable micrometastasis)(131).

Role of the microenvironment and host organ

In congruence with the “seed and soil” hypothesis(132-134), defined by the propensity of some tumor cells (seeds) to spread and grow in a specific target organ (soil), there is indeed evidence that host factors may actually be critical in the progression of secondary metastatic lesions. For example, there may be expression of specific receptor on

cancer cells, such as epidermal growth factor receptor, concurrently with the expression of specific factors in the tissue, like transforming growth factor-α(135-138). For CRCLM, the different types of cells encountered in the hepatic sinusoids have been shown to play a role in cancer cells extravasation and establishment of metastasis(139). More precisely, the different sinusoidal cells have a critical role in the extravasation step, as they are in close contact when tumor cells arrest in the liver microcirculatory system. A multitude of pathways mediate this complex process, and involves production of cytokines and growth factors, expression of adhesion molecules and reactive oxygen species, and immune response(140-142). Regarding the arrest of cancer cells in the hepatic sinusoids, it is thought to be a process rather based on mechanical factors: cancer cells size average 20um whereas small sinusoidal vessels average 3-8um(143) causing the cells to physically stop in this microcirculation(125,144-148). The subsequent growth of cancer cells into a definite metastasis is mediated by molecular factors that are based on the interaction between the liver and tumor cells.

Metastatic cascade

In addition to the interaction between the organ microenvironment and the cancer cells, which regulate metastatic growth, molecular pathways have been shown in experimental studies to be implicated in the progression of metastases. As an example, in response to the interactions between chemokines and their receptors, intracellular pathways such as the Ras/MAPK signaling pathway can become activated, leading to events mediating proliferation, invasion and progression of tumors(149). Whether activated by chemokines, cytokines, growth factors or other mechanisms, the implication of the Ras signaling pathway in metastatic progression is well established(150-156), even in the activation of micrometastases from dormancy(148). Moreover, in order to survive and form a macrometastasis in the distant site, cancer cells must undergo a reversal of the initial

epithelial-mesenchymal transition (which allowed them to escape the primary and intravasate), termed a mesenchymal-epithelial transition (MET)(157); this process is thought to be mediated by the extra-cellular matrix(158).

X. Histological growth patterns

Liver metastases from colorectal cancer have been demonstrated to grow in three distinct histological growth patterns(159). First, desmoplastic lesions are defined as the presence of a desmoplastic rim separating tumor cells from the liver, in addition to a rich infiltrate of inflammatory cells at the interface. Replacement lesions on the other hand are known to be the infiltrative lesions; they are defined as tumor cells invading the surrounding liver parenchyma, resulting in an overlap of metastasis and hepatocytes at the interface, where the hepatocytes are “replaced” by tumor cells. Finally the pushing growth pattern is characterized as the liver plate surrounding the metastasis being pushed by the tumor; although no invasion and overlap is present at the interface, there is direct contact between tumor cells and hepatocytes but with the absence of a desmoplastic reaction and inflammatory cells found in the desmoplasic pattern. These growth patterns have been validated and described in several subsequent studies(160,161) and have also been each associated with different tumor vascularization(162). In fact it was noted that the replacement pattern display a more mature vasculature and utilize a process called vessel co-option, whereby a tumor uses nearby mature vasculature in order to get its blood supply. On the other hand, desmoplastic lesions have been characterized to utilize angiogenesis to supply the tumors. Although investigators suggested a possible prognostic role of the growth patterns, the clinical heterogeneity of the lesions evaluated in previous studies as well as the lack of statistically significant differences in long-term outcomes make the clinical utility of the growth patterns unclear so far. Nevertheless, as these patterns seem to

display markedly distinct vascularization processes, it has been hypothesized that such differences may explain the heterogeneity of biological response of colorectal liver metastasis.

TABLES

Table 1. Results of liver resection series for metastatic colorectal cancer (disease-free survival and overall survival)

Study	n	Perioperative chemotherapy (% of patients)	Major resection (% of patients)	Mortality (%)	5-year DFS (%)	5-year OS (%)
Hughes et al, 1986 (7)	607	-	-	-	-	33
Scheele et al, 1995 (163)	434	-	-	4.4	33	39
Nordlinger et al, 1996 (9)	1568	35%	64%	0.04-2.9[a]	15	28
Jamison et al, 1997 (10)	280	24%	28%	-	-	27
Fong et al, 1999 (11)	1001	-	63%	2.8	-	37
Iwatsuki et al, 1999 (12)	305	66%	80%	0.9	48	74
Choti et al, 2002 (13)	133	52%	47%	0-2.2[b]	20	40
Abdalla et al, 2004 (14)	190	-	64%	-	30	58
Fernandez et al, 2004 (15)	100	-	75%	-	35	59
Wei et al, 2006 (16)	423	32%	65%	1.7	27	47
Rees et al, 2008 (17)	929	55%	64%	1.5	24	36
De Jong et al, 2009 (18)	1669	43%	45%	-	30	47
Morris et al, 2010 (19)	3116	-	-	-	-	44

Abbreviations: OS: overall survival; DFS: disease-free survival
a: minor vs. major resection. b: late vs. recent period

Table 2. Results of randomized controlled trials first-line treatment for metastatic colorectal cancer (progression free survival and overall survival)

Study	Type of study	n	Comparative groups	PFS/TTP (months)	OS (months)
Scheithauer et al, 1993 [51]	RCT	40	5FU		11.0*
			supportive care	-	5.0
De Gramont et al, 2000 [52]	RCT	420	5FU/LV + OX	9.0*	16.2
			5FU/LV	6.2	14.7
Douillard et al, 2000 [53]	RCT	387	5FU + Iri	6.7*	17.4*
			5FU	4.4	14.1
Saltz et al, 2000 [54]	RCT	683	5FU + Iri	7.0*	14.8*
			5FU	4.3	12.6
Goldberg et al, 2004 [4]	RCT	795	FOLFOX	8.7*	19.5*
			IFL	6.9	15.0
			IROX	6.5	17.4
Tournigand et al, 2004 [55]	RCT	220	FOLFIRI	14.2	21.5
			FOLFOX6	10.9	20.5
Hurwitz et al, 2004 [57]	RCT	813	IFL + Bev	10.6*	20.3*
			IFL	6.2	15.6
Hochster et al, 2008 [164] (TREE study)	RCT	383	mFOLFOX6	8.7	19.2
			mFOLFOX6 + Bev	9.9	26.1
			bFOL	6.9	17.9
			bFOL + Bev	8.3	20.4
			CapeOX	5.9	17.2
			CapeOX + Bev	10.3	24.6
Saltz et al, 2007 [6] (NO16966)	RCT	1401	XELOX/FOLFOX + Bev	9.4*	21.3
			XELOX/FOLFOX	8.0	19.9
Fuchs et al, 2007 [56] (BICC-C)	RCT	547[a]	FOLFIRI + Bev	9.0	n/a[b]
			FOLFIRI[a]	7.6	23.1
			mIFL + Bev	8.3	19.2
			mIFL[a]	5.8	17.6
			CapeIRI + Bev	-	-
			CapeIRI	5.7	18.9

*: significant difference (p-value<0.05). a: n=430 patients randomized to FOLFIRI, mIFL or CapeIRI prior to protocol modification that included Bev. b: median not reached (median follow-up of 29 months).
Abbreviations: PFS: progression-free survival. TTP: time to progression. OS: overall survival. RCT: randomized controlled trial. FU: fluorouracil. LV: leucovorin. OX: oxaliplatin. CapeOX: capecitabine+oxaliplatin. Iri: Irinotecan. FOLFOX: 5-FU+leucovorin+oxaliplatin. FOLFIRI: 5FU+leucovorin+irinotecan. mIFL: modified irinotecan, 5FU infusion and leucovorin bolus. IROX: irinotecan+oxaliplatin. CapeIRI: capecitabine + irinotecan. bFOL: bolus 5FU, leucovorin + oxaliplatin. XELOX: capecitabine + oxaliplatin. Bev: Bevacizumab

FIGURES

Figure 1. Segmental anatomy of the liver

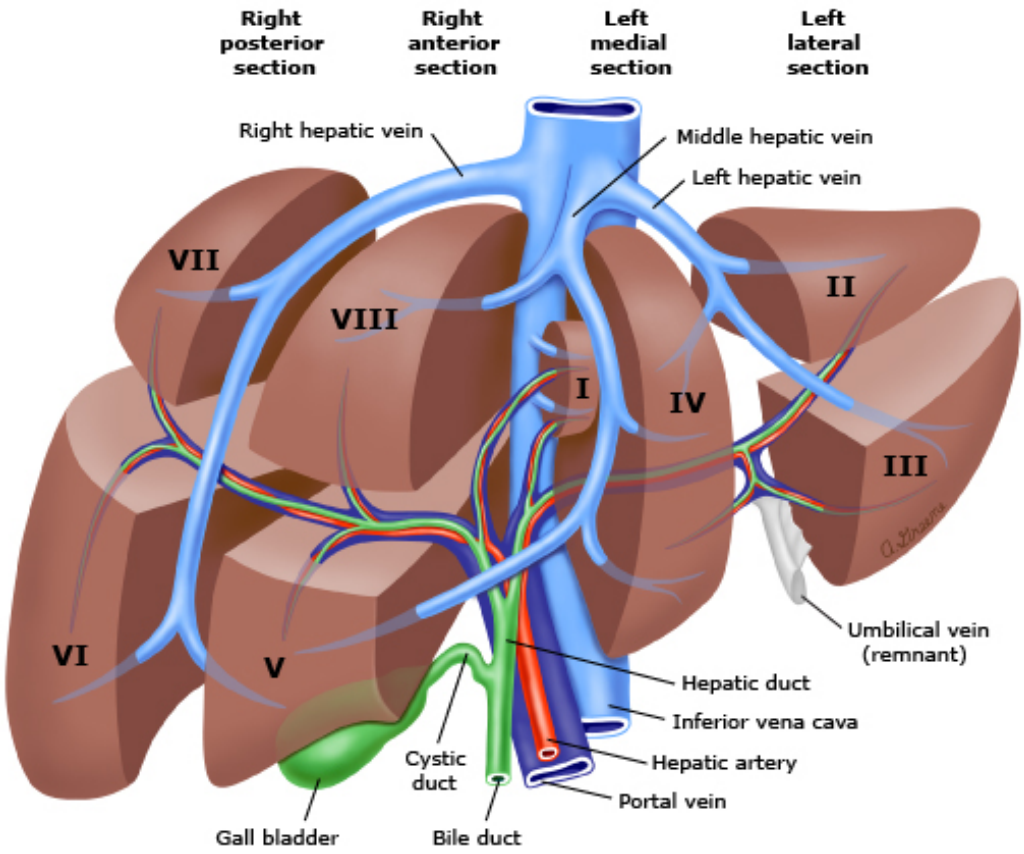

(www.uptodate.com)

Figure 2. The surgical management of colorectal liver metastasis relies on the adequate future liver remnant

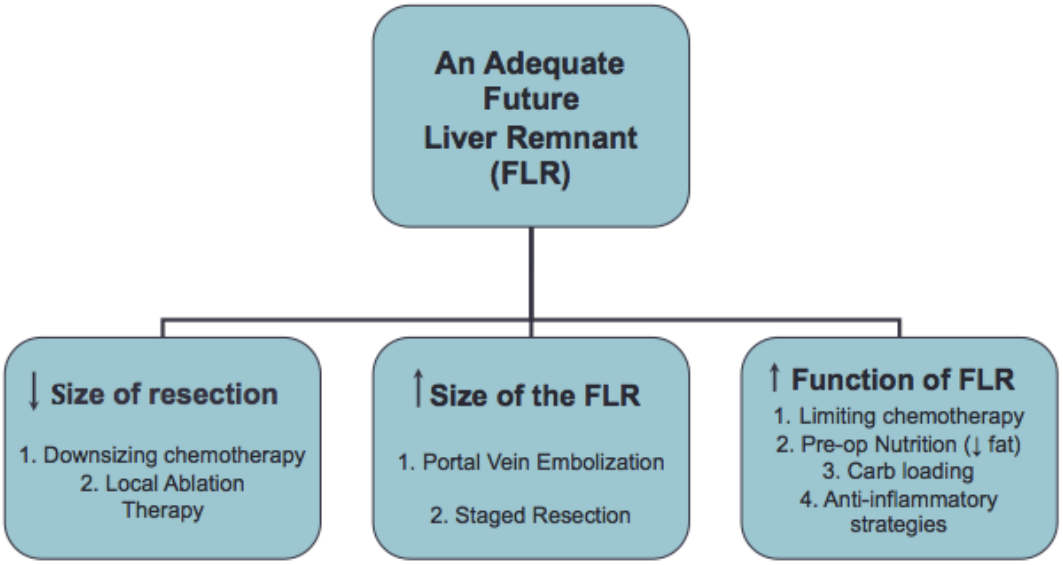

XI. Thesis Manuscript I

Published HPB journal

Podium presentation at the American Hepato-Pancreatico-Biliary Association, March 2011

ORIGINAL ARTICLE

Portal vein embolization stimulates tumour growth in patients with colorectal cancer liver metastases

Eve Simoneau[1], Murad Aljiffry[1,4], Ayat Salman[1], Nasser Abualhassan[1], Tatiana Cabrera[2], David Valenti[2], Arwa El Baage[5], Mohammad Jamal[1], Petr Kavan[3], Saleh Al-Abbad[1], Prosanto Chaudhury[1], Mazen Hassanain[1,5*] & Peter Metrakos[1,5*]

[1]Section of Solid Organ Transplant and Hepatopancreatobiliary Surgery, Departments of [2]Radiology and [3]Oncology, McGill University Health Center, Montreal, QC, Canada, [4]Department of Surgery, College of Medicine, King Abdul Aziz University, Jeddah, Saudi Arabia and [5]Department of Surgery, College of Medicine, King Saud University, Riyadh, Saudi Arabia

Abstract

Objectives: Portal vein embolization (PVE) can facilitate the resection of previously unresectable colorectal cancer (CRC) liver metastases. Bevacizumab is being used increasingly in the treatment of metastatic CRC, although data regarding its effect on post-embolization liver regeneration and tumour growth are conflicting. The objective of this observational study was to assess the impact of pre-embolization bevacizumab on liver hypertrophy and tumour growth.

Methods: Computed tomography scans before and 4 weeks after PVE were evaluated in patients who received perioperative chemotherapy with or without bevacizumab. Scans were compared with scans obtained in a control group in which no PVE was administered. Future liver remnant (FLR), total liver volume (TLV) and total tumour volume (TTV) were measured. Bevacizumab was discontinued ≥ 4 weeks before PVE.

Results: A total of 109 patients and 11 control patients were included. Portal vein embolization induced a significant increase in TTV: the right lobe increased by 33.4% in PVE subjects but decreased by 34.8% in control subjects ($P < 0.001$), and the left lobe increased by 49.9% in PVE subjects and decreased by 33.2% in controls ($P = 0.022$). A total of 52.8% of the study group received bevacizumab and 47.2% did not. There was no statistical difference between the two chemotherapy groups in terms of tumour growth. Median FLR after PVE was similar in both groups (28.8% vs. 28.7%; $P = 0.825$).

Conclusions: Adequate liver regeneration was achieved in patients who underwent PVE. However, significant tumour progression was also observed post-embolization.

Keywords

colorectal cancer liver metastases, tumour growth, portal vein embolization, bevacizumab, liver regeneration, degree of hypertrophy

Received 15 December 2011; accepted 30 March 2012

Correspondence

Mazen Hassanain, Department of Surgery, McGill University Health Center, S10.26-687 Pine Avenue West, Montreal, QC H3A 1A1 Canada. Tel: + 1 514 843 1600. Fax: + 1 514 843 1503. E-mail: mazen.hassanain@mail.mcgill.ca

Introduction

Colorectal cancer is diagnosed in approximately 142 570 Americans annually.[1] Of these, 51 370 will die from the disease.[1] Metastasis is the most common cause of death and occurs in the majority of patients.[2,3] In recent decades, outcomes in patients with colorectal liver metastases (CRLM) have improved as a result of enhancements in chemotherapy and hepatic resection.[4] In selected patients, the combination of chemotherapy and resection has increased 5-year survival to up to 50%, compared with only 10% in patients treated with chemotherapy alone.[5,6] Perioperative chemotherapy regimens for patients with CRLM are based on either

*These authors contributed equally to this paper as senior authors.

This manuscript was presented at the annual AHPBA 2011 meeting, Miami and at the 2010 IHPBA meeting.

© 2012 International Hepato-Pancreato-Biliary Association

oxaliplatin or irinotecan. Bevacizumab, a human monoclonal antibody and an inhibitor of vascular endothelial growth factor (VEGF), has become part of first-line chemotherapy.[7] VEGF plays a major role in tumour angiogenesis and is required for both tumour proliferation and healing of injured tissue. Randomized controlled trials have demonstrated that the addition of bevacizumab to standard chemotherapy increases tumour response, resectability rate and progression-free survival compared with chemotherapy alone.[8–11]

Unfortunately, despite the downsizing effect of preoperative chemotherapy, the majority of patients still have unresectable disease. The size of the future liver remnant (FLR) plays a major role in determining resectability. Therefore, strategies aimed at increasing the FLR if it is estimated to represent < 20–30% of organ size (in the absence of chronic liver disease) must be developed. Preoperative portal vein embolization (PVE) has been shown to be a safe and effective method of stimulating liver hypertrophy, increasing FLR and reducing post-hepatectomy complications.[12–15]

The regenerative process following PVE mirrors the regeneration stimulated after partial hepatectomy. Recent literature supports the safety of using preoperative chemotherapy in liver regeneration following PVE.[16–18] Despite its increasing clinical usage, however, there are currently very few data regarding the effect of bevacizumab on liver regeneration after PVE.[17] Moreover, the potential effect of PVE on tumour growth has been a subject of concern. In fact, some studies have suggested that, as well as causing hypertrophy of normal liver parenchyma, PVE also stimulates the growth of any tumour that is still present within the regenerating liver, including embolized and non-embolized sides.[19–25]

It is evident that the progression of tumours secondary to PVE could potentially affect resectability and overall survival in patients with CRLM. Any effect of pre-embolization chemotherapy on this potential tumour growth would therefore be an important clinical consideration. Therefore, the objectives of this observational study were to assess the effect of PVE on the volume of existing CRLM and to evaluate the effect of pre-embolization therapy, particularly the use of bevacizumab, on the volumes of metastases and FLR.

Materials and methods

Guidelines for meeting STROBE (*st*rengthening the *r*eporting of *ob*servational studies in *e*pidemiology) criteria were used in the preparation of this manuscript.

Patients

This study was authorized by the Director of Professional Services at the McGill University Health Center as per institutional protocol. All patients who underwent PVE in preparation for liver resection (trisegmentectomy or staged resection, according to tumour board recommendations) were identified. The criteria for PVE were an FLR of < 30% or staged resection. Between January 2003 and May 2011, 168 patients underwent PVE; 127 of these had a diagnosis of CRLM and 41 had alternative diagnoses. Of the 127 CRLM patients, 18 were excluded because computed tomography (CT) scans were missing; therefore comparative volumes could be calculated in 109 patients. Only 89 of the 109 patients could be assigned to the bevacizumab and non-bevacizumab groups with certainty because some patients had received chemotherapy in other institutions (Fig. 1). Patients were also excluded if they had not received preoperative chemotherapy or were known to have biliary obstruction or cirrhosis. Basic demographic data, disease characteristics, surgery and chemotherapy data were reviewed retrospectively. To assess the effects of pre-embolization chemotherapy, the study group was subdivided into those who had received bevacizumab prior to embolization ($n = 47$) and those who had not ($n = 42$). A control group of patients with CRLM who had not undergone PVE was identified ($n = 11$). Control patients were selected if they had received neoadjuvant chemotherapy, had two CT scans both performed off-chemotherapy and before surgical resection, and if the time between scans was comparable with the corresponding interval in the PVE population.

Portal vein embolization

Portal vein embolization was administered prior to a planned trisegmentectomy or as part of a staged liver resection. The procedure was performed via an ipsilateral approach using 90–180-μm polyvinyl alcohol (PVA) particles and coils to occlude segmental branch origins. In patients undergoing right-sided embolization, the first embolization included both the anterior and posterior branches of the right portal vein. Patients who failed to achieve the recommended FLR underwent a subsequent embolization of any remaining segments in the right liver with or without embolization of segment IV branches. In general, standard chemotherapy alone was discontinued approximately 4 weeks prior to embolization, and regimens including bevacizumab were discontinued 6 weeks prior to embolization.

Volumetry

To obtain volumetric data, pre- and post-PVE CT scans were analysed using GE Medical Systems Advantage Windows 4.3 workstations (GE Healthcare, Chalfont St Giles, UK) with dedicated three-dimensional volume calculation software. Two radiologists were blinded to the patients' chemotherapy treatment. The volume of the FLR and total liver volume (TLV) were measured on the portal phase of thin-slice helical CT scans. Routine scans were performed prior to PVE and 3–4 weeks after PVE. The ratio between the FLR and TLV was determined before and after PVE and the absolute difference between these two ratios was defined as the degree of hypertrophy. Total tumour volumes (TTVs) and tumour volumes (TVs) in both embolized and non-embolized lobes were measured in all patients pre- and post-embolization.

Statistics

Statistical analyses were performed using JMP Version 8.0 (SAS Institute, Inc., Cary, NC, USA). Normally distributed data

© 2012 International Hepato-Pancreato-Biliary Association

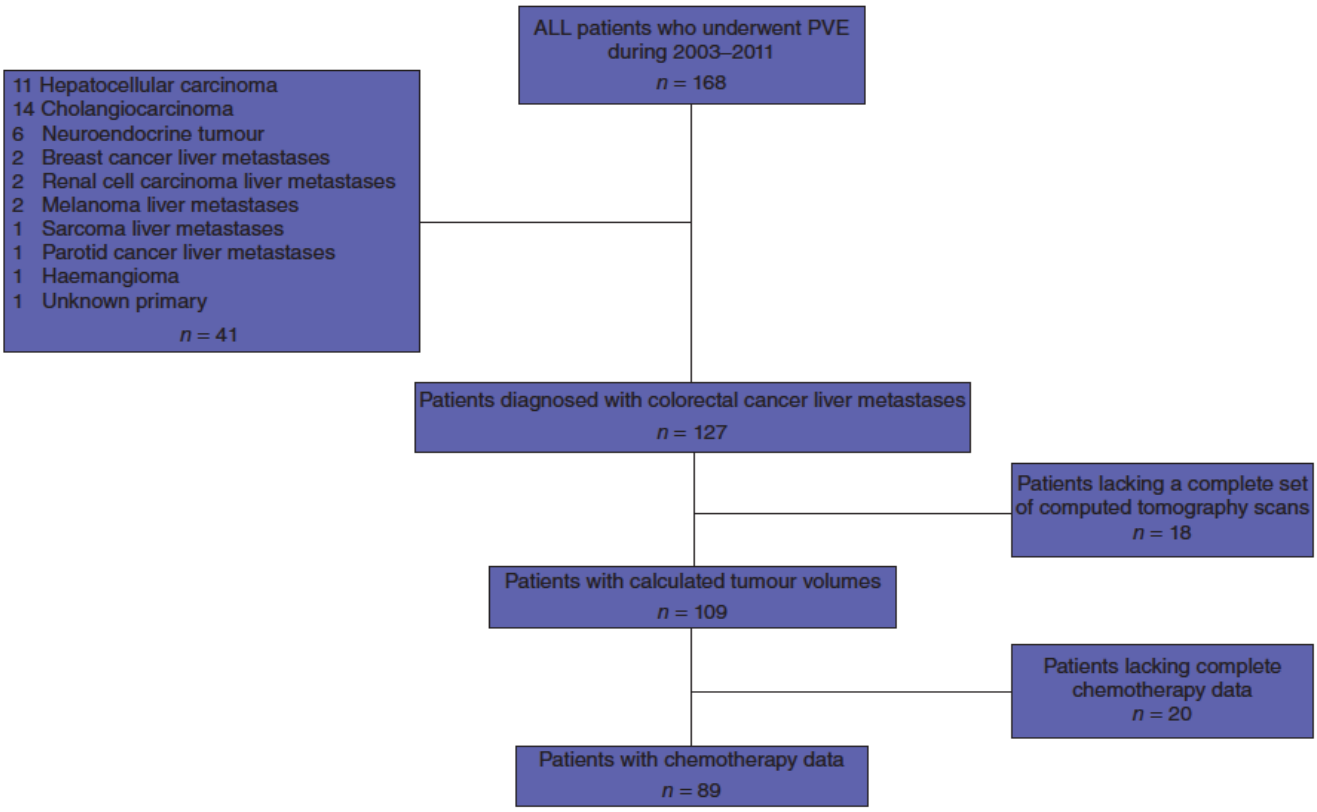

Figure 1 Distribution of patients who underwent portal vein embolization (PVE) during 2003–2011

were expressed as means and standard deviations; otherwise medians and ranges (interquartile ranges) were used. Nominal data were expressed as percentages. Differences in tumour growth against PVE and the use of bevacizumab were established using paired *t*-tests or Mann–Whitney *U*-tests as appropriate for continuous data. The chi-squared test was used for nominal data. Between-group differences were considered statistically significant at $P < 0.05$.

Results

Patients

A total of 127 CRLM patients who underwent PVE prior to liver resection were initially identified. Patients were excluded from the study group if they lacked two CT scans for volumetric calculations and thus 109 patients remained for tumour volume analysis (Fig. 1). Eleven control patients with two appropriately timed CT scans were also identified.

Patient demographics and preoperative variables are shown in Table 1. Among the 109 patients who received pre-embolization chemotherapy, receipt of bevacizumab was confirmed in 89 patients, 47 (52.8%) of whom were given pre-embolization bevacizumab. Complete details of the chemotherapy regimen were missing for some patients (Fig. 1) because they had been treated at a different institution. Chemotherapy was oxaliplatin-based in 22 and 17 patients in the bevacizumab and non-bevacizumab groups, respectively, and irinotecan-based in 13 and 12 patients in the bevacizumab and non-bevacizumab groups, respectively. One patient in the bevacizumab group and two in the non-bevacizumab group received chemotherapy using both oxaliplatin and irinotecan. Patients received a median of six (range: five to nine) chemotherapy cycles prior to embolization and the median time interval for all patients was 70 days (interquartile range: 51–100 days). Sixty patients (67.4%) underwent resection, including 30 patients (63.8%) in the bevacizumab group and 30 (71.4%) in the non-bevacizumab group ($P = 0.167$).

Portal vein embolization

Baseline characteristics and embolization data for patients who underwent PVE, by chemotherapy group (bevacizumab and non-bevacizumab), compared with those who did not undergo PVE, are shown in Table 1. In total, 105 patients (96.3%) underwent a right-sided embolization and four patients, all in the bevacizumab group, underwent segment IV and right portal vein embolization. One of these four patients had an extended right hepatectomy.

© 2012 International Hepato-Pancreato-Biliary Association

Table 1 Baseline characteristics in the total study population

	PVE		No PVE	*P*-value
	Bev (*n* = 47)	Non-bev (*n* = 42)	Bev (*n* = 11)	
Male, *n* (%)	26 (55.3)	28 (66.7)	9 (81.8)	0.191
Primary tumour, *n* (%)				
Colon	33 (70.2)	28 (66.7)	6 (54.5)	0.042[a]
Rectum	6 (12.8)	12 (28.6)	5 (45.5)	
Missing data	8 (17.0)	2 (4.8)	0	
Lesions, *n* (%)				
Synchronous	37 (70.2)	37 (88.1)	7 (63.6)	0.051
Metachronous	3 (6.4)	3 (7.1)	3 (27.3)	
Missing data	7 (14.9)	2 (4.8)	1 (9.1)	
Chemotherapy cycles, median (range)	6.0 (5–9)	7.5 (6–9)	7.0 (6–16)	0.266
Chemotherapy regimen, *n* (%)				
Oxaliplatin-based	22 (46.8)	17 (40.4)	5 (45.5)	0.701
Irinotecan-based	13 (27.7)	12 (28.6)	2 (18.2)	0.701
Both	1 (2.2)	2 (4.8)	0	
Missing	11 (23.3)	11 (26.2)	4 (36.3)	
Resected, *n* (%)	30 (63.8)	30 (71.4)	10 (90.9)	0.167
Staged	18 (60.0)	15 (50.0)	2 (20.0)	0.316
Trisegmentectomy	12 (40.0)	15 (50.0)	8 (80.0)	
Right-sided embolization, *n* (%)	46 (97.8)	41 (97.6)	NA	
Segment IV embolization[b], *n* (%)	4 (8.5)	0	NA	
Resected	1 (25.0)			
Unresectable	2 (50.0)			
Missing	1 (25.0)			
Days between CT scans, median (range)	72 (52–116)	65 (51–117)	68 (47–92)	0.581
Days from chemotherapy to second CT scan, median (range)	51 (30–107)	44 (27–100)	70 (47–116)	0.220

[a]There were more cases of rectal cancer in the control group; no difference was seen when comparing bev vs. non-bev in the PVE group ($P = 0.179$).
[b]Right-sided and segment VI embolization.
PVE, portal vein embolization; bev, bevacizumab; CT, computed tomography; NA, not available.

The median FLR in the 109 patients with CRLM who underwent PVE was 21.7% (range: 15.9–26.3%) before embolization and 28.7% (range: 23.2–35.4%) after embolization ($P < 0.001$). The median degree of hypertrophy was 6.0 (range: 1.6–10.2).

Tumour volumes

Overall, 77.1% of patients had an increase in TV. Statistically significant increases in TV were seen in both liver lobes (Tables 2 and 3); changes in TV in the PVE group differed markedly from those in the control group of patients who did not undergo PVE. Patients in the PVE group demonstrated a 33.4% increase in TV in the right lobe, whereas control subjects showed a 34.8% decrease in TV in the right lobe ($P < 0.001$). These percentages corresponded to a positive growth rate of 0.07 cm^3/day (range: 0–0.27 cm^3/day) in the PVE group and a negative rate of 0.06 cm^3/day (range: 0.18–0.01 cm^3/day) in the controls ($P < 0.001$). Patients in the PVE group showed an increase in TV of 49.9% in the left lobe, whereas control subjects demonstrated a decrease in TV of 33.2% in the left lobe ($P = 0.022$). Eight patients in the PVE group demonstrated unilateral disease on the first CT scan and developed new lesions on the second CT scan (i.e. after PVE), an event that was not observed in any patient in the control group. This difference did not reach statistical significance ($P = 0.427$).

The effects of pre-embolization chemotherapy in the bevacizumab and non-bevacizumab groups on tumour growth after PVE are shown in Tables 4 and 5. The percentage increase in tumour growth was higher in the non-bevacizumab group than in the bevacizumab group, but the difference was not statistically significant. Rates of tumour growth in the non-bevacizumab and bevacizumab groups, respectively, were 56.2% vs. 34.5% ($P = 0.764$) in the right lobe, and 54.3% vs. 30.1% ($P = 0.612$) in the left lobe.

© 2012 International Hepato-Pancreato-Biliary Association

Table 2 Tumour volumetry in the right lobe in patients who did and did not undergo portal vein embolization (PVE)

	PVE (n = 109)	No PVE (n = 11)	P-value
Tumour volume, cm^3, median (range)			
First CT scan[a]	21.2 (4.5–76.4)	10.6 (3.2–14.8)	0.080
Second CT scan	34.8 (11.5–112)	6.6 (2.0–9.9)	< 0.001
P-value[b]	< 0.001	0.002	
Change in tumour volume, % (range)	33.4 (– 0.5 to 168.0)	– 34.8 (– 40.7 to – 26.1)	< 0.001[a]

[a]Tumour volumes calculated from first and second CT scans (with embolization during interval time for study group only).
[b]Difference between pre- and post-embolization values.
CT, computed tomography.

Table 3 Tumour volumetry in the left lobe in patients who did and did not undergo portal vein embolization (PVE)

	PVE (n = 109)	No PVE (n = 11)	P-value
Tumour volume, cm^3, median (range)			
Pre-PVE	0 (0–3.2)	0 (0–7.4)	0.694
Post-PVE	0 (0–6.0)	0 (0–3.6)	0.805
P-value	< 0.001	0.625	
Change in tumour volume[a], % (range)	49.9 (– 24.2 to 118.0)	– 33.2 (– 58.0 to 6.0)	0.022
New bilateral disease[b], n (%)	8 (7.3)	0	0.595

[a]Difference in tumour volumes in the left lobe between patients receiving PVE and control subjects, expressed as a percentage.
[b]New lesions in the left lobe on the second computed tomography scan (i.e. after embolization in the PVE group).

Table 4 Tumour volumetry in the right lobe in patients who underwent portal vein embolization (PVE) with and without bevacizumab (bev)

	Bev (n = 47)	Non-bev (n = 42)	P-value
Tumour volume, cm^3, median (range)			
Pre-PVE	16.4 (3–75.5)	22.4 (6.2–65.5)	0.370
Post-PVE	21.2 (8.4–82.6)	33.7 (11.7–117.0)	0.255
P-value	0.003	< 0.001	
Change in tumour volume[a], % (range)	34.5 (– 2.5 to 212.2)	56.2 (3.6–165.0)	0.764

[a]Change in tumour volumes in the right lobe, expressed as a percentage, in patients who did and did not receive bevacizumab (all received PVE).

Table 5 Tumour volumetry in the left lobe in patients who underwent portal vein embolization (PVE) with and without bevacizumab (bev)

	Bev (n = 47)	Non-bev (n = 42)	P-value
Tumour volume, cm^3, median (range)			
Pre-PVE	0 (0–3.3)	0 (0–2.6)	0.435
Post-PVE	0 (0–5.2)	0 (0–5.6)	0.654
P-value	0.123	0.021	
Change in tumour volume[a], % (range)	30.1 (– 62.4 to 190.6)	54.3 (– 23.9 to 100.1)	0.612

[a]Change in tumour volumes in the left lobe, expressed as a percentage, in patients who did and did not receive bevacizumab (all received PVE).

Liver regeneration after PVE

A clinically significant increase in FLR volume was observed in both groups after PVE. Both groups had similar TLV prior to ($P = 0.617$) and after ($P = 0.581$) embolization.

The addition of bevacizumab to chemotherapy did not affect the pre- to post-embolization change in FLR volume. The proportion of the FLR increased from 20.8% to 28.8% in the bevacizumab group, and from 21.3% to 28.7% in the non-bevacizumab group ($P = 0.825$). Correspondingly, the mean degree of hypertrophy was comparable in the two groups (Table 6).

Correlation of the percentage growth in the FLR with the percentage growth in TV revealed a statistically significant positive

© 2012 International Hepato-Pancreato-Biliary Association

Table 6 Liver volumetry by chemotherapy group in patients who underwent portal vein embolization (PVE) with and without bevacizumab (bev)

	Bev (n = 47)	Non-bev (n = 42)	P-value
Total liver volume, cm^3, median (range)			
Pre-PVE	1588 (1444–2000)	1685 (1377–2073)	0.617
Post-PVE	1635 (1415–2037)	1766 (1385–2135)	0.581
Future liver remnant, %, median (range)			
Pre-PVE	20.8 (15.1–23.8)	21.3 (14.9–26.4)	0.373
Post-PVE	28.8 (21.9–34.5)	28.7 (24.8–35.7)	0.825
Degree of hypertrophy	7.5 (3.4–11.2)	5.1 (1.0–12.5)	0.127

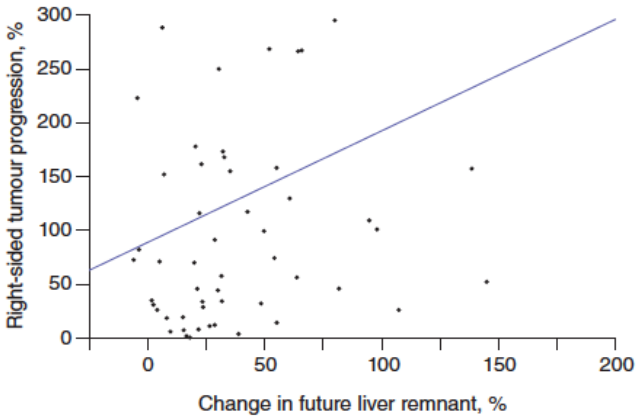

Figure 2 Correlation between percentage of future liver remnant growth and right-sided tumour progression

linear correlation between the growth of the remnant liver and the growth of tumours in the right lobe of the liver (P = 0.043) (Fig. 2).

Discussion

Portal vein embolization is an important strategy in the optimization of resectability rates in CRLM and is reported to be safe and effective in stimulating contralateral liver growth, which can be a major limitation in the resectability of CRLM. There are concerns that PVE may simultaneously stimulate tumour growth and this may limit its use. This study has demonstrated that PVE stimulates tumour growth in both embolized and non-embolized lobes of the liver compared with control lobes in a group of patients who had not received PVE and had been off preoperative chemotherapy for a duration similar to that of the PVE patients. The addition of bevacizumab to chemotherapy administered before embolization trended towards a relative protective effect (although this did not reach statistical significance), reducing this enhanced tumour growth without affecting liver hypertrophy. To the authors' knowledge, this is the largest study to demonstrate the effects of PVE on liver hypertrophy and tumour growth in patients with CRLM.

Bevacizumab has been shown to improve pathologic response rates when combined with cytotoxic agents and has also been reported to exert a protective effect against sinusoidal injuries induced by oxaliplatin-based chemotherapy.[26] Nevertheless, the inclusion of bevacizumab in treatment regimens for patients scheduled to undergo PVE and hepatic resection has been tempered by concerns regarding impaired wound healing and tissue regeneration, both of which are greatly dependent on angiogenesis and VEGF expression. Consistent with findings by Gruenberger and colleagues,[27] the present study found no increased risk for morbidity post-resection in patients receiving perioperative chemotherapy with bevacizumab.[28] However, existing data regarding the effects of bevacizumab on post-embolization hypertrophy remain scarce and inconsistent.[29,30] In a retrospective study conducted at the MD Anderson Center, University of Texas, preoperative chemotherapy plus bevacizumab did not impair liver regeneration after PVE.[29] Patients included in that study received oxaliplatin-based chemotherapy with (n = 26; median six cycles) or without (n = 17; median five cycles) bevacizumab, or received no chemotherapy before embolization (n = 22). After a median of 4 weeks post-PVE, no significant difference in the degree of hypertrophy was found among patients who had no chemotherapy, patients who received chemotherapy with bevacizumab and patients who received chemotherapy without bevacizumab (mean values 10.0%, 8.8% and 6.8%, respectively; P = 0.11). Conversely, Aussilhou and colleagues[30] reported a significantly smaller increase in mean FLR volume in 13 patients receiving bevacizumab plus standard chemotherapy compared with 26 patients treated with chemotherapy only (561 cm^3 vs. 667 cm^3; P < 0.03).[30] In that study, 30% of patients underwent portal vein ligation instead of embolization. Importantly, the mean number of bevacizumab cycles was 12, and the number of cycles above six was found to significantly reduce liver growth, as was age ≥ 60 years. It is noteworthy that prolonged chemotherapy has been identified previously as a factor contributing to impaired liver regeneration.[31,32]

In the present study, patients received a median of six chemotherapy cycles (five to nine in the bevacizumab group; six to nine in the non-bevacizumab group). This is consistent with the duration of treatment in the MD Anderson study.[29] Volumetric CT assessments were completed within 3–4 weeks after PVE in the present study; this is in concordance with published data showing

© 2012 International Hepato-Pancreato-Biliary Association

that the greatest increase in post-embolization liver volume (about 75%) occurs within 3 weeks after the procedure and is followed by a plateau phase of minimal regeneration.[33]

The progression of metastases after embolization was first described by Elias *et al.*, who showed that four of five patients had tumour growth after PVE.[20] However, that study included a small number of patients, lacked a control group and included patients with heterogeneous liver pathologies. In 2001, Kokudo *et al.* evaluated tumour proliferation after PVE using the Ki-67 labelling index, and showed that PVE induced a higher rate of proliferation compared with that in PVE-free controls.[19] Although these authors included more patients (18 patients in the study group and 29 controls), there was no mention of peri-embolization chemotherapy. In 2007, Ribero *et al.* observed no changes in tumour size in 80 patients undergoing PVE.[22] The authors did not, however, report the proportions of patients in whom tumour size increased or decreased and measured tumour diameters rather than volumes. It is the present authors' belief that tumour volume measurements are more accurate, especially when metastatic lesions are numerous, heterogeneous and uneven.

In the current study, significant increases in median TV were observed in both liver lobes (33.4% and 49.9% in the right and left lobes, respectively) in the PVE population, compared with the control group (decreases of 34.8% and 33.2% in the right and left lobes, respectively). Growth within the left lobe would potentially have more impact on resectability and therefore patient survival. The current study included eight patients (7.3%) who developed new lesions within the remnant liver lobe after embolization, seven of whom were rendered unresectable. None of the patients in the control group developed new lesions within the left lobe during the time interval between the scans. This difference is of major clinical significance as it may have an impact on patient survival. These results suggest that metastases that respond to chemotherapy continue to do so for some time after chemotherapy is stopped and that the regenerative milieu stimulated by the PVE is of a magnitude that reverses this effect. The fact that new lesions appear in some patients may indicate that micrometastases are being recruited in this regenerative environment.

Additionally, the current study demonstrated that patients who underwent PVE and who received pre-embolization bevacizumab had less pronounced overall tumour progression than patients who received chemotherapy only. However, this difference did not reach statistical significance. The addition of bevacizumab has been shown to improve pathologic response, as evidenced by a significant reduction in viable tumour cells and an increase in tumour fibrosis, resulting in a protective effect against sinusoidal injuries induced by oxaliplatin-based chemotherapy.[34–36] The increased response rate and/or fibrosis may explain the less pronounced growth observed in the bevacizumab group after PVE. A prospective examination of pathology specimens is needed to confirm this theory.

The limitations of the current study are those inherent to retrospective analyses and make it impossible to make specific recommendations regarding treatment regimens. Prospective studies with homogeneous populations would be required to assess the optimal type and timing of treatment regimens in relation to PVE in patients with CRLM. Prospective studies are also required to assess the impact of PVE-induced tumour growth on outcomes such as resectability and longterm survival. In general, a single CT scan is performed between the end of chemotherapy and liver resection at this institution, which explains the relatively small number of control patients who underwent two CT scans between the cessation of chemotherapy and surgery.

In conclusion, the current study reports on the effects of pre-embolization bevacizumab on liver regeneration and tumour growth observed after PVE in the largest cohort of patients studied to date. These findings provide evidence that PVE induces significant tumour growth in patients with CRLM. Although PVE is an essential tool in the management of CRLM, its effectiveness can be enhanced by developing strategies that limit tumour growth without suppressing liver regeneration.

Acknowledgements

The authors thank the Deanship of Scientific Research, College of Medicine Research Centre, King Saud University for funding this work through research group project no. RGP-VPP-082, and the McGill University Health Center Hepatopancreatobiliary and Transplant Center Research Unit.

Conflicts of interest

None declared.

References

1. Jemal A, Siegel R, Xu J, Ward E. (2010) Cancer statistics 2010. *CA Cancer J Clin* 60:277–300.
2. Siegel R, Naishadham D, Jemal A. (2012) Cancer statistics, 2012. *CA Cancer J Clin* 62:10–29.
3. American Joint Committee on Cancer. (2010) *Cancer Staging Manual*, 7th edn. Edge SB, Byrd DR, Compton CC, Fritz AG, Greene FL, Trotti A, eds. New York, NY: Springer, p. 143.
4. Kopetz S, Chang GJ, Overman MJ, Eng C, Sargent DJ, Larson DW *et al.* (2009) Improved survival in metastatic colorectal cancer is associated with adoption of hepatic resection and improved chemotherapy. *J Clin Oncol* 27:3677–3683.
5. Shah SA, Haddad R, Al-Sukhni W, Kim RD, Greig PD, Grant DR *et al.* (2006) Surgical resection of hepatic and pulmonary metastases from colorectal carcinoma. *J Am Coll Surg* 202:468–475.
6. Sanoff HK, Sargent DJ, Campbell ME, Morton RF, Fuchs CS, Ramanathan RK *et al.* (2008) Five-year data and prognostic factor analysis of oxaliplatin and irinotecan combinations for advanced colorectal cancer: N9741. *J Clin Oncol* 26:5721–5727.
7. Engstrom PF, National Comprehensive Cancer Network. (2008) Systemic therapy for advanced or metastatic colorectal cancer: National Comprehensive Cancer Network guidelines for combining anti-vascular endothelial growth factor and anti-epidermal growth factor receptor monoclonal antibodies with chemotherapy. *Pharmacotherapy* 28 (11 Pt 2):18–22.
8. Hurwitz H, Fehrenbacher L, Novotny W, Cartwright T, Hainsworth J, Heim W *et al.* (2004) Bevacizumab plus irinotecan, fluorouracil, and leucovorin for metastatic colorectal cancer. *N Engl J Med* 350:2335–2342.

© 2012 International Hepato-Pancreato-Biliary Association

9. Hochster HS, Hart LL, Ramanathan RK, Childs BH, Hainsworth JD, Cohn AL *et al*. (2008) Safety and efficacy of oxaliplatin and fluoropyrimidine regimens with or without bevacizumab as first-line treatment of metastatic colorectal cancer: results of the TREE Study. *J Clin Oncol* 26:3523–3529.
10. Loupakis F, Bria E, Vaccaro V, Cuppone F, Milella M, Carlini P *et al*. (2010) Magnitude of benefit of the addition of bevacizumab to first-line chemotherapy for metastatic colorectal cancer: meta-analysis of randomized trials. *J Exp Clin Cancer Res* 29:58–66.
11. Welch S, Spithoff K, Rumble RB, Maroun J, Gastrointestinal Cancer Disease Site Group. (2010) Bevacizumab combined with chemotherapy for patients with advanced colorectal cancer: a systematic review. *Ann Oncol* 21:1152–1162.
12. Hemming AW, Reed AI, Howard RJ, Fujita S, Hochwald SN, Caridi JG *et al*. (2003) Preoperative portal vein embolization for extended hepatectomy. *Ann Surg* 237:686–691.
13. Abdalla EK, Barnett CC, Doherty D, Curley SA, Vauthey JN. (2002) Extended hepatectomy in patients with hepatobiliary malignancies with and without preoperative portal vein embolization. *Arch Surg* 137:675–680; discussion 680–681.
14. Abulkhir A, Limongelli P, Healey AJ, Curley SA, Vauthey JN. (2008) Preoperative portal vein embolization for major liver resection: a meta-analysis. *Ann Surg* 247:49–57.
15. Wicherts DA, de Haas RJ, Andreani P, Sotirov D, Salloum C, Castaing D *et al*. (2010) Impact of portal vein embolization on longterm survival of patients with primarily unresectable colorectal liver metastases. *Br J Surg* 97:240–250.
16. Nafidi O, Désy D, Létourneau R, Côté J, Plasse M, Vandenbroucke F *et al*. (2009) Hypertrophy of the non-embolized liver after chemotherapy. *HPB* 11:103–107.
17. Covey AM, Brown KT, Jarnagin WR, Brody LA, Schwartz L, Tuorto S *et al*. (2008) Combined portal vein embolization and neoadjuvant chemotherapy as a treatment strategy for resectable hepatic colorectal metastases. *Ann Surg* 247:451–455.
18. Tanaka K, Kumamoto T, Matsuyama R, Takeda K, Nagano Y, Endo I. (2010) Influence of chemotherapy on liver regeneration induced by portal vein embolization or first hepatectomy of a staged procedure for colorectal liver metastases. *J Gastrointest Surg* 14:359–368.
19. Kokudo N, Tada K, Seki M, Ohta H, Azekura K, Ueno M *et al*. (2001) Proliferative activity of intrahepatic colorectal metastases after preoperative hemihepatic portal vein embolization. *Hepatology* 34:267–272.
20. Elias D, De Baere T, Roche A, Ducreux M, Leclere J, Lasser P. (1999) During liver regeneration following right portal embolization the growth rate of liver metastases is more rapid than that of the liver parenchyma. *Br J Surg* 86:784–788.
21. Barbaro B, Di Stasi C, Nuzzo G, Vellone M, Giuliante F, Marano P. (2003) Preoperative right portal vein embolization in patients with metastatic liver disease. Metastatic liver volumes after RPVE. *Acta Radiol* 44:98–102.
22. Ribero D, Abdalla EK, Madoff DC, Donadon M, Loyer EM, Vauthey JN. (2007) Portal vein embolization before major hepatectomy and its effect on regeneration, resectability and outcome. *Br J Surg* 94:1386–1394.
23. Heinrich S, Jochum W, Graf R, Clavien PA. (2006) Portal vein ligation and partial hepatectomy differentially influence growth of intrahepatic metastasis and regeneration in mice. *J Hepatol* 45:35–42.
24. Maggiori L, Bretagnol F, Sibert A, Paradis V, Vilgrain V, Panis Y. (2010) Selective portal vein ligation and embolization induce different tumoral responses in the rat liver. *Surgery* 149:496–503.
25. van Gulik TM, van den Esschert JW, de Graaf W, van Lienden KP, Busch OR, Heger M *et al*. (2008) Controversies in the use of portal vein embolization. *Dig Surg* 25:436–444.
26. Zalinski S, Bigourdan JM, Vauthey JN. (2010) Does bevacizumab have a protective effect on hepatotoxicity induced by chemotherapy? *J Chir (Paris)* 147 (Suppl 1):18–24.
27. Gruenberger B, Tamandl D, Schueller J, Scheithauer W, Zielinski C, Herbst F *et al*. (2008) Bevacizumab, capecitabine, and oxaliplatin as neoadjuvant therapy for patients with potentially curable metastatic colorectal cancer. *J Clin Oncol* 26:1830–1835.
28. Chaudhury P, Hassanain M, Bouganim N, Salman A, Kavan P, Metrakos P. (2010) Perioperative chemotherapy with bevacizumab and liver resection for colorectal cancer liver metastasis. *HPB* 12:37–42.
29. Zorzi D, Chun YS, Madoff DC, Abdalla EK, Vauthey JN. (2008) Chemotherapy with bevacizumab does not affect liver regeneration after portal vein embolization in the treatment of colorectal liver metastases. *Ann Surg Oncol* 15:2765–2772.
30. Aussilhou B, Dokmak S, Faivre S, Paradis V, Vilgrain V, Belghiti J. (2009) Preoperative liver hypertrophy induced by portal flow occlusion before major hepatic resection for colorectal metastases can be impaired by bevacizumab. *Ann Surg Oncol* 16:1553–1559.
31. Sturesson C, Keussen I, Tranberg KG. (2010) Prolonged chemotherapy impairs liver regeneration after portal vein occlusion – an audit of 26 patients. *Eur J Surg Oncol* 36:358–364.
32. Vauthey JN, Zorzi D. (2009) In search of the black sheep: is it bevacizumab or extended chemotherapy? *Ann Surg Oncol* 16:1463–1464.
33. Donadon M, Ribero D, Morris-Stiff G, Abdalla EK, Vauthey JN. (2007) New paradigm in the management of liver-only metastases from colorectal cancer. *Gastrointest Cancer Res* 1:20–27.
34. Ribero D, Wang H, Donadon M, Zorzi D, Thomas MB, Eng C *et al*. (2007) Bevacizumab improves pathologic response and protects against hepatic injury in patients treated with oxaliplatin-based chemotherapy for colorectal liver metastases. *Cancer* 110:2761–2767.
35. Rubbia-Brandt L, Giostra E, Brezault C, Roth AD, Andres A, Audard V *et al*. (2007) Importance of histological tumour response assessment in predicting the outcome in patients with colorectal liver metastases treated with neoadjuvant chemotherapy followed by liver surgery. *Ann Oncol* 18:299–304.
36. Maru DM, Kopetz S, Boonsirikamchai P, Agarwal A, Chun YS, Wang H *et al*. (2010) Tumour thickness at the tumour–normal interface: a novel pathologic indicator of chemotherapy response in hepatic colorectal metastases. *Am J Surg Pathol* 34:1287–1294.

XII. Transition to manuscript II

We previously showed in the largest published series on portal vein embolization that portal vein embolization had an effect on tumor progression.(165) The impact of tumor progression post portal vein embolization has yet to be established. In fact, multiple studies looked at long-term outcomes in PVE patients and compared them to patients not receiving PVE. In terms of overall survival, results from these studies were conflicting as some studies reported a lower survival compared to controls (25% vs. 50% 5-year survival)(166) whereas some others stated that overall survival were similar (47% vs. 40% 5-year survival for PVE and non-PVE respectively)(167). Similarly, reports of disease-free survival from studies comparing PVE and non-PVE patients were ranging from worse disease-free survival (30% vs. 50% 5-year disease-free survival)(168) to similar disease-free survival in PVE patients.(167) One study even reported less intrahepatic recurrence in PVE patients. (169) Most of the studies looking at long-term outcomes also reported the resectability rate of the PVE patients. Since not all PVE patients proceeded to surgical resection, this further contributed to the heterogeneity of the PVE group, hence resulting in conflicting results among studies.

There is no literature on the effect of tumor progression on long-term outcomes. We wanted to investigate in a large series of PVE patients the impact of tumor progression on resectability. We also aimed to evaluate the overall survival and disease-free survival of PVE patients, both with and without tumor progression post-PVE, and compared it to a cohort of patients who underwent major hepatectomy but did not require preoperative portal vein embolization.

XIII. Thesis Manuscript II

Published in British Journal of Surgery

Podium presentation at the American College of Surgeons, October 29th 2014

Original article

Portal vein embolization and its effect on tumour progression for colorectal cancer liver metastases

E. Simoneau[1], M. Hassanain[2,4], M. Shaheen[1], M. Aljiffry[5], N. Molla[3], P. Chaudhury[1,2], S. Anil[4], A. Khashper[3], D. Valenti[3] and P. Metrakos[1]

[1]Department of Surgery, Division of Hepatopancreatobiliary Surgery, [2]Division of Oncology, Department of Surgery, and [3]Department of Radiology, McGill University, Montreal, Quebec, Canada, and [4]Department of Surgery, King Saud University, Riyadh, and [5]Department of Surgery, Faculty of Medicine, King Abdulaziz University, Jeddah, Saudi Arabia

Correspondence to: Dr P. Metrakos, Royal Victoria Hospital, 687 Pine Avenue West, S10.26, Montreal, Quebec, Canada, H3A 1A1 (e-mail: peter.metrakos@mcgill.ca)

Background: The aim of this study was to evaluate the long-term outcomes of patients with colorectal cancer liver metastasis (CRCLM) exhibiting disease progression after portal vein embolization (PVE).

Methods: Patients with CRCLM requiring PVE before hepatectomy between 2003 and 2014 were included. Clinical variables, and liver and tumour volumes determined by three-dimensional CT volumetry were assessed before and after PVE. Overall and disease-free survival data were obtained. Univariable and multivariable logistic regression analyses were performed to identify predictors of tumour progression after PVE.

Results: Of 141 patients who underwent PVE, 93 (66·0 per cent) had tumour progression and 17 (12·1 per cent) developed new contralateral lesions. Significantly fewer patients had resectable disease in the group with disease progression than among those with stable disease: 43 (46 per cent) of 93 *versus* 36 (75 per cent) of 48 respectively ($P = 0·001$). Median survival was similar in patients with and without tumour growth after PVE: 22·5 *versus* 26·0 months for patients with unresectable tumours ($P = 0·706$) and 46·2 *versus* 52·2 months for those with resectable disease ($P = 0·953$). However, disease-free survival for patients with tumour progression after PVE was shorter than that for patients with stable disease (6·0 *versus* 20·2 months; $P = 0·045$). Response to neoadjuvant chemotherapy was the only significant factor associated with tumour progression in multivariable analysis.

Conclusion: Tumour progression after PVE did not affect overall survival, but patients with resected tumours who had tumour growth after embolization experienced earlier recurrence. A borderline response to neoadjuvant chemotherapy seemed to be associated with tumour progression after PVE.

Presented to the American College of Surgeons Clinical Congress, San Francisco, California, USA, October 2014; published in abstract form as *J Am Coll Surg* 2014; **219**(Suppl): e19

Paper accepted 14 May 2015

Published online 24 June 2015 in Wiley Online Library (www.bjs.co.uk). **DOI:** 10.1002/bjs.9872

Introduction

Surgical resection of colorectal cancer liver metastasis (CRCLM) is the only chance of cure. Advanced treatment strategies take advantage of the liver's capacity to regenerate after injury. An adequate future liver remnant (FLR) in both size and function is one of the major determinants of resectability[1–4]. Preoperative portal vein embolization (PVE) has become the standard method for inducing atrophy of the embolized segments and hypertrophy of the contralateral (non-embolized) segments (the FLR), in an attempt to convert the disease in more patients from an unresectable to a resectable state[4–7]. Long-term outcome studies[3,5,8–11] have supported the use of PVE by comparing patients who have PVE, of whom a proportion become resectable, with patients without PVE, whose tumours remain unresectable. Most of these studies have also demonstrated similar survival between patients with and without PVE. The benefit of preoperative PVE for initially unresectable CRCLM is well established as it allows such metastasis to become resectable[3,5,12,13], thereby offering a survival advantage.

© 2015 BJS Society Ltd
Published by John Wiley & Sons Ltd

Tumour progression following PVE is a concern that has been reported in multiple studies[2,10,14–18]. It has been shown that metastases can progress in 30–82 per cent of patients undergoing preoperative embolization[3,9,16,17,19,20] and that unresectability after PVE may be attributed to tumour progression[2,15]. The impact of disease progression on long-term outcomes following preoperative embolization is not well defined. The primary objective of this study was to evaluate the impact of tumour growth after PVE on resectability, overall survival and disease-free survival. A secondary objective was to identify clinical predictors of tumour progression after PVE, in an attempt to identify patients at higher risk of progression at an early stage.

Methods

All adult patients with CRCLM between January 2003 and June 2014 who required PVE before liver resection were included. PVE was carried out before a trisegmentectomy or as part of a staged liver resection. The decision to undertake PVE was based on the tumour board recommendations (FLR less than 25 per cent[13] or part of a staged resection). Patients were excluded from the study if they did not have adequate cross-sectional imaging before or after PVE for assessment of tumour volumetrics. Although the groups compared were within the PVE cohort (progression *versus* stable disease after PVE), an additional cohort of patients with CRCLM who underwent a single major hepatectomy without PVE during the same interval served as a control group. Major hepatectomy was defined as the resection of three or more liver segments. The control group also underwent volumetric assessment of the liver and metastases in order to match the PVE and non-PVE (control) group by baseline total tumour volume (TTV) and by age. Patients in the control group were not offered preoperative PVE because they were judged to have an adequate preoperative FLR. The ethics review board at McGill University approved this study.

Data collection

For all patients, clinical characteristics, disease characteristics, chemotherapy data and information on recurrence were collected in the Liver Disease Data Registry. For patients with adequate imaging before and after neoadjuvant chemotherapy, the chemotherapy response was evaluated objectively based on Response Evaluation Criteria in Solid Tumours (RECIST) guidelines (version 1.1)[21]. The hepatic lesions were assessed by triphasic CT before and after systemic chemotherapy. Briefly, a complete response was defined as complete disappearance of all lesions on follow-up imaging, whereas a partial response and progression of disease were defined as a decrease of at least 30 per cent and an increase of at least 20 per cent in the total diameter of the target metastatic lesions respectively. Any differences falling in between these cut-offs were judged to represent stable disease. Disease progression also included patients who developed new lesions or extrahepatic disease while receiving chemotherapy regardless of changes in lesion diameter[21].

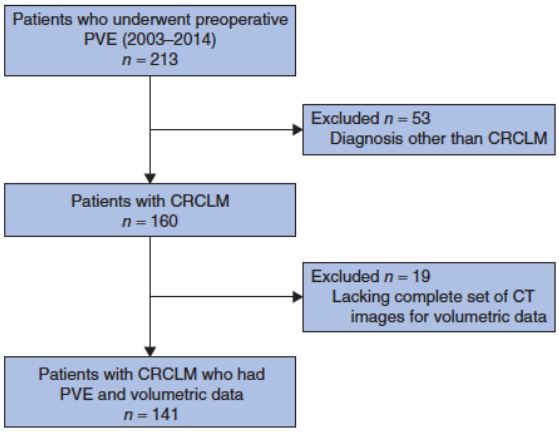

Fig. 1 Study flow chart. PVE, portal vein embolization; CRCLM, colorectal cancer liver metastasis

Although discrepancy exists in the definition of resectability[22,23], surgeons at this institution declined patients for resection if new extrahepatic disease developed in the interval before resection, significant intrahepatic progression occurred further reducing the amount of spared liver, new lesions developed in the liver remnant that were not amenable to resection or local ablative therapy, and if it was judged impossible for the remnant liver to have adequate bile drainage, portal and hepatic arterial blood supply and venous drainage.

Overall survival was calculated from the date of diagnosis of liver metastasis until the date of death (obtained from the provincial data registry) or alternatively the date of last follow-up. Disease-free survival was calculated from the date of resection until the date of recurrence or last follow-up.

Portal vein embolization

The procedure was performed via an ipsilateral approach using 90–180-mm polyvinyl alcohol particles and coils (early part of study) or histoacryl glue (later years) to occlude segmental vessels. The embolization endpoint

© 2015 BJS Society Ltd
Published by John Wiley & Sons Ltd

Table 1 Demographic and tumour characteristics for patients who had portal vein embolization

	No tumour progression after PVE ($n = 48$)	Tumour progression after PVE ($n = 93$)	P§
Age (years)*	58(11)	58(10)	0·992¶
Sex ratio (M : F)	12 : 36	34 : 59	0·165
Primary tumour characteristics			
Tumour site			0·122
Colon	30 (63)	70 (75)	
Rectum	18 (37)	23 (25)	
Tumour category‡			0·198#
T1	0 (0)	1 (3)	
T2	1 (6)	2 (6)	
T3	8 (50)	25 (74)	
T4	7 (44)	6 (18)	
Node status‡			0·171#
N0	3 (19)	5 (15)	
N1	8 (50)	9 (26)	
N2	5 (31)	20 (59)	
Differentiation‡			1·000#
Poor	2 (13)	4 (12)	
Moderate	13 (81)	28 (82)	
Unknown	1 (6)	2 (6)	
Metastases			
Timing			0·613
Synchronous	40 (83)	81 (87)	
Metachronous	8 (17)	12 (13)	
Bilateral lesions	27 (56)	35 (38)	0·035
No. of lesions at diagnosis†	4 (3–7)	5 (3–8)	0·987**
Largest lesion at diagnosis (cm)†	3·6 (2·1–5·9)	3·7 (2·1–5·8)	0·922**
Extrahepatic disease	4 (8)	9 (10)	1·000
Volumetry before PVE†			
Tumour volume, right lobe (cm^3)	33·1 (13·1–100·7)	10·2 (2·9–42·6)	0·495**
Tumour volume, left lobe (cm^3)	0 (0–3·6)	0 (0–1·8)	0·819**
Total tumour volume (cm^3)	41·9 (13·6–107·0)	19·8 (3·9–56·2)	0·543**
Total liver volume (cm^3)	1716 (1048–2006)	1613 (1382–1888)	0·548**
Future liver remnant (cm^3)	376·2 (301·5–533·1)	336·0 (258·4–502·5)	0·728**

Values in parentheses are percentages unless indicated otherwise; values are *mean(s.d.) and †median (i.q.r.). ‡Only 50 pathological primary colonic specimens (16 in group with stable disease and 34 in group with progression) were available for review. PVE, portal vein embolization. §χ^2 test, except ¶t test, #Fisher's exact test and **Mann–Whitney U test.

was stasis. All but six patients underwent a right-sided embolization and the majority (79·4 per cent) of the embolizations were achieved in a single session where the embolization included both the anterior and posterior branches of the right portal vein. Patients who failed to achieve an adequate FLR underwent subsequent embolization of any remaining segments in the right liver with or without embolization of segment IV branches. The majority of patients undergoing PVE had cytotoxic chemotherapy discontinued at least 4 weeks before embolization[24,25] in accordance with standard practice at this institution; if the regimen included bevacizumab, it was discontinued approximately 6 weeks before embolization[26,27]. Adjuvant chemotherapy was administered routinely to all patients after resection[28].

Liver and tumour volumetry

Because patients undergoing PVE do not receive any treatment (chemotherapy is stopped before PVE until resection), disease status was evaluated before and after PVE using three-dimensional tumour volumes, as the RECIST classification is a validated method for measurement of treatment response. To calculate liver and tumour volumes before and after embolization, all included patients had triphasic CT before PVE (at the discontinuation of neoadjuvant chemotherapy) and after embolization (follow-up imaging after 3–4 weeks). The scans at these two time points were assessed with dedicated three-dimensional volume calculation software, on a GE Medical Systems Advantage Windows® 4.3 workstation (GE Healthcare, Milwaukee, Wisconsin, USA). Volume

© 2015 BJS Society Ltd
Published by John Wiley & Sons Ltd

Table 2 Chemotherapy and embolization data

	No tumour progression after PVE ($n = 48$)	Tumour progression after PVE ($n = 93$)	P¶
Chemotherapy			
Chemonaive	0 (0)	5 (5)	0·165
Oxaliplatin-based	36 of 44 (82)	56 of 82 (68)	0·103
Irinotecan-based	8 of 44 (18)	24 of 79 (30)	0·129
Bevacizumab	26 of 41 (63)	47 of 82 (57)	0·516
No. of neoadjuvant cycles*	6 (6–7)	6 (6–8)	0·384#
Response†			< 0·001
Disease progression	1 of 45 (2)	24 of 81 (30)	
Stable disease	19 of 45 (42)	38 of 81 (47)	
Partial response	25 of 45 (56)	19 of 81 (23)	
Interval between chemotherapy and CT for RECIST assessment (days)*	102 (90–293)	110 (87–164)	0·841#
Embolization			
Two-stage PVE‡	7 (15)	27 (29)	0·057
Interval between chemotherapy and PVE (days)*	36 (28–67)	66 (33–104)	0·035#
Segment IV embolization	0 (0)	3 (3)	0·551**
Hepatic vein embolization	0 (0)	2 (2)	0·548**
Side of PVE			0·664**
Right-sided	47 (98)	88 (95)	
Left-sided	1 (2)	5 (5)	
Part of staged resection§	13 of 47 (28)	38 of 92 (41)	0·114

Values in parentheses are percentages unless indicated otherwise; *values are median (i.q.r.). †According to Response Evaluation Criteria in Solid Tumours (RECIST). ‡Embolization of consecutive anterior and posterior segments. §Minor resection followed by portal vein embolization (PVE) and subsequent second hepatectomy. ¶χ^2 test, except #Mann–Whitney U test and **Fisher's exact test.

measurements were performed on axial view images in the portovenous phase from 2·5-mm thick slices, and all volumes were expressed in cubic centimetres[3].

To characterize the liver hypertrophy, the size of the FLR and the total liver volume (TLV) were measured before and after PVE. The FLR was defined as the liver portion predicted to remain after surgical resection, and the degree of hypertrophy was defined as the difference in percentage FLR ((FLR/TLV) × 100) before and after PVE[4]. To evaluate the metastases, TTV and tumour volume (TV) on the right and left sides were measured. Disease progression after PVE was defined as a percentage change in TTV of at least 15 per cent ($(TTV_{after} - TTV_{before})/TTV_{before} \times 100$), based on previous studies[29,30]. If new lesions developed after embolization, patients were also categorized as having disease progression after PVE.

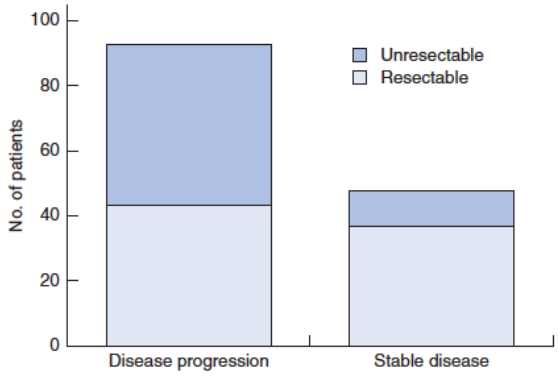

Fig. 2 Tumour resectability among patients with tumour progression or stable disease after portal vein embolization. $P = 0·001$ (χ^2 test)

Statistical analysis

Normally distributed data are expressed as mean(s.d.) and non-normally distributed data as median (i.q.r.); the t test and Mann–Whitney U test respectively were used for comparison of values. Categorical data were compared using χ^2 or Fisher's exact test as appropriate. Overall and disease-free survival were obtained using the Kaplan–Meier method, and comparisons between groups were made by means of the log rank test. $P < 0·050$ was considered statistically significant. To evaluate factors associated with tumour progression after PVE, univariable logistic regression was carried out for variables found to be marginally or highly significantly different ($P < 0·100$) between the groups with stable disease *versus* progression. Variables with $P < 0·050$ in the univariable analysis were entered into a multivariable logistic regression model. Crude and adjusted risk ratios were calculated in univariable and multivariable logistic regression models respectively, both with 95 per cent c.i. Data were analysed in R version 3.1.1 (R Project for Statistical Computing,

© 2015 BJS Society Ltd
Published by John Wiley & Sons Ltd

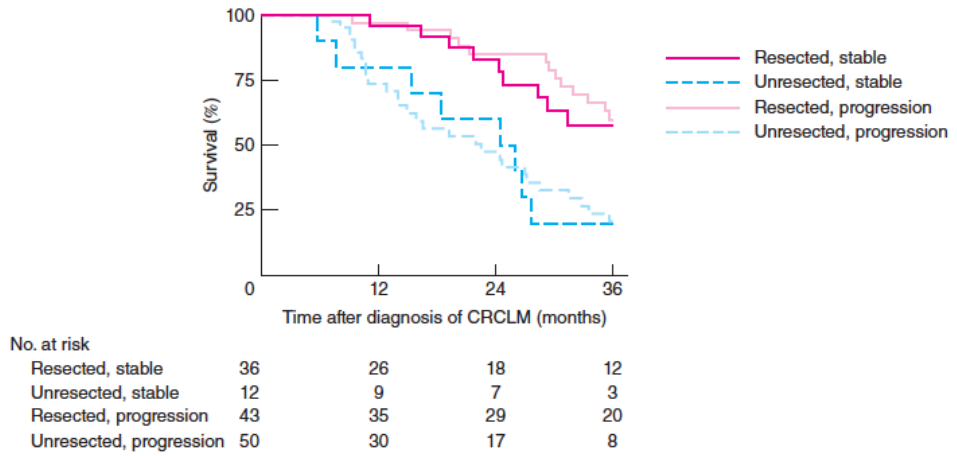

Fig. 3 Kaplan–Meier survival curves for patients with stable disease or progression after portal vein embolization, who did or did not have tumour resection. CRCLM, colorectal cancer liver metastasis. $P < 0{\cdot}001$ (log rank test)

Table 3 Baseline clinical characteristics of patients who had resected colorectal cancer liver metastasis with or without preoperative portal vein embolization

	Resected with PVE ($n = 79$)	Resected without PVE ($n = 60$)	P§
Age (years)*	58(11)	59(10)	0·477¶
Sex ratio (M : F)	57 : 22	37 : 23	0·205
Disease characteristics			
Total tumour volume (cm^3)†	14·3 (4·3–41·1)	13·8 (8·4–43·3)	0·300#
Synchronous	65 (82)	37 (62)	0·011
No. of lesions†	4 (3–7)	2 (1–3)	< 0·001#
Neoadjuvant chemotherapy	76 (96)	44 (73)	< 0·001
No. of cycles†	6 (6–7)	6 (5–7)	0·835#
Resection margin‡			0·167
R0–R1	53 (78)	50 (88)	
R2	15 (22)	7 (12)	

Values in parentheses are percentages unless indicated otherwise; values are *mean(s.d.) and †median (i.q.r.). ‡Based on available pathological specimens: 68 in portal vein embolization (PVE) group and 57 in no-PVE group). §χ^2 test, except ¶t test and #Mann–Whitney U test.

Vienna, Austria) as well as GraphPad Prism® version 6.0 (GraphPad Software, San Diego, California, USA).

Results

A total of 141 patients were included in the study (*Fig. 1*). Hepatic metastatic progression was present at PVE in 93 patients (66·0 per cent), whereas 48 patients (34·0 per cent) had no tumour progression; overall changes in TTV were +90·8 (29·0 to 235·2) and −12·9 (−31·8 to 1·3) per cent respectively ($P < 0{\cdot}001$). Seventeen patients (12·1 per cent) developed new contralateral lesions after PVE. Baseline clinical characteristics according to disease outcome after PVE are outlined in *Tables 1* and *2*. Patients with and without tumour progression were similar for most baseline characteristics, except for significant differences in the presence of bilateral lesions on presentation, response to neoadjuvant chemotherapy group assessed by RECIST, and interval between the end of neoadjuvant chemotherapy and PVE. Of note, most patients (80·2 per cent) who had PVE had disease control on neoadjuvant chemotherapy (34·9 per cent partial response, 45·2 per cent stable disease), contrasting with 66·0 per cent of the cohort who exhibited progression after embolization.

Patients with disease progression after PVE were more likely to have unresectable disease than those not exhibiting tumour growth: 50 (54 per cent) of 93 *versus* 12 (25 per cent) of 48 (*Fig. 2*). In the progression group, the reason for unresectability was tumour growth in all patients except one who refused the surgery after embolization. The reason for unresectability in the group with stable disease after PVE was failure to achieve an adequate FLR (23·3 (21·8–28·5) per cent FLR) and degree of hypertrophy (6·22 (0·78–8·78)) after PVE.

Liver hypertrophy and atrophy

Among those with disease progression after PVE, all 43 patients who underwent resection achieved an adequate FLR (31·3 (26·3–36·6) per cent FLR) and degree of hypertrophy (9·20 (5·24–13·12)). Of the 50 patients with disease progression after PVE who did not undergo resection, 14 (28 per cent) failed to achieve an adequate FLR in addition to having disease progression; the FLR in these patients

© 2015 BJS Society Ltd
Published by John Wiley & Sons Ltd

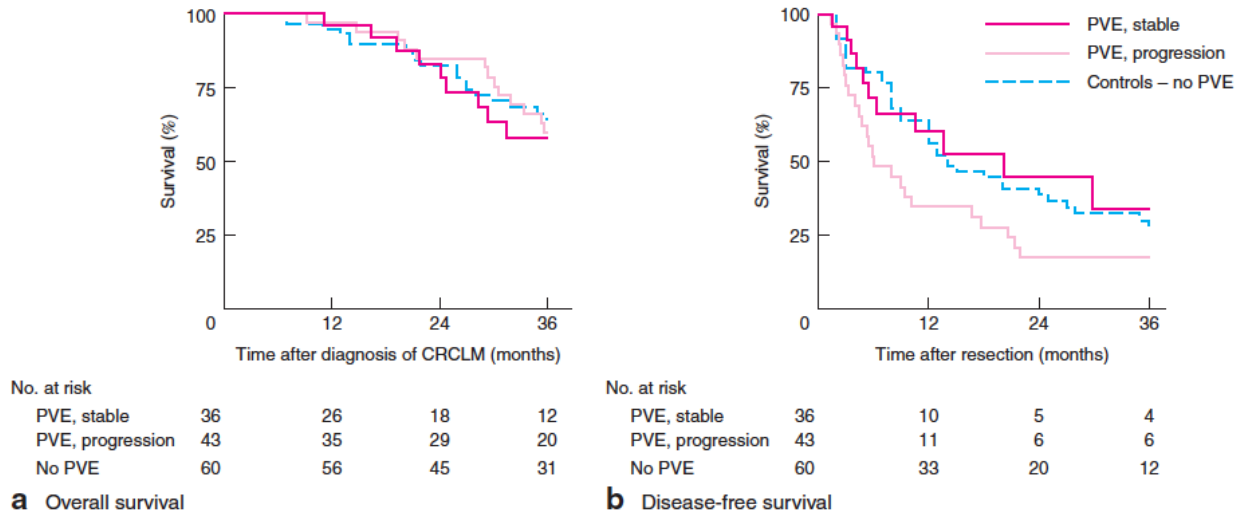

Fig. 4 Kaplan–Meier **a** overall and **b** disease-free survival curves for patients with resected tumours who had stable disease or progression after portal vein embolization (PVE), or did not undergo PVE. CRCLM, colorectal cancer liver metastasis. **b** $P = 0{\cdot}045$; stable disease *versus* progression after PVE; $P = 0{\cdot}015$, progression after PVE *versus* no PVE (log rank test)

was similar to that of the patients with disease progression who had tumour resection (27·6 (21·7–35·4) *versus* 31·3 (26·3 to 36·6) per cent FLR; $P = 0{\cdot}094$). Overall, the proportion of patients with progression and stable disease who achieved adequate hypertrophy was similar, although there was a trend towards more patients achieving an adequate FLR (over 25 per cent) in the progression group: 79 (85 per cent) of 93 *versus* 36 (75 per cent) of 48 respectively ($P = 0{\cdot}172$).

The TLVs in the progression and stable disease groups were similar, both before PVE (1613 (1382–1888) *versus* 1716 (1048–2006) cm^3 respectively; $P = 0{\cdot}548$) and after (1647 (1412–2110) *versus* 1712 (1420–2473) cm^3 respectively; $P = 0{\cdot}854$) embolization. Regarding the embolized lobe specifically, the median volume of embolized liver was also similar between the groups with progression and stable disease, both before (1279 (1061–1510) *versus* 1354 (990–1593) cm^3; $P = 0{\cdot}674$) and after (1151 (918–1488) *versus* 1197 (979–1403) cm^3; $P = 0{\cdot}972$) PVE. On examination of the difference in embolized liver volumes to evaluate the atrophy of the embolized lobe, there was no difference between the progression and stable disease groups: −65·8 (−198·4 to 57·0) and −128·0 (−215·0 to 44·1) cm^3 respectively ($P = 0{\cdot}307$).

Overall survival

Irrespective of resectability status, the 93 patients with tumour progression after embolization had similar overall survival to the 48 patients with stable disease (32·1 *versus* 31·5 months respectively; $P = 0{\cdot}395$). The groups were further divided based on whether tumours were resected or not following PVE, creating four subgroups: unresected with (50) and without (12) tumour growth after PVE, and resected with (43) and without (36) tumour growth after PVE. There was a significant difference in median survival for patients who did and those who did not undergo resection (52·2 *versus* 24·5 months respectively; $P < 0{\cdot}001$), but no difference based on tumour growth after PVE: median survival 22·5 *versus* 26·0 months for patients with and those without tumour growth after PVE who had unresectable disease ($P = 0{\cdot}706$), and 46·2 *versus* 52·2 months respectively for patients who had tumour resection ($P = 0{\cdot}953$) (*Fig. 3*).

Overall survival among 79 patients who had tumour resection after PVE was compared with that in a control group of 60 patients who had resection of CRCLM without PVE, matched by age and TTV (*Table 3*). The control group had a median survival of 50·0 months, similar that of patients with resectable disease who showed disease progression after PVE ($P = 0{\cdot}569$) (*Fig. 4a*).

Disease-free survival

Among patients who underwent resection, the 43 patients who exhibited tumour progression after PVE had worse disease-free survival than the 36 patients who had stable disease after PVE (median 6·0 *versus* 20·2 months respectively; $P = 0{\cdot}045$). The 60 patients who had resection without PVE had a median disease-free survival of

© 2015 BJS Society Ltd
Published by John Wiley & Sons Ltd

Table 4 Univariable and multivariable logistic regression analyses of variables associated with tumour progression after portal vein embolization

	Univariable analysis		Multivariable analysis	
	Crude risk ratio	*P*	Adjusted risk ratio	*P*
Site of primary tumour				
Colon	1·27 (0·93, 1·73)	0·114	–	–
Rectum	1·00 (reference)			
Bilateral lesions	0·77 (0·59, 0·99)	0·049	0·51 (0·18, 1·38)	0·103
Response to chemotherapy*				
Disease progression	1·00 (reference)		1·00 (reference)	
Stable disease	0·69 (0·56, 0·85)	0·004	0·12 (0·01, 0·72)	0·041
Partial response	0·45 (0·31, 0·63)	< 0·001	0·05 (0·00, 0·32)	0·023
Interval between chemotherapy and PVE (days)	1·01 (1·00, 1·02)	0·039	1·01 (1·00, 1·02)	0·234
Two-stage PVE	1·21 (0·96, 1·53)	0·138	–	–

Values in parentheses are 95 per cent c.i. *According to Response Evaluation Criteria in Solid Tumours. PVE, portal vein embolization.

14·0 months, similar to that of the patients with stable disease after PVE ($P = 0·759$) but significantly greater than that in the disease progression group ($P = 0·015$) (*Fig. 4b*). The pattern of recurrence was similar, however; the most common site of recurrence was intrahepatic (19 of 29 and 9 of 11 patients with and without tumour growth) followed by the lungs (7 of 29 and 2 of 11 respectively).

Predictors of tumour progression after portal vein embolization

Univariable analysis showed that progression of hepatic metastasis after PVE was 23 per cent less likely in patients with bilateral lesions (*Table 4*). Patients showing a partial response and stable disease on neoadjuvant chemotherapy were 55 per cent ($P < 0·001$) and 31 per cent ($P = 0·004$) less likely to have tumour progression after PVE respectively compared with those who had disease progression. An increase of 1 day between chemotherapy and PVE increased the risk of post-PVE tumour progression by 1 per cent ($P = 0·039$) (*Table 4*). All patients except one who were categorized as having progressive disease on chemotherapy had tumour progression after embolization. On multivariable analysis adjusting for bilateral lesions and time interval between end of chemotherapy and PVE, only stable disease or partial response to chemotherapy was significantly associated with a lower risk of tumour progression after PVE (*Table 4*).

Discussion

This study evaluated the impact of tumour progression following PVE on overall and disease-free survival. The results suggest that resectability is a more important determinant of overall survival than disease progression after PVE. Among patients who had liver resection, overall survival was similar between those who had PVE (with or without disease progression) and controls without PVE, as reported in other studies[3,8,9,11]. However, disease-free survival was reduced in patients with tumour progression after PVE. Although it is well established that hepatic resection for CRCLM confers the best long-term outcomes[31–33], tumour progression before a planned resection remains a controversial point to consider in terms of outcomes. A landmark study by Adam and colleagues[34] reported significant differences in overall and disease-free survival after resection for patients with disease progression on neoadjuvant chemotherapy compared with those without progression, suggesting that tumour control before surgery may actually be crucial in order to benefit from surgical resection, although this has been challenged by other investigators[35]. Nevertheless, such results may not be directly applicable to patients undergoing PVE. As the majority of the present patients had their disease under control before embolization (80·2 per cent with stable disease or partial response based on RECIST), the authors believe that progression after PVE in a patient who previously had tumour control on neoadjuvant chemotherapy represents a different scenario from disease progression on neoadjuvant chemotherapy.

The present results also indicate that the only factor associated with a likelihood of progression after PVE is response to neoadjuvant chemotherapy. Similarly, Pommier and co-workers[36] also reported an association between response to neoadjuvant chemotherapy and tumour progression after PVE, although the patients were classified into two response groups based on the number of chemotherapy cycles received. Response to chemotherapy was measured using the RECIST classification in the present study and the findings further highlight the importance of tumour control on neoadjuvant chemotherapy

© 2015 BJS Society Ltd
Published by John Wiley & Sons Ltd

in this context, as well as an important role of tumour biology.

The data also demonstrate that liver tumours are more likely to be unresectable in patients with disease progression after PVE. The rate of unresectable disease after PVE of 44·0 per cent approaches previously reported failure rates, which range between 33 and 40 per cent[3,9,37]. Therefore, considering that PVE is offered to patients whose liver disease would otherwise remain unresectable, preoperative PVE for patients with CRCLM with a small FLR is still recommended, in order to facilitate resection. In that perspective, the present results also demonstrated that patients with postembolization tumour growth whose tumours were not resectable had a median survival (22·5 months) comparable to that for patients with unresectable CRCLM on chemotherapy alone[38–40]. This supports the view that PVE (when indicated) should still be offered to patients before resection, as it is unlikely to result in shorter overall survival than treatment with chemotherapy alone. The present survival data were calculated from the date of diagnosis of liver metastasis, allowing comparison with survival data reported in large series of unresectable CRCLM treated with chemotherapy only.

Despite the number of patients included, this study has several limitations, such as its retrospective nature and the fact that the data represent a single-institution experience. Despite this, the results underline the need for further research to identify and target higher-risk patients, such as those with a borderline chemotherapy response. Ultimately, this may lead to the development of treatment algorithms that would reduce the failure rate of surgery.

The benefit of surgery is clear in terms of overall survival; whether patients have tumour growth or not after PVE does not seem to affect this. Therefore, the decision to operate should not be influenced by the presence of disease progression after PVE, as long as the liver remnant allows safe hepatic resection. The only pitfall is that such patients may harbour slightly more aggressive disease, which translates into early recurrence based on the present findings. Such patients may benefit from a tailored approach, especially in the adjuvant setting. However, preventing tumour progression may have the greatest impact on achieving resectability and therefore provide the best possible outcome for patients. Prospective studies integrating clinical and possibly molecular or genetic markers are needed to stratify better patients with CRCLM, identify those who may be at risk of tumour growth in this context, and attempt treatment strategies that would impede tumour growth after PVE.

Acknowledgements

The authors thank the Radiology Department at McGill University Health Centre for support in providing access to the three-dimensional volume calculation software, and A. Salman for assistance with the ethics approval.
Disclosure: The authors declare no conflict of interest.

References

1 Elias D, Debaere T, Roche A, Bonvallot S, Lasser P. Preoperative selective portal vein embolizations are an effective means of extending the indications of major hepatectomy in the normal and injured liver. *Hepatogastroenterology* 1998; **45**: 170–177.
2 Ribero D, Abdalla EK, Madoff DC, Donadon M, Loyer EM, Vauthey J-N. Portal vein embolization before major hepatectomy and its effects on regeneration, resectability and outcome. *Br J Surg* 2007; **94**: 1386–1394.
3 Azoulay D, Castaing D, Smail A, Adam R, Cailliez V, Laurent A *et al*. Resection of nonresectable liver metastases from colorectal cancer after percutaneous portal vein embolization. *Ann Surg* 2000; **231**: 480–486.
4 Abdalla EK, Adam R, Bilchik AJ, Jaeck D, Vauthey J-N, Mahvi D. Improving resectability of hepatic colorectal metastases: expert consensus statement. *Ann Surg Oncol* 2006; **13**: 1271–1280.
5 Shindoh J, Tzeng CW, Aloia TA, Curley SA, Zimmitti G, Wei SH *et al*. Portal vein embolization improves rate of resection of extensive colorectal liver metastases without worsening survival. *Br J Surg* 2013; **100**: 1777–1783.
6 Abulkhir A, Limongelli P, Healey AJ, Damrah O, Tait P, Jackson J *et al*. Preoperative portal vein embolization for major liver resection. *Ann Surg* 2008; **247**: 49–57.
7 Farges O, Belghiti J, Kianmanesh R, Regimbeau JM, Santoro R, Vilgrain V *et al*. Portal vein embolization before right hepatectomy: prospective clinical trial. *Ann Surg* 2003; **237**: 208–217.
8 Ardito F, Vellone M, Barbaro B, Grande G, Clemente G, Giovannini I *et al*. Right and extended-right hepatectomies for unilobar colorectal metastases: impact of portal vein embolization on long-term outcome and liver recurrence. *Surgery* 2013; **153**: 801–810.
9 Mueller L, Hillert C, Möller L, Krupski-Berdien G, Rogiers X, Broering DC. Major hepatectomy for colorectal metastases: is preoperative portal occlusion an oncological risk factor? *Ann Surg Oncol* 2008; **15**: 1908–1917.
10 Kokudo N, Tada K, Seki M, Ohta H, Azekura K, Ueno M *et al*. Proliferative activity of intrahepatic colorectal metastases after preoperative hemihepatic portal vein embolization. *Hepatology* 2001; **34**: 267–272.
11 Oussoultzoglou E, Bachellier P, Rosso E, Scurtu R, Lucescu I, Greget M *et al*. Right portal vein embolization before right hepatectomy for unilobar colorectal liver metastases reduces the intrahepatic recurrence rate. *Ann Surg* 2006; **244**: 71–79.

© 2015 BJS Society Ltd
Published by John Wiley & Sons Ltd

12 Abdalla EK. Portal vein embolization (prior to major hepatectomy) effects on regeneration, resectability, and outcome. *J Surg Oncol* 2010; **102**: 960–967.
13 Hemming AW, Reed AI, Howard RJ, Fujita S, Hochwald SN, Caridi JG *et al*. Preoperative portal vein embolization for extended hepatectomy. *Ann Surg* 2003; **237**: 686–691.
14 Elias D, De Baere T, Roche A, Ducreux M, Leclere J, Lasser P. During liver regeneration following right portal embolization the growth rate of liver metastases is more rapid than that of the liver parenchyma. *Br J Surg* 1999; **86**: 784–788.
15 Barbaro B, Di Stasi C, Nuzzo G, Vellone M, Giuliante F, Marano P. Preoperative right portal vein embolization in patients with metastatic liver disease. Metastatic liver volumes after RPVE. *Acta Radiol* 2003; **44**: 98–102.
16 Simoneau E, Aljiffry M, Salman A, Abualhassan N, Cabrera T, Valenti D *et al*. Portal vein embolization stimulates tumour growth in patients with colorectal cancer liver metastases. *HPB (Oxford)* 2012; **14**: 461–468.
17 Hoekstra LT, van Lienden KP, Doets A, Busch ORC, Gouma DJ, van Gulik TM. Tumor progression after preoperative portal vein embolization. *Ann Surg* 2012; **256**: 812–187.
18 de Graaf W, van den Esschert JW, van Lienden KP, van Gulik TM. Induction of tumor growth after preoperative portal vein embolization: is it a real problem? *Ann Surg Oncol* 2009; **16**: 423–430.
19 Treska V, Skalicky T, Liska V, Sutnar A, Ferda J, Mirka H *et al*. Prognostic value of the number and volume of liver tumours on portal vein embolization outcomes. *Hepatogastroenterology* 2012; **59**: 448–452.
20 Pamecha V, Levene A, Grillo F, Woodward N, Dhillon A, Davidson BR. Effect of portal vein embolisation on the growth rate of colorectal liver metastases. *Br J Cancer* 2009; **100**: 617–622.
21 Eisenhauer EA, Therasse P, Bogaerts J, Schwartz LH, Sargent D, Ford R *et al*. New response evaluation criteria in solid tumours: revised RECIST guideline (version 1.1). *Eur J Cancer* 2009; **45**: 228–247.
22 Folprecht G, Gruenberger T, Bechstein WO, Raab H-R, Lordick F, Hartmann JT *et al*. Tumour response and secondary resectability of colorectal liver metastases following neoadjuvant chemotherapy with cetuximab: the CELIM randomised phase 2 trial. *Lancet Oncol* 2010; **11**: 38–47.
23 O'Reilly DA, Chaudhari M, Ballal M, Ghaneh P, Wu A, Poston GJ. The Oncosurge strategy for the management of colorectal liver metastases – an external validation study. *Eur J Surg Oncol* 2008; **34**: 538–540.
24 Beal IK, Anthony S, Papadopoulou A, Hutchins R, Fusai G, Begent R *et al*. Portal vein embolisation prior to hepatic resection for colorectal liver metastases and the effects of periprocedure chemotherapy. *Br J Radiol* 2006; **79**: 473–478.
25 Sturesson C, Keussen I, Tranberg KG. Prolonged chemotherapy impairs liver regeneration after portal vein occlusion – an audit of 26 patients. *Eur J Surg Oncol* 2010; **36**: 358–364.
26 Reddy SK, Morse MA, Hurwitz HI, Bendell JC. Addition of bevacizumab to irinotecan- and oxaliplatin-based preoperative chemotherapy regimens does not increase morbidity after resection of colorectal liver metastases. *J Am Coll Surg* 2008; **206**: 96–106.
27 Kesmodel SB, Ellis LM, Lin E, Chang GJ, Abdalla EK, Kopetz S *et al*. Preoperative bevacizumab does not significantly increase postoperative complication rates in patients undergoing hepatic surgery for colorectal cancer liver metastases. *J Clin Oncol* 2008; **26**: 5254–5260.
28 Nordlinger B, Sorbye H, Glimelius B, Poston GJ, Schlag PM, Rougier P *et al*. Perioperative FOLFOX4 chemotherapy and surgery *versus* surgery alone for resectable liver metastases from colorectal cancer (EORTC 40983): long-term results of a randomised, controlled, phase 3 trial. *Lancet Oncol* 2013; **14**: 1208–1215.
29 Ak G, Metintas M, Metintas S, Yildirim H, Ozkan R, Ozden H. Three-dimensional evaluation of chemotherapy response in malignant pleural mesothelioma. *Eur J Radiol* 2010; **74**: 130–135.
30 Jeon D-G, Kong C-B, Cho WH, Song WS, Cho SH, Choi SW *et al*. Examination of the cutoff value of postchemotherapy increase in tumor volume as a predictor of subsequent oncologic events in stage IIB osteosarcoma. *J Surg Oncol* 2014; **109**: 275–279.
31 Fernandez FG, Drebin JA, Linehan DC, Dehdashti F, Siegel BA, Strasberg SM. Five-year survival after resection of hepatic metastases from colorectal cancer in patients screened by positron emission tomography with F-18 fluorodeoxyglucose (FDG-PET). *Ann Surg* 2004; **240**: 438–447.
32 Abdalla EK, Vauthey J-N, Ellis LM, Ellis V, Pollock R, Broglio KR *et al*. Recurrence and outcomes following hepatic resection, radiofrequency ablation, and combined resection/ablation for colorectal liver metastases. *Ann Surg* 2004; **239**: 818–825.
33 Scheele J, Stangl R, Altendorf-Hofmann A. Hepatic metastases from colorectal carcinoma: impact of surgical resection on the natural history. *Br J Surg* 1990; **77**: 1241–1246.
34 Adam R, Pascal G, Castaing D, Azoulay D, Delvart V, Paule B *et al*. Tumor progression while on chemotherapy: a contraindication to liver resection for multiple colorectal metastases? *Ann Surg* 2004; **240**: 1052–1061.
35 Neumann UP, Thelen A, Röcken C, Seehofer D, Bahra M, Riess H *et al*. Nonresponse to pre-operative chemotherapy does not preclude long-term survival after liver resection in patients with colorectal liver metastases. *Surgery* 2009; **146**: 52–59.
36 Pommier R, Ronot M, Cauchy F, Gaujoux S, Fuks D, Faivre S *et al*. Colorectal liver metastases growth in the embolized and non-embolized liver after portal vein embolization: influence of initial response to induction chemotherapy. *Ann Surg Oncol* 2014; **21**: 3077–3083.

© 2015 BJS Society Ltd
Published by John Wiley & Sons Ltd

37 Pamecha V, Glantzounis G, Davies N, Fusai G, Sharma D, Davidson B. Long-term survival and disease recurrence following portal vein embolisation prior to major hepatectomy for colorectal metastases. *Ann Surg Oncol* 2009; **16**: 1202–1207.
38 Hochster HS, Hart LL, Ramanathan RK, Childs BH, Hainsworth JD, Cohn AL *et al*. Safety and efficacy of oxaliplatin and fluoropyrimidine regimens with or without bevacizumab as first-line treatment of metastatic colorectal cancer: results of the TREE Study. *J Clin Oncol* 2008; **26**: 3523–3529.
39 Saltz LB, Clarke S, Díaz-Rubio E, Scheithauer W, Figer A, Wong R *et al*. Bevacizumab in combination with oxaliplatin-based chemotherapy as first-line therapy in metastatic colorectal cancer: a randomized phase III study. *J Clin Oncol* 2008; **26**: 2013–2019.
40 Fuchs CS, Marshall J, Mitchell E, Wierzbicki R, Ganju V, Jeffery M *et al*. Randomized, controlled trial of irinotecan plus infusional, bolus, or oral fluoropyrimidines in first-line treatment of metastatic colorectal cancer: results from the BICC-C Study. *J Clin Oncol* 2007; **25**: 4779–4786.

XIV. Transition to manuscript III

Tumor progression after PVE has been investigated in many experimental studies involving animal models. Evidence suggests different mechanisms of tumor progression during liver regeneration: portal vein occlusion seems to be dependent on hepatic arterial redistribution in the occluded lobe whereas partial hepatectomy may be relying on extracellular matrix remodeling(170). Results from these studies suggest that many important cytokines and growth factors are released during the liver regeneration process(26,94), many of which are known to be pro-tumorigenic(171-173). Moreover, it was suggested that portal occlusion may promote cancer progression through increased angiogenesis, as a consequence from an initial hypoxic environment(174). Most of these studies in fact describe extracellular factors potentially involved in this complex process, but the data is sparse regarding intracellular pathways involved in cancer progression following portal occlusion.

Despite the evidence derived from small patient series showing that portal vein occlusion promotes tumor progression and proliferation, there is no data from clinical studies about the molecular networks and potential mechanisms involved in this process. Moreover, experimental studies do not reflect the clinical scenario where patients exhibit tumor progression after receiving neoadjuvant chemotherapy, which may result in different activated pathways. To understand the molecular networks involved in colorectal liver metastasis progression after portal vein embolization, we conducted a prospective study where metastatic tumor tissue was obtained prior to and following portal vein embolization and compared in a paired analysis using high throughput technology. In this study we aimed to evaluate the transcriptional changes in tumors of patients exhibiting tumor growth by gene expression profiling using RNA Seq.

XV. Thesis Manuscript III

For submission

Next generation sequencing of progressive colorectal liver metastases after portal vein embolization

Eve Simoneau[1], Jarred Chicoine[2], Sarita Negi[1], Ayat Salman[1], Anthoula Lazaris[1,3], Mazen Hassanain,[4,5] Nicole Beauchemin,[2,5,6,7] Stephanie Petrillo,[1] David Valenti,[8] Ramila Amre,[9] Peter Metrakos[1,3,9]

[1]Department of Surgery, McGill University Health Center, Montreal, Canada; [2]Department of Medicine, McGill University, Montreal, Canada; [3]McGill University Health Center Research Institute, Montreal, Canada; [4]Department of Surgery, King Saud University, Riyadh, Saudi Arabia; [5]Department of Oncology, McGill University, Montreal, Canada; [6]Goodman Cancer Center, Montreal, Canada, [7]Department of Biochemistry, McGill University, Montreal, Canada; [8]Department of Radiology, McGill University Health Center, Montreal, Canada; [9]Department of Pathology, McGill University Health Center, Montreal, Canada

Corresponding author:

Dr. Peter Metrakos, MD, CM, FRCSC
Department of Surgery, Royal Victoria Hospital, McGill University Health Center
1001 Decarie Boulevard
Montreal (Quebec), Canada
H4A 3J1
Fax: (514) 843-1503
Tel: (514) 934-1934 ext 34042
E-mail: peter.metrakos@mcgill.ca

Running title: RNA Seq of colorectal cancer liver metastasis

List of abbreviations :

CRCLM : colorectal cancer liver metastasis
PVE : portal vein embolization
RNA : ribonucleic acid
FLR : future liver remnant
RIN : RNA intergrity score
CT : computed tomography
TLV : total liver volume
TV : tumor volume
TTV : total tumor volume
PD_{PVE}: progression of disease post-PVE
SD_{PVE}: stable disease post-PVE
RECIST: Response Evaluation Criteria In Solid Tumors
CR: complete response
PR: partial response
PD: progression of disease
SD: stable disease
DEG: differentially expressed genes
qRT-PCR: quantitative reverse transcription polymerase chain reaction
rRNA: ribosomal ribonucleic acid
FDR: false discovery rate

Financial support:

E.S. was supported by a salary grant from FRQS (*Fonds de Recherche du Québec en Santé*) and by the CIHR (*Canadian Institute of Health and Research*)/FRSQ training grant in cancer research FRN 53888 of the McGill Integrated Cancer Research Training Program.

Abstract

Background and Aims: Portal vein embolization (PVE) can be required to stimulate liver regeneration before hepatectomy for colorectal liver metastasis (CRCLM), however, PVE may also trigger CRCLM progression in patients initially exhibiting chemotherapy response. Using RNA-seq, we aimed to determine the molecular networks involved in metastatic progression in this context. Methods: A prospective study including all CRCLM patients undergoing PVE prior to hepatectomy was conducted. Paired biopsies of metastatic lesions were obtained prior to and after PVE and total RNA was isolated and used to prepare Illumina rRNA-depleted TruSeq stranded cDNA libraries for HiSeq 100bp paired-end sequencing. Patients were classified with progression of disease (PD_{PVE}) or stable disease (SD_{PVE}) post-PVE using 3D-CT tumor volumetric analysis. Results: Twenty patients were included, 13 (65.0%) in the PD_{PVE} group (median 58.0 % (18.6-234.3) increase in tumor volume) and 7 (35.0%) in the SD_{PVE} group exhibiting continuous chemotherapy response (median -14.3 % (-40.8- -2.8) decrease in tumor volume) ($p<0.0001$). Our results showed that progressive CRCLM after PVE undergo gene expression changes that indicate activation of core cancer pathways (IL-17 ($p=5.94 \times 10^{-03}$), PI3K ($p=8.71 \times 10^{-03}$), IL6 and IGF-1 signaling pathways), consistent with changes driven by cytokines and growth factors.. Differential expression analysis in a paired model of progression (EdgeR, DeSeq) identified significantly dysregulated genes in the PD_{PVE} group (FOS, FOSB, RAB20, IRS2). Conclusion: Differentially expressed genes and pathways with known links to cancer and metastasis were identified post-PVE in patients with disease progression. Highlighting these molecular changes is a crucial first step towards development of targeted therapeutic strategies that may mitigate the effects of PVE on tumor growth.

Keywords: Colon cancer hepatic metastasis; tumor growth; liver regeneration; RNA-Sequencing; expression analysis

INTRODUCTION

Colorectal cancer is the third most common cancer in North America and is the third leading cause of cancer-related death(Siegel et al., 2013). Approximately 50% of patients will be diagnosed with colorectal cancer liver metastasis (CRCLM) during the course of their disease. Untreated, patients with CRCLM will typically survive for a few months (Scheele et al., 1990) whereas modern chemotherapy can extend median survival to 20-24 months(Hurwitz et al., 2004; Hochster et al., 2008; Saltz et al., 2008.) Liver resection is increasingly offering eligible patients an improved survival and even a potential cure. The long-term benefit of surgery, combined with modern chemotherapy regimens, is now irrefutable as shown in multiple large series reporting 5-year survival of 32-58% (Fernandez et al., 2004; Simmonds et al., 2006).

For patients exhibiting greater overall disease burden and/or maldistribution of lesions, strategies have been developed to convert some of these patients to a resectable state. Conversion can be accomplished by downsizing tumor burden with neo-adjuvant chemotherapy, by a staged resection strategy (which requires two or more consecutive liver resections), and by preoperative portal vein embolization (PVE) to increase the size of a small future liver remnant (which is the predicted amount of liver left after surgery). By embolizing the portal venous flow supplying the side of the liver that is to be resected, the contralateral side of the liver undergoes hypertrophy, thus allowing for an adequately sized future liver remnant. In large series of patients reported by several centers, PVE has thus been shown to be a safe and effective method to stimulate liver hypertrophy, generating an adequate future liver remnant (FLR) and allowing more patients to be resected (Madoff et al., 2005; Abulkhir et al., 2008). However, multiple reports have shown that PVE can also stimulate tumor growth as the liver is regenerating(Elias et al., 1999; Kokudo et al., 2001; Barbaro et al., 2003; Pamecha et al., 2009; Simoneau et al., 2012). These reports found

that patients undergoing PVE can have significant disease progression with increasing tumor volume and development of new lesions. This phenomenon seems to occur in 30-80% of the patients undergoing preoperative embolization, depending on the study(Mueller et al., 2008; Hoekstra et al., 2012; Simoneau et al., 2012). Moreover, the majority of patients who undergo portal vein embolization receive neoadjuvant chemotherapy with adequate radiological response(Adam et al., 2004; Nordlinger et al., 2013). Tumor progression after PVE thus reflects a reversion to a proliferative state that had been halted by neoadjuvant chemotherapy, since initially responding patients subsequently develop disease progression. The objective of the current study was to perform RNA sequencing to identify pathways and genes that may be activated in metastatic tumors that progress after stimulus from portal vein embolization.

METHODS

Patient population and procedures

Informed consent was obtained from every patient before enrollment into this study and the protocol conformed to the ethical guidelines of the 1975 Declaration of Helsinki as reflected by its approval by the Royal Victoria Hospital institutional review board (protocol number GEN 11-140). All patients had a diagnosis of CRCLM with no extra-hepatic disease other than resectable lung metastasis and were considered good candidates for liver resection except for an inadequate FLR, and thus required a preoperative portal vein embolization (see Supplementary Tables 1 for further details on the patient cohort). Decision to undergo portal vein embolization was made by the treating team and based on tumor board recommendations prior to a planned trisegmentectomy (major liver resection) or staged liver resection (more than one consecutive hepatectomy required). The indication for PVE

was because of a small predicted future liver remnant (<25%). (Abdalla, 2010) The procedure was performed by infusion of histoacryl glue to occlude all segmental portal branches of the lobe to be resected, in order to induce hypertrophy of the contralateral (non-embolized) lobe (*i.e*. liver remnant) in preparation for the surgery.

Tissue collection

Paired biopsies from the metastatic lesions were procured prior to and following the embolization (time of tumor progression). The pre-PVE biopsy was performed under ultra-sound guidance and with a 16 gauge-needle biopsy just prior to the PVE, on the side of the liver to be embolized. The post-PVE biopsy was obtained 8 weeks later at the time of surgical resection with a core-biospy needle from the same metastatic lesion. All metastatic lesions, including newly developed lesions, were also biopsied intraoperatively. All biospies were specifically taken from tumor-rich areas and were carefully dissected macroscopically to obtain metastatic tumor tissue only. Samples were then immediately snap-frozen in liquid-nitrogen and kept at -80C until RNA extraction. Samples selected for next generation sequencing had RIN scores >6.0 (Supplementary Table 4).

Volumetric analysis and chemotherapy response

Tri-phasic computed tomography (CT) scans were done for all patients, prior to and 3 weeks following the PVE. These CT scans were used for volumetric analysis to obtain the following measurements: total liver volume (TLV), pre- and post-future liver remnant (FLR), pre- and post-tumor volumes (TV) in embolized and non-embolized liver lobes and total tumor volume (TTV). The assessment was performed with the portal phase of thin-sliced helical CT scans and volumes were expressed in cm^3. Volumetric data was obtained using GE Medical Systems Advantage Windows 4.3 workstations with dedicated three-dimensional volume calculation software (GE Healthcare, Chalfont St Giles, UK). The

evaluator was blinded to the clinical information and the sequencing data of the patients. For the purpose of this study, patients were considered to have disease progression post-PVE (PD_{PVE}) if they had a radiological increase of TTV by at least 15% (Ak et al., 2010; Jeon et al., 2014) and/or if new metastatic lesions appeared post-PVE, or stable disease post PVE (SD_{PVE}) if <15% increase or a decrease in TTV was noted on imaging. Chemotherapy response prior to PVE was assessed by RECIST criteria. (Eisenhauer et al., 2009) Briefly, a complete response (CR) denotes disappearance of all lesions, partial response (PR) is a ≥ 30% decrease in total diameter of the target lesion, progression of disease (PD) for a ≥ 20% increase in total diameter of the lesion and stable disease (SD) for anything in between PR and PD.

RNA-Seq library preparation, sequencing and data analysis

From 20 patients that were enrolled in the study, 12 paired samples from a subset of 6 patients (4 with disease progression (P4, P8, P9, P10) and 2 with stable disease (P2, P11), see Supplementary Table 5 for samples details) were initially included for the RNA Seq analysis, the remaining patients' samples were kept as a validation pool. After RNA quality control, the pre-PVE sample from patient 2 (P2-A) did not meet quality standards and this pair was therefore excluded from further analysis. Since only one pair was available for the stable disease group, the comparison of stable vs. progressive pairs was not statistically valid, we therefore elected to include only 8 paired samples (pairs from 4 patients with progression) in a paired model of progression, and to subsequently compare patients with stable disease using the validation cohort. The RNA Sequencing was done (HiSeq - Paired-ends 100bp sequencing lanes, Illumina) with the Illumina HiSeq 2000. For functional annotation and biological significance, the data was also analyzed with the Ingenuity pathway analysis (IPA) (Ingenuity pathways, Qiagen). Further methodology details regarding library preparation, sequencing and data analysis are provided in the

Supplement.

Validation of RNA-Seq results

Candidate differentially expressed genes (DEG) were selected for validation by quantitative real-time PCR (qRT-PCR). Independent tumor samples (n=14 samples, 6 pre- and 8 post-PVE) were procured and used as biological replicates. It is important to note that the validation cohort did not consist of paired samples since some patients in the study remained unresectable, and one patient (P5) did not have enough viable tissue in the pre-PVE biopsy. RNA was extracted (RNEasy minikit (Qiagen)), reverse transcribed (Superscript III reverse transcriptase, Invitrogen) and used for qRT-PCR (MyiQ2 real-time detection system (BioRad)). Primer sequences for selected genes and a housekeeping gene (HPRT1) were purchased (Qiagen) and PCR reactions were carried in duplicate as per protocol (SYBR green, Applied Bioscience) with cDNA from each sample (See Supplementary Table 6). Expression values were normalized to HPRT1 levels and fold changes were calculated from the average values in each patient category (pre- and post-PVE time points, unpaired samples) $2^{-\Delta\Delta Ct}$ (Livak) Method.

Immunohistochemistry

To compare patients with progression and stable disease post-PVE, tumor proliferation was assessed by immunohistochemistry. This was performed using a validation cohort of 22 post-PVE CRCLM samples as well as 21 controls resected without PVE. Ki-67 immunostaining was performed according to the manufacturer's recommendations, using the Mib-1 clone (1:300 dilution; 24-minute incubation; DAKO, Carpinteria, CA; and Ventana BenchMark LT Staining Platform; CC1 Standard Retrieval; iVIEW DAB Detection, Ventana Medical System Inc. Arizona, USA). A pathologist, blinded to the clinical information, scored the stained slides and attributed a percentage of Ki-67 positive tumor cells and when

available, two representative blocks per lesion were analyzed.

Statistical Analysis

For analyses not related to RNA-Seq raw data, normally distributed data were expressed as means ± standard deviations and non-normally distributed data as medians with interquartile ranges. Comparison of categorical data was done using the Chi-Square and Fisher's exact test as appropriate and the t-test or Mann-Whitney was used for continuous data. Statistical significance was considered when $p<0.05$. Statistical analyses were performed using JMP Version 8.0 (SAS Institute, Inc., Cary, NC, USA) and Graph Pad Prism version 6.0 (Graph Pad Software, San Diego, CA).

RESULTS

Patients and Volumetric Analysis

From 30 patients initially screened, 20 were included in the study as depicted in supplementary Figure 1. Baseline clinical characteristics are provided in Table 1. Four patients (20.0%) developed new metastatic lesions in the liver on follow-up scan and 3 of those had new lesions located on the contralateral (non-embolized) side (See Supplementary Table 1 for individual patients details). Thirteen (65.0%) patients had tumor progression while the remaining (n=7, 35.0%) had stable disease post-PVE. Patients with progression post-PVE had a median increase of 58.0 (18.6-234.3) % in total tumor volume as opposed to those with stable disease having a median decrease of -14.3 (-40.8- -2.8) % in tumor volume ($p<0.0001$). Overall, an adequate degree of hypertrophy was achieved after the PVE for most patients, reaching an FLR (%) of 31.70 (27.67-34.50) from a baseline of 21.33 (18.77-23.80) ($p<0.0001$) (Supplementary Tables 2 and 3).

RNA Sequencing and mapping

An average of 150 million raw reads per sample was obtained (ranging from 111.1 to 208.8 million) and an average of 91.8% genomic alignment was achieved (Supplementary Table 5 for details on samples statistics). The coverage of our samples was 63X on average (ranging between 36X and 78X with only one sample having the lowest coverage of 36X). Only 2.5% of our reads mapped to rRNA, suggesting an efficient filtering of ribosomal RNA. Over 30,000 unique transcripts were initially detected in each sample (unfiltered dataset). Multidimensional scaling plot and hierarchical clustering demonstrated differences between pre and post PVE samples and also for samples corresponding to PD_{PVE} and SD_{PVE} (Supplementary Figure 2) between the pre-PVE baseline samples. The Spearman correlation matrix demonstrated good correlation distance for each pair of samples, and the heat map of the most varying transcripts showed differences between samples with and without tumor progression (Supplementary Figure 3).

Differential gene expression data analysis and validation

The gene expression analysis focused on pairs with disease progression (count-based paired analysis (EdgeR, DeSeq)) and the resulting dataset (n=34,999 genes) was filtered by number of reads (≥ 4 reads for all samples), fold change (≥ 2.0) and false discovery rate (<0.1), resulting in 1345 differentially expressed genes (DEG) (available as a Supplementary Table 7). A larger proportion of downregulated genes were noted (1208 downregulated genes and 137 upregulated genes). Functional analysis of these 1345 differentially expressed genes revealed enrichment for top networks related to cancer, cellular development, cellular growth and proliferation, cell cycle and cell-cell signaling and interaction (score 32) (see Figure 1A), as well as metabolic disease and lipid metabolism (score 25 and 23). Enriched of several canonical pathways were also highlighted by the

analysis, such as IL-17 signaling pathway (p=5.94 x 10-03), PI3K signaling (p=8.71 x 10-03), and IL6 and IGF-1 signaling pathways (Figure 1B). A list of significant dysregulated genes related to these top networks is shown in Table 2. The top significantly enriched functions were protein synthesis ($p=1.90 \times 10^{-13}$), gene expression ($p=4.92 \times 10^{-13}$), cellular development ($p=1.07x10^{-05}$), cellular growth and proliferation ($p=1.07 \times 10^{-05}$) and cell cycle ($p=3.21 \times 10^{-05}$). These results show that genes involved in these networks are suggestive of metabolically active tumors and reflect active processes of cancer progression. Additionally, the analysis of this dataset revealed several predicted upstream regulators (Table 3) that are known to act as secreted mediators of liver regeneration (Taub, 2004; Fausto et al., 2006; Michalopoulos, 2007), which is the biological process activated by portal vein occlusion.(Lim et al., 2013) Again, these findings support the validity of our data by pointing to relevant upstream regulators that are specifically related to a liver regeneration environment and that are mediating downstream events indicative of active tumors. Five candidate genes (FOS, IRS2, RAB20, CC1 and IL8) significantly upregulated in the progressive paired samples were selected for biological validation based on functional annotations, FDR and fold change (Figure 2A). Quantitative real-time PCR determined that four of the five genes (FOS, IRS2, RAB20 and CC1) exhibited similar up-regulation profiles in an independent validation cohort of 14 samples (6 pre-PVE, 8 post-PVE; see figure 2B).

Tumor proliferation

A validation cohort of metastatic lesion consisting of post-PVE tumors (progressive (n=13) and non-progressive lesions (n=9)), as well as a set of controls (CRCLM without PVE (n=21)) was identified and used to test whether the proliferative index of metastases post-PVE were specific to those exhibiting disease progression as opposed to a result of the PVE. Significantly higher proliferative index was shown in post-PVE tumors demonstrating

disease progression, compared to post-PVE tumors that did not progress after the embolization. In fact, tumors post-PVE without progression did not differ from tumors exhibiting optimal chemotherapy response (Figure 3), supporting the hypothesis that altered expression of the pathways identified through RNA sequencing lead to increased tumor proliferation in CRCLM post portal vein embolization.

DISCUSSION

Tumor growth after portal vein embolization can affect the resectability rate, which may subsequently impair patients' outcomes. The peculiarity of tumors that progress after PVE is that they show reversal of chemotherapy response, since the majority of patients respond to the neoadjuvant chemotherapy prior to the portal vein embolization. This suggests that progressive metastases after PVE, which occur in 32-80% of cases (Mueller et al., 2008; Hoekstra et al., 2012; Simoneau et al., 2012) likely harbor different biological properties. This study used state-of-the art RNA sequencing technology to identify potential candidate genes that may alter CRCLM response after PVE stimulation. There is still a paucity of evidence on PVE-induced tumor growth and the molecular pathways involved. Most of the evidence has been derived from experimental studies attempting to replicate the PVE environment using animal models of portal vein occlusion or partial hepatectomy(De Jong et al., 1995; Picardo et al., 1998; Heinrich et al., 2006; Maggiori et al., 2011; Momiyama et al., 2012). The immediate events occurring within the embolized liver are still poorly understood, likely due to the technical challenges of performing the embolization in animal models. Overall, these studies seem to indicate that different mechanisms of tumor progression exist after hepatectomy than after portal venous occlusion(Lim et al., 2013). In fact, portal vein occlusion is thought to trigger arterial blood flow redistribution in the occluded liver (Richter et al., 2001; Yokoyama et al., 2006; Kollmar et al., 2007), further

feeding the liver metastases (Eveno et al., 2012), whereas partial hepatectomy causes remodeling of the extracellular matrix in the contralateral remnant liver(Lim et al., 2013). In addition, animal models do not account for a crucial component, which is a model of tumor progression after neoadjuvant chemotherapy response.

Through a prospective clinical cohort study allowing us to procure biopsies prior to surgery (outside of the standard of care) and combined with next generation sequencing, we report the first gene expression profiling of paired PVE tumor samples prior to and after the intervention. We identified and validated candidate genes involved in relevant molecular functions, and networks that seem to mediate metastatic progression in this context. FOS, FOSB and ATF3 are all part of the AP-1 (activator protein 1) transcription factor. The AP-1 transcription factor is a dimeric complex made of several protein families, notably FOS, JUN, MAF (musculoaponeurotic fibrosarcoma) and ATF (activating transcription factor) proteins. (Eferl and Wagner, 2003) The FOS proteins are known to be associated with angiogenesis and invasiveness, through regulation of the matrix metalloproteinases (MMPs) (Hu et al., 1994), although none of the MMPs were significantly dysregulated in our data. Additionally, there is evidence that FOS proteins are associated with more advanced (late-stage) tumors (Reichmann et al., 1992), and unlike JUN proteins; they also mediate epithelial-to-mesenchymal transition, a hallmark of metastasis. The transcription factor AP-1 is an important mediator downstream of the Ras-MAPK signaling pathway (Eferl and Wagner, 2003) and has several known downstream target genes modulating invasion and motility (Hennigan et al., 1994). Among them is a member of the protocadherin family (PCDHGC3), whose downregulation has been shown to mediate the invasiveness of FOS-transformed cells (McGarry et al., 2004). Accordingly in this current RNA-Seq analysis, three protocadherin members (PCDH18, PCDHB5 and PCDH9) were found to be significantly downregulated in the paired samples with progression, suggesting a role of this protocadherin superfamily in this process. In fact, protocadherin -9 and -18 were recently

proposed to act as tumor suppressors in pancreatic cancer (Jones et al., 2008) while others such as PCDH8 (not significantly dysregulated in our data) were implicated in breast cancer (Yu et al., 2008), although the potential involvement of these three protocadherins in colon cancer is novel to our knowledge. In addition, metastasis suppressor 1 (MTSS1) was significantly downregulated in the progressive tumors, in accordance with several previous studies reporting repression of MTSS1 in more aggressive and metastatic cancers(Lee et al., 2002; Liu et al., 2010; Dawson et al., 2012). AP-1 is rapidly induced by cytokines and growth factors, resulting in cell proliferation, survival and differentiation. (Angel and Karin, 1991) Most importantly, several of these growth factors and cytokines, which are released and play important roles during the liver regeneration process (Taub, 2004; Fausto et al., 2006; Michalopoulos, 2007), were predicted to be significantly active upstream regulators from our data-driven pathway analysis. Also, despite that some of the pathways highlighted in our study were also previously reported to be upregulated in the regenerating liver as a result of the regeneration cascade(Rauchfuss et al., 2012), the samples analyzed in our study were obtained from metastatic tissue located on the embolized (atrophying) lobe, suggesting that our data is likely not reflecting downstream pathways occurring in the background liver during regeneration.

Although the precise molecular mechanisms underlying our observations remain to be elucidated, they are beyond the scope of this proof-of-principle translational study, which has some acknowledged limitations. First, almost all patients with stage VI colon cancer receive neoadjuvant chemotherapy (Nordlinger et al., 2013) as per standard of care, which may affect the tissue quality because of necrosis and treatment effects. However we selected samples with an adequate RNA quality for this pilot study, and all patients interrupt systemic treatment at least 6 weeks prior to any procedure, thereby reducing the risk of observing treatment effects in the sequencing data. Second, because some patients' disease progressed to an un-resectable state, we were unable to procure some of the

follow-up tissue biopsies, which reduced the sample size of our cohort. We therefore elected to select a subset of high-quality paired tissue biopsy material to investigate potential pathways and gene expression changes using high-throughput RNA-Seq analysis, and to further validate our findings in additional biological samples, including fresh frozen and formalin-fixed paraffin-embedded samples.

It is important to clarify that since PVE allows conversion of initially unresectable patients to a resectable state, it is still justified and standard of care to provide this preoperative intervention when indicated. The clinical impact would lie in stratifying patients prior to PVE and resection, to determine which patients would benefit the most from this procedure and which could potentially have disease progression and may therefore benefit from an alternate form of intervention. In the future, it will be critical to investigate metastatic lesions prior to the intervention, to determine molecular signatures that may be predictive of disease progression post-PVE. Such predictive models could guide physicians in selecting patients for this intervention, which if successful and leading to resectability, can provide these patients with the best possible long-term outcomes.

CONCLUSION

In summary, our study shows that colorectal liver metastases that progress post-PVE are susceptible tumors that undergo gene expression changes, likely cytokine and growth factors-driven, resulting in enhanced tumor proliferation and activation of core cancer pathways. Highlighting mechanisms of tumor progression in this context is a first step towards patient stratification and development of targeted therapeutic strategies that may mitigate the unwanted effects of portal vein embolization on tumor growth. Determining a signature predictive of post-PVE tumor growth would be crucial in early identification of patients at risk of disease progression.

Acknowledgements:

This study was supported by the Liver Disease Biobank (McGill University Health Center). We would like to thank Dr Bia Dias, as well as the interventional radiology fellows and angiography technicians of the McGill University Health Center Radiology Department. We also would like to thank Genome Quebec for the sequencing and bioinformatics platforms.

REFERENCES

Abdalla, E.K. (2010). Portal vein embolization (prior to major hepatectomy) effects on regeneration, resectability, and outcome. *J Surg Oncol* **102**, 960–967 doi:10.1002/jso.21654.

Abulkhir, A., Limongelli, P., Healey, A.J., Damrah, O., Tait, P., Jackson, J., Habib, N., and Jiao, L.R. (2008). Preoperative Portal Vein Embolization for Major Liver Resection. *Ann. Surg.* **247**, 49–57 doi:10.1097/SLA.0b013e31815f6e5b.

Adam, R., Pascal, G., Castaing, D., Azoulay, D., Delvart, V., Paule, B., Levi, F., and Bismuth, H. (2004). Tumor progression while on chemotherapy: a contraindication to liver resection for multiple colorectal metastases? *Ann. Surg.* **240**, 1052–61–discussion1061–4.

Ak, G., Metintas, M., Metintas, S., Yildirim, H., Ozkan, R., and Ozden, H. (2010). Three-dimensional evaluation of chemotherapy response in malignant pleural mesothelioma. *Eur J Radiol* **74**, 130–135 doi:10.1016/j.ejrad.2009.02.002.

Angel, P., and Karin, M. (1991). The role of Jun, Fos and the AP-1 complex in cell-proliferation and transformation. *Biochim. Biophys. Acta* **1072**, 129–157.

Barbaro, B., Di Stasi, C., Nuzzo, G., Vellone, M., Giuliante, F., and Marano, P. (2003). Preoperative right portal vein embolization in patients with metastatic liver disease. Metastatic liver volumes after RPVE. *Acta Radiol* **44**, 98–102.

Dawson, J.C., Bruche, S., Spence, H.J., Braga, V.M.M., and Machesky, L.M. (2012). Mtss1 promotes cell-cell junction assembly and stability through the small GTPase Rac1. *PLoS ONE* **7**, e31141 doi:10.1371/journal.pone.0031141.

De Jong, K.P., Lont, H.E., Bijma, A.M., and Brouwers, M. (1995). The effect of partial hepatectomy on tumor growth in rats: in vivo and in vitro studies. ….

Eferl, R., and Wagner, E.F. (2003). AP-1: a double-edged sword in tumorigenesis. *Nat.*

Rev. Cancer **3**, 859–868 doi:10.1038/nrc1209.

Eisenhauer, E.A., Therasse, P., Bogaerts, J., Schwartz, L.H., Sargent, D., Ford, R., Dancey, J., Arbuck, S., Gwyther, S., Mooney, M., Rubinstein, L., Shankar, L., Dodd, L., Kaplan, R., Lacombe, D., and Verweij, J. (2009). New response evaluation criteria in solid tumours: revised RECIST guideline (version 1.1). *Eur. J. Cancer* **45**, 228–247 doi:10.1016/j.ejca.2008.10.026.

Elias, D., De Baere, T., Roche, A., Mducreux, Leclere, J., and Lasser, P. (1999). During liver regeneration following right portal embolization the growth rate of liver metastases is more rapid than that of the liver parenchyma. *Br J Surg* **86**, 784–788 doi:10.1046/j.1365-2168.1999.01154.x.

Eveno, C., Le Henaff, C., Audollent, R., Soyer, P., Rampanou, A., Nemeth, J., Brouland, J.-P., Dupuy, E., Pocard, M., and Bonnin, P. (2012). Tumor and non-tumor liver angiogenesis is traced and evaluated by hepatic arterial ultrasound in murine models. *Ultrasound Med Biol* **38**, 1195–1204 doi:10.1016/j.ultrasmedbio.2012.03.004.

Fausto, N., Campbell, J.S., and Riehle, K.J. (2006). Liver regeneration. *Hepatology* **43**, S45–S53 doi:10.1002/hep.20969.

Fernandez, F.G., Drebin, J.A., Linehan, D.C., Dehdashti, F., Siegel, B.A., and Strasberg, S.M. (2004). Five-year survival after resection of hepatic metastases from colorectal cancer in patients screened by positron emission tomography with F-18 fluorodeoxyglucose (FDG-PET). *Ann. Surg.* **240**, 438–47–discussion447–50.

Heinrich, S., Jochum, W., Graf, R., and Clavien, P.-A. (2006). Portal vein ligation and partial hepatectomy differentially influence growth of intrahepatic metastasis and liver regeneration in mice. *J. Hepatol.* **45**, 35–42 doi:10.1016/j.jhep.2006.02.020.

Hennigan, R.F., Hawker, K.L., and Ozanne, B.W. (1994). Fos-transformation activates genes associated with invasion. *Oncogene* **9**, 3591–3600.

Hochster, H.S., Hart, L.L., Ramanathan, R.K., Childs, B.H., Hainsworth, J.D., Cohn, A.L., Wong, L., Fehrenbacher, L., Abubakr, Y., Saif, M.W., Schwartzberg, L., and Hedrick, E. (2008). Safety and Efficacy of Oxaliplatin and Fluoropyrimidine Regimens With or Without Bevacizumab As First-Line Treatment of Metastatic Colorectal Cancer: Results of the TREE Study. *J. Clin. Oncol.* **26**, 3523–3529 doi:10.1200/JCO.2007.15.4138.

Hoekstra, L.T., van Lienden, K.P., Doets, A., Busch, O.R.C., Gouma, D.J., and van Gulik, T.M. (2012). Tumor progression after preoperative portal vein embolization. *Ann. Surg.* **256**, 812–7–discussion817–8 doi:10.1097/SLA.0b013e3182733f09.

Hu, E., Mueller, E., Oliviero, S., Papaioannou, V.E., Johnson, R., and Spiegelman, B.M. (1994). Targeted disruption of the c-fos gene demonstrates c-fos-dependent and -independent pathways for gene expression stimulated by growth factors or oncogenes. *Embo J.* **13**, 3094–3103.

Hurwitz, H., Fehrenbacher, L., Novotny, W., Cartwright, T., Hainsworth, J., Heim, W., Berlin, J., Baron, A., Griffing, S., Holmgren, E., Ferrara, N., Fyfe, G., Rogers, B., Ross, R., and Kabbinavar, F. (2004). Bevacizumab plus Irinotecan, Fluorouracil, and Leucovorin for Metastatic Colorectal Cancer. *N. Engl. J. Med.* **350**, 2335–2342 doi:10.1056/NEJMoa032691.

Jeon, D.-G., Kong, C.-B., Cho, W.H., Song, W.S., Cho, S.H., Choi, S.W., and Lee, S.-Y. (2014). Examination of the cutoff value of postchemotherapy increase in tumor volume as a predictor of subsequent oncologic events in stage IIB osteosarcoma. *J Surg Oncol* **109**, 275–279 doi:10.1002/jso.23496.

Jones, S., Zhang, X., Parsons, D.W., Lin, J.C.-H., Leary, R.J., Angenendt, P., Mankoo, P., Carter, H., Kamiyama, H., Jimeno, A., Hong, S.-M., Fu, B., Lin, M.-T., Calhoun, E.S., Kamiyama, M., Walter, K., Nikolskaya, T., Nikolsky, Y., Hartigan, J., Smith, D.R., Hidalgo, M., Leach, S.D., Klein, A.P., Jaffee, E.M., Goggins, M., Maitra, A., Iacobuzio-Donahue, C., Eshleman, J.R., Kern, S.E., Hruban, R.H., Karchin, R., Papadopoulos, N., Parmigiani, G., Vogelstein, B., Velculescu, V.E., and Kinzler, K.W. (2008). Core signaling pathways in human pancreatic cancers revealed by global genomic analyses. *Science* **321**, 1801–1806 doi:10.1126/science.1164368.

Kokudo, N., Tada, K., Seki, M., Ohta, H., Azekura, K., Ueno, M., Ohta, K., Yamaguchi, T., Matsubara, T., Takahashi, T., Nakajima, T., Muto, T., Ikari, T., Yanagisawa, A., and Kato, Y. (2001). Proliferative activity of intrahepatic colorectal metastases after preoperative hemihepatic portal vein embolization. *Hepatology* **34**, 267–272 doi:10.1053/jhep.2001.26513.

Kollmar, O., Corsten, M., Scheuer, C., Vollmar, B., Schilling, M.K., and Menger, M.D. (2007). Portal branch ligation induces a hepatic arterial buffer response, microvascular remodeling, normoxygenation, and cell proliferation in portal blood-deprived liver tissue. *Am. J. Physiol. Gastrointest. Liver Physiol.* **292**, G1534–G1542 doi:10.1152/ajpgi.00503.2006.

Lee, Y.-G., Macoska, J.A., Korenchuk, S., and Pienta, K.J. (2002). MIM, a Potential Metastasis Suppressor Gene in Bladder Cancer. *Neoplasia* **4**, 291–294 doi:10.1038/sj.neo.7900231.

Lim, C., Cauchy, F., Azoulay, D., Farges, O., Ronot, M., and Pocard, M. (2013). Tumour progression and liver regeneration-insights from animal models. *Nat Rev Gastroenterol Hepatol* doi:10.1038/nrgastro.2013.55.

Liu, K., Wang, G., Ding, H., Chen, Y., Yu, G., and Wang, J. (2010). Downregulation of metastasis suppressor 1(MTSS1) is associated with nodal metastasis and poor outcome in Chinese patients with gastric cancer. *BMC Cancer* **10**, 428 doi:10.1186/1471-2407-10-428.

Madoff, D.C., Abdalla, E.K., and Vauthey, J.-N. (2005). Portal vein embolization in preparation for major hepatic resection: evolution of a new standard of care. *J Vasc Interv Radiol* **16**, 779–790 doi:10.1097/01.RVI.0000159543.28222.73.

Maggiori, L., Bretagnol, F., Sibert, A., Paradis, V., Vilgrain, V., and Panis, Y. (2011). Selective portal vein ligation and embolization induce different tumoral responses in the rat liver. *Surgery* **149**, 496–503 doi:10.1016/j.surg.2010.10.012.

McGarry, L.C., Winnie, J.N., and Ozanne, B.W. (2004). Invasion of v-Fos(FBR)-transformed cells is dependent upon histone deacetylase activity and suppression of histone deacetylase regulated genes. *Oncogene* **23**, 5284–5292 doi:10.1038/sj.onc.1207687.

Michalopoulos, G.K. (2007). Liver regeneration. *J. Cell. Physiol.* **213**, 286–300 doi:10.1002/jcp.21172.

Momiyama, M., Kumamoto, T., Suetsugu, A., Kishimoto, H., Chishima, T., Tanaka, K., Akiyama, H., Ichikawa, Y., Bouvet, M., Endo, I., and Hoffman, R.M. (2012). Major liver resection stimulates stromal recruitment and metastasis compared with repeated minor resection. *J. Surg. Res.* **178**, 280–287 doi:10.1016/j.jss.2012.03.020.

Mueller, L., Hillert, C., Möller, L., Krupski-Berdien, G., Rogiers, X., and Broering, D.C. (2008). Major hepatectomy for colorectal metastases: is preoperative portal occlusion an oncological risk factor? *Ann. Surg. Oncol.* **15**, 1908–1917 doi:10.1245/s10434-008-9925-y.

Nordlinger, B., Sorbye, H., Glimelius, B., Poston, G.J., Schlag, P.M., Rougier, P., Bechstein, W.O., Primrose, J.N., Walpole, E.T., Finch-Jones, M., Jaeck, D., Mirza, D., Parks, R.W., Mauer, M., Tanis, E., Van Cutsem, E., Scheithauer, W., Gruenberger, T., EORTC Gastro-Intestinal Tract Cancer Group, Cancer Research UK, Arbeitsgruppe Lebermetastasen und–tumoren in der Chirurgischen Arbeitsgemeinschaft Onkologie (ALM-CAO), Australasian Gastro-Intestinal Trials Group (AGITG), Fédération Francophone de Cancérologie Digestive (FFCD) (2013). Perioperative FOLFOX4 chemotherapy and surgery versus surgery alone for resectable liver metastases from colorectal cancer (EORTC 40983): long-term results of a randomised, controlled, phase 3 trial. *Lancet Oncol.* **14**, 1208–1215 doi:10.1016/S1470-2045(13)70447-9.

Pamecha, V., Levene, A., Grillo, F., Woodward, N., Dhillon, A., and Davidson, B.R. (2009). Effect of portal vein embolisation on the growth rate of colorectal liver metastases. *Br. J. Cancer* **100**, 617–622 doi:10.1038/sj.bjc.6604872.

Picardo, A., Karpoff, H.M., Ng, B., Lee, J., Brennan, M.F., and Fong, Y. (1998). Partial hepatectomy accelerates local tumor growth: potential roles of local cytokine activation. *Surgery* **124**, 57–64.

Rauchfuss, F., Lambeck, S., Claus, R.A., Ullmann, J., Schulz, T., Weber, M., Katenkamp, K., Guthke, R., Bauer, M., and Settmacher, U. (2012). Sustained liver regeneration after portal vein embolization --a human molecular pilot study. *Dig Liver Dis* **44**, 681–688 doi:10.1016/j.dld.2012.04.002.

Reichmann, E., Schwarz, H., Deiner, E.M., and Leitner, I. (1992). Activation of an inducible c-FosER fusion protein causes loss of epithelial polarity and triggers epithelial-fibroblastoid cell conversion. *Cell*.

Richter, S., Vollmar, B., Mücke, I., Post, S., and Menger, M.D. (2001). Hepatic arteriolo-portal venular shunting guarantees maintenance of nutritional microvascular supply in hepatic arterial buffer response of rat livers. *J. Physiol. (Lond.)* **531**, 193–201.

Saltz, L.B., Clarke, S., and Díaz-Rubio, E. (2008). Bevacizumab in combination with oxaliplatin-based chemotherapy as first-line therapy in metastatic colorectal cancer: a randomized phase III study. *Journal of Clinical …*.

Scheele, J., Stangl, R., and Altendorf-Hofmann, A. (1990). Hepatic metastases from colorectal carcinoma: impact of surgical resection on the natural history. *Br J Surg* **77**, 1241–1246.

Siegel, R., Naishadham, D., and Jemal, A. (2013). Cancer statistics, 2013. *CA: a Cancer Journal for Clinicians* **63**, 11–30 doi:10.3322/caac.21166.

Simmonds, P.C., Primrose, J.N., Colquitt, J.L., Garden, O.J., Poston, G.J., and Rees, M.

(2006). Surgical resection of hepatic metastases from colorectal cancer: a systematic review of published studies. *Br. J. Cancer* **94**, 982–999 doi:10.1038/sj.bjc.6603033.

Simoneau, E., Aljiffry, M., Salman, A., Abualhassan, N., Cabrera, T., Valenti, D., Baage, El, A., Jamal, M., Kavan, P., Al-Abbad, S., Chaudhury, P., Hassanain, M., and Metrakos, P. (2012). Portal vein embolization stimulates tumour growth in patients with colorectal cancer liver metastases. *HPB (Oxford)* **14**, 461–468 doi:10.1111/j.1477-2574.2012.00476.x.

Taub, R. (2004). Liver regeneration: from myth to mechanism. *Nat. Rev. Mol. Cell Biol.* **5**, 836–847 doi:10.1038/nrm1489.

Yokoyama, Y., Wawrzyniak, A., Sarmadi, A.M., Baveja, R., Gruber, H.E., Clemens, M.G., and Zhang, J.X. (2006). Hepatic arterial flow becomes the primary supply of sinusoids following partial portal vein ligation in rats. *J. Gastroenterol. Hepatol.* **21**, 1567–1574 doi:10.1111/j.1440-1746.2006.04460.x.

Yu, J.S., Koujak, S., Nagase, S., Li, C.-M., Su, T., Wang, X., Keniry, M., Memeo, L., Rojtman, A., Mansukhani, M., Hibshoosh, H., Tycko, B., and Parsons, R. (2008). PCDH8, the human homolog of PAPC, is a candidate tumor suppressor of breast cancer. *Oncogene* **27**, 4657–4665 doi:10.1038/onc.2008.101.

TABLES

Table 1. Baseline clinical characteristics of study population (n=20)

Variable	Value
Age, mean ± SD	61 ± 11
Male gender, n (%)	14 (70.0)
Chemotherapy cycles prior to PVE (number), mean ± SD	6 ± 3
Neoadjuvant chemotherapy agent, n (%)	
Oxaliplatin	16 (80.0)
Irinotecan	2 (10.0)
Bevacizumab	8 (40.0)
Chemo-naive[a]	3 (15.0)
Interval time between CT scans (days), median (range)	70 (60-100)
Right-sided PVE, n (%)	20 (100)
Staged resection, n (%)	6 (30.0)
Number of lesions pre PVE, median (IQ range)	
Right side	4 (2-6)
Left side	0 (0-1)
Tumour volume pre PVE (cm^3), median (IQ range)	
Right side	9.34 (3.05-31.75)
Left side	0.00 (0.00-1.30)

a: 2 patients who never received chemotherapy; 1 patient who received chemotherapy >1 year before the onset of liver metastases.

Table 2. Differentially expressed genes in CRCLM paired samples with progression related to top networks from functional analysis

Gene name	Gene ID	Fold change	EdgeR p-value	Adjusted p-value (FDR)
FOS	ENSG00000170345	5.88	1.20 E-06	0.0034
FOSB	ENSG00000125740	14.43	4.50 E-05	0.0078
CXCL5	ENSG00000163735	25.54	0.00021	0.0132
NR4A1	ENSG00000123358	5.52	0.0011	0.0255
RAB20	ENSG00000139832	12.95	0.0018	0.0311
IRS2	ENSG00000185950	15.08	0.0019	0.0320
AQP8	ENSG00000103375	38.38	0.0039	0.0476
ATF3	ENSG00000162772	3.24	0.0043	0.0492
PCDH18	ENSG00000189184	-3.70	0.004	0.048
PCDHB5	ENSG00000113209	-4.50	0.00094	0.0237
PCDH9	ENSG00000184226	-5.19	0.0015	0.0291
MTSS1	ENSG00000170873	-4.76	0.0018	0.0313

Abbreviations: CRCLM: colorectal cancer liver metastasis. FDR: false discovery rate

Table 3. Prediction of upstream regulators during metastatic progression after portal vein embolization

Upstream regulator	Molecule type	Activation Z-score[a]	p-value of overlap[b]
PDGF-BB	Complex	2.635	4.13×10^{-05}
HGF	Growth factor	2.371	3.17×10^{-03}
EGF	Growth factor	2.349	2.55×10^{-03}
IL6	Cytokine	2.192	1.45×10^{-02}
NFκB	Complex	2.182	2.65×10^{-02}
Insulin	Group	2.167	3.53×10^{-03}
IL1	Group	2.132	2.63×10^{-03}
IL1B	Cytokine	2.065	3.36×10^{-06}
VEGF-A	Growth factor	1.995	4.06×10^{-03}

a: A molecule was predicted to be an activated upstream regulator as indicated by the positive z-score. b: The p-value was calculated by Fischer's exact test and based on the number of genes connected by the upstream regulator (Ingenuity Pathway Analysis)

Supplementary Tables

Supplementary Table 1. Baseline patient characteristics and metastatic lesions

Patient	Age	Gender	# cycles chemo[a]	Response[b]	Number of lesions – right lobe		Number of lesions – left lobe		New lesions post PVE
					Pre-PVE	Post-PVE	Pre-PVE	Post-PVE	
1	52	M	6	SD	7	7	3	3	-
2	59	F	5	PR	2	2	1	1	-
3	70	M	0	-	1	1	0	0	-
4	80	M	0	-	5	5	0	0	-
5	52	M	6	SD	7	7	1	1	-
6	75	F	3	PD	2	5	0	1	+
7	67	M	6	PR	4	5	0	0	+
8	50	M	4	SD	2	2	0	0	-
9	59	F	6	SD	1	1	0	0	-
10	77	M	6	PR	3	3	2	2	-
11	68	M	4	PR	6	6	0	0	-
12	52	M	6	SD	3	3	0	0	-
13	54	F	6	PR	15	15	1	1	+
14	54	F	6	PR	8	8	0	0	-
15	64	M	2	SD	2	2	1	1	-
16	53	M	14	PR	2	2	2	2	-
17	51	M	6	SD	6	8	0	4	+
18	63	M	6	PR	3	3	2	2	-
19	39	M	0	-	5	n/a[b]	0	n/a	n/a
20	64	F	6	PR	5	5	0	0	-

a: neoadjuvant chemotherapy prior to portal vein embolization. b: For those receiving neoadjuvant chemotherapy only: as per RECIST criteria: CR: complete response, PR: partial response, SD: stable disease, PD: progressive disease. c: CT scan post PVE with suboptimal liver protocol for 3D CT volumetric analysis.

Supplementary Table 2. Tumor volumetric data[a]

Patient	Tumor volumes – Right lobe			Tumor volumes – Left lobe			% **Δ**Total TV	New lesion	Outcome post PVE
	Pre-PVE	Post-PVE	% **Δ**TV	Pre-PVE	Post-PVE	% **Δ**TV			
1	150.347	165.269	9.93	1.234	2.226	80.39	+ 10.50	+	PD
2	295.593	228.891	-22.57	93.147	58.734	-36.94	- 26.01	-	SD
3	1.724	2.876	66.82	0	0	-	+ 66.82	-	PD
4	3.337	21.281	537.73	0	0	-	+ 537.73	-	PD
5	1.397	1.393	-0.29	0.341	0.365	7.04	1.15	-	SD
6	25.221	25.991	3.05	0	0.314	-	+ 4.30	+	PD
7	11.878	15.752	32.61	0	0	-	+ 32.61	+	PD
8	2.964	9.910	234.35	0	0	-	+ 234.35	-	PD
9	3.637	5.747	58.01	0	0	-	+ 58.01	-	PD
10	30.595	42.252	38.10	8.936	4.653	-47.93	+ 18.65	-	PD
11	35.23	16.513	-53.13	0	0	-	- 53.13	-	SD
12	8.863	7.403	-14.25	0	0	-	-14.25	-	SD
13	2.522	3.533	40.09	0.561	1.045	86.27	+48.49	+	PD
14	46.000	109.408	137.84	0	0	-	+137.84	-	PD
15	10.037	5.749	-42.72	3.504	2.271	-35.19	-40.77	-	SD
16		34.544			5.222				PD
17	21.555	117.264	444.02	0	3.586	-	+460.65	+	PD
18	2.286	2.488	8.83	1.517	0.932	-38.56	-10.07	-	SD
19	1.472			0	0				PD[b]
20	5.453	5.301	-2.79				-2.79	-	SD

Abbreviations: PVE: portal vein embolization; TV: tumor volume; PD: progression of disease; SD: stable disease. a: all tumor volumes expressed in cm^3. b: 3D volumetric analysis not feasible secondary to suboptimal liver protocol; disease outcome (PD) based on small lesion seen on ultra-sound post-PVE prior to resection.

Supplementary Table 3. Liver volumetric data and measurement of liver regeneration

Patient	Outcome post PVE	Future liver remnant (%)[a], pre-PVE	Future liver remnant (%), post-PVE	Degree of hypertrophy[b]
1	PD	14.33	23.11	8.78
2	SD	20.88	31.11	10.22
3	PD	19.61	33.19	13.58
4	PD	22.79	34.57	11.78
5	SD	23.36	35.20	11.84
6	PD	20.98	31.73	10.75
7	PD	24.75	31.66	6.91
8	PD	18.57	27.50	8.94
9	PD	9.99	16.28	6.29
10	PD	23.95	36.43	12.48
11	SD	24.81	37.23	12.42
12	SD	28.61	33.60	4.99
13	PD	21.03	29.95	8.92
14	PD	13.32	25.79	12.47
15	SD	23.27	34.28	11.01
16	PD	21.62	28.18	6.56
17	PD	11.97	24.77	12.80
18	SD	19.35	35.36	16.01
19	PD	22.08	28.91	6.83
20	SD	24.04	33.66	9.62

Abbreviations: PVE: portal vein embolization; FLR: future liver remnant; PD: progression of disease; SD: stable disease

a: all future liver remnant expressed as % (future liver remnant (cm^3) / total liver volume (cm^3) * 100). b: degree of hypertrophy= FLR (%) post – FLR (%) pre

Supplementary Table 4. RNA extraction data for samples selected for RNA Seq

Patient ID	Outcome post PVE	Time point to PVE	Yield (ng/uL)[a]	RIN
P4	PD	Pre	1049	7.8
		Post	720.2	7.4
P8	PD	Pre	612.1	7.5
		Post	302.9	6.1
P9	PD	Pre	909.8	8.5
		Post	281.6	7.2
P10	PD	Pre	121.0	9.0
		Post	153.0	6.5
P11	SD	Pre	32.0	6.1
		Post	56.6	7.0
P2	SD	Pre	3.679	2.3[b]
		Post	202.4	6.8

Abbreviations: PVE: portal vein embolization; RIN: RNA integrity score
a: volume of 40uL (with buffer). b: sample excluded from further sequencing

Supplementary Table 5. Statistics of CRCLM transcriptome after trimming and alignment steps

Sample	Raw reads	Surviving reads (%)	Aligned reads (%)	Alternative alignments (%)	rRNA reads (%)	Coverage	Exonic rate	Genes
P4-A	163,742,800	160,458,606 (97.99)	150,168,402 (93.59)	20,516,034 (13.66)	5,979,705 (3.73)	58	0.8268	26,384
P4-B	143,653,432	139,912,538 (97.40)	131,001,380 (93.63)	17,170,073 (13.11)	5,125,035 (3.66)	74	0.6760	28,778
P8-A	164,428,210	160,570,904 (97.65)	149,681,162 (93.22)	23,648,993 (15.80)	7,982,945 (4.97)	77	0.6854	29,629
P8-B	111,069,472	108,033,938 (97.27)	97,332,149 (90.09)	21,754,484 (22.35)	5,528,368 (5.12)	36	0.4533	31,469
P9-A	135,569,978	132,273,228 (97.57)	122,921,350 (92.93)	14,087,304 (11.46)	2,752,577 (2.08)	78	0.7201	28,360
P9-B	151,287,158	147,570,302 (97.54)	135,922,057 (92.11)	22,977,364 (16.90)	6,235,560 (4.23)	67	0.5524	32,038
P10-A	134,060,526	131,339,400 (97.97)	119,734,097 (91.16)	13,040,363 (10.89)	2,494,540 (1.90)	56	0.6415	29,576
P10-B	165,097,758	161,077,874 (97.57)	144,436,781 (89.67)	27,606,100 (19.11)	5,227,600 (3.25)	56	0.4303	34,701
P11-A	122,898,662	119,700,576 (97.40)	105,685,475 (88.29)	18,781,477 (17.77)	3,275,404 (2.74)	34	0.3996	34,140
P11-B	208,820,958	204,123,052 (97.75)	183,540,569 (89.92)	29,318,380 (15.97)	7,602,800 (3.72)	69	0.5181	35,271
P2-B*	149,308,466	145,899,388 (97.72)	136,457,700 (93.53)	19,395,411 (14.21)	5,439,340 (3.73)	61	0.5778	29,876

*P2-A excluded.

FIGURE LEGENDS

Figure 1:

Title: Top enriched networks, functional analysis (Ingenuity Pathway analysis)

Legend: Top networks: Cancer; Cellular development, growth and proliferation; Cell-Cell signaling (score 32)

Figure 2:

Title: Differentially expressed genes, paired comparison of CRCLM samples pre and post embolization

Legend:

A) Differentially expressed genes (count-based (edgeR), tumors pre- and post-PVE with progression post embolization.
B) Validation of candidate genes from RNA-Seq data by quantitative rt-PCR

Figure 3:

Title: Proliferation index of metastatic lesions post embolization and controls without PVE (n=43 lesions)

Legend:

A) Colorectal liver metastasis post-PVE with progression (n=13)
B) Colorectal liver metastasis post-PVE with stable disease (n=9)
C) Colorectal liver metastasis with partial response to chemotherapy (controls without PVE, n=14)
D) Colorectal liver metastasis with complete response to chemotherapy (controls without PVE, n=7)
E) Comparison of Ki67 positive cells (%) across groups

Supplementary Figure 1:

Title: Consort diagram, CRCLM patients requiring preoperative portal vein embolization

Supplementary Figure 2:

Title: Multidimensional scaling and unsupervised hierarchical clustering plots

Legend :

A) Multidimensional Scaling plot (2D) of the gene log_2 values (count per million (CPM)), representing samples (progression group) pre- and post-intervention (red dashed and full line respectively) and samples (stable disease group) pre and post-intervention (green dashed and full-line respectively).
B) Hierarchical clustering based on the correlation distance, log2 (CPM) (samples 10, 17 and 19 from SD group)

Supplementary Figure 3:

Title: Comparison of transcriptional profiles across samples

A) Heat map of most varying transcripts by log_2 standard deviation (Fragments Per Kilobase of transcript per Million mapped reads (FPKM))
B) Clustering of the mean absolute difference distance for gene log_2 (count per million (CPM)) values: heat map showing the hierarchically clustered Spearman correlation matrix for each pair of samples.

FIGURES

Figure 1.

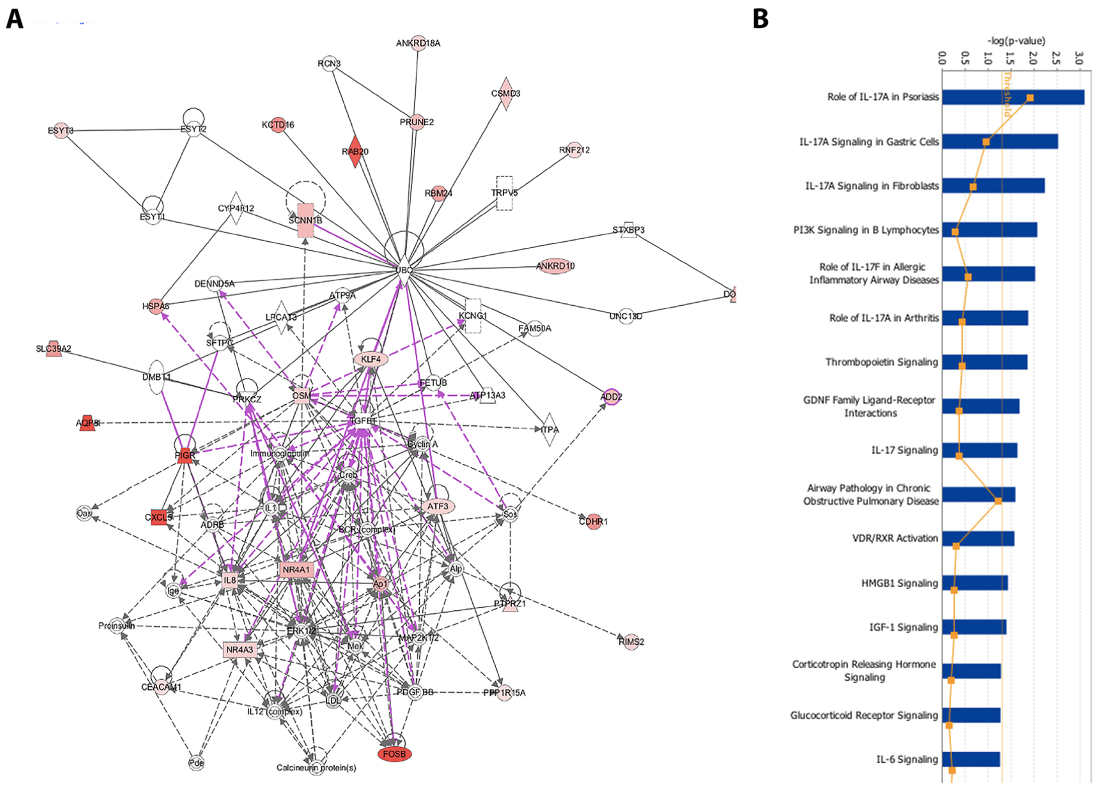

Figure 2.

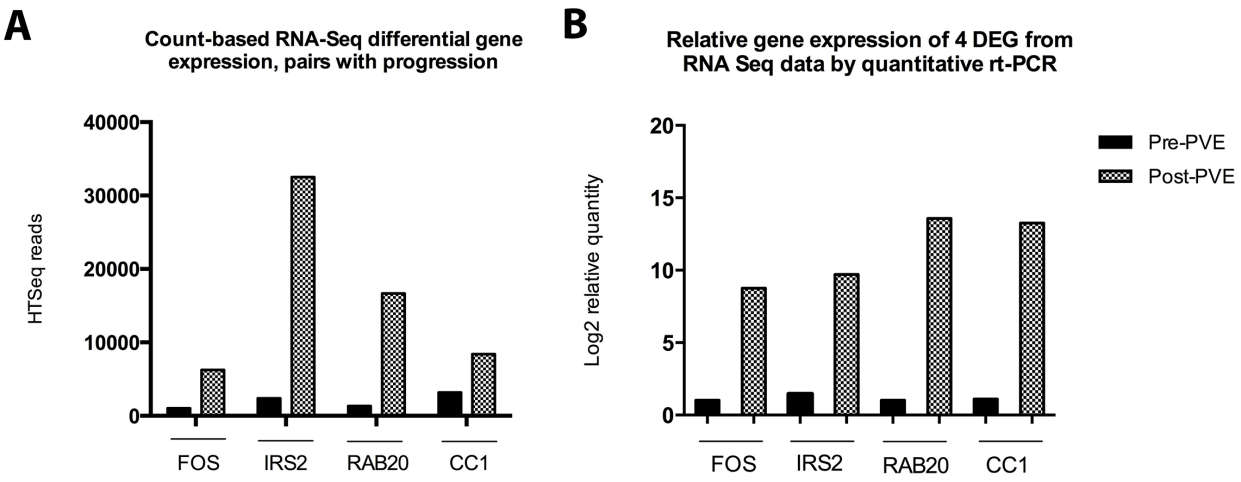
A
Count-based RNA-Seq differential gene expression, pairs with progression
HTSeq reads
40000
30000
20000
10000
0
FOS
IRS2
RAB20
CC1
B
Relative gene expression of 4 DEG from RNA Seq data by quantitative rt-PCR
Log2 relative quantity
20
15
10
5
0
FOS
IRS2
RAB20
CC1
Pre-PVE
Post-PVE

Figure 3.

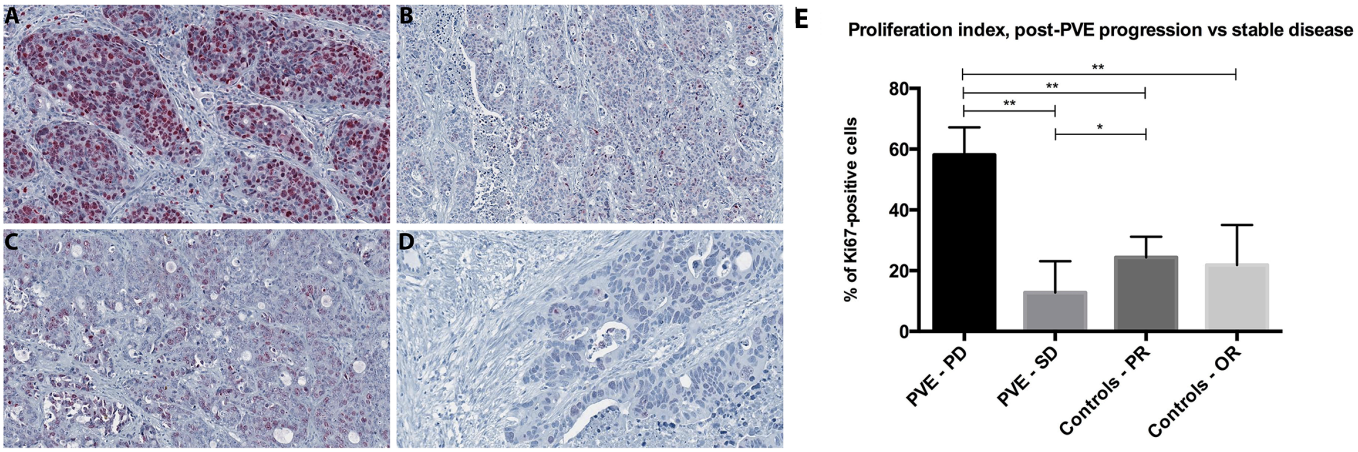
A
B
C
D
E
Proliferation index, post-PVE progression vs stable disease
% of Ki67-positive cells
80
60
40
20
0
**
**
**
*
PVE - PD
PVE - SD
Controls - PR
Controls - OR

Supplementary Figure 1.

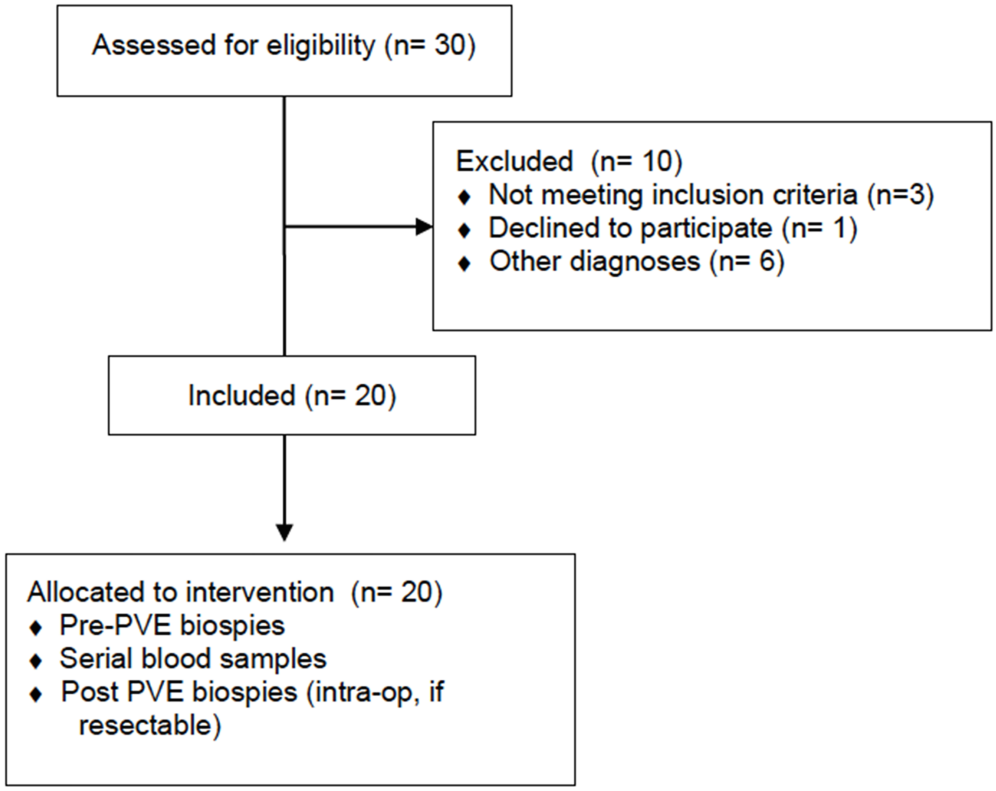

Supplementary Figure 2.

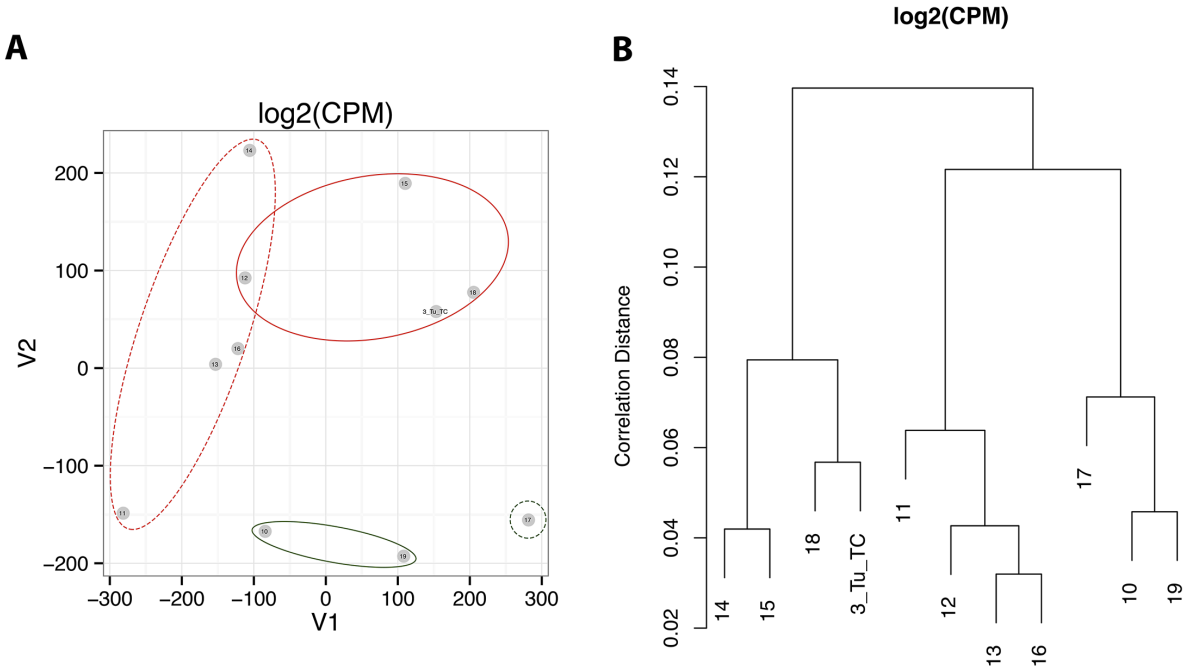

Supplementary Figure 3.

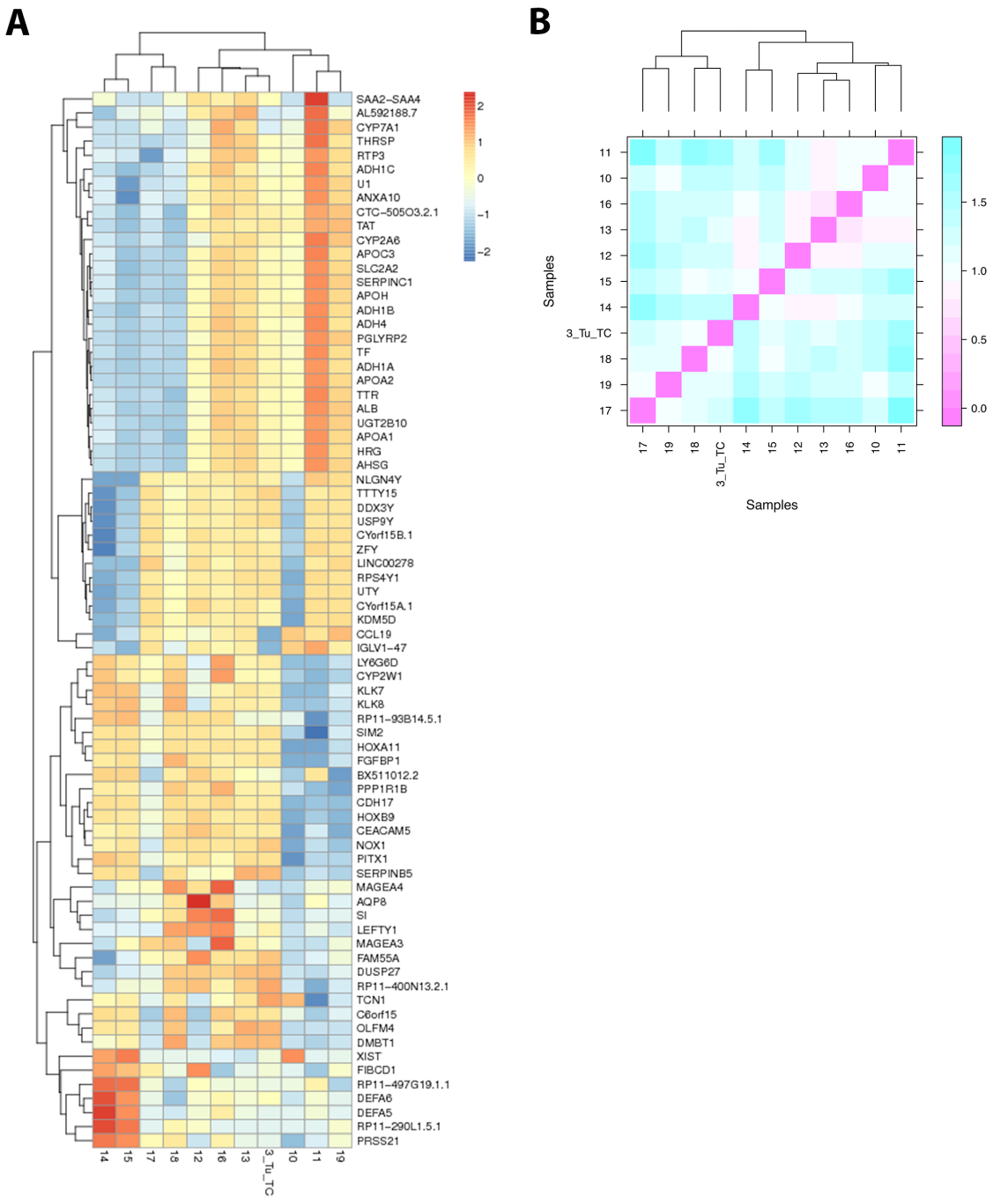

XVI. Transition to manuscript IV

The heterogenous biological behavior of colorectal liver metastasis suggests the presence of different subtypes of liver metastases. In fact, it was described that liver metastasis grow in different histological growth patterns, each of which are being associated with different tumor vascularization processes(159,162). Thus desmoplastic pattern is known to be utilizing angiogenesis whereas replacement utilizes a process known as vessel co-option. The latter is characterized by the tumor using nearby mature vasculature in order to obtain its blood supply, in opposition to harboring neovascularization. In this context, it was hypothesized that such distinct patterns and vascularization may in fact explain the heterogenous responses of colorectal liver metastases to systemic therapy, more precisely to targeted therapy against angiogenesis.

Indeed, despite encouraging results from experimental studies and clinical trials in other types of cancer suchs as glioblastoma, the use of the monoclonal antibody to vascular endothelial growth factor Bevacizumab has demonstrated a rather disapointing impact in the treatment of colorectal liver metastasis. In fact, although some trials have shown a better disease-free and progression-free survival, no clinical trial have yet shown a survival benefit from the addition of Bevacizumab to systemic perioperative chemotherapy.

The aim of the next study was to investigate the role of the growth patterns and vessel co-option in neoadjuvant treatment resistance with Bevacizumab for colorectal liver metastasis.

XVII. Thesis Manuscript IV

Under revision at Nature Medicine

Vessel co-option mediates resistance to anti-angiogenic therapy in liver metastases

Eve Simoneau[3†], Sophia Frentzas[1,2†], Victoria L. Bridgeman[1†], Peter B. Vermeulen[1,4†], Shane Foo[1], Eleftherios Kostaras[1], Mark Nathan[1], Andrew Wotherspoon[2], Zu-hua Gao[3], Yu Shi[3], Gert Van den Eynden[4], Ayat Salman[3], Anthoula Lazaris[3], Frances Daley[5], Patrycja Gazinska[6], Tracy J. Berg[1], Zak Eltahir[2], Clare Peckitt[2], Laila Ritsma[7], Jacco Van Rheenen[7], Alla Khashper[3], Gina Brown[2], Hanna Nystrom[8], Malin Sund[8], Steven Van Laere[4], Evelyne Loyer[9], Luc Dirix[4], David Cunningham[2,10] Peter Metrakos[3,10] & Andrew R. Reynolds[1,10]

[1]Tumour Biology Team, The Breast Cancer Now Toby Robins Research Centre, Mary-Jean Mitchell Green Building, The Institute of Cancer Research (ICR), London SW3 6JB, UK

[2]The Royal Marsden (RM), London SW3 6JJ, UK

[3]McGill University Health Centre (MUHC), Montreal, Quebec H3A 2B4, Canada

[4]Translational Cancer Research Unit (TCRU), GZA Hospitals St. Augustinus, Wilrijk 2610, Antwerp, Belgium

[5]Breakthrough Centre Histopathology Core Facility, RM, London SW3 6JJ, UK

[6]Breakthrough Breast Cancer Research Unit, Guy's Hospital, King's College London School of Medicine, London SE1 9RT, UK

[7]Hubrecht Institute, University Medical Center Utrecht, Utrecht 3584CT, Netherlands

[8]Department of Surgical and Perioperative Sciences, Umeå University, Umea SE-90185, Sweden

[9]The University of Texas MD Anderson Cancer Center (MDACC), Houston, TX 77030, USA

[†]These authors contributed equally.

[10]Co-senior authors.

Correspondence:

Andrew Reynolds

Tumour Biology Team, ICR, London, UK

Tel: +44 (0)207 153 5235

Email: andrew.reynolds@icr.ac.uk

Running title: Vessel co-option in bevacizumab resistance

Abstract

The efficacy of angiogenesis inhibitors in cancer is limited by resistance mechanisms that are poorly understood. Importantly, instead of inducing angiogenesis, many cancers can also vascularize by the non-angiogenic mechanism of vessel co-option. Here we show that vessel co-option is associated with a poor response to the anti-angiogenic agent bevacizumab in patients with colorectal cancer liver metastases. Moreover, we find that vessel co-option prevails in human breast cancer liver metastases, a setting where results with anti-angiogenic therapy have been disappointing. In our preclinical mechanistic studies, we show that cancer cell motility mediated by Arp2/3 is required for vessel co-option in liver metastases *in vivo* and that combined inhibition of angiogenesis and vessel co-option is more effective than inhibiting angiogenesis alone in this setting. Vessel co-option is therefore a clinically relevant mechanism of resistance to anti-angiogenic therapy and combined inhibition of angiogenesis and vessel co-option may be a warranted therapeutic strategy.

Introduction

Metastases can vascularize through sprouting angiogenesis that is stimulated by vascular endothelial growth factor-A (VEGF-A). This prompted the clinical development of anti-angiogenic agents, including the VEGF-A targeted antibody, bevacizumab[1,2]. Bevacizumab combined with chemotherapy can extend progression-free and / or overall survival in several indications, including metastatic colorectal cancer (CRC)[3,4]. Indeed, bevacizumab combined with chemotherapy (bev-chemo) is now an approved treatment for metastatic CRC. Despite this fact, the survival benefit achieved with the addition of bevazicumab to chemotherapy is modest, measured only in terms of months. Moreover, in other indications, including metastatic breast cancer, anti-angiogenic therapy has yet to demonstrate a survival benefit in patients[5,6]. Importantly, the mechanisms that limit the therapeutic efficacy of anti-angiogenic therapy in patients are still poorly understood.

However, it now emerges that some metastases can also vascularize by the non-angiogenic mechanism of vessel co-option, a process whereby cancer cells incorporate pre-existing vessels from surrounding tissue instead of inducing new vessel growth[7-10]. Importantly, although anti-angiogenic agents (including bevacizumab) were designed to target sprouting angiogenesis, they were not designed to target the process of vessel co-option. Because of this, vessel co-option has been suggested as a potential mechanism of resistance to anti-angiogenic therapy[6,10,11]. In the current study, we provide the first evidence that vessel co-option is a clinically relevant mechanism of resistance to anti-angiogenic therapy in liver metastases and that combined inhibition of angiogenesis and vessel co-option is more effective than targeting angiogenesis alone.

Results

CRC liver metastases with a replacement growth pattern respond poorly to bevacizumab

The liver is the most common site of involvement in metastatic CRC, and surgical removal of CRC liver metastases (CRCLMs) is now recommended practice for eligible patients[12]. Careful histopathological examination of human CRCLMs has shown that these tumors can present with three different histopathological growth patterns (HGPs): the desmoplastic HGP, the pushing HGP or the replacement HGP (Fig. 1a and Supplementary Fig. S1)[8,13]. Moreover, it has been shown that whilst CRCLMs with a desmoplastic or pushing HGP utilize angiogenesis, CRCLMs with a replacement HGP utilize vessel co-option i.e. the tumor actively incorporates pre-existing vessels instead of promoting angiogenesis[8,13,14]. Although bevacizumab was not designed to target vessel co-option, no study has addressed whether vessel co-option is associated with resistance to bevacizumab in liver metastases.

To address this question, we took advantage of the fact that some patients with metastatic CRC receive preoperative therapy with bev-chemo in the months that precede surgical removal of CRCLMs[15-17]. We evaluated the HGPs and the pathological response to therapy in 59 CRCLMs resected from 33 patients that were treated preoperatively with bev-chemo at The Royal Marsden (RM) (Fig. 1b) (for patient details see Supplementary Fig. S2 and Table S1). Since CRCLMs can present with a mixture of HGPs[13], the percentage of desmoplastic, pushing and replacement HGP was quantified in each lesion. To measure response to therapy, the pathological response in each lesion was scored in quartiles (>75%, 50-75%, 25-49% or <25% viable tumor). Lesions with <25% viable tumor were considered good responders, whilst lesions with ≥25% viable tumor were considered poor responders.

Importantly, lesions having a substantial (≥50%) replacement component were significantly enriched in the poor responder group when compared to the good

responder group (Fig. 1b, *P*<0.001). In contrast, lesions having a substantial (≥50%) desmoplastic component were significantly enriched in the good responders when compared to poor responders (Fig. 1b, *P*<0.001). Examples of lesions examined are shown (Fig. 1c-e). In a univariate analysis of other clinical variables, only the HGPs showed a statistically significant association with pathological response (Supplementary Table S2).

To provide an alternative measure of treatment response, we also evaluated radiological response in the same lesions. Recently published guidelines recommend that response to bev-chemo should be evaluated from computed tomography (CT) scans using novel morphological response criteria which correlate better with outcome than RECIST-based criteria[12,18]. Importantly, lesions with ≥50% replacement HGP were significantly enriched in the poor response group according to morphological response criteria (Fig. 2; *P*=0.006). However, no correlation was observed with RECIST-based criteria (Supplementary Fig. S3).

To validate the association between the HGPs and pathological response to therapy, we then examined a larger series of 128 CRCLMs from 59 patients that were treated preoperatively with bev-chemo at Montreal University Health Centre (MUHC) (for patient details see Supplementary Fig. S4 and Table S3). Again, lesions with ≥50% replacement HGP were significantly enriched in the poor responder group (Fig. 1f, *P*<0.001), whilst lesions with ≥50% desmoplastic HGP were significantly enriched in the good responder group (Fig. 1f, *P*<0.001). In a univariate analysis, the HGPs were the strongest predictors of pathological response (Supplementary Table S4).

Included in these analyses were patients that presented with solitary liver metastasis and patients that presented with multiple liver metastases. To control for this, we also examined the subset of patients that presented with a single lesion only. Importantly, the HGPs also correlated with pathological response in this subset of patients (Supplementary Fig S5). To determine whether the association between the

HGPs and pathological response remains significant when controlling for the effect of other clinical variables, we performed a multivariate analysis using pooled data from RM and MUHC (187 lesions from 92 patients). Importantly, the replacement HGP was still significantly associated with a poor pathological response (P<0.0001) in this analysis, whilst the desmoplastic HGP was significantly associated with a good pathological response (P<0.0001). Taken together, these data demonstrate that the replacement HGP is associated with a poor pathological response to bev-chemo in CRCLMs.

Cancer cells infiltrate the hepatic plates and co-opt sinusoidal blood vessels in the replacement growth pattern

We then investigated the mechanism of tumor vascularization in replacement HGP CRCLMs by examining, in detail, the relationship between cancer cells and the normal liver in this growth pattern. In normal liver, staining for hepatocyte specific antigen (HSA) identified hepatocytes within the hepatic plates, whilst collagen-3 staining identified the intervening sinusoidal blood vessels (SV; Fig. 3a). In the replacement HGP, co-staining for cancer cells (pan-cytokeratin) and hepatocytes (HSA) demonstrated that invading cancer cells line-up neatly with hepatocytes within the hepatic plates at the tumor-liver interface (Fig. 3b). Replacement of hepatocytes by invading cancer cells was clearly observed (Fig. 3c). Behind the invasive tumor front, near complete replacement of hepatocytes by cancer cells was evident and flattened displaced hepatocytes were frequently observed at the edge of cancer cell nests (Fig. 3d). However, cancer cells clearly respected the spaces occupied by SV (Fig. 3b-d). Therefore, in the replacement HGP, cancer cells (a) invade the liver parenchyma, (b) replace hepatocytes and (c) co-opt SV.

Further evidence for vessel co-option was obtained by staining for the endothelial marker CD31. In the replacement HGP, SV were frequently observed where one end of the vessel was physically located in the normal liver (*arrows* in Fig.

3e-g), whilst the other end was embedded in the tumor (*arrowheads* in Fig. 3e-g), showing that these tumors co-opt SV as they infiltrate the liver parenchyma (see also Supplementary Fig. S6a,b). However, this was not observed in the desmoplastic or pushing HGPs (Supplementary Fig. S6c-f). In addition, co-staining of tumors for CD31 and HSA demonstrated that tumor vessels at the periphery of the replacement HGP were often still physically associated with hepatocytes, providing additional evidence that these vessels are co-opted sinusoidal vessels and that they are not newly formed vessels. However, this was not observed in the desmoplastic or pushing HGPs (Supplementary Fig. S7). Therefore, whilst replacement HGP CRCLMs co-opt pre-existing sinusoidal vessels, the desmoplastic and pushing CRCLMs do not.

Prevalence of the replacement growth pattern in disease that progresses following bevacizumab treatment

Unfortunately, patients can progress following treatment with bev-chemo by developing new CRCLMs[19]. Here we define new CRCLMs as lesions that present in the liver after the initiation of bev-chemo treatment that were not evident on pre-treatment scans. In our analyses of treatment response described above (Fig. 1) we only examined resected CRCLMs that were detected on pre-treatment scans prior to treatment initiation and we specifically excluded any new CRCLMs, even if they were resected. Given that these new CRCLMs represent progressive disease that is clearly resistant to bev-chemo, we identified these new CRCLMs and examined their HGP. In the MUHC case series, 35 new CRCLMs from 13 patients were available for assessment (for patient details see Supplementary Table S5). We compared the HGPs in these new CRCLMs with two control groups from MUHC: CRCLMs from bev-chemo treated patients that were detected on pre-treatment scans prior to treatment initiation (128 CRCLMs from 59 patients; for patient details see Supplementary Table S4) and CRCLMs resected from MUHC patients that did not

receive any pre-operative therapy (32 CRCLMs from 19 patients; for patient details see Supplementary Table S6). Importantly, the replacement HGP was significantly increased in new CRCLMs compared to both of these control groups (P<0.001; Fig. 4a). These data provide evidence for an increased prevalence of the replacement HGP in patients that progress following treatment with bev-chemo.

Patients with replacement growth pattern liver metastases achieve less clinical benefit from bevacizumab

We then examined whether the HGPs of liver metastasis could impact on the clinical benefit achieved with anti-angiogenic therapy in terms of patient survival. Kaplan-Meier estimates of overall survival (OS) were calculated for a cohort of 62 patients from MUHC that were treated preoperatively with bev-chemo between 2008 and 2013 (Figure 4a) and for a cohort of 29 patients from MUHC that were treated preoperatively with chemotherapy alone during the same period (Figure 4b). Patients were stratified into groups based on their liver metastasis growth pattern: predominant replacement, predominant desmoplastic or predominant pushing.

In the bev-chemo cohort, the replacement HGP patients had a significantly poorer OS when compared to the desmoplastic HGP patients (P = 0.0022; Fig. 4b) and the HGP was the only variable associated with overall survival in a multivariate analysis (P = 0.0023; Supplementary Table S7). However, no significant difference in OS was observed between the replacement and desmoplastic HGP patients in the cohort treated with chemotherapy only (P = 0.846; Fig. 4c). Using the same data set, we also examined whether patients with a predominant desmoplastic HGP achieved more benefit from the addition of bevacizumab to chemotherapy than patients with a predominant replacement HGP. A trend towards improved OS was observed in the desmoplastic HGP patients treated bevacizumab and chemotherapy compared to the desmoplastic HGP patients treated with chemotherapy alone (P = 0.0605, Fig 4d). However, OS was comparable in the replacement HGP patients treated with

bevacizumab and chemotherapy compared to the replacement HGP patients treated with chemotherapy alone (P = 0.433, Fig 4e). Taken together, these data suggest that patients with replacement HGP liver metastases achieve less clinical benefit from bevacizumab than patients with desmoplastic HGP liver metastases.

A comparison of the replacement group with the desmoplastic group showed that the patients were similar in terms of their clinical characteristics (Supplementary Table S8). However, the interval between last dose of therapy and resection tended to be longer in the replacement group compared to the desmoplastic group (P = 0.030). We also examined for differences in clinical characteristics between the bev-chemo treated cohort and the cohort treated with chemotherapy alone (Supplementary Table S9). The cohorts were similar except for a larger proportion of patients receiving irinotecan-based chemotherapy in the bev-chemo cohort compared to the chemotherapy alone cohort (P = 0.019).

When stratifying patients based on their liver metastasis HGPs, only two patients were allocated to the predominant pushing group (one patient treated with bev-chemo and one patient treated with chemotherapy alone). Both of these patients died within 2 years of diagnosis of liver metastasis (Figure 4b,c). This is consistent with the findings of a previous study, which showed that the pushing HGP is an independent predictor of poor overall survival at 2 years of follow-up[20]. It is therefore possible that the pushing HGP of CRCLMs is associated with a poor outcome regardless of the treatment modality utilized.

The replacement HGP is prevalent in breast cancer liver metastases

Thus far, disappointing results have been obtained with anti-angiogenic therapy in metastatic breast cancer[5,6]. Therefore, we also examined the HGPs in breast cancer liver metastasis samples obtained from 17 patients (for patient details see Supplementary Table S10). The replacement HGP was predominant in 16 of 17 cases examined, with only one case presenting with a predominant desmoplastic HGP (Figure 5a). Further histopathological characterization of replacement HGP BCLMs was also performed (Figure 5b-g). Breast cancer cells colonized the liver by replacing resident hepatocytes (Figure 5d) with no desmoplastic stroma present at the tumor-liver interface (Figure 5e). The vascular architecture of the adjacent liver was preserved at the tumor-liver interface (Figure 5f) and the co-option of sinusoidal vessels was observed (Figure 6g). These data show that the replacement HGP, which vascularizes by vessel co-option, predominates in breast cancer liver metastases.

Combined inhibition of vessel co-option and angiogenesis is more effective than inhibition of angiogenesis alone

Vessel co-option in the liver requires the infiltration of cancer cells into the normal liver parenchyma (for example see Fig. 2). We therefore reasoned that cancer cell motility may be required for vessel co-option. The Arp2/3 complex, which mediates the nucleation of actin filaments, has been previously implicated in the motility and invasion of both breast and colorectal cancer cells[21-23]. In order to confirm Arp2/3 expression in human liver metastases, we performed staining for the Arp2/3 subunit ARPC3 using a well-validated antibody. ARPC3 was expressed in cancer cells in all human specimens we examined. Moreover, ARPC3 expression was significantly higher in replacement HGP metastases when compared to desmoplastic HGP metastases (Supplementary Fig S8).

To then address whether cancer cell motility mediated by Arp2/3 could play a functional role in the process of vessel co-option *in vivo*, we utilized a preclinical model where HT29 colorectal cancer cells are directly injected into mouse liver (Supplementary Fig. S9). This model is commonly used to replicate the advanced stage of CRCLMs where patients are treated in the metastatic setting[24-26]. Importantly, the CRCLMs generated in this model have a mixed HGP, being mainly composed of replacement HGP areas (Fig. 6a) and, to a lesser extent, desmoplastic HGP areas (Fig. 6b), thus recapitulating the two prevalent HGPs observed in human CRCLMs. We knocked-down ARPC3 expression in HT29 cells using two independent shRNA oligonucleotides. Knockdown of ARPC3 significantly suppressed the migration of HT29 cells (Fig. 6c,d) without any confounding effect on cell proliferation (Supplementary Fig. S10). Most importantly, knockdown of ARPC3 significantly decreased the replacement HGP *in vivo*, whilst significantly increasing the desmoplastic HGP (Fig. 6e). These data confirm that suppression of Arp2/3-mediated cancer cell motility inhibits the replacement HGP *in vivo* and therefore also blocks the ability of these tumors to co-opt pre-existing vessels *in vivo.*

We then evaluated whether combined inhibition of vessel co-option and angiogenesis is more effective at limiting tumor growth when compared to angiogenesis inhibition alone. Mice with established control- or ARPC3-knockdown tumors were treated with the VEGF-A inhibitory antibody B20-4.1.1[27] combined with capecitabine (Fig. 6f-h). In control tumors, which have a predominantly replacement HGP (Fig. 6f), no significant inhibition of tumor burden was observed in response to treatment when compared to vehicle control (Fig. 6g). However, in ARPC3 knockdown tumors, which have a predominantly desmoplastic HGP (Fig. 6f), tumor burden was significantly suppressed by treatment (Fig. 6g). In addition, although treatment with B20-4.1.1 led to a reduced tumor vessel density in both control- and ARPC3 knockdown-tumors, this effect was more pronounced when vessel co-option was also suppressed by knockdown of ARPC3 (Fig. 6h, Supplementary Fig. S11).

The administration of capecitabine alone did not significantly suppress tumor burden or tumor vessel density in either control- or ARPC3-knockdown tumors (Supplementary Fig S12). These data suggest that simultaneous inhibition of angiogenesis and vessel co-option may be a more effective strategy for the treatment of liver metastasis than current strategies that target angiogenesis alone.

Discussion

When cancers metastasize to highly vascular organs (including the liver) they can sometimes utilize vessel co-option, instead of angiogenesis, as a mechanism to obtain a vascular supply[10]. Here we addressed whether vessel co-option is a significant mechanism of resistance to anti-angiogenic therapy in patients with colorectal cancer liver metastases. We found that: (a) vessel co-option occurs in ~50% of lesions we examined, (b) metastases that utilize vessel co-option respond poorly to bev-chemo, (c) vessel co-option is prevalent in patients that progress following treatment with bev-chemo, and (d) patients with metastases that utilize vessel co-option obtain less clinical benefit from bev-chemo in terms of overall survival. These observations confirm that vessel co-option can blunt the therapeutic benefit achieved with anti-angiogenic therapy in metastatic colorectal cancer.

Our findings also have relevance for breast cancer. Phase 3 trials of bevacizumab combined with chemotherapy in metastatic breast cancer have consistently failed demonstrate a survival benefit for the addition of bevacizumab[28-32]. Here we found that the majority of breast cancer liver metastases utilize vessel co-option. In addition, vessel co-option occurs in breast cancer metastases to the lymph nodes[33,34], skin[35], lungs[7,36,37] and brain[38-40]. The prevalence of vessel co-option in breast cancer may explain, at least in part, why anti-angiogenic therapy has been a disappointing therapeutic approach in this cancer.

Biomarkers that are predictive of response to anti-angiogenic therapy in patients remain elusive[6,11,41]. Our data suggest that patients who present with desmoplastic HGP liver metastases may derive more benefit from bevacizumab than patients who present with replacement HGP liver metastases, which identifies the HGPs as potential biomarkers for anti-angiogenic therapy. There are some characteristics that are present on high resolution MRI and CT imaging of the liver that might be exploited to determine the HGPs of liver metastases prior to treatment. By using imaging to identify liver metastasis HGPs in this way, it may eventually be

possible to select-out the patients with desmoplastic HGP liver metastases who are more likely to benefit from anti-angiogenic therapy.

However, in the longer term, we believe that therapeutic strategies which can block vessel co-option in tumors should also be developed. In this regard, here we show that knockdown of Arp2/3-mediated cancer cell motility suppresses vessel co-option in a preclinical model of advanced liver metastasis. Moreover, we recently showed that acquired resistance to the anti-angiogenic drug sorafenib in hepatocellular carcinoma occurs due to increased cancer cell invasion in the liver, which mediates co-option of pre-existing liver vessels[42]. Taken together, these data suggest a key role for cancer cell motility in the process of vessel co-option and that targeting cancer cell motility might be an effective means to block vessel co-option in tumors.

In the current manuscript, we also present the first preclinical evidence that combined inhibition of angiogenesis and vessel co-option is more effective at controlling tumour burden than targeting either mechanism alone. We propose therefore that therapies which are designed to inhibit both angiogenesis and vessel co-option should be explored in patients, as these may yield greater therapeutic benefit than current therapies that are designed to target angiogenesis alone.

Acknowledgments

The study was supported by Breakthrough Breast Cancer (recently merged with Breast Cancer Campaign forming Breast Cancer Now) and NHS funding to the NIHR Biomedical Research Centre at RM / ICR (London), the Liver Disease Biobank (Montreal) and De Stichting tegen Kanker (Antwerp). We thank the Liver Metastasis Research Network, Ian Hart, Kairbaan Hodivala-Dilke, Clare Isacke, Robert Kerbel and Andrew Tutt for critical comments on the work. We thank Xianming Tan and James Campbell for assistance with statistical analysis and Mat Balazsi for assistance with digital pathology.

References

1. Ferrara, N., Hillan, K.J., Gerber, H.P. & Novotny, W. Discovery and development of bevacizumab, an anti-VEGF antibody for treating cancer. *Nat Rev Drug Discov* **3**, 391-400 (2004).
2. Kerbel, R.S. Tumor angiogenesis. *N Engl J Med* **358**, 2039-2049 (2008).
3. Hurwitz, H.*, et al.* Bevacizumab plus irinotecan, fluorouracil, and leucovorin for metastatic colorectal cancer. *The New England journal of medicine* **350**, 2335-2342 (2004).
4. Cunningham, D.*, et al.* Bevacizumab plus capecitabine versus capecitabine alone in elderly patients with previously untreated metastatic colorectal cancer (AVEX): an open-label, randomised phase 3 trial. *Lancet Oncol* **14**, 1077-1085 (2013).
5. Ebos, J.M. & Kerbel, R.S. Antiangiogenic therapy: impact on invasion, disease progression, and metastasis. *Nat Rev Clin Oncol* **8**, 210-221 (2011).
6. Vasudev, N.S. & Reynolds, A.R. Anti-angiogenic therapy for cancer: current progress, unresolved questions and future directions. *Angiogenesis* **17**, 471-494 (2014).
7. Pezzella, F.*, et al.* Angiogenesis in primary lung cancer and lung secondaries. *Eur J Cancer* **32A**, 2494-2500 (1996).
8. Vermeulen, P.B.*, et al.* Liver metastases from colorectal adenocarcinomas grow in three patterns with different angiogenesis and desmoplasia. *The Journal of pathology* **195**, 336-342 (2001).
9. Dome, B., Hendrix, M.J., Paku, S., Tovari, J. & Timar, J. Alternative vascularization mechanisms in cancer: Pathology and therapeutic implications. *Am J Pathol* **170**, 1-15 (2007).
10. Donnem, T.*, et al.* Vessel co-option in primary human tumors and metastases: an obstacle to effective anti-angiogenic treatment? *Cancer Med* **2**, 427-436 (2013).
11. Jayson, G.C., Kerbel, R., Ellis, L.M. & Harris, A.L. Antiangiogenic therapy in oncology: current status and future directions. *Lancet* (2016).
12. Adams, R.B.*, et al.* Selection for hepatic resection of colorectal liver metastases: expert consensus statement. *HPB (Oxford)* **15**, 91-103 (2013).
13. Van den Eynden, G.G.*, et al.* The multifaceted role of the microenvironment in liver metastasis: biology and clinical implications. *Cancer research* **73**, 2031-2043 (2013).
14. Stessels, F.*, et al.* Breast adenocarcinoma liver metastases, in contrast to colorectal cancer liver metastases, display a non-angiogenic growth pattern that preserves the stroma and lacks hypoxia. *Br J Cancer* **90**, 1429-1436 (2004).
15. Gruenberger, B.*, et al.* Bevacizumab, capecitabine, and oxaliplatin as neoadjuvant therapy for patients with potentially curable metastatic colorectal cancer. *J Clin Oncol* **26**, 1830-1835 (2008).
16. Chaudhury, P.*, et al.* Perioperative chemotherapy with bevacizumab and liver resection for colorectal cancer liver metastasis. *HPB* **12**, 37-42 (2010).
17. Wong, R.*, et al.* A multicentre study of capecitabine, oxaliplatin plus bevacizumab as perioperative treatment of patients with poor-risk colorectal liver-only metastases not selected for upfront resection. *Ann Oncol* **22**, 2042-2048 (2011).
18. Chun, Y.S.*, et al.* Association of computed tomography morphologic criteria with pathologic response and survival in patients treated with bevacizumab for colorectal liver metastases. *JAMA* **302**, 2338-2344 (2009).
19. Boonsirikamchai, P.*, et al.* CT findings of response and recurrence, independent of change in tumor size, in colorectal liver metastasis treated

with bevacizumab. *AJR. American journal of roentgenology* **197**, W1060-1066 (2011).
20. Van den Eynden, G.G.*, et al.* The histological growth pattern of colorectal cancer liver metastases has prognostic value. *Clin Exp Metastasis* **29**, 541-549 (2012).
21. Nurnberg, A., Kitzing, T. & Grosse, R. Nucleating actin for invasion. *Nature reviews* **11**, 177-187 (2011).
22. Otsubo, T.*, et al.* Involvement of Arp2/3 complex in the process of colorectal carcinogenesis. *Modern pathology : an official journal of the United States and Canadian Academy of Pathology, Inc* **17**, 461-467 (2004).
23. Iwaya, K.*, et al.* Correlation between liver metastasis of the colocalization of actin-related protein 2 and 3 complex and WAVE2 in colorectal carcinoma. *Cancer science* **98**, 992-999 (2007).
24. Kopetz, S.*, et al.* Synergistic activity of the SRC family kinase inhibitor dasatinib and oxaliplatin in colon carcinoma cells is mediated by oxidative stress. *Cancer research* **69**, 3842-3849 (2009).
25. Nyati, M.K.*, et al.* The potential of 5-fluorocytosine/cytosine deaminase enzyme prodrug gene therapy in an intrahepatic colon cancer model. *Gene therapy* **9**, 844-849 (2002).
26. Gray, M.J.*, et al.* Therapeutic targeting of Id2 reduces growth of human colorectal carcinoma in the murine liver. *Oncogene* **27**, 7192-7200 (2008).
27. Liang, W.C.*, et al.* Cross-species vascular endothelial growth factor (VEGF)-blocking antibodies completely inhibit the growth of human tumor xenografts and measure the contribution of stromal VEGF. *J Biol Chem* **281**, 951-961 (2006).
28. Miller, K.D.*, et al.* Randomized phase III trial of capecitabine compared with bevacizumab plus capecitabine in patients with previously treated metastatic breast cancer. *J Clin Oncol* **23**, 792-799 (2005).
29. Miller, K.*, et al.* Paclitaxel plus bevacizumab versus paclitaxel alone for metastatic breast cancer. *The New England journal of medicine* **357**, 2666-2676 (2007).
30. Miles, D.W.*, et al.* Phase III study of bevacizumab plus docetaxel compared with placebo plus docetaxel for the first-line treatment of human epidermal growth factor receptor 2-negative metastatic breast cancer. *J Clin Oncol* **28**, 3239-3247 (2010).
31. Robert, N.J.*, et al.* RIBBON-1: randomized, double-blind, placebo-controlled, phase III trial of chemotherapy with or without bevacizumab for first-line treatment of human epidermal growth factor receptor 2-negative, locally recurrent or metastatic breast cancer. *J Clin Oncol* **29**, 1252-1260 (2011).
32. Brufsky, A.M.*, et al.* RIBBON-2: a randomized, double-blind, placebo-controlled, phase III trial evaluating the efficacy and safety of bevacizumab in combination with chemotherapy for second-line treatment of human epidermal growth factor receptor 2-negative metastatic breast cancer. *J Clin Oncol* **29**, 4286-4293 (2011).
33. Naresh, K.N., Nerurkar, A.Y. & Borges, A.M. Angiogenesis is redundant for tumour growth in lymph node metastases. *Histopathology* **38**, 466-470 (2001).
34. Jeong, H.S.*, et al.* Investigation of the Lack of Angiogenesis in the Formation of Lymph Node Metastases. *J Natl Cancer Inst* **107**(2015).
35. Colpaert, C.G.*, et al.* Cutaneous breast cancer deposits show distinct growth patterns with different degrees of angiogenesis, hypoxia and fibrin deposition. *Histopathology* **42**, 530-540 (2003).
36. Breast-Cancer-Progression-Working-Party. Evidence for novel non-angiogenic pathway in breast-cancer metastasis. *Lancet* **355**, 1787-1788 (2000).

37. Szabo, V.*, et al.* Mechanism of tumour vascularization in experimental lung metastases. *The Journal of pathology* **235**, 384-396 (2015).
38. Carbonell, W.S., Ansorge, O., Sibson, N. & Muschel, R. The vascular basement membrane as "soil" in brain metastasis. *PLoS One* **4**, e5857 (2009).
39. Valiente, M.*, et al.* Serpins promote cancer cell survival and vascular co-option in brain metastasis. *Cell* **156**, 1002-1016 (2014).
40. Bugyik, E.*, et al.* Lack of angiogenesis in experimental brain metastases. *J Neuropathol Exp Neurol* **70**, 979-991 (2011).
41. Jain, R.K.*, et al.* Biomarkers of response and resistance to antiangiogenic therapy. *Nat Rev Clin Oncol* **6**, 327-338 (2009).
42. Kuczynski, E.*, et al.* Co-option of liver vessels and not sprouting angiogenesis drives acquired sorafenib resistance in hepatocellular carcinoma. *Journal of the National Cancer Institute (in press)* (2016).

Figure legends

Figure 1 Correlation between HGP and pathological response in CRC patients treated preoperatively with bevacizumab

a. Diagrams illustrate the morphology of normal liver or the morphology of the tumor-liver interface in liver metastases with a desmoplastic, pushing or replacement HGP (see also Supplementary Fig. S1). **b.** The HGPs and the pathological response to bev-chemo were scored in 59 CRCLMs from 33 patients that were treated preoperatively with bev-chemo at RM. Graph shows % HGP (replacement, desmoplastic, pushing) scored in each individual lesion and the data are grouped by pathological response score: >75%, 50-75%, 25-49% or <25% viable tumor. **c-e.** Examples of H&E-stained specimens from this cohort. In **c**, a lesion scored as >75% viable with HGP score of 100% replacement. Note the close contact between tumor cells and liver parenchyma in the infiltrative replacement HGP (*arrows*). In **d**, a lesion scored as <25% viable with HGP score of 100% desmoplastic. Note the entire circumference of the tumor is desmoplastic (*arrowheads*) and well encapsulated. A large central area of infarct-like necrosis (ILN), indicative of a strong treatment response, is labeled (*asterisks*). In **e**, a lesion scored as <25% viable with a mixed HGP (79% desmoplastic, 19% replacement, 2% pushing). Note the desmoplastic areas (*arrowheads*) and two peripheral nodules with a replacement HGP (*arrows*). Areas of ILN are labeled (*asterisks*). **f.** The HGPs and the pathological response to bev-chemo were scored in 128 CRCLMs from 59 patients treated with bev-chemo at MUHC. Graph shows % HGP (replacement, desmoplastic, pushing) scored in each individual lesion and the data are grouped by pathological response score: >75%, 50-75%, 25-49% or <25% viable tumor. The χ^2-test was used to determine statistical significance (see 2x2 contingency tables in panels **b** and **f**). Scale bars, 1 mm.

Figure 2 Correlation between HGP and morphological response on CT-imaging in patients treated preoperatively with bevacizumab

a-f. Serial CT scans of the liver obtained in patients treated preoperatively with bevacizumab in combination with chemotherapy at RM. Examples of lesions scored as undergoing an optimal**,** partial or absent response (according to morphological response criteria) are shown. **a,b.** Optimal response: CRC liver metastasis in liver segment VII from a 29 year old male (*arrowheads*). In the pre-treatment image (**a**), the lesion has heterogeneous attenuation and a poorly defined tumor-liver interface (group-3 metastasis). The same lesion imaged after 4 cycles of bevacizumab in combination with CAPOX (**b**) now appears as a homogeneous, low attenuation lesion with a sharply defined tumor-liver interface (group-1 metastasis). **c,d.** Partial response: CRC liver metastasis present in liver segment II from a 66 year old female (*arrowheads*). In the pre-treatment image (**c**), the lesion has heterogeneous attenuation and a poorly defined tumor-liver interface (group-3 metastasis). The same lesion imaged after 4 cycles of bevacizumab in combination with CAPOX (**d**) now appears to be less heterogeneous in terms of attenuation and has a better-defined tumor-liver interface (group-2 metastasis). **e,f.** Absent response: CRC liver metastasis present in liver segment VI from 67 year old male (*arrowheads*). In the pre-treatment image (**e**), the lesion has heterogeneous attenuation and a poorly defined tumor-liver interface (group-3 metastasis). The same lesion imaged after 6 cycles of bevacizumab in combination with FOLFIRI (**f**) is still classed as a group-3 metastasis. **g.** Morphological response criteria (absent response, AR; partial response, PR; optimal response, OR) and HGP were scored in 52 liver metastases of CRC resected from 31 patients treated preoperatively with bevacizumab and chemotherapy at RM. Graph shows the % HGP scored in each individual lesion (replacement, desmoplastic, pushing). Lesions are grouped according to response: AR, PR or OR. Lesions scored as having an absent morphological response (AR) were considered to be poor responders, whilst those undergoing a partial (PR) or optimal (OR) morphological response were considered to be good responders. Lesions with ≥50% replacement HGP were significantly enriched in the group of lesions undergoing a poor radiological response according to morphological response criteria (P=0.006). The χ^2-test was used to determine statistical significance (see 2x2 contingency table in panel **g**).

Figure 3 Cancer cells infiltrate the hepatic plates and co-opt sinusoidal blood vessels in the replacement HGP

a. An area of normal liver is shown. Staining for hepatocyte specific antigen (HSA, green) to detect hepatocytes and collagen-3 (col-3, red) to detect sinusoidal blood vessels (SV). **b-d.** Staining for cancer cells (CK, red) and hepatocytes (HSA, green) at the tumor-liver interface (**b,c**) and within the tumor mass (**d**) in the replacement HGP. Displaced hepatocytes are marked (*arrowheads*). **e-g.** Staining for cytokeratin 20 (CK20, brown) to identify cancer cells and CD31 to identify vessels (blue). Note vessels where one end of the vessel is physically located in the liver parenchyma (*arrows*) and the other end is surrounded by cancer cells (*arrowheads*). Asterisk, tumor; Lv, normal liver; SV, sinusoidal blood vessel. Scale bars, 25 μM.

Figure 4 The replacement HGP occurs in progressive disease and is associated with a poor outcome in patients treated with bevacizumab

a. Left: HGPs in CRCLMs resected from patients that did not receive preoperative therapy (untreated CRCLMs). n = 32 lesions from 19 MUHC patients. Middle: HGPs in lesions that were resected from patients treated preoperatively with bev-chemo and that were detected on baseline imaging prior to therapy (pre-existing CRCLMs). n = 128 lesions from 59 MUHC patients. Right: HGPs in new CRCLMs (lesions that were absent from baseline pre-treatment liver scans, but presented after the initiation of bev-chemo treatment and were subsequently resected). n = 35 lesions from 13 MUHC patients. Graphs show % replacement (R), desmoplastic (D) and pushing (P) HGP per lesion ± SEM. The % replacement HGP was significantly increased in new CRCLMs (right panel) when compared to both untreated CRCLMs (left panel) and treated pre-existing CRCLMs (middle panel) (**P*<0.001), which was mirrored by a concomitant significant decrease in the desmoplastic HGP (**P*<0.001) (Kruskal-Wallis test). **b.** Kaplan-Meier estimates of overall survival for 62 MUHC patients treated preoperatively with bev-chemo. Patients were stratified into three groups: predominant replacement HGP (26 patients), predominant desmoplastic HGP (35 patients) and predominant pushing HGP (1 patient). **c.** Kaplan-Meier survival estimates for 29 MUHC patients treated preoperatively with chemotherapy alone. Patients were stratified into three groups: predominant replacement HGP (12 patients), predominant desmoplastic HGP (16 patients) and predominant pushing HGP (1 patient). **d.** Kaplan-Meier estimates of overall survival for 51 MUHC patients with a predominant desmoplastic HGP. Patients were stratified into two groups: desmoplastic HGP treated with bev-chemo (35 patients) and desmoplastic HGP treated with chemotherapy alone (16 patients). **e.** Kaplan-Meier estimates of overall survival for 38 MUHC patients with a predominant replacement HGP. Patients were stratified into two groups: replacement HGP treated with bev-chemo (26 patients) and replacement HGP treated with chemotherapy alone (12 patients). The Log-Rank test was used to determine statistical significance.

Figure 5 The replacement HGP predominates in breast cancer liver metastases

a. The HGPs were examined in breast cancer liver metastases (BCLMs) from 17 patients. Graph shows the % HGP (replacement, desmoplastic, pushing) scored in each case. The cases are grouped by intrinsic subtype of breast cancer. Lum A, luminal A; Lum B (HER2-), luminal B HER2 negative; Lum B (HER2+), luminal B HER2 positive; TN, triple negative.

b-g. Morphology of the replacement growth pattern of BCLMs. Diagram of the tumor-liver interface in the replacement HGP (**b**). H&E-stained human BCLM sample illustrating the tumor-liver interface (**c**). Co-staining for hepatocyte specific antigen (HSA) to label hepatocytes and pan-cytokeratin (CK) to label cancer cells confirms that breast cancer cells infiltrate the liver parenchyma and replace hepatocytes in BCLM (**d**). Co-staining for alpha smooth muscle actin (αSMA) to label fibroblasts and CK confirms the absence of a desmoplastic stroma in BCLM (**e**). Co-staining for collagen-3 (col-3) to label sinusoidal vessels and CK shows that the vascular architecture of the adjacent liver is preserved at the tumor-liver interface in BCLM (**f**). Co-staining for CD31 to label blood vessels and cytokeratin 19 (CK19) to label cancer cells confirms the infiltrative pattern of tumor growth that facilitates vessel co-option (**g**). Asterisk, cancer cells; Lv, normal liver. Scale bars, 50 μM.

Figure 6 Combined inhibition of vessel co-option and angiogenesis is more effective than inhibition of angiogenesis alone

a,b. The replacement and desmoplastic HGPs are recapitulated in a preclinical (HT29 cell line) model of advanced liver metastasis. Areas of replacement (**a**) and desmoplastic (**b**) HGP are shown with staining for H&E, CK and HSA, CK and col-3, CK and αSMA or cytokeratin 20 (CK20) and CD31. **c,d.** Characterization of parental HT29 cells (parent) and HT29 cells transduced with control non-targeting shRNA (control-shRNA) or shRNAs designed to target ARPC3 (ARPC3-shRNA-1, ARPC3-shRNA-2 or ARPC3-shRNA-3). In **c**, ARPC3 expression was quantified by western blotting. Graph shows ARPC3 expression relative to parental HT29 cells ± SEM (n = 3 independent western blots): ARPC3-shRNA-2 and ARPC3-shRNA-3 significantly knockdown ARPC3 expression whereas control-shRNA and ARPC3-shRNA-1 do not. In **d**, cell motility measured by manually tracking cells in time-lapse microscopy movies. Graph shows cell velocity (μm/min) relative to parental HT29 cells ± SEM (n = 30 tracked cells per group pooled from 2 independent experiments). **e.** Quantification of the HGPs in control and ARPC3 knockdown tumors. Graph shows the % replacement (R), desmoplastic (D) and pushing (P) HGP per group ± SEM (n = 6 mice per group). **f-h.** Tumors with normal ARPC3 levels (control-shRNA) or ARPC3 knockdown (ARPC3-shRNA-3) were established in the livers of mice and treated with B20-4.1.1 plus capecitabine (B/C) or vehicle alone (Vh) for two weeks followed by histopathological analysis (n = 8 mice per group). Graph in **f** shows the % HGP per group ± SEM. Graph in **g** shows liver tumor burden expressed in terms of lesion area ± SEM. Graph in **h** shows tumor vessel density in terms of vessels per mm^2 ± SEM. For statistical analysis, Student's t-test (panels **c,g**,**h)** or Mann Whitney U-test (panels **d,e,f**) were used. **P*<0.05, ***P*<0.01 ****P*<0.001, *****P*<0.0001. ns, no significant difference. Asterisk, cancer cells; DS, desmoplastic stroma; Lv, normal liver. Scale bars, 50 μM.

Figure 1

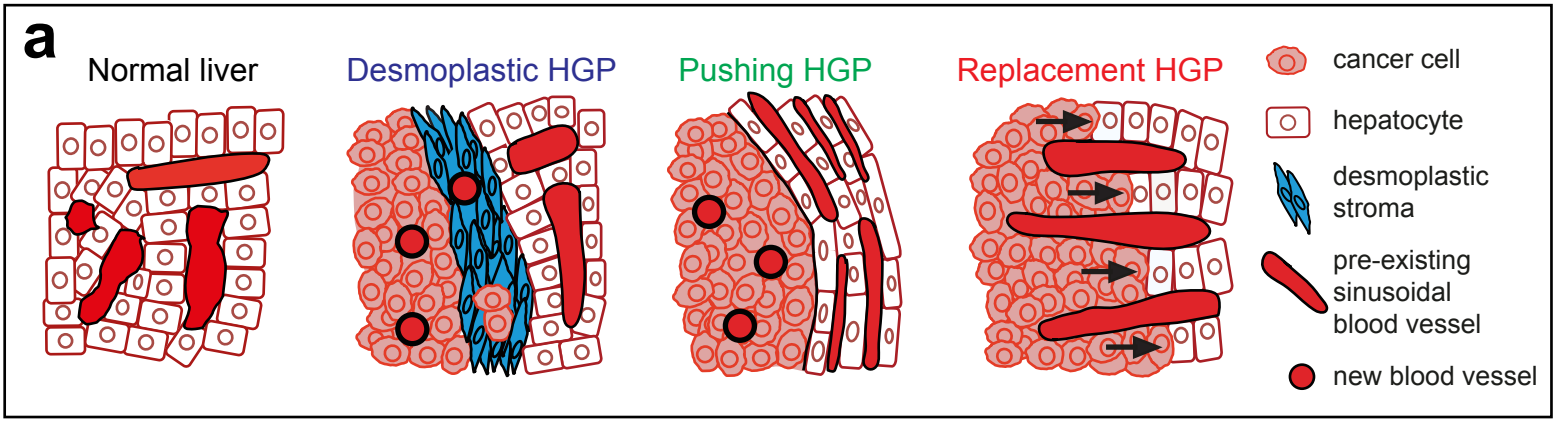

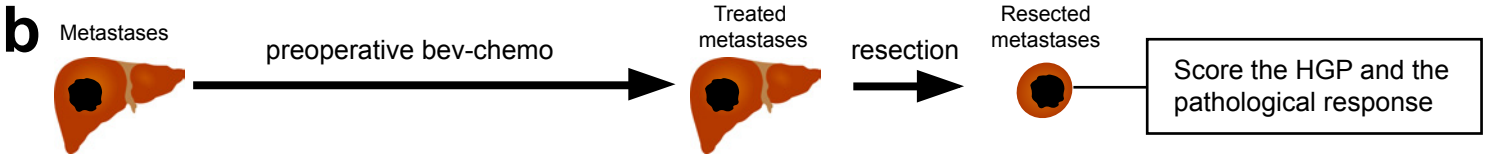

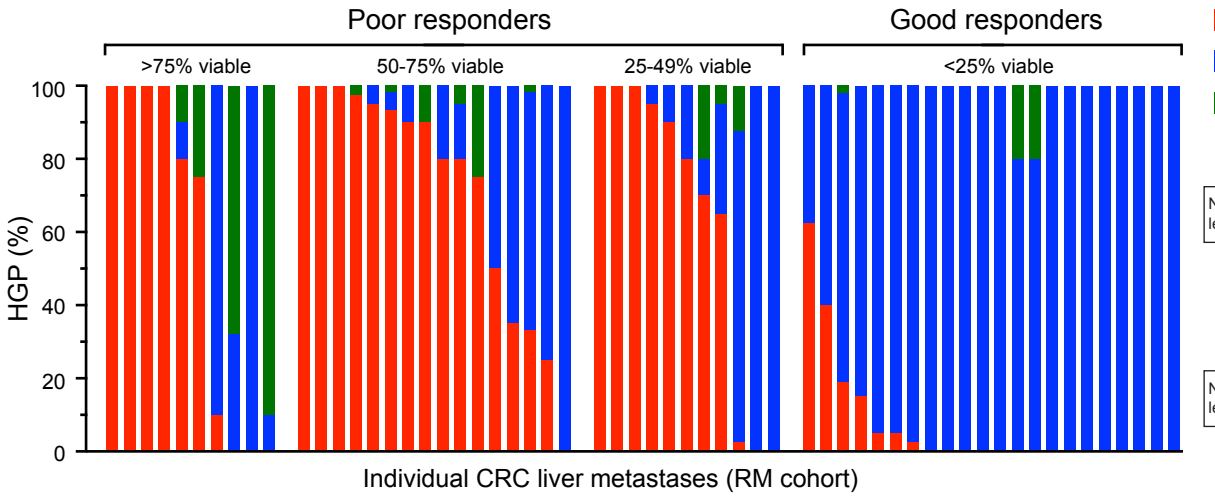

		Response		
		Poor	Good	Total
No. of lesions	<50% replacement	11	21	32
	≥50% replacement	26	1	27
	Total	37	22	59

P<0.001

		Response		
		Poor	Good	Total
No. of lesions	<50% desmoplastic	27	1	28
	≥50% desmoplastic	10	21	31
	Total	37	22	59

P<0.001

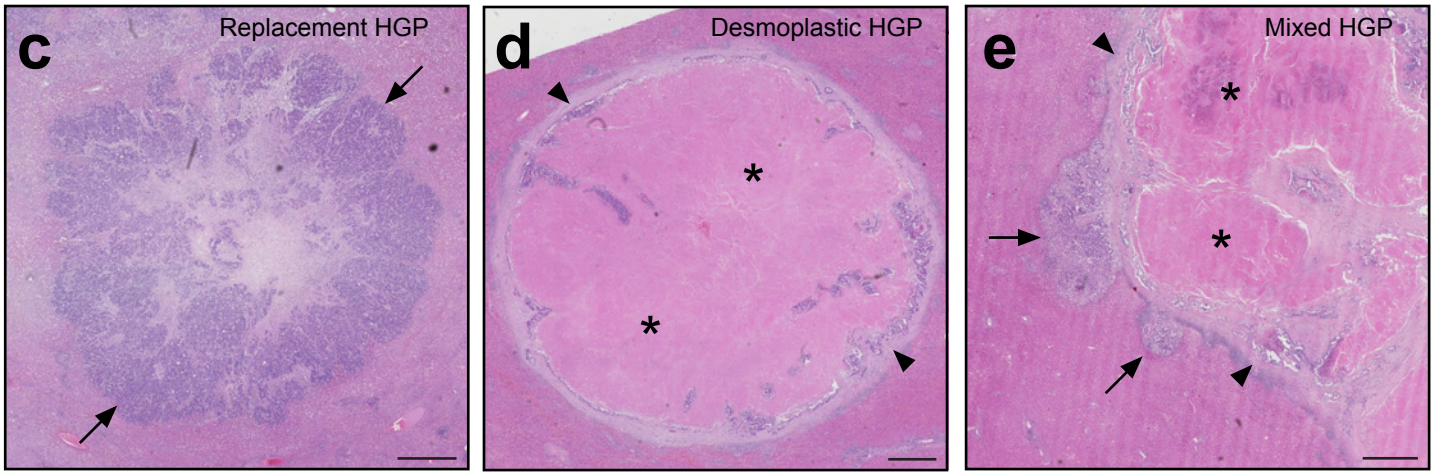

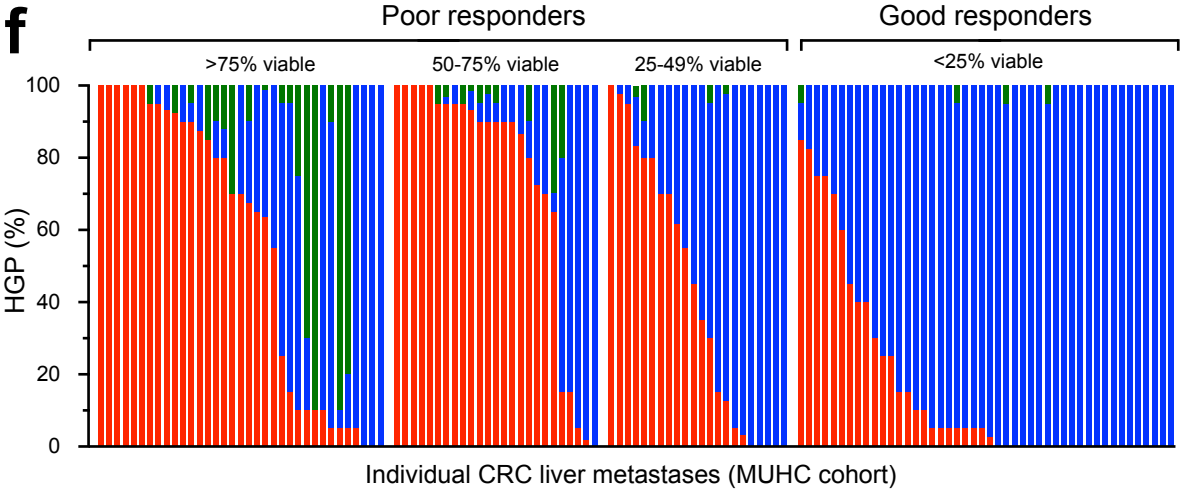

		Response		
		Poor	Good	Total
No. of lesions	<50% replacement	30	40	70
	≥50% replacement	52	6	58
	Total	82	46	128

P<0.001

		Response		
		Poor	Good	Total
No. of lesions	<50% desmoplastic	56	6	62
	≥50% desmoplastic	26	40	66
	Total	82	46	128

P<0.001

Figure 2

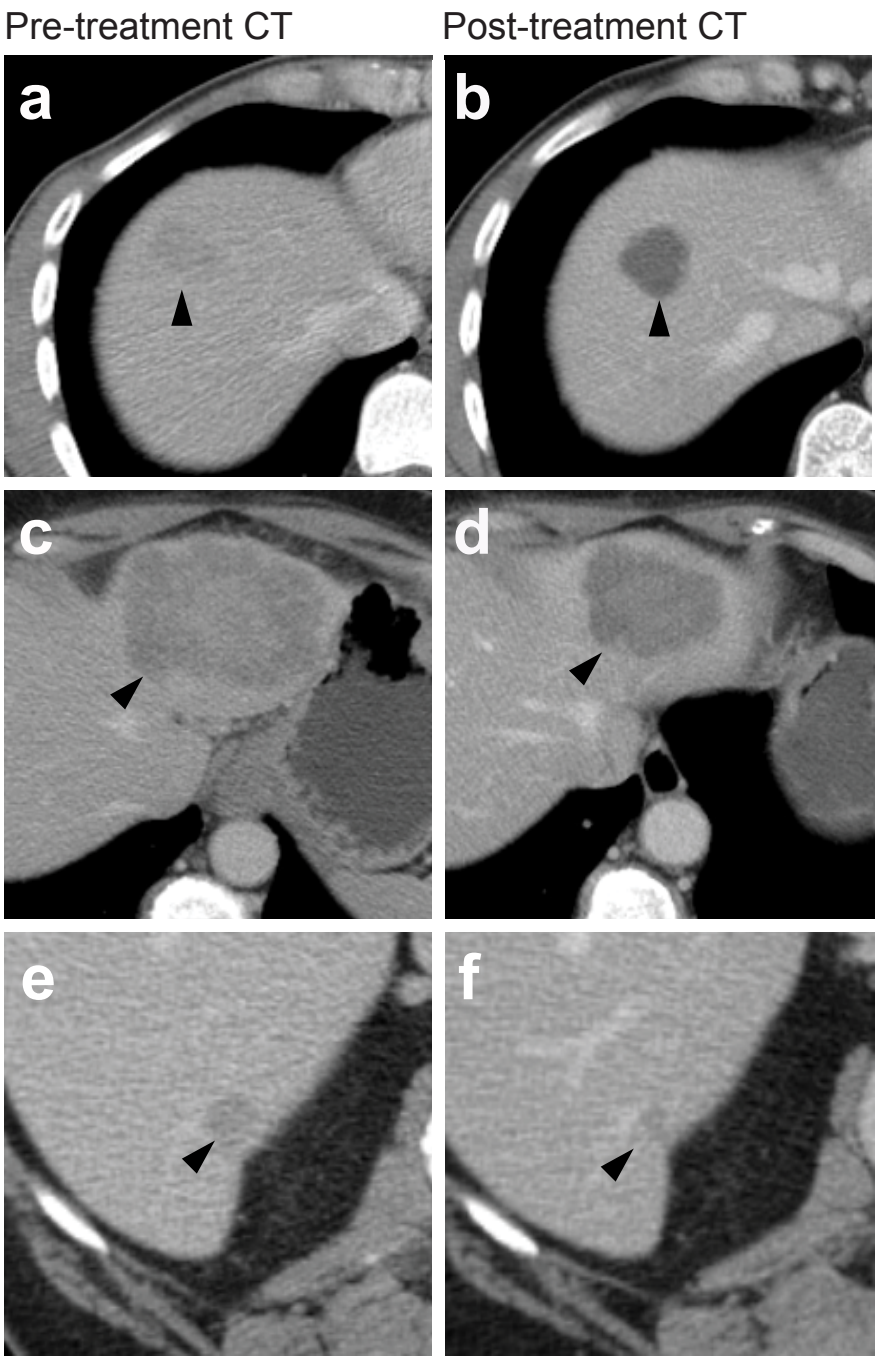

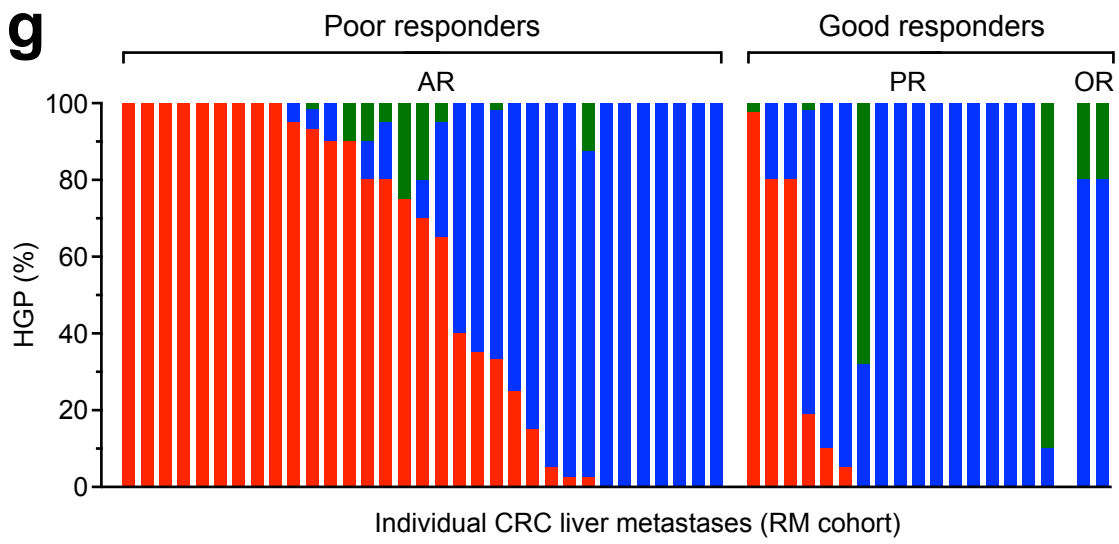

		Response		
		Poor	Good	Total
No. of lesions	<50% replacement	15	16	31
	≥50% replacement	18	3	21
	Total	33	19	52

P= 0.006

Figure 3

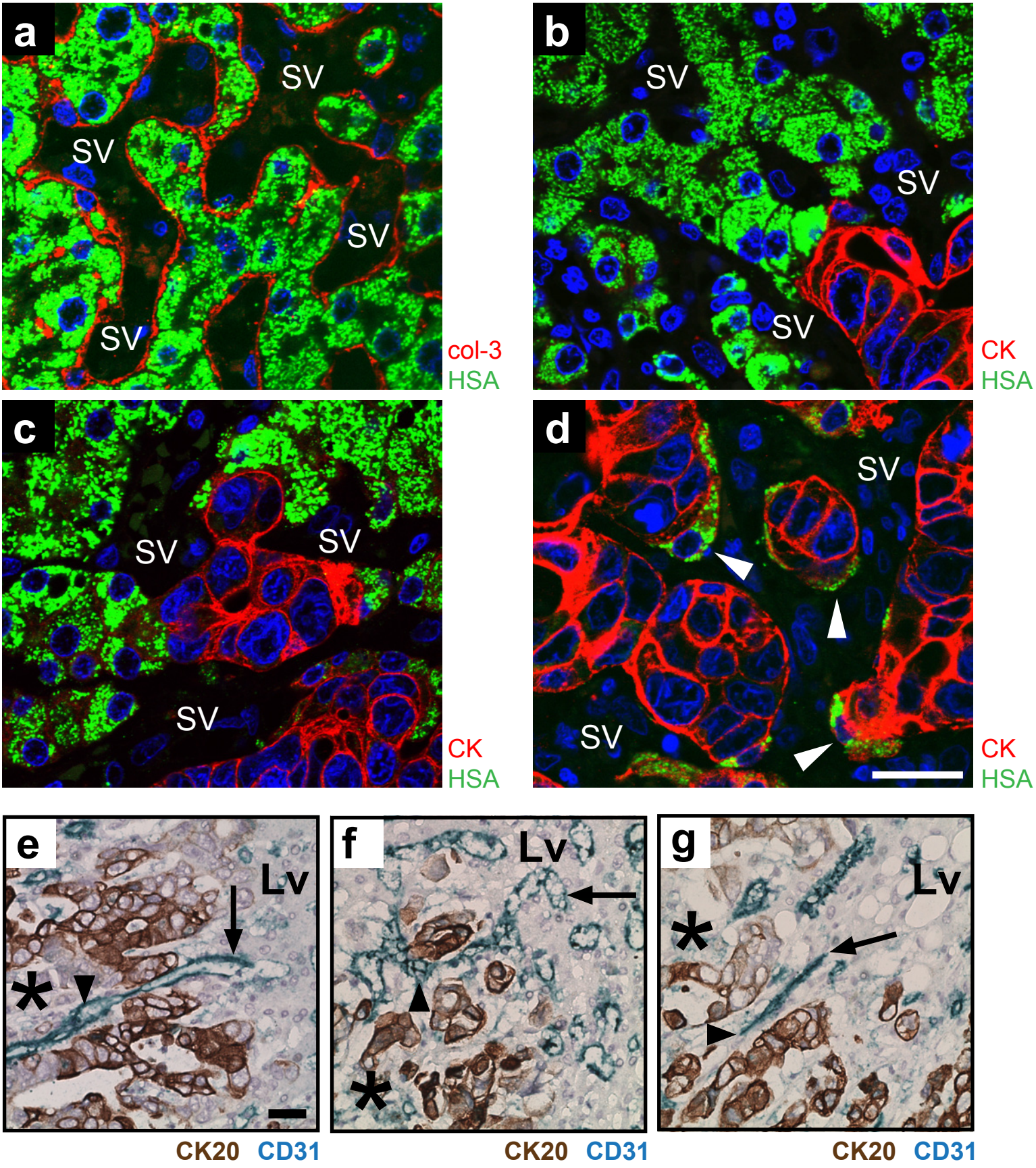
a
SV
SV
SV
SV
col-3
HSA
b
SV
SV
SV
CK
HSA
c
SV
SV
SV
CK
HSA
d
SV
SV
CK
HSA
e
Lv
CK20 CD31
f
Lv
CK20 CD31
g
Lv
CK20 CD31

Figure 4

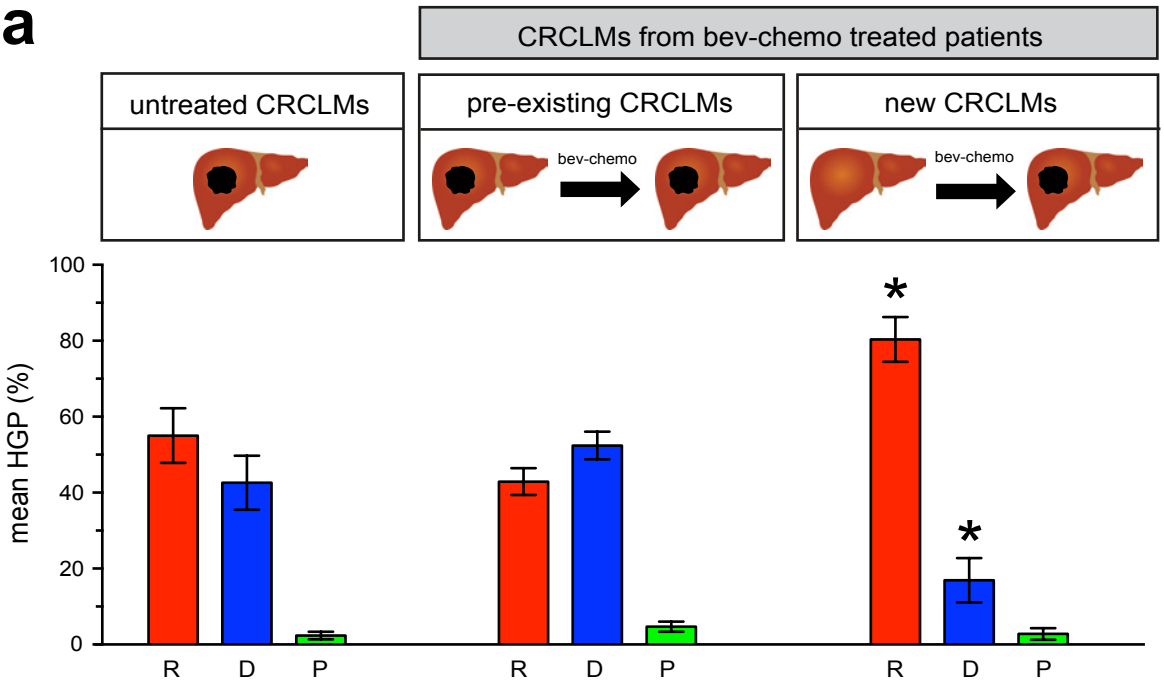

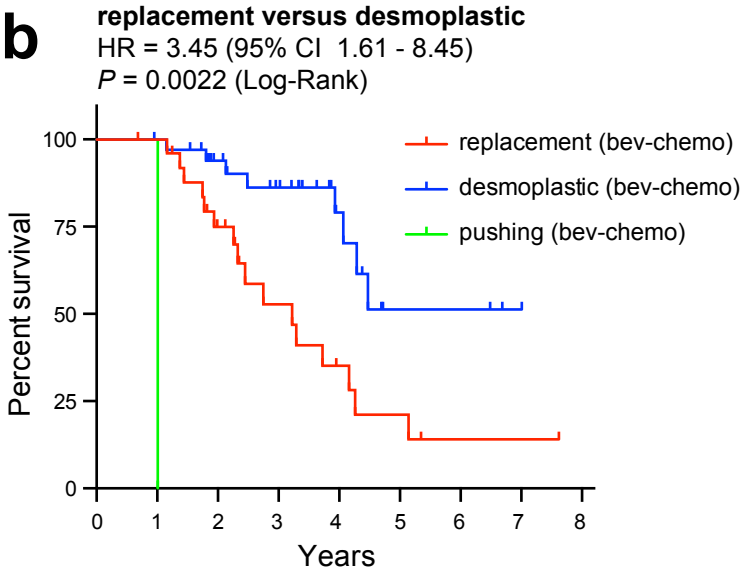

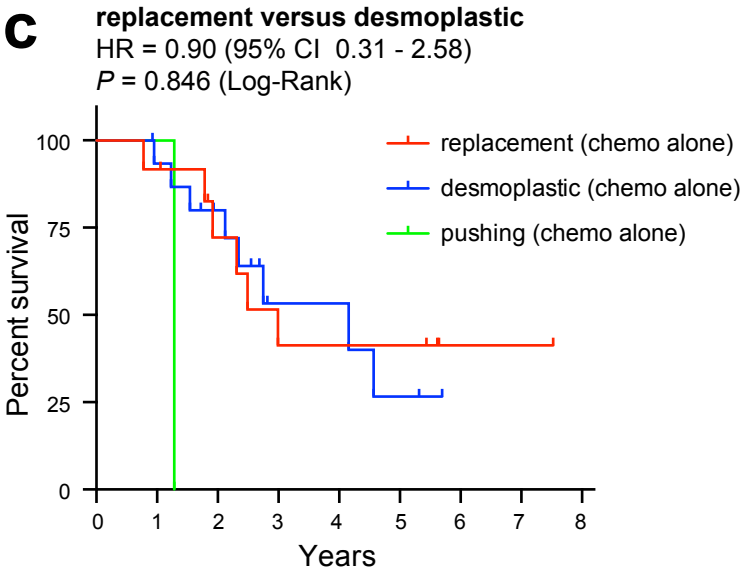

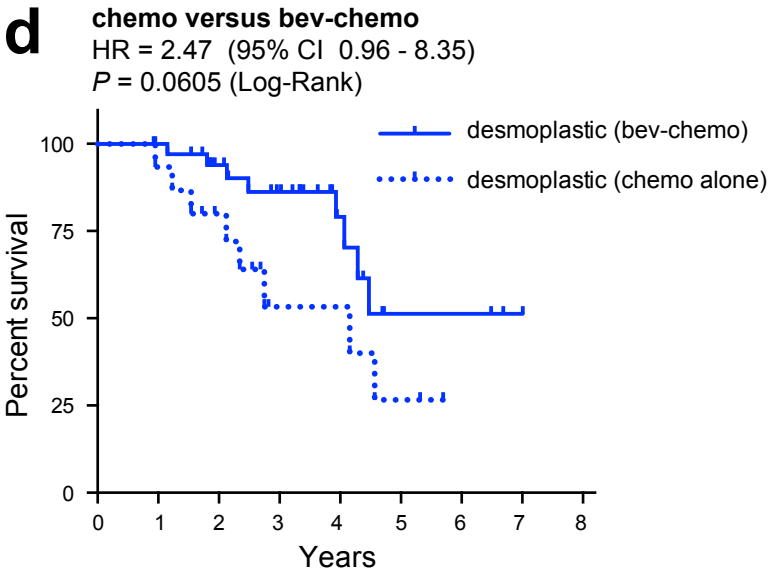

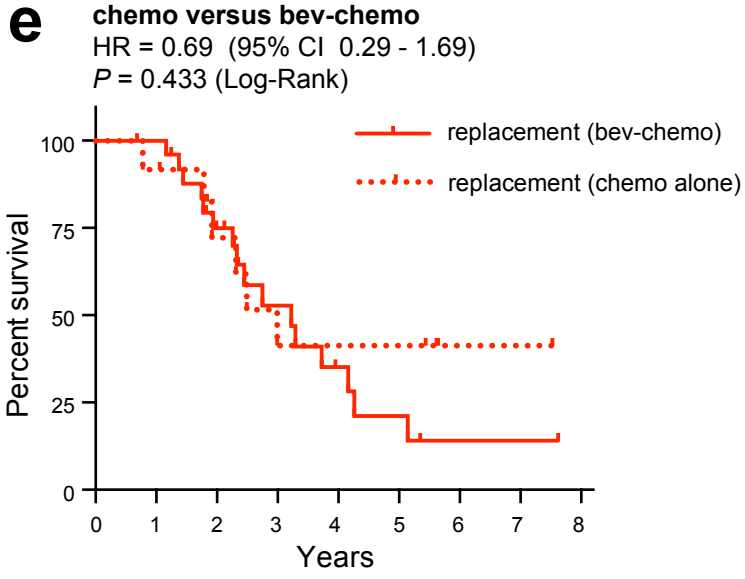

f

Treatment	HGP	n	Median OS	3-year OS	5-year OS
bev-chemo	replacement	26 patients	39.2 months	52.8%	21.1%
bev-chemo	desmoplastic	35 patients	median not reached	86.3%	51.2%
chemo alone	replacement	12 patients	36.4 months	41.3%	41.3%
chemo alone	desmoplastic	16 patients	50.6 months	53.3%	26.7%

Figure 5

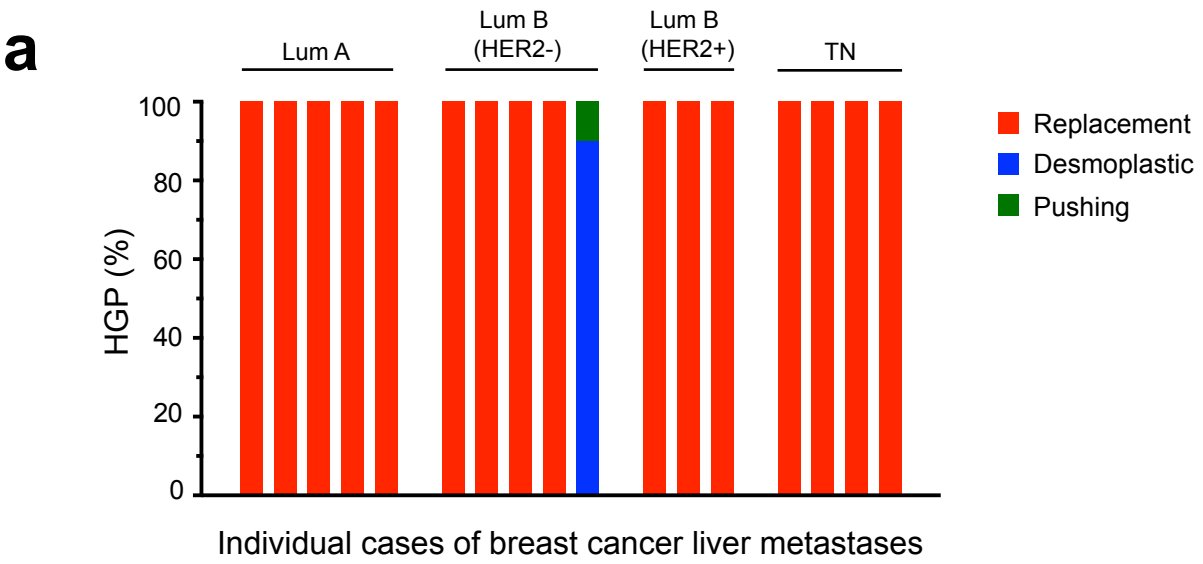
a
Lum A
Lum B (HER2-)
Lum B (HER2+)
TN
100
80
60
40
20
0
HGP (%)
Replacement
Desmoplastic
Pushing
Individual cases of breast cancer liver metastases

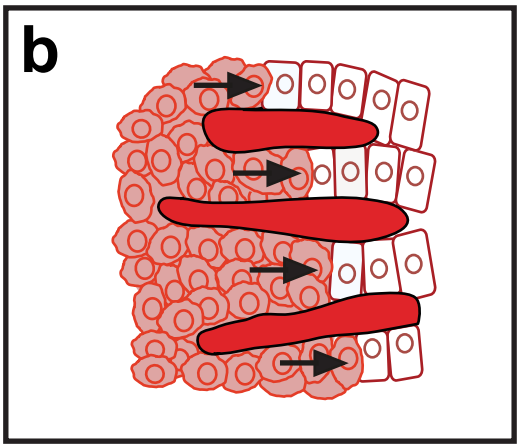
b

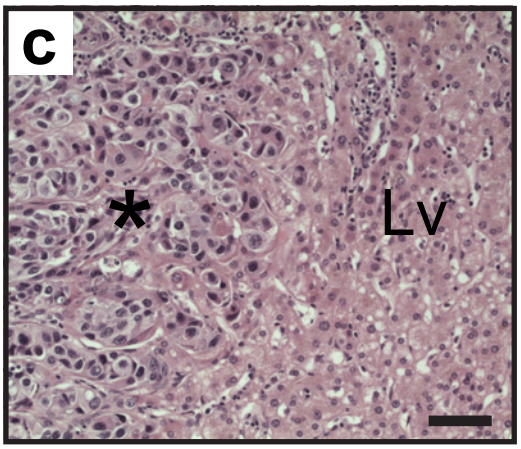
c
*
Lv

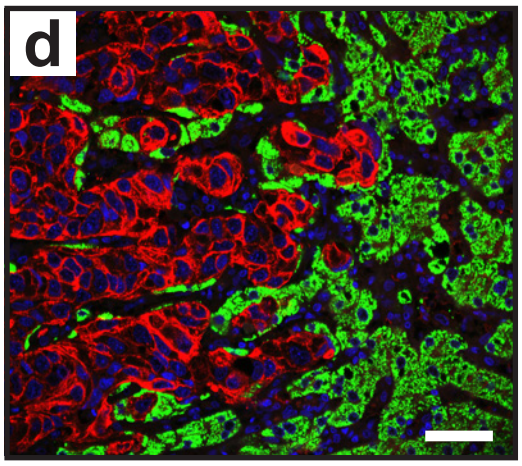
d
CK HSA

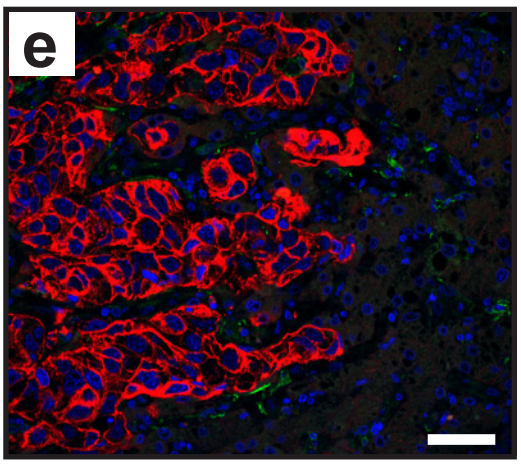
e
CK col-3

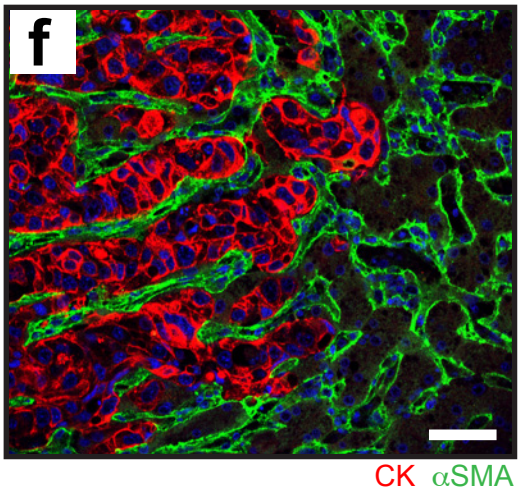
f
CK αSMA

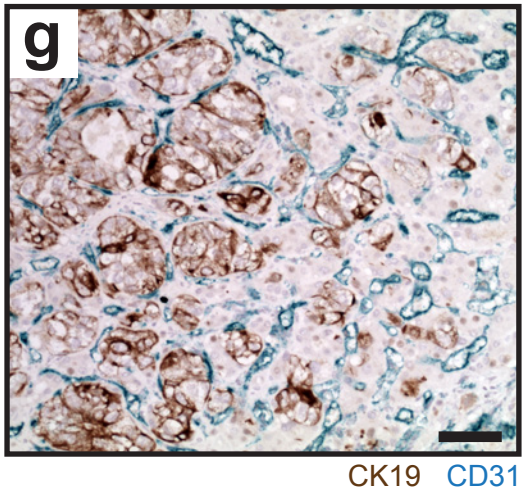
g
CK19 CD31

Figure 6

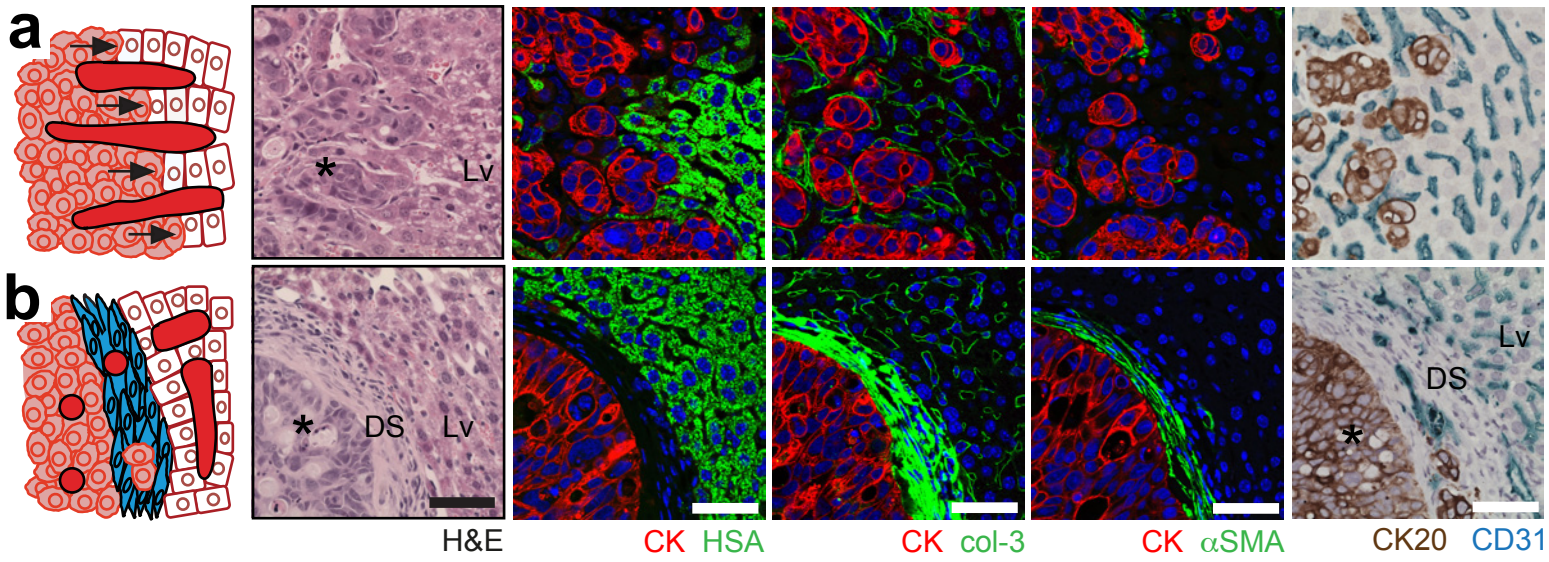
a
b
Lv
DS
H&E
CK HSA
CK col-3
CK αSMA
CK20 CD31

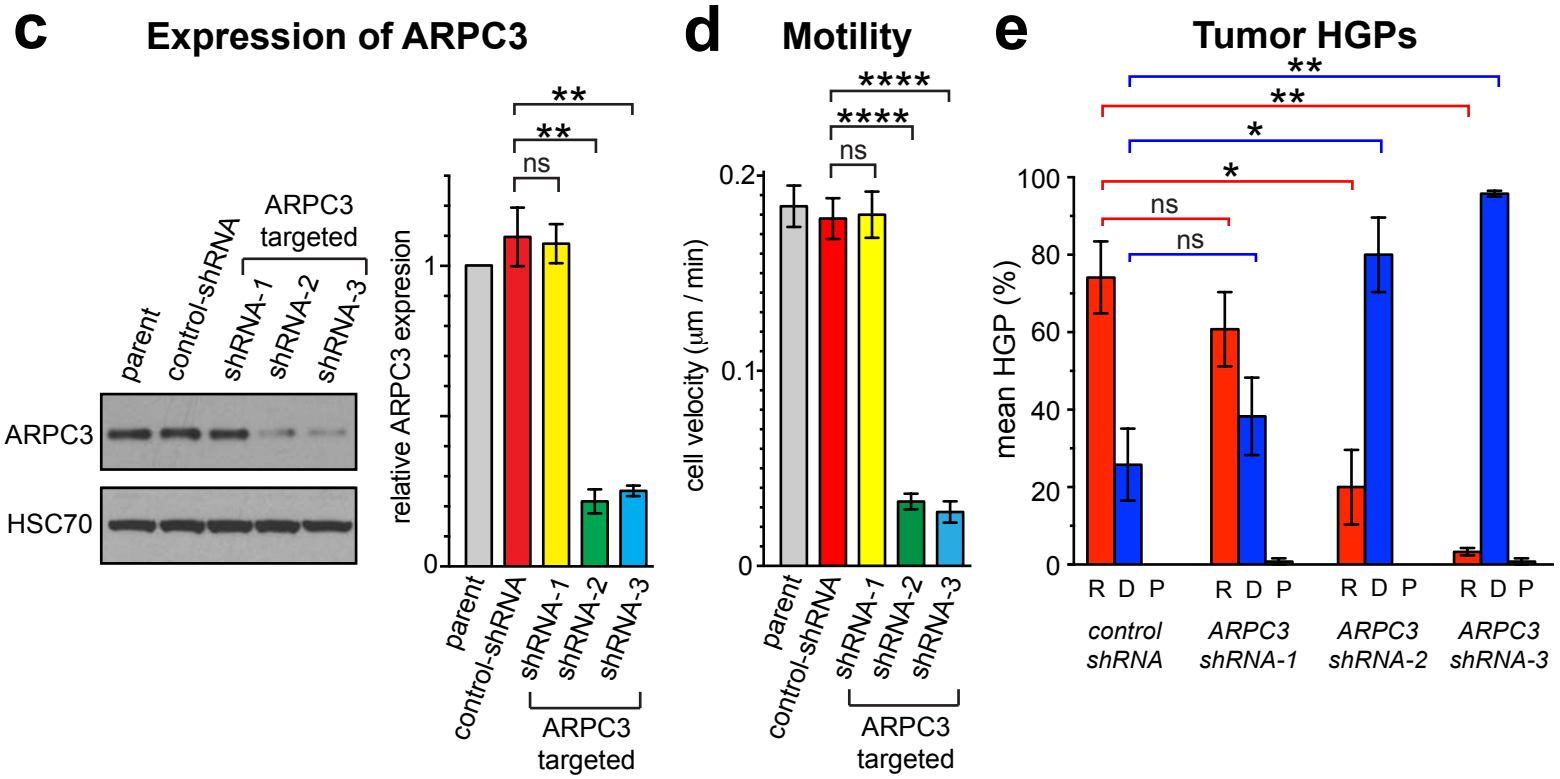
c
Expression of ARPC3
parent
control-shRNA
ARPC3 targeted
shRNA-1
shRNA-2
shRNA-3
ARPC3
HSC70
relative ARPC3 expresion
ns
d
Motility
cell velocity (μm / min)
e
Tumor HGPs
mean HGP (%)
R D P
control shRNA
ARPC3 shRNA-1
ARPC3 shRNA-2
ARPC3 shRNA-3

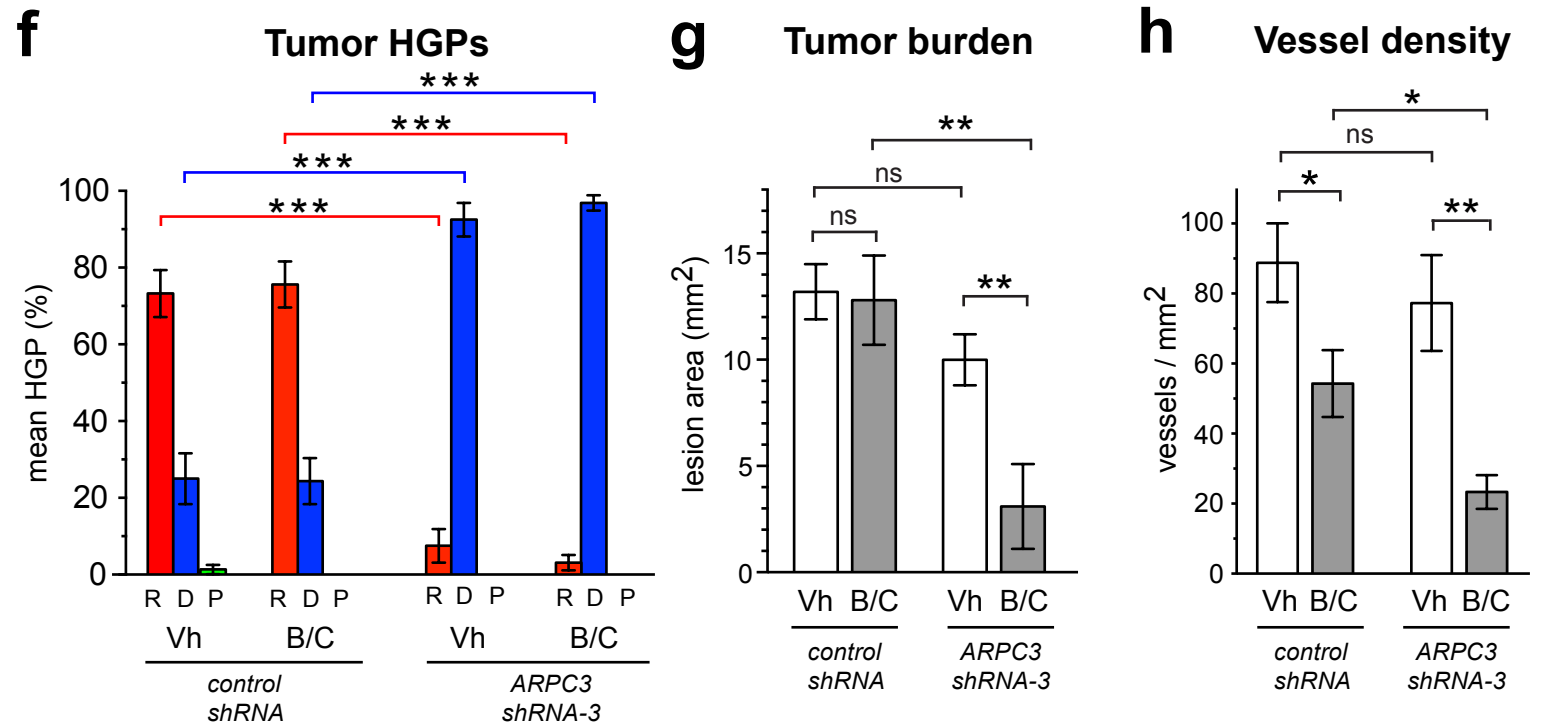
f
Tumor HGPs
mean HGP (%)
Vh
B/C
control shRNA
ARPC3 shRNA-3
g
Tumor burden
lesion area (mm2)
h
Vessel density
vessels / mm2

Supplementary Figure S1

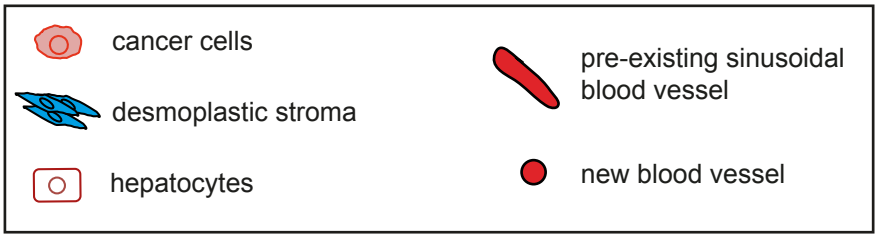

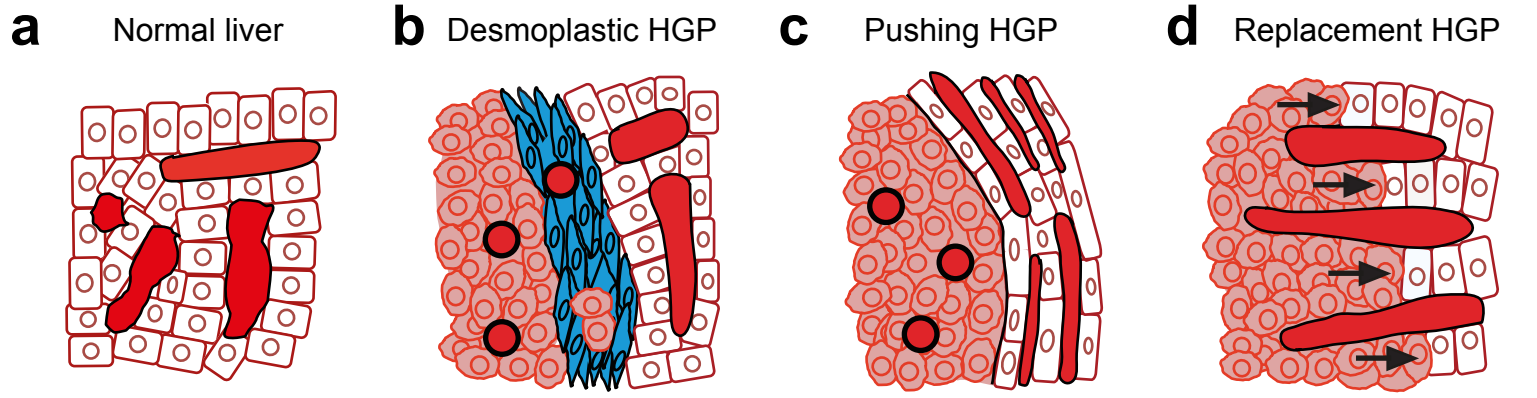

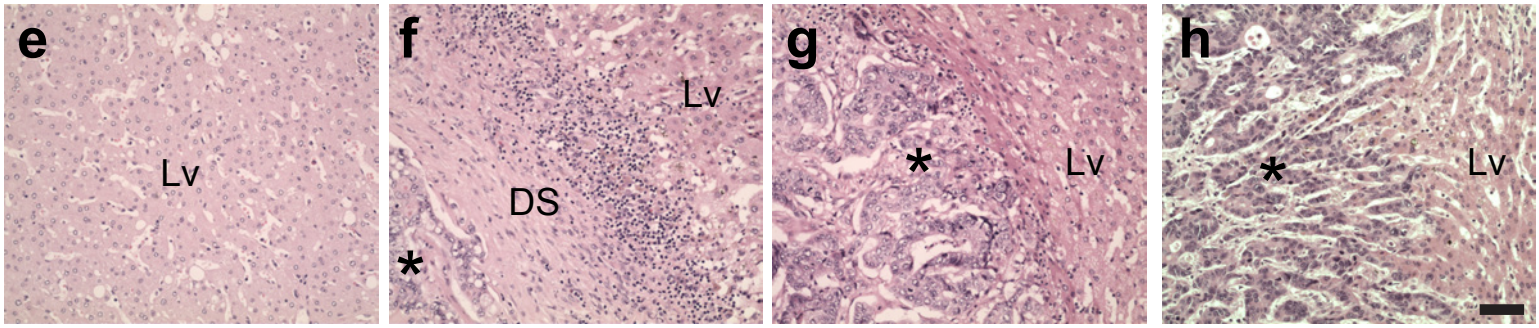

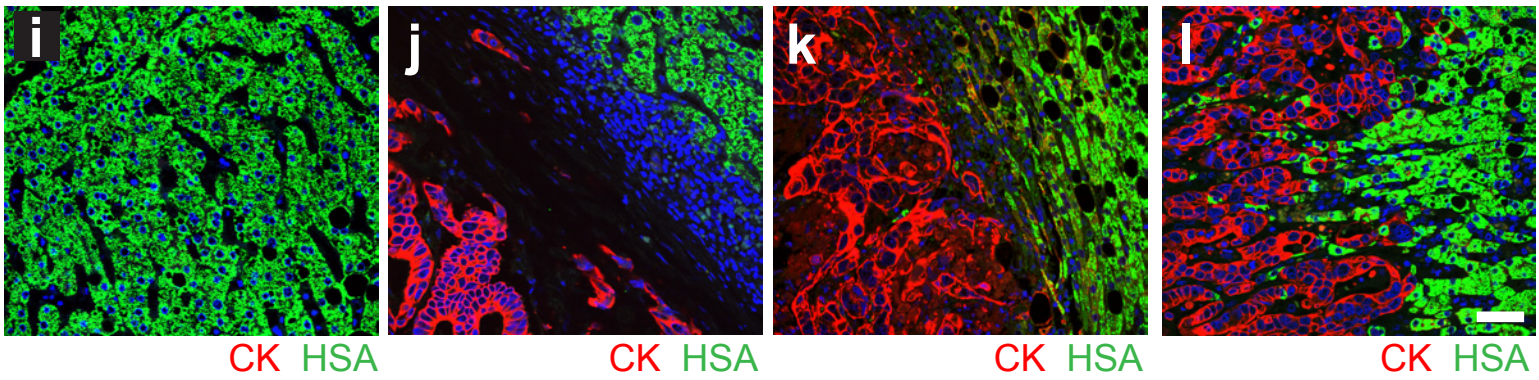

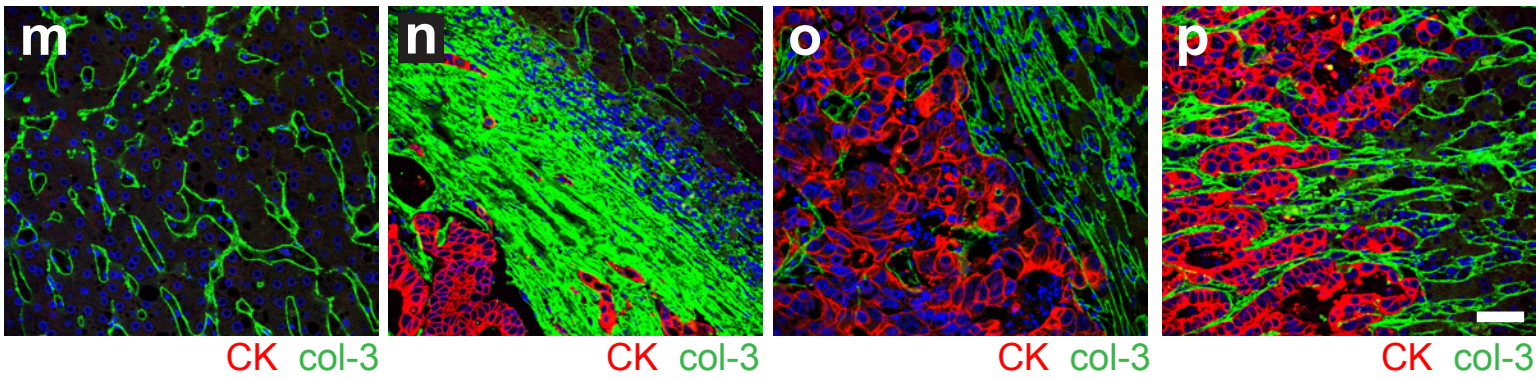

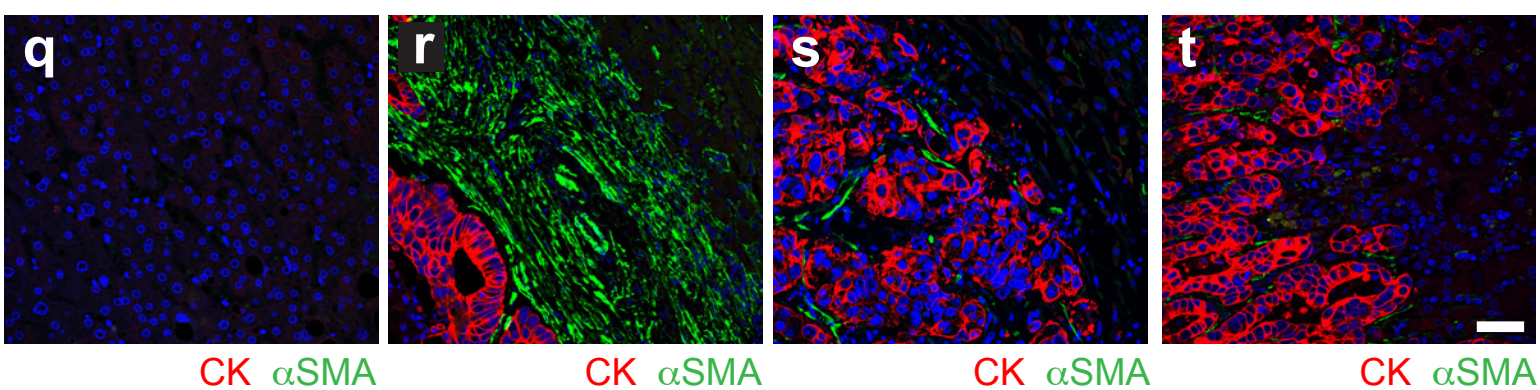

See overleaf for figure legend

Supplementary Figure S1 Morphology of the three histopathological growth patterns (HGPs) of colorectal cancer liver metastases

a-h. Diagrams and H&E-stainings illustrate the morphology of normal liver or the morphology of the tumor-normal liver interface in human CRC liver metastases with a desmoplastic, pushing or replacement HGP.

i-t. To confirm the distinct tumor-stroma interaction that occurs in each HGP, we performed additional staining for hepatocyte specific antigen (HSA), collagen-3 (col-3) and alpha smooth muscle actin (αSMA). In **normal liver**, HSA labeled hepatocytes (**i**), col-3 labeled sinusoidal blood vessels (**m**), whilst αSMA labeled neither hepatocytes nor sinusoidal blood vessels (**q**). In the **desmoplastic HGP**, a desmoplastic stroma physically separates cancer cells from normal liver (**b,f**). Co-staining for pan-cytokeratin (CK) to detect cancer cells and HSA to detect hepatocytes confirmed physical separation of cancer cells and normal liver (**j**), whilst co-staining for pan-cytokeratin and col-3, or pan-cytokeratin and αSMA, confirmed the presence of a desmoplastic stroma abundant in collagen (**n**) and αSMA-positive fibroblasts (**r**), respectively. In the **pushing HGP**, cancer cells and normal liver are in close contact with no intervening desmoplastic stroma (**c,g**) which was confirmed by co-staining for CK and HSA (**k**) or CK and αSMA (**s**). Another feature of the pushing HGP, physical compression of sinusoidal vessels in adjacent normal liver tissue, was confirmed by co-staining for pan-cytokeratin and col-3 (**o**). In the **replacement HGP**, cancer cells infiltrate the liver parenchyma and replace hepatocytes without disturbing the vascular architecture of the liver; no desmoplastic stroma is observed (**d,h**). Supporting this, co-staining for CK and HSA confirmed the invasion of cancer cells into liver parenchyma (**l**). Co-staining for CK and col-3 showed that the vascular architecture of the adjacent liver was preserved at the tumor-liver interface (**p**). Lack of αSMA staining confirmed the absence of a desmoplastic stroma (**t**). Scale bars, 50 μM.

Supplementary Figure S2

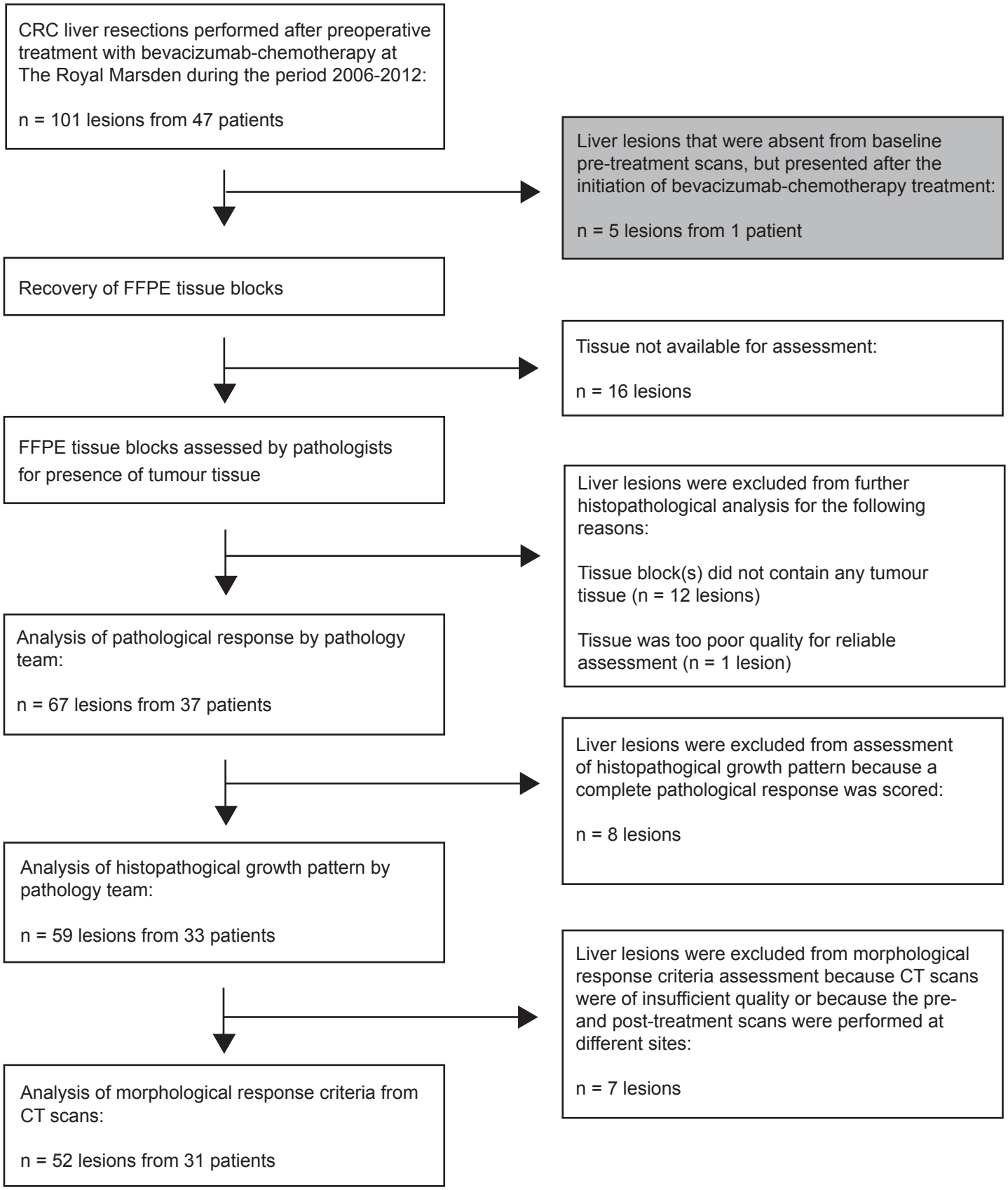

Supplementary Figure S2 Consort diagram for The Royal Marsden cohort
Consort diagram to illustrate how cases of CRC liver metastases from patients treated preoperatively with bevacizumab-chemotherapy at The Royal Marsden were selected for inclusion in the study or excluded.

Supplementary Table S1 Characteristics of bev-chemo treated CRC patients in The Royal Marsden cohort

Characteristics of 33 patients (n = 59 lesions) treated preoperatively with bevacizumab and chemotherapy prior to liver resection at The Royal Marsden.

Demographics	
Gender, number of patients (%)	
Male	21 (63.6)
Female	12 (36.4)
Age, median (range)	63 (29-79)
Primary tumor	
Site of primary tumor, number of patients (%)	
Rectum	7 (21.2)
Recto-sigmoid	14 (42.4)
Colon	12 (36.4)
Lymph node status, number of patients (%)	
Positive	26 (78.8)
Negative	7 (21.2)
Histological grade, number of patients (%)	
High grade	4 (12.1)
Low grade	29 (87.9)
Adjuvant therapy, number of patients (%)	
Yes	10 (30.3)
No	23 (69.7)
Liver metastasis	
No. of liver lesions at presentation, number of patients (%)	
Solitary lesion	11 (33.3)
Multiple lesions	22 (66.7)
Baseline lesion size, median (range)	21 mm (5-110)
Preoperative therapy administered, number of patients (%)	
CAPOX + bevacizumab	21 (63.6)
FOLFOX + bevacizumab	5 (15.2)
FOLFIRI + bevacizumab	7 (21.2)
Cycles of preoperative therapy, median (range)	6 (4-12)
Interval between last bevacizumab dose and resection, median (range)	76 days (41-362)

Footnote: CAPOX, capecitabine and oxaliplatin; FOLFOX, infusional 5-fluorouracil and oxaliplatin; FOLFIRI, infusional 5-fluorouracil and irinotecan.

Supplementary Table S2 Univariate analysis of The Royal Marsden cohort

Univariate analysis of predictors of pathological response in 59 lesions (from 33 patients) treated preoperatively with bevacizumab and chemotherapy prior to liver resection (The Royal Marsden cohort).

Variables	Total number of lesions	Lesions with <25% viable tumor, no. (%)	*P*-value
Demographics			
Gender			
Male	34	12 (35.3)	0.712
Female	25	10 (40)	
Age			
< 60 years	17	6 (35.3)	0.840
≥ 60 years	42	16 (38.1)	
Primary tumor			
Site of primary tumor			
Rectum	13	4 (30.8)	0.599
Recto-sigmoid	24	8 (33.3)	
Colon	22	10 (45.5)	
Lymph node status			
Positive	48	19 (39.6)	0.446
Negative	11	3 (27.3)	
Histological grade			
High grade	8	5 (62.5)	0.113
Low grade	51	17 (33.3)	
Adjuvant therapy			
Yes	18	4 (22.2)	0.113
No	41	18 (43.9)	
Liver metastasis			
No. of liver lesions at presentation			
Solitary	11	5 (45.5)	0.535
Multiple	48	17 (35.4)	
Baseline lesion size			
<20 mm	24	11 (45.8)	0.261
≥20 mm	35	11 (31.4)	
Preoperative therapy administered			
CAPOX + bevacizumab	37	16 (42.1)	0.475
FOLFOX + bevacizumab	9	2 (22.2)	
FOLFIRI + bevacizumab	13	4 (30.8)	
Cycles of preoperative therapy			
≤6 cycles	44	16 (36.4)	0.801
>6 cycles	15	6 (40.0)	
Interval between last bevacizumab dose and resection			
<70 days	24	10 (41.7)	0.565
≥70 days	35	12 (34.3)	

Table continues overleaf

Supplementary Table S2 continued

Variables	Total number of lesions	Lesions with <25% viable tumor, no (%)	*P*-value
Response measures			
Change in lesion size by RECIST			
PR	34	15 (44.1)	0.206
SD or PD	25	7 (28.0)	
Morphological response on CT			
Yes (OR or PR)	19	11 (57.9)	0.051
No (AR)	33	10 (30.3)	
Histopathological growth pattern			
Replacement HGP			
<25%	28	20 (71.4)	<0.001
≥25%	31	2 (6.5)	
Replacement HGP			
<50%	32	21 (65.6)	<0.001
≥50%	27	1 (3.7)	
Desmoplastic HGP			
<25%	25	0 (0)	<0.001
≥25%	34	22 (64.7)	
Desmoplastic HGP			
<50%	28	1 (3.6)	<0.001
≥50%	31	21 (67.7)	

Footnote: CAPOX, capecitabine and oxaliplatin; FOLFOX, infusional 5-fluorouracil and oxaliplatin; FOLFIRI, infusional 5-fluorouracil and irinotecan; N/A, data not available.

Supplementary Figure S3

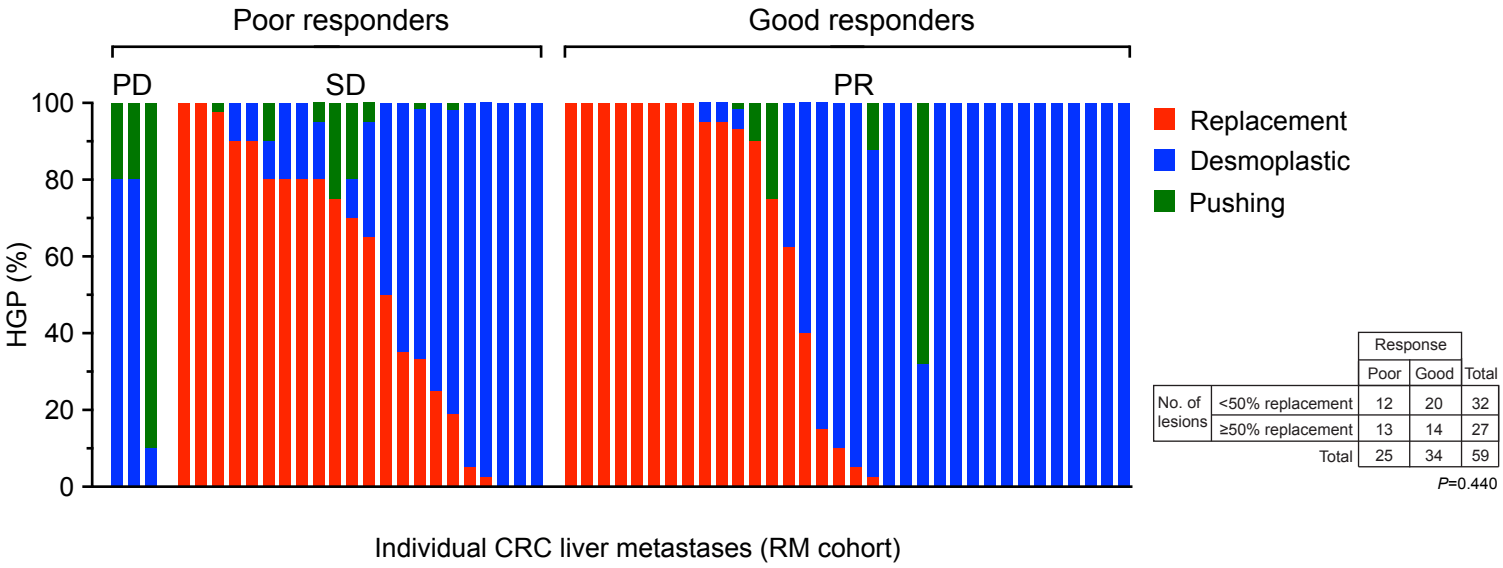

		Response		
		Poor	Good	Total
No. of lesions	<50% replacement	12	20	32
	≥50% replacement	13	14	27
	Total	25	34	59

P=0.440

Supplementary Figure S3 The HGPs do not correlate with response when using RECIST criteria as a response measure

Response to bev-chemo was scored using RECIST criteria in order to categorise individual lesions as: progressive disease (PD), stable disease (SD) or partial response (PR). Graph shows the % HGP scored in each individual lesion (replacement, desmoplastic, pushing) with lesions grouped according to response: PD, SD or PR (n = 59 liver metastases from 33 patients). Lesions scored as PD or SD were considered to be poor responders, whilst lesions scored as PR were considered to be good responders. Lesions with a substantial (≥50%) replacement HGP were not significantly enriched in the poor responder group when compared with good responders (*P*=0.440). The χ2-test was used to determine statistical significance (see 2x2 contingency table).

Supplementary Figure S4

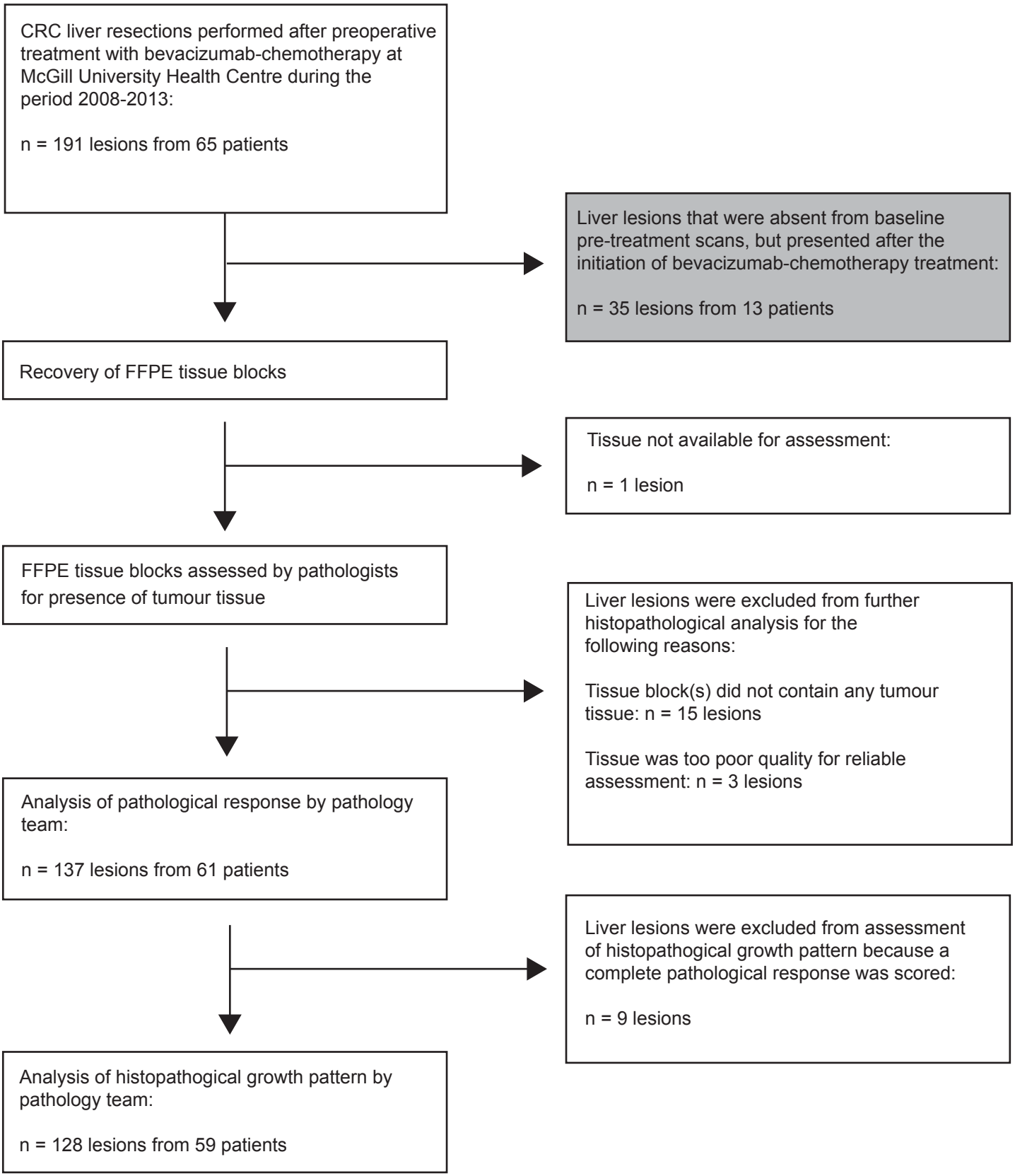

Supplementary Figure S4 Consort diagram for McGill University Health Centre cohort
Consort diagram to illustrate how cases of CRC liver metastases from patients treated preoperatively with bevacizumab-chemotherapy at the McGill University Health Centre were selected for inclusion in the study or excluded.

Supplementary Table S3 Characteristics of bev-chemo treated CRC patients in McGill University Health Centre cohort

Characteristics of 59 patients (n = 128 lesions) treated preoperatively with bevacizumab and chemotherapy at McGill University Health Centre.

Demographics	
Gender, number of patients (%)	
Male	35 (59.3)
Female	24 (40.7)
Age, median (range)	63 (30-85)
Primary tumor	
Site of primary tumor, number of patients (%)	
Rectum	11 (18.6)
Recto-sigmoid	9 (15.3)
Colon	39 (66.1)
Lymph node status, number of patients (%)	
Positive	32 (54.2)
Negative	8 (13.6)
N/A	19 (32.2)
Histological grade, number of patients (%)	
High grade	4 (6.8)
Low grade	36 (61.0)
N/A	19 (32.2)
Adjuvant therapy, number of patients (%)	
Yes	12 (20.3)
No	46 (78.0)
N/A	1 (1.7)
Liver metastasis	
No. of liver lesions at presentation, number of patients (%)	
Solitary lesion	18 (30.5)
Multiple lesions	41 (69.5)
Baseline lesion size, median (range)	26 (5 – 190)*
Preoperative therapy administered, number of patients (%)	
FOLFOX + bevacizumab	47 (79.7)
FOLFIRI + bevacizumab	12 (20.3)
Cycles of preoperative therapy, median (range)	6 (2 – 13)
Interval between last bevacizumab dose and resection, median (range)	64 (23 – 237)

Footnote: FOLFOX, infusional 5-fluorouracil and oxaliplatin; FOLFIRI, infusional 5-fluorouracil and irinotecan; N/A, data not available. *Information on baseline lesion size was available for 113 out of 128 lesions.

Supplementary Table S4 Univariate analysis of McGill University Health Centre cohort

Univariate analysis of predictors of pathological response in 128 lesions (from 59 patients) treated preoperatively with bevacizumab and chemotherapy prior to liver resection (McGill University Health Centre cohort).

Variables	Total number of lesions	Lesions with <25% viable tumor, no. (%)	*P*-value
Demographic			
Gender			
Male	88	29 (32.9)	0.297
Female	40	17 (42.5)	
Age			
< 60 years	53	18 (34.0)	0.695
≥ 60 years	75	28 (37.3)	
Primary tumor			
Site of primary tumor			
Rectum	21	5 (23.8)	0.022
Recto-sigmoid	14	8 (57.1)	
Colon	93	33 (35.5)	
Lymph node status			
Positive	66	20 (30.3)	0.032
Negative	11	7 (63.6)	
Histological grade			
High grade	6	1 (16.7)	0.279
Low grade	72	28 (38.9)	
Adjuvant therapy			
Yes	24	6 (25)	0.204
No	103	40 (38.8)	
Liver metastasis			
No. of liver lesions at presentation			
Solitary	18	7 (38.9)	0.778
Multiple	110	39 (35.4)	
Baseline lesion size			
<20 mm	40	13 (32.5)	0.447
≥20 mm	73	29 (39.7)	
Preoperative therapy administered			
FOLFOX + bevacizumab	108	42 (38.9)	0.048
FOLFIRI + bevacizumab	20	4 (20.0)	
Cycles of preoperative therapy			
6 cycles	86	37 (43)	0.017
>6 cycles	42	9 (21.4)	
Interval between last bevacizumab dose and resection			
<70 days	58	22 (37.9)	0.669
≥70 days	70	24 (34.3)	

Table continues overleaf

Supplementary Table S4 continued

Variables	Total number of lesions	Lesions with <25% viable tumor, no (%)	*P*-value
Response measures			
Change in lesion size by RECIST			
PR	44	22 (50)	0.024
SD or PD	69	20 (29)	
Histopathological growth pattern			
Replacement HGP			
<25%	60	34 (56.7)	<0.001
≥25%	68	23 (17.7)	
Replacement HGP			
<50%	70	40 (57.1)	<0.001
≥50%	58	6 (10.3)	
Desmoplastic HGP			
<25%	48	2 (4.2)	<0.001
≥25%	80	44 (55)	
Desmoplastic HGP			
<50%	62	6 (9.7)	<0.001
≥50%	66	40 (60.6)	

Footnote: FOLFOX, infusional 5-fluorouracil and oxaliplatin; FOLFIRI, infusional 5-fluorouracil and irinotecan; N/A, data not available.

Supplementary Figure S5

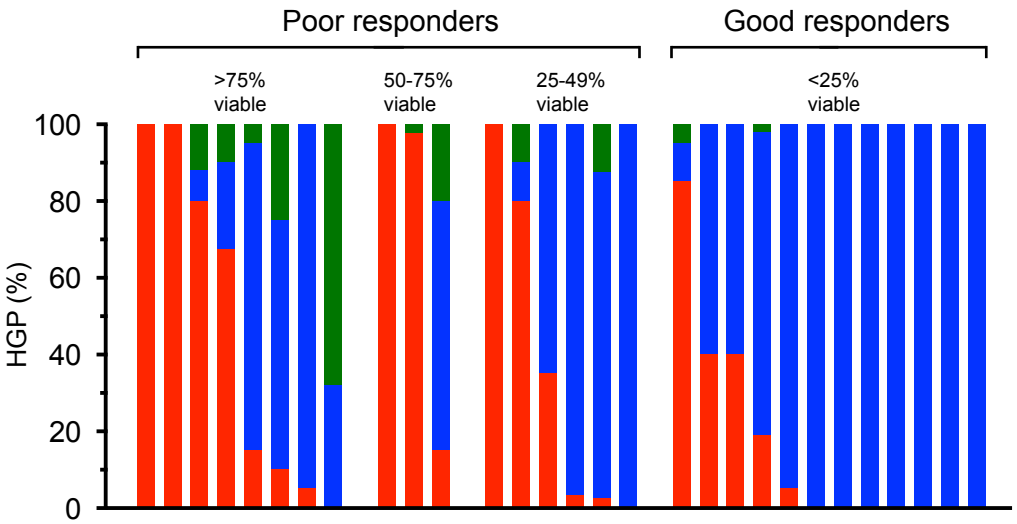

		Response		
		Poor	Good	Total
No. of lesions	<50% replacement	9	11	20
	≥50% replacement	8	1	9
	Total	17	12	29

P=0.0264

Supplementary Figure S5 The HGPs correlate with pathological response in patients presenting with a single lesion only

Graph shows the % HGP (replacement, desmoplastic, pushing) scored in 29 patients that presented with a single lesion only. Lesions scored as 25-49%, 50-75% or >75% viable were considered to be poor responders, whilst lesions scored as <25% viable were considered good responders. Lesions with a substantial (≥50%) replacement HGP were significantly enriched in the poor responder group when compared with good responders (*P*=0.0264). The χ2-test was used to determine statistical significance (see 2x2 contingency table).

Supplementary Figure S6

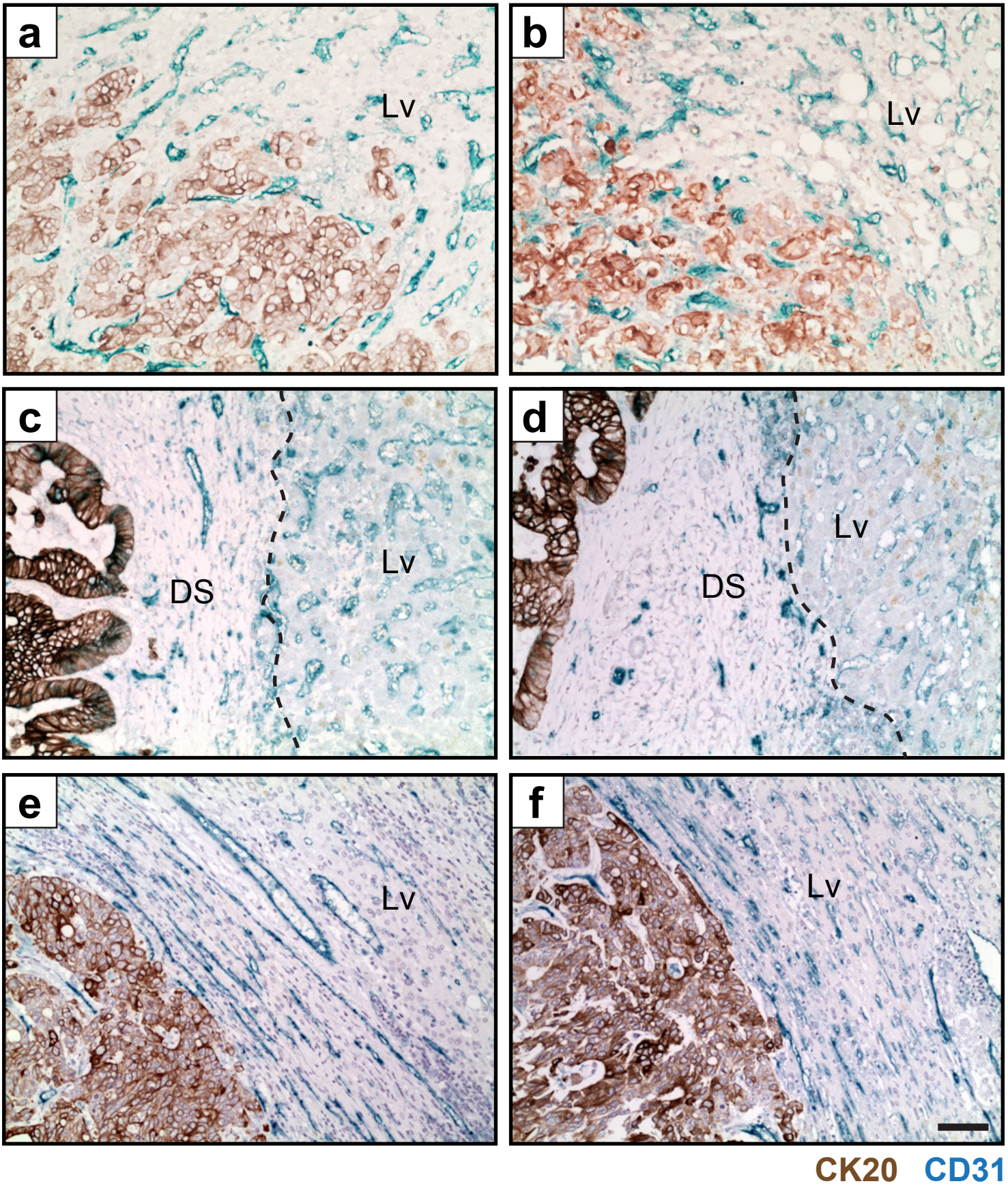

Supplementary Figure S6 Staining for blood vessels in the different histopathological growth patterns
Resection specimens of CRCLMs corresponding to the three different HGPs were stained for cytokeratin 20 (CK20) to identify cancer cells (brown) and CD31 to identify vessels (blue). **a,b.** Replacement HGP. Co-option of sinusoidal vessels by invading cancer cells is observed. **c,d.** Desmoplastic HGP. Co-option of sinusoidal vessels by cancer cells is physically precluded by the desmoplastic stroma (DS) that separates cancer cells from the normal liver (Lv). Dashed line indicates where the desmoplastic rim of the tumor meets the normal liver. **e,f.** Pushing HGP. Sinusoidal vessels that are present in the normal liver adjacent to the tumor are compressed, highly elongated and run in parallel with the tumor-liver interface, a topology that physically precludes the co-option of these vessels by invading cancer cells. DS, desmoplastic stroma; Lv, normal liver. Scale bar, 50 µM.

Supplementary Figure S7

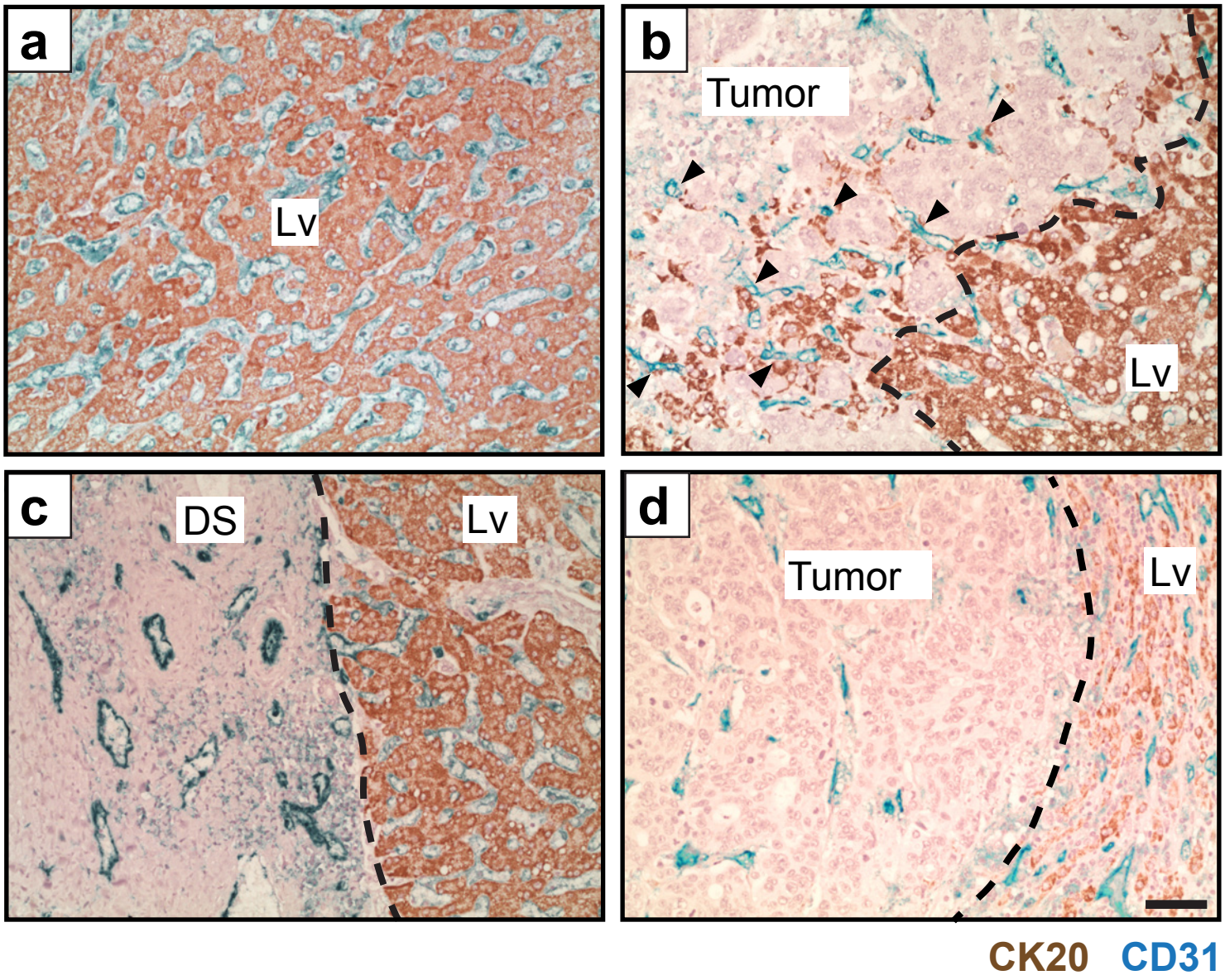

Supplementary Figure S7 Co-staining for blood vessels and hepatocytes in the different histopathological growth patterns

Resection specimens of CRCLMs were stained for HSA to identify hepatocytes (brown) and CD31 to identify vessels (blue). **a.** Normal liver, **b.** replacement HGP, **c.** desmoplastic HGP, and **d**. pushing HGP. Dashed line indicates the interface where the tumor meets the normal liver. Arrowheads indicate co-opted sinusoidal vessels that are still associated with hepatocytes. DS, desmoplastic stroma; Lv, normal liver. Scale bar, 50 μM.

Supplementary Table S5 Characteristics of CRC patients that presented with new lesions after bev-chemo treatment was initiated

Characteristics of 13 patients (n = 35 lesions) that presented with new liver metastases after treatment with a combination of bevacizumab and chemotherapy was initiated.

Demographics	
Gender, number of patients (%)	
Male	9 (69.2)
Female	4 (30.8)
Age, median (range)	65 (46-78)
Primary tumor	
Site of primary tumor, number of patients (%)	
Rectum	2 (15.4)
Recto-sigmoid	3 (23.1)
Colon	8 (61.5)
Lymph node status, number of patients (%)	
Positive	10 (76.9)
Negative	0
N/A	3 (23.1)
Histological grade, number of patients (%)	
High grade	2 (15.4)
Low grade	8 (61.5)
N/A	3 (23.1)
Adjuvant therapy, number of patients (%)	
Yes	4 (30.8)
No	9 (69.2)
Liver metastasis	
Quantity of liver lesions present when treatment started, number of patients (%)	
No lesion*	2 (15.4)
Solitary lesion	2 (15.4)
Multiple lesions	9 (69.2)
Quantity of new liver lesions presenting after treatment started, number of patients (%)	
Solitary lesion	7 (53.8)
Multiple lesions	6 (46.2)
Preoperative therapy administered, number of patients (%)	
FOLFOX + bevacizumab	9 (69.2)
FOLFIRI + bevacizumab	4 (30.8)
Cycles of preoperative therapy, median (range)	6 (5-12)
Interval between last bevacizumab dose and resection, median (range)	67 days (43-126)

Footnote: *Two patients were administered bevacizumab-chemotherapy prior to detection of liver metastases: one patient was receiving adjuvant bevacizumab-chemotherapy when liver disease was detected and a second patient was receiving bevacizumab-chemotherapy for CRC lung metastasis when liver disease was detected. N/A, data not available.

Supplementary Table S6 Characteristics of untreated CRC patients

Characteristics of 19 patients (n = 32 lesions) that did not receive preoperative therapy prior to liver resection.

Demographics	
Gender, number of patients (%)	
Male	11 (57.9)
Female	8 (42.1)
Age, median (range)	70 (33 - 80)
Primary tumor	
Site of primary tumor, number of patients (%)	
Rectum	5 (26.3)
Recto-sigmoid	1 (5.3)
Colon	13 (68.4)
Lymph node status, number of patients (%)	
Positive	10 (52.6)
Negative	5 (26.3)
N/A	4 (21.1)
Histological grade, number of patients (%)	
High grade	1 (5.3)
Low grade	10 (52.6)
N/A	8 (42.1)
Adjuvant therapy, number of patients (%)	
Yes*	4 (21.1)
No (completely chemonaive)	15 (78.9)
Baseline features of the liver metastases	
No. of liver lesions at presentation, number of patients (%)	
Solitary lesion	12 (63.2)
Multiple lesions	7 (36.8)
Baseline lesion size, median (range)	13.5 mm (4 - 77)

Footnote: *patients were only included if the last dose of adjuvant therapy was administered ≥ 365 days prior to diagnosis of liver metastasis (median interval between last dose of adjuvant therapy and diagnosis of liver metastasis in these 4 patients was 1161 days, range was 789 – 1667 days). Adjuvant therapy consisted of chemotherapy only and no patients received adjuvant bevacizumab. N/A, data not available.

Supplementary Table S7 Multivariate analysis of charateristics associated with overall survival in patients treated preoperatively with bev-chemo

Analysis was performed on 61 patients from MUHC that received preoperative therapy with bev-chemo (composed of 26 patients with a predominant replacement HGP and 35 patients with a predominant desmoplastic HGP).

	***P*-value**
Demographics	
Gender (Male / Female)	0.421
Age (Years)	0.357
Primary tumour	
Primary tumour site (Rectum / Recto-sigmoid / Colon)	0.437
Lymph nodes (Positive / Negative)	0.783
Histological grade (High / Low)	0.467
Treated with adjuvant therapy (Yes / No)	0.162
Liver metastasis	
Number of lesions at presentation	0.605
Preoperative therapy (FOLFOX + bevacizumab / FOLFIRI + bevacizumab)	0.078
Number of cycles of preoperative therapy administered	0.181
Interval between last bevacizumab dose and resection	0.582
Mean baseline lesion size	0.268
HGP (predominant replacement / predominant desmoplastic)	0.0023

Supplementary Table S8 Analysis for differences in characteristics between patients with a predominant replacement HGP and patients with a predominant desmoplastic HGP

Analysis was performed on 89 patients from MUHC that received preoperative therapy with bev-chemo or chemotherapy alone (composed of 38 patients with a predominant replacement HGP and 51 patients with a predominant desmoplastic HGP).

	Total number of patients	Number of replacement patients (%)	Number of desmoplastic patients (%)	*P*-value
Demographics				
Gender				
Male	56	28 (50)	28 (50)	0.070
Female	33	10 (30.3)	23 (69.7)	
Age				
< 60 years	35	15 (42.9)	20 (57.1)	0.980
≥ 60 years	54	23 (42.6)	31 (57.4)	
Primary tumour				
Primary tumour site				
Rectum	20	7 (35)	13 (65)	0.544
Recto-sigmoid	17	9 (52.9)	8 (47.1)	
Colon	32	22 (68.8)	10 (31.2)	
Lymph nodes				
Positive	44	20 (45.5)	24 (54.5)	0.522
Negative	14	5 (35.7)	9 (64.3)	
Histological grade				
High	6	4 (66.7)	2 (33.3)	0.149
Low	55	20 (36.4)	35 (63.6)	
Treated with adjuvant therapy				
Yes	16	8 (50)	8 (50)	0.543
No	72	30 (41.7)	42 (58.3)	
Liver metastasis				
Number of lesions at presentation				
No lesion*	3	3 (100)	0 (0)	0.046
Solitary lesion	27	8 (29.6)	19 (70.4)	
Multiple lesions	59	27 (45.8)	32 (54.2)	
Therapy				
FOLFOX	24	11 (45.8)	13 (54.2)	0.679
FOLFIRI	1	0 (0)	1 (100)	
FOLFIRINOX	2	1 (50)	1 (50)	
5-FU	1	0	1 (100)	
FOLFOX + bev	49	19 (38.8)	30 (61.2)	
FOLFIRI + bev	12	7 (58.3)	5 (41.7)	
Number pre-op cycles				
≤6	62	26 (41.9)	36 (58.1)	0.826
>6	27	12 (44.4)	15 (55.6)	

Table continues overleaf

Supplementary Table S8 continued

Interval between last therapy dose & resection				
<70 days	47	15 (31.9)	32 (68.1)	0.030
≥70 days	38	21 (55.3)	17 (44.7)	
Mean baseline lesion size				
<20 mm	25	9 (36)	16 (64)	0.666
≥20 mm	56	23 (41.1)	33 (58.9)	

Footnote: *Three patients were administered therapy prior to detection of liver metastases: one patient was receiving adjuvant bevacizumab-chemotherapy when liver disease was detected, one patient was receiving bevacizumab-chemotherapy for CRC lung metastasis when liver disease was detected and one patient was receiving adjuvant chemotherapy alone when liver disease was detected.

FOLFOX, infusional 5-fluorouracil and oxaliplatin; FOLFIRI, infusional 5-fluorouracil and irinotecan; FOLFIRINOX, infusional 5-fluorouracil and irinotecan and oxaliplatin; infusional 5-FU only. N/A, data not available.

Supplementary Table S9 Analysis for differences in characteristics between patients that received bev-chemo and patients that received chemotherapy alone

Analysis was performed on 91 patients from MUHC (comparing 62 patients that received pre-operative bev-chemo and 29 patients that received preoperative chemotherapy only).

	Total number of patients	Number of bev-chemo patients (%)	Number of chemo alone patients (%)	*P*-value
Demographics				
Gender				
Male	57	37 (64.9)	20 (35.1)	0.393
Female	34	25 (73.5)	9 (26.5)	
Age				
< 60 years	36	25 (69.4)	11 (30.6)	0.828
≥ 60 years	55	37 (67.3)	18 (32.7)	
Primary tumor				
Primary tumour site				
Rectum	21	12 (57.1)	9 (42.9)	0.206
Recto-sigmoid	17	10 (58.8)	7 (41.2)	
Colon	53	40 (75.5)	13 (24.5)	
Lymph nodes				
Positive	45	35 (77.8)	10 (22.2)	0.129
Negative	14	8 (57.1)	6 (42.9)	
Histological grade				
High	6	5 (83.3)	1 (16.7)	0.468
Low	55	38 (69.1)	17 (30.9)	
Treated with adjuvant therapy				
Yes	18	13 (72.2)	5 (27.8)	0.652
No	72	48 (66.7)	24 (33.3)	
Liver metastases				
Number of lesions at presentation				
No lesion*	4	2 (50)	2 (50)	0.695
Solitary lesion	27	18 (66.7)	9 (33.3)	
Multiple lesions	60	42 (70)	18 (30)	
Type of chemotherapy administered				
FOLFOX	75	50 (66.7)	25 (33.3)	0.019
FOLFIRI	13	12 (92.3)	1 (7.7)	
FOLFIRINOX	2	0 (0)	2 (100)	
5-FU	1	0 (0)	1 (100)	
Number pre-op cycles				
≤6	63	41 (65.1)	22 (34.9)	0.349
>6	28	21 (75)	7 (25)	

Table continues overleaf

Supplementary Table S9 continued

Interval between last therapy dose & resection				
<70 days	48	35 (72.9)	13 (27.1)	0.527
≥70 days	39	26 (66.7)	13 (33.3)	
Mean baseline lesion size				
<20 mm	25	14 (56)	11 (44)	0.125
≥20 mm	56	41 (73.2)	15 (26.8)	

Footnote: *Four patients were administered therapy prior to detection of liver metastases: one patient was receiving adjuvant bevacizumab-chemotherapy when liver disease was detected, one patient was receiving bevacizumab-chemotherapy for CRC lung metastasis when liver disease was detected and two patients were receiving adjuvant chemotherapy alone when liver disease was detected.

FOLFOX, infusional 5-fluorouracil and oxaliplatin; FOLFIRI, infusional 5-fluorouracil and irinotecan; FOLFIRINOX, infusional 5-fluorouracil and irinotecan and oxaliplatin; infusional 5-FU only. N/A, data not available.

Supplementary Table S10 Characteristics of breast cancer liver metastasis patients

Characteristics of the 17 patients from whom breast cancer liver metastasis samples were obtained. All samples were obtained from GZA Hospitals St Augustinus.

Details of primary	
Age at diagnosis of primary breast cancer, median (range)	47 (36-77)
Primary was resected, number of patients (%)	
Yes	15 (88.2)
No	2 (11.8)
Ductal or lobular histology, number of patients (%)	
Ductal	13 (76.5)
Lobular	3 (17.6)
Mixed	1 (5.9)
T-stage, number of patients (%)	
T1	6 (35.3)
T2	6 (35.3)
T3	2 (11.8)
T4	1 (5.9)
N/A	2 (11.8)
Lymph nodes, number of patients (%)	
Positive	9 (52.9)
Negative	6 (35.3)
N/A	2 (11.8)
Treatment received prior to obtaining liver metastasis sample	
Form of treatment received, number of patients (%)	
Endocrine therapy	14 (82.4)
Chemotherapy	12 (70.6)
Herceptin	2 (11.8)
Everolimus	1 (5.9)
Iressa	1 (5.9)
Zometa	1 (5.9)
Details of liver metastasis sample	
Age when sample was obtained, median (range)	54 (43-81)
Source of material, number of patients (%)	
Resection	11 (64.7)
Autopsy	6 (35.3)
Intrinsic subtype, number of patients (%)	
Luminal A	5 (29.4)
Luminal B HER2 negative	5 (29.4)
Luminal B HER2 positive	3 (17.7)
HER2 positive (non-luminal)	0 (0)
Triple negative	4 (23.5)

Footnote: N/A, data not available.

Supplementary Figure S8

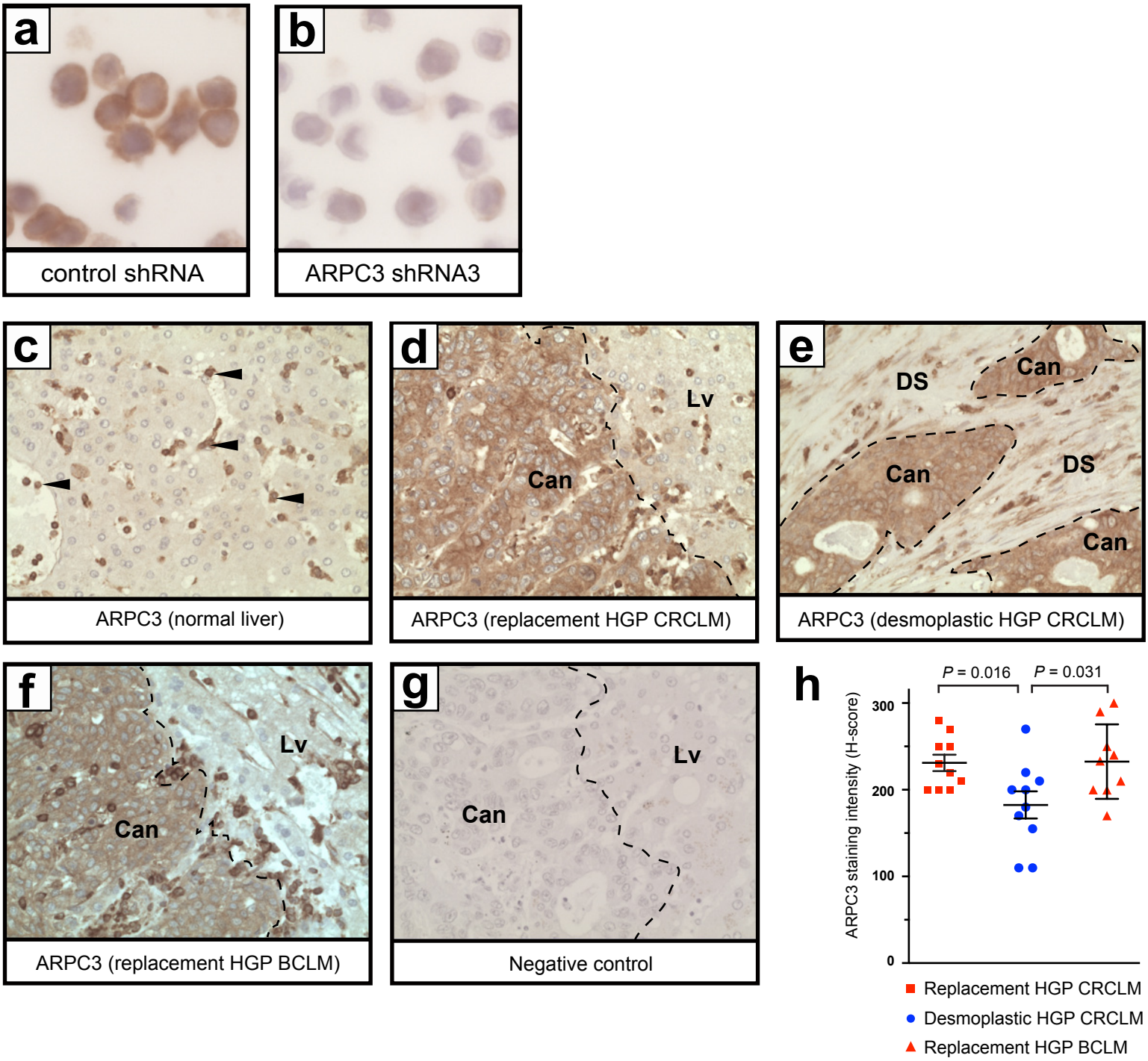

Supplementary Figure S8 Expression of the Arp2/3 subunit ARPC3 in human liver metastases

a,b. Validation of anti-ARPC3 antibody staining specificity
HT29 cells stably transfected with a control non-targeting shRNA (**a**) or ARPC3-targeted shRNA (**b**) were prepared for FFPE sections and then stained using an anti-ARPC3 antibody (MABT95, Millipore). Loss of antigenicity in the knockdown cells (**b**) compared to the control cells (**a**) indicates that this antibody is specific for ARPC3.

c-e. Examples of ARPC3 staining in human liver metastasis specimens
Samples of human liver metastasis were stained using the anti-ARPC3 antibody. **c.** ARPC3 staining in normal liver. ARPC3 staining is limited to Kuppfer cells and immune cells within the lumen of vessels (arrowheads) and staining is absent / weak in hepatocytes. **d-f.** ARPC3 staining in cancer cells (Can) of a replacement HGP CRCLM (**d**), a desmoplastic HGP CRCLM (**e**) and a replacement HGP breast cancer liver metastasis (BCLM) (**f**). Panel **g** shows a negative control, where the same staining protocol was performed but the primary antibody was omitted. Can, cancer cells. Lv, normal liver parenchyma. DS, desmoplastic stroma.

h. Quantification of ARPC3 staining in human liver metastasis specimens
The intensity of ARPC3 staining was scored in replacement HGP CRCLMs (n = 10), desmoplastic HGP CRCLMs (n = 10) and replacement HGP BCLMs (n = 9). Each data point on the graph is the intensity (H-score) for an individual case. Bars show the mean ± SEM. Student's t-test was used to compare groups.

Supplementary Figure S9

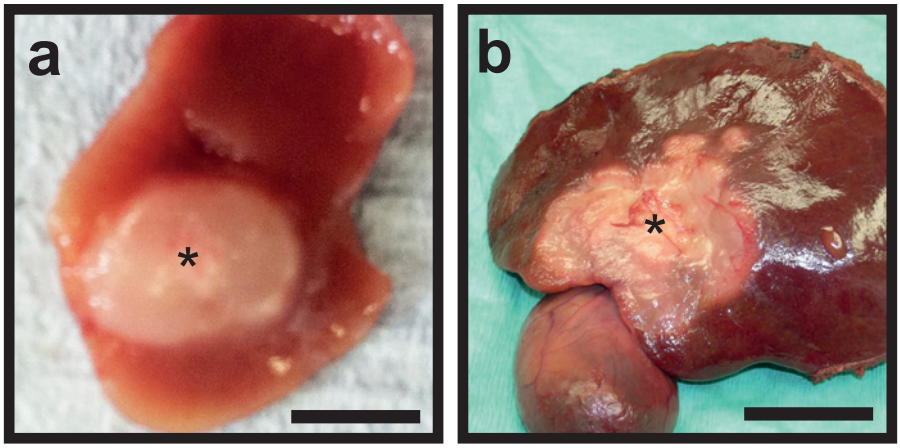

Supplementary Figure S9 Preclinical model of advanced liver metastasis
a. Macroscopic appearance of tumor formation in the left main lobe of the mouse liver after injection of HT29 cells. **b.** Macroscopic appearance of a human CRC liver metastasis resected from a patient (picture is courtesy of Mr Ali Majeed). Scale bar, 5 mm (**a**) or 5 cm (**b**). Tumor is indicated by an asterisk.

Supplementary Figure S10

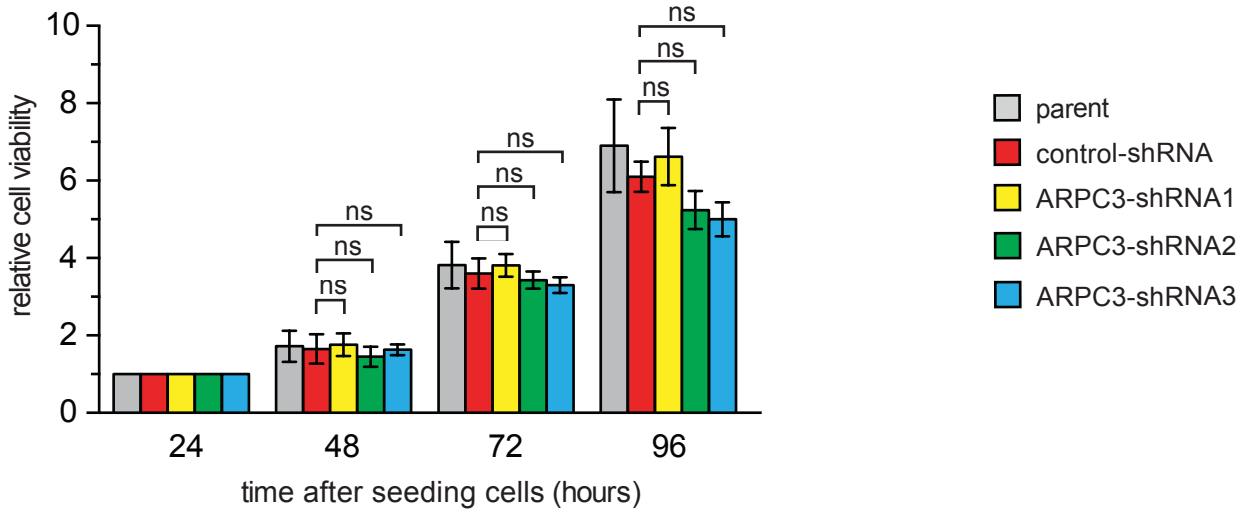

Supplementary Figure S10 Knockdown of ARPC3 in HT29 cells does not alter cell proliferation
Proliferation of parental HT29 cells (parent) and HT29 cells stably transduced with control-shRNA, ARPC3-shRNA-1, ARPC3-shRNA-2 or ARPC3-shRNA-3. The quantity of viable cells is expressed relative to the quantity measured at 24 hours ± SEM (n = 3 independent experiments). ns, no significant difference (Student's t-test).

Supplementary Figure S11

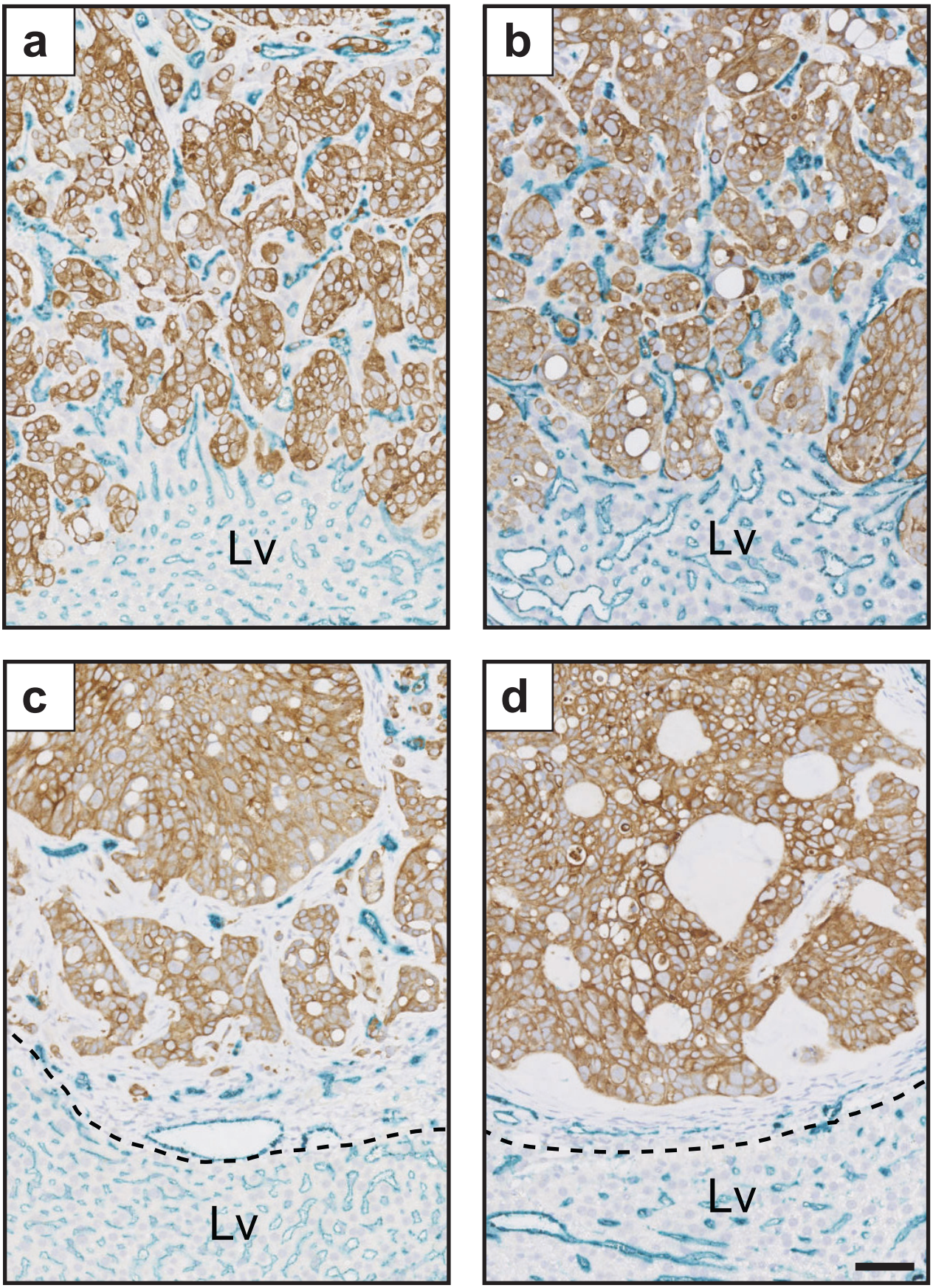

Supplementary Figure S11 Staining for CD31 in HT29 tumours treated with B20-4.1.1 and capecitabine *in vivo*

a-d. HT29 tumors with normal ARPC3 levels (control-shRNA) or ARPC3 knockdown (ARPC3-shRNA-3) were established in the livers of mice and treated with B20-4.1.1 plus capecitabine (B/C) or vehicle (Vh) alone. Liver specimens harvested after two weeks of treatment were stained for CK20 to label tumor cells and CD31 to label blood vessels. Representative images of the tumour-liver interface are shown for control-shRNA tumors treated with Vh (**a**) or B/C (**b**) and for ARPC3 knockdown tumors treated with Vh (**c**) or B/C (**d**). Dashed line in panels **c** and **d** indicates where the desmoplastic rim of the tumor meets the normal liver. Lv, normal liver. Scale bar, 60 μM.

Supplementary Figure S12

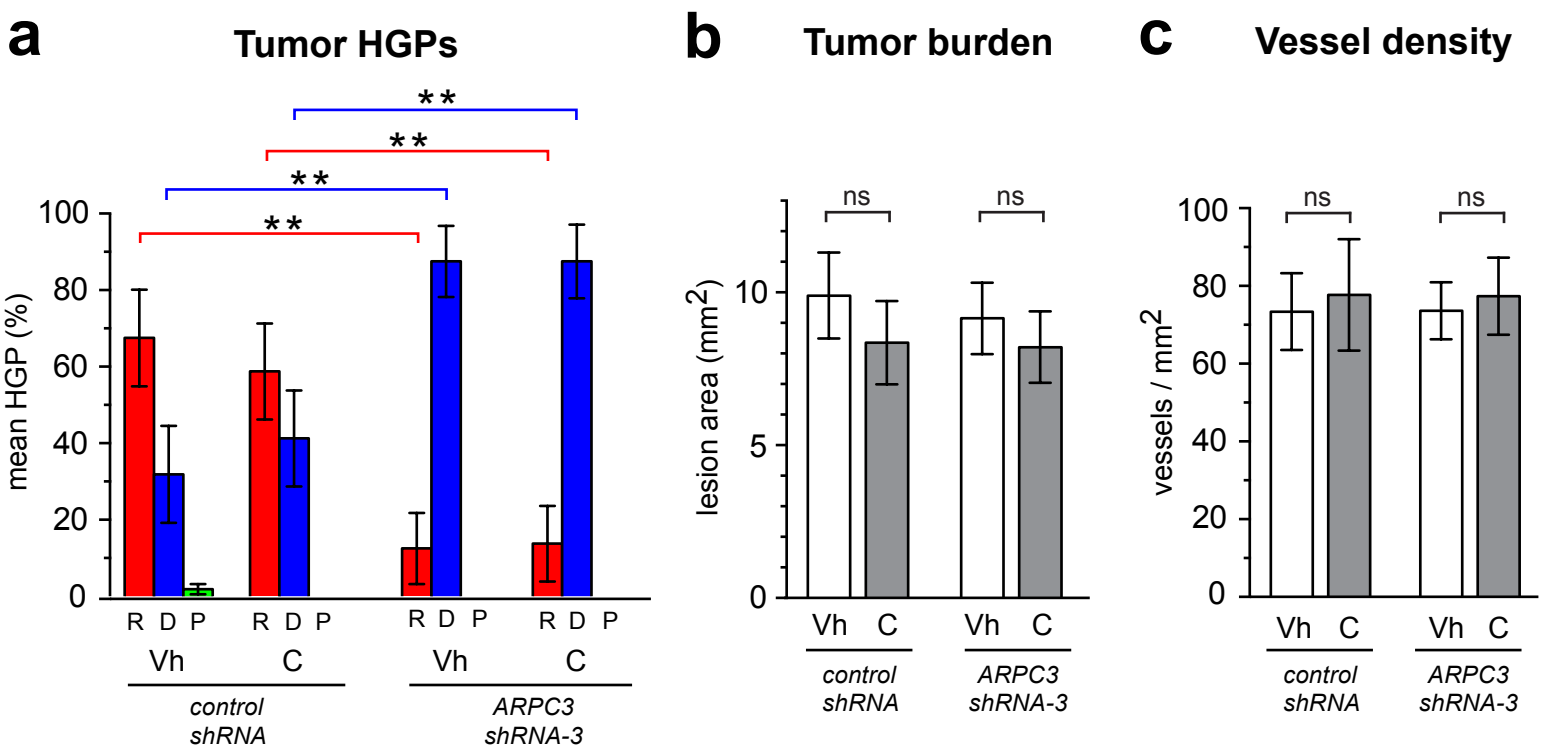

Supplementary Figure S12 Knockdown of ARPC3 does not effect tumor burden or tumor vessel density in mice treated with capecitabine alone

a-c. Tumors with normal ARPC3 levels (control-shRNA) or ARPC3 knockdown (ARPC3-shRNA-3) were established in the livers of mice. Mice were then treated with capecitabine (C) or vehicle alone (Vh) for two weeks followed by histopathological analysis of the liver tumors (n = 8 mice per group). Graph in **a** shows the % HGP per group ± SEM. Graph in **b** shows liver tumor burden expressed in terms of lesion area ± SEM. Graph in **c** shows tumor vessel density in terms of vessels per mm^2 ± SEM. For statistical analysis, Mann Whitney U-test (panel **a**) or Student's t-test (panels **b,c**) were used. ***P*<0.01. ns, no significant difference.

Supplementary Figure S13

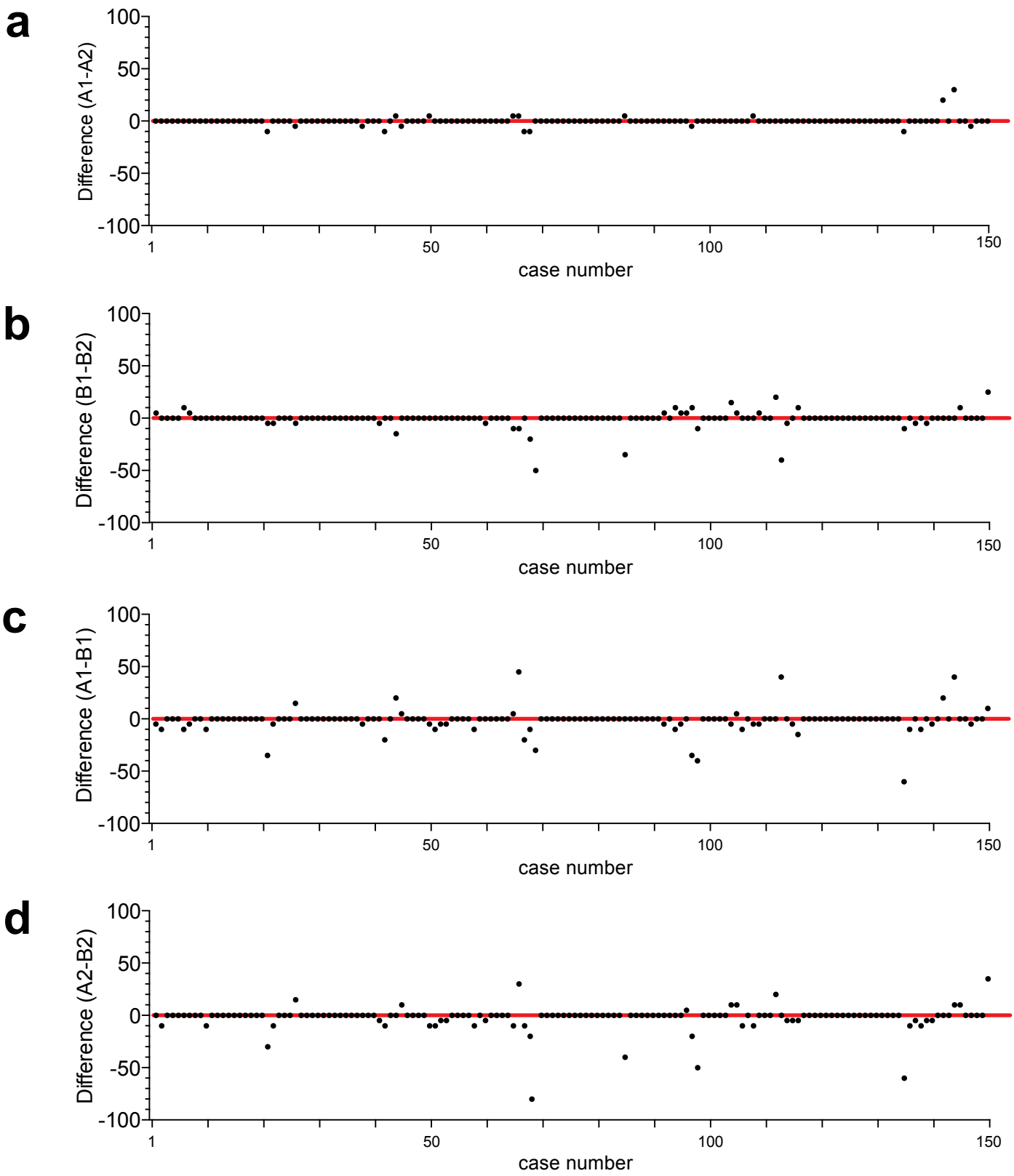

Supplementary Figure S13 Difference in % HGP scores between observers for the intra-observer and inter-observer agreement of HGP scoring

Two observers scored the HGP (% replacement, % desmoplastic, % pushing) in 150 tissue sections of colorectal cancer liver metastasis. The graphs show the difference between the two % replacement scores for every case for the following comparisons:

a. intra-observer agreement: observer A first score (A1) minus observer A second score (A2), **b.** intra-observer agreement: observer B first score (B1) minus observer B second score (B2), **c.** inter-observer agreement: observer A first score (A1) minus observer B first score (B1) and **d.** inter-observer agreement: observer A second score (A2) minus observer B second score (B2).

Data points which lie on the red line indicate cases for which there was complete agreement between the two scores, whilst data points either side of the line are cases for which there was disagreement between the two scores.

Supplementary Figure S14

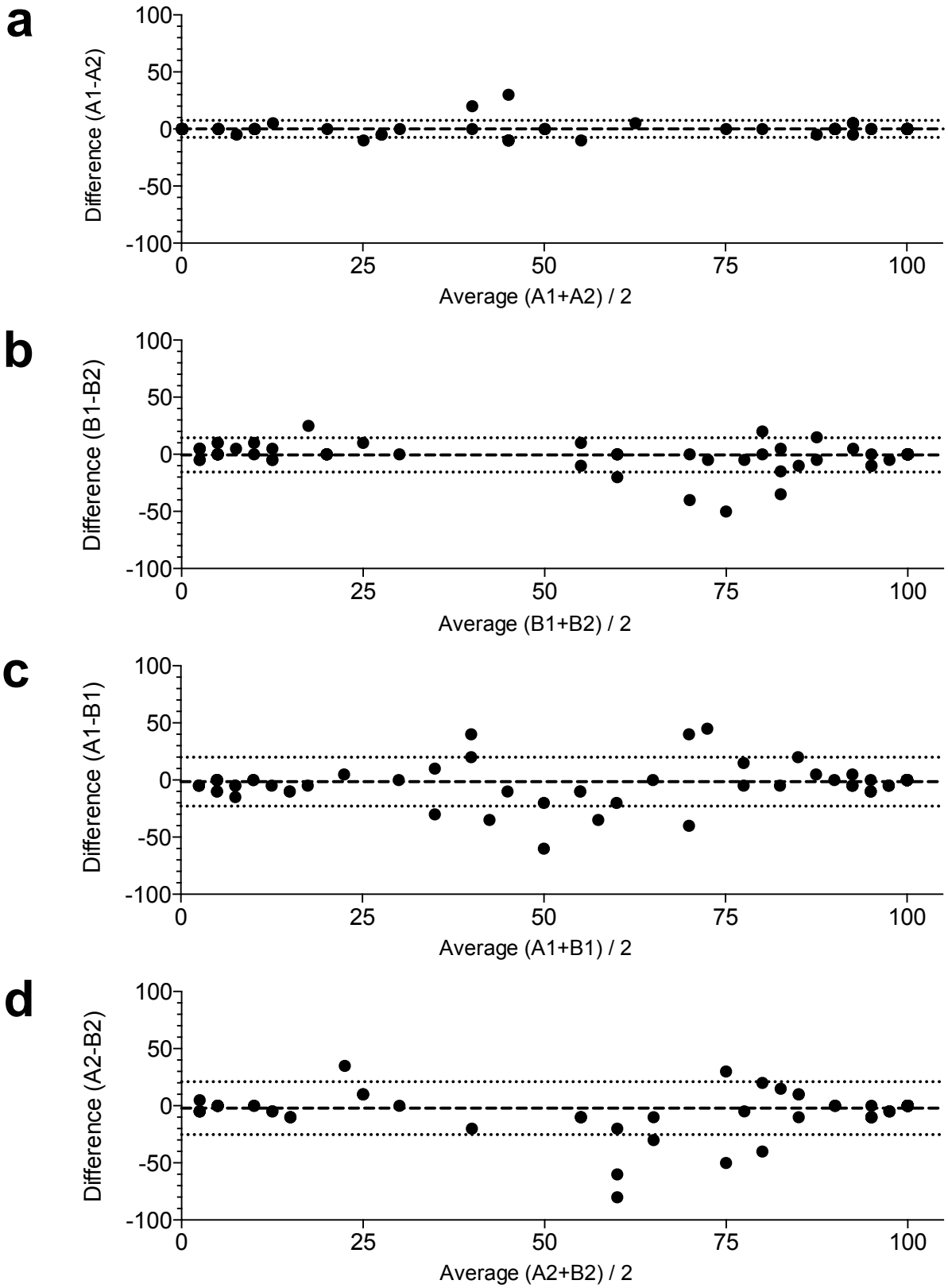

Supplementary Figure S14 Bland-Altman plots for intra-observer and inter-observer agreement of HGP scoring
Two observers scored the HGP (% replacement, % desmoplastic, % pushing) in 150 tissue sections of colorectal cancer liver metastasis. Bland-Altman plots show the difference between the two % replacement scores plotted against the average of the two % replacement scores for the following comparisons:
a. Intra-observer agreement: observer A first score (A1) versus observer A second score (A2). Mean difference between scores (-0.033) and limits of agreement (-7.431 to 7.497). **b.** Intra-observer agreement: observer B first score (B1) versus observer B second score (B2). Mean difference between scores (-0.633) and limits of agreement (-15.663 to 14.397). **c.** Inter-observer agreement: observer A first score (A1) versus observer B first score (B1). Mean difference between scores (-1.500) and limits of agreement (-22.88 to 19.88). **d.** Inter-observer agreement: observer A second score (A2) versus observer B second score (B2). Mean difference between scores (-2.167) and limits of agreement (-25.287 to 20.953).
Bold dashed line indicates the mean difference between scores whilst the flanking dotted lines show the limits of agreement. Note: since a large proportion of the 150 data points in each graph have identical x and y co-ordinates, many of the data points depicted constitute multiple overlaping data points.

Online Methods

Human samples

Specimens were obtained from patients treated at The Royal Marsden (RM) in London, at McGill University Health Centre (MUHC) in Montreal and at GZA Hospitals St Augustinus in Antwerp. Informed consent was obtained from all patients included in the study. Ethical approval for the study was granted by the local Research Ethics Committee at The Royal Marsden (London), by the Surgical Techniques, Medical Devices and Reproductive Technologies Research Ethics Board at the McGill University Health Centre (Montreal) and by the local Research Ethics Committee of the GZA Hospitals St. Augustinus (Antwerp).

We identified all cases of CRC liver metastases resected from patients treated preoperatively with a combination of bevacizumab and chemotherapy (bev-chemo) at RM from 2006-2012 (101 metastases resected from 47 patients). Of these, 59 liver metastases from 33 patients were eligible for our study correlating HGP with pathological response. A consort diagram illustrates how these 59 cases were selected for inclusion in the study (Supplementary Fig. S2). For patient characteristics see Supplementary Table S1. For our study correlating HGP with morphological response on imaging, 52 lesions from 31 patients were eligible for inclusion (see Supplementary Fig. S2). For our study correlating HGP with response using change in lesion size (RECIST criteria) as a response measure, all 59 liver metastases from 33 patients were eligible for inclusion.

We identified all CRC liver metastases resected from patients treated preoperatively with bev-chemo at MUHC from 2008-2013 (191 CRC liver metastases from 65 patients). Of these, 128 liver metastases from 59 patients were eligible for our study correlating HGP with pathological response (see consort diagram in Supplementary Fig. S5). For patient characteristics see Supplementary Table S3.

For the analysis of new CRC liver metastases (i.e. lesions that only presented after the initiation of bev-chemo but were not present on baseline scans) we identified 35 resected lesions from 13 patients treated preoperatively with bev-chemo at MUHC (see grey box in Supplementary Fig. S4). For patient characteristics see Supplementary Table S5. For the analysis of CRC liver metastases from patients that did not receive pre-operative therapy with bev-chemo, we identified 32 lesions from 19 patients at MUHC. For patient characteristics see Supplementary Table S6.

For the analysis of CRC liver metastases from patients treated with chemotherapy alone we identified all cases of CRC liver metastases resected from patients treated preoperatively with chemotherapy alone at MUHC from 2008-2014 (81 metastases resected from 29 patients). Of these, 76 liver metastases from 29 patients were eligible for our study correlating HGP with overall survival.

For the analysis of breast cancer liver metastases, all breast cancer liver metastasis cases obtained via resection or autopsy at GZA Hospitals St. Augustinus from 2004-2015 were examined (17 patients). For patient characteristics see Supplementary Table S7.

Details of therapy administration

Patients that received preoperative treatment with bevacizumab in combination with chemotherapy were treated with one of three different regimens.

CAPOX plus bevacizumab: a 21 day treatment cycle consisting of a 15 minute intravenous infusion of bevacizumab (7.5 mg/kg) and a 2 hour intravenous infusion of oxaliplatin (130 mg/m^2) on day one, followed by daily oral capecitabine (1700 mg/m^2) in two divided doses from days 1 to 14.

FOLFOX plus bevacizumab: a 14 day treatment cycle consisting of a 10 minute intravenous infusion of bevacizumab (5 mg/kg), a 2 hour intravenous infusion of oxaliplatin (85 mg/m^2), a 2 hour intravenous infusion of folinic acid (400mg/m^2) with a bolus dose of 5-

FU (400 mg/m^2) on day one, followed by a 48 hour continuous intravenous infusion of 5-FU (1200mg/m^2/day).

FOLFIRI plus bevacizumab: a 14 day treatment cycle consisting of a 10 minute intravenous infusion of bevacizumab (5 mg/kg), a 1 hour intravenous infusion of irinotecan (180 mg/m^2), a 1 hour intravenous infusion of folinic acid (400mg/m^2) with a bolus dose of 5-FU (400 mg/m^2) on day one, followed by a 48 hour continuous intravenous infusion of 5-FU (1200mg/m^2/day).

For patients that received preoperative treatment with chemotherapy alone, patients received either FOLFOX or FOLFIRI, which were administered as described above, but without the addition of bevacizumab.

The decision to administer neoadjuvant therapy, the type of therapy and the number of cycles were based on the recommendation of the local mutidisciplinary team based on tumor board recommendations. Patients received oxaliplatin or irinotecan-based regimens with the addition of bevacizumab preferentially, as long there were no contraindications to administer bevacizumab, such as uncontrolled hypertension, history of gastrointestinal perforation, history of arterial or venous thromboembolic events, history of significant bleeding, recent surgery or nephrotic syndrome. In the case that the patient was deemed unsuitable for administration of bevacizumab, the patient received chemotherapy alone. There was no bias in terms of period (year) as patients in the current study were included in a time period where bevacizumab was approved and available at the institutions.

Scoring of HGPs

Sections (5 μm thickness) were prepared from formalin fixed paraffin-embedded (FFPE) liver resection specimens, stained with hematoxylin and eosin (H&E) and then scored for HGP by two pathologists with extensive experience of scoring the HGPs. In brief, the tumor-liver interface was categorized as being desmoplastic, pushing or replacement

HGP according to the following criteria. Desmoplastic HGP: there was no direct contact between cancer cells and liver parenchyma and the cancer cells were separated from the liver parenchyma by a layer of desmoplastic stroma. Pushing HGP: close contact between cancer cells and normal liver tissue was observed, without an intervening desmoplastic stroma. The normal liver was compressed by the tumor and no invasion of cancer cells into the hepatic plates was observed. Replacement HGP: close contact between cancer cells and liver parenchyma was observed, without an intervening desmoplastic stroma. The cancer cells invaded into the hepatic plates and replaced the hepatocytes without destroying the vascular architecture of the liver. To account for the fact that some lesions present with a mixture of different HGPs, in the current study the percentage of the tumor-liver interface adopting a desmoplastic, pushing or replacement HGP was scored in intervals of 5% in all available tissue blocks. Where multiple blocks were available, the mean average score was calculated to produce a single score for % desmoplastic, % pushing and % replacement for each lesion.

In some cases, invasion of cancer cells into the hepatic plates (which is a defining feature of the replacement HGP and required for vessel co-option) was also accompanied by some compression of the liver parenchyma. When invasion of cancer cells into the hepatic plates was also accompanied by some compression of the liver parenchyma, this was scored as replacement HGP and not pushing HGP. This subtle but important refinement to the criteria for scoring the HGPs helps to explain why, in the current study, the incidence of the replacement HGP in colorectal cancer liver metastases is higher than in some previous studies.

The level of inter- and intra-observer agreement for scoring the HGPs was good, with an interclass correlation co-efficient (ICC) value of 0.931 for the inter-observer agreement and ICC values of 0.995 (observer 1) and 0.977 (observer 2) for the intra-observer agreement.

Scoring of pathological response to therapy

For scoring of the pathological response to bev-chemo from H&E-stained specimens, the extent of viable carcinoma was assessed semi-quantitatively as a percentage relative to the total tumor surface area. Each lesion was assigned as belonging to one of four categories: >75%, 50-75%, 25-49% or <25% viable carcinoma[1], with areas of usual necrosis being considered part of the viable tumor fraction, whilst areas of infarct-like necrosis were considered to be non-viable[2]. Pathological response was scored independently by three experienced pathologists using the criteria described above. Any difference in score that occurred between pathologists was resolved by consensus to produce a single score for each lesion.

Scoring of morphological response criteria from CT scans

Pre- and post-treatment contrast-enhanced CT scans of suitable quality were available for 52 lesions from 31 patients for this analysis (see consort diagram, Supplementary Fig. S2). The response to therapy in contrast-enhanced CT scans was evaluated using a method based on previously published morphological response criteria[3,4] and is described below.

The appearance of each lesion on both the pre-treatment scan and the post-treatment scan was scored as belonging to one of three morphology groups (group-1, group-2 or group-3). A homogeneous, low attenuation lesion with a thin, sharply defined tumor-liver interface was defined as a group-1 metastasis. A lesion having heterogeneous attenuation and a thick, poorly defined tumor-liver interface was defined as a group-3 metastasis. A lesion having morphology that was intermediate between group-1 and group-3, having a moderate degree of heterogeneous attenuation and a moderately defined tumor-liver interface, was defined as a group-2 metastasis.

Morphological response was defined as an optimal response (OR) if the lesion changed in appearance from a group-3 or group-2 metastasis to a group-1 metastasis following treatment; a partial response (PR) if the metastasis changed in appearance from a group-3 to a group-2 metastasis following treatment; and an absent response (AR) if the metastasis either did not change group following treatment or if the appearance increased from a group-2 to a group-3 metastasis following treatment. When present, a peripheral rim of hyperattenuating contrast enhancement was designated as a group-3 characteristic, and resolution of this enhancement was classified as group-2 if it was partially resolved following treatment and a group-1 if it was completely resolved following treatment. Morphological response was scored independently by two observers. Any difference in scores was resolved by consensus to produce a single score for each lesion. Lesions scored as AR were considered to be poor responders, whilst lesions scored as PR or OR were considered to be good responders. Scorers were blinded as to the HGP and pathological response data.

Scoring of response according to RECIST criteria

Change in lesion size was determined from MRI scan data, by calculating the change in lesion diameter that occurred between the pre- and post-treatment scans. The lesion size measurements were obtained from the patient records and were therefore blinded, because the original reporting radiologist had no prior knowledge of our retrospective HGP and pathological response data. For this analysis, MRI scans of suitable quality were available for 59 lesions from 33 patients. Lesions were classified as partial response (PR), stable disease (SD) or progressive disease (PD) according to the following criteria: PR (lesion underwent ≥30% decrease in size between pre- and post-treatment scan), SD (lesion underwent <30% decrease in size and <20% increase in size between pre- and post-treatment scan) and PD (lesion underwent ≥20% increase in size between

pre- and post-treatment scan).

Kaplan-Meier estimates of overall survival

For the purposes of examining the association between HGP and overall survival, patients were allocated to one of three groups: predominant replacement, predominant desmoplastic or predominant pushing. To allocate patients to each group, the mean percentage of replacement HGP, desmoplastic HGP and pushing HGP was calculated for each patient using the data available from all lesions. Those patients with a mean replacement HGP of >50% were allocated to the predominant replacement group, those patients with a mean desmoplastic HGP of >50% were allocated to the predominant desmoplastic group and those patients with a mean pushing HGP of >50% were allocated to the predominant pushing group. This method allowed unambiguous allocation of patients to the three groups (i.e. there were no patients scored as having a 50:50 score for two growth patterns). Overall survival was calculated from the date of diagnosis of liver metastases to the date of death or to the date of last follow-up.

Immunohistochemistry

For staining of human and mouse tissue, sections of 5 μm thickness were prepared from FFPE blocks. Sections were de-paraffinized and rehydrated by standard protocols. Depending on the antibodies used, antigen retrieval was performed either at pH 6 in a pressure cooker or at pH 9 in a microwave. Sections were incubated in blocking buffer (1% BSA in PBS-T) for 1 hr followed by incubation with primary antibodies in blocking buffer for 2 hr, all at room temperature. Primary antibodies were: mouse anti-ARPC3 (MABT95, Millipore), mouse-anti-human CD31 (M0823, Dako), rabbit anti-mouse CD31 (DIA310, Dianova), rabbit anti-collagen-3 (ab7778, Abcam), mouse anti-human cytokeratin-19 (M0888, Dako), mouse anti-human cytokeratin-20 (M7019, Dako), mouse anti-human

estrogen receptor alpha (M3643, Dako), mouse anti-hepatocyte specific antigen (sc-58693, Santa Cruz Biotechnology), mouse anti-human pan-cytokeratin (M3515, Dako), rabbit anti-human pan-cytokeratin (Z0622, Dako), mouse anti-human Ki67 (M7240, Dako), mouse anti-human progesterone receptor (M3643, Dako) and rabbit anti-alpha smooth muscle actin (ab5694, Abcam).

For immunofluorescence, primary antibodies were detected with Alexa-488 or Alexa-555 fluorescently-conjugated secondary antibodies (Invitrogen) diluted in blocking buffer supplemented with DAPI for 30 mins at room temperature, followed by mounting under glass coverslips in MOWIOL mountant supplemented with antifade (0.1% w/v 1,4-diazabicyclo[2.2.2]octane) (Sigma). For DAB and TMB staining, primary antibodies were detected with Envision Flex system (K8002, Dako), followed by a light counterstain with hematoxylin before mounting under glass coverslips in DPEX mountant. For HER2 we used the HercepTest kit (SK001, Dako). Images were captured using a confocal laser-scanning microscope (Leica) or a light microscope (Olympus), as appropriate.

Scoring intrinsic molecular subtypes in breast cancer liver metastasis cases

Cases of breast cancer liver metastasis were characterized for intrinsic molecular subtype: luminal A, luminal B-HER2 negative, luminal B-HER2 positive, HER2 positive (non-luminal) and triple negative. For this purpose, we used surrogate immunohistochemical markers as recommended in recently published guidelines[5]. In brief, FFPE tissue sections were stained for ER, PgR, HER2 and Ki67, which were then scored by a pathologist. For both ER and PgR, positive staining in ≥1% of tumor cell nuclei was required in order for the case to be considered receptor positive[6]. For HER2, the following system was utilized: 0 (HER2 negative), 1+ (also HER2 negative), 2+ (HER2 borderline), or 3+ (HER2 positive)[7]. Cases scored as HER2 borderline underwent additional testing with the HER2 CISH pharmDx kit (SK109, Dako) to test for HER2 amplification according to the

manufacturer's instructions. The presence of HER2 amplification was considered to indicate that the case was HER2 positive. Cases were deemed Ki67 'low' if <14% of nuclei were Ki67 positive, otherwise they were considered to be Ki67 'high.' The results of the ER, PgR, HER2 and Ki67 analysis were then used to assign each case to an intrinsic molecular subtype according to the criteria shown below (adapted from Goldhirsch et al 2013):

Intrinsic subtype	**Criteria**
Luminal A	ER and PgR positive HER2 negative Ki67 'low'
Luminal B HER2 negative	ER positive HER2 negative Ki67 'high'
Luminal B HER2 positive	ER positive HER2 positive Any Ki67 Any PgR
HER2 positive (non-luminal)	HER2 positive ER and PgR absent
Triple negative	ER negative PgR negative HER2 negative

Cell culture

The HT29 cells used were luciferase-tagged (HT-29-luc2 from Caliper Life Sciences). Cells were authenticated by STR typing and were regularly tested for mycoplasma and shown to be contamination free. HT29 cells were cultured in complete DMEM supplemented with 10% FCS, L-glutamine and penicillin/streptomycin at 37°C in an atmosphere of 5% CO_2.

Generation of knockdown cell lines

HT29 cells were stably transduced with shRNA oligonucleotides using lentiviral particles. We utilized three different shRNA oligonucleotides designed to target ARPC3 (ARPC3-shRNA-1, ARPC3-shRNA-2, ARPC3-shRNA-3) and a control oligonucleotide with

a validated non-targeting sequence (control-shRNA). The sequence of these oligonucleotides was as follows:

Oligonucleotide	**Sequence**
ARPC3-shRNA-1	5'CACCCGCTTAATAAGAATAAGTACGAATACTTATTCTTATTAAGCG3'
ARPC3-shRNA-2	5'CACCGAAATGTATACGCTGGGAATCCGAAGATTCCCAGCGTATACATTTC3'
ARPC3-shRNA-3	5'CACCGCCAAGGTGAGAAAGAAATGTCGAAACATTTCTTTCTCACCTTGGC3'
control-shRNA	5'CACCTAAGGCTATGAAGAGATACCGAAGTATCTCTTCATAGCCTTA3'

Oligonucleotides were ligated into the pENTR/U6 Gateway system entry vector (Invitrogen) according to the manufacturer's instructions. Oligonucleotide sequences were verified by sequencing and then transferred, together with the U6 promoter, into the Gateway-modified pSEW lentiviral vector (this vector also contains the EGFP gene under the control of an independent SFFV promoter). Viral supernatants were generated by lipofectamine-2000 co-transfection of this expression vector and two packaging vectors (psPAX2 and pMD2.G) into HEK293T cells. Viral supernatants were collected and stored at -80°C until use. Adherent HT29 cells were infected with viral supernatant for 24 hours. Following this, the infecting medium was aspirated and replaced by DMEM complete. At 3-5 days after infection, HT29 cells were trypsinized and sorted for GFP expression by flow cytometry on a FACS ARIA instrument (BD Biosciences).

Western blotting

Western blotting was performed essentially as previously described[8]. In brief, cell lysates were separated on 10% SDS-PAGE gels at 150 V for 1 hr. Transfer to nitrocellulose membranes was then performed at 100 V for 1 hr. Membranes were blocked using blocking buffer (TBS-T supplemented with 5% milk) and then probed with mouse anti-

ARPC3 antibodies (sc-136020, Santa Cruz Biotechnology) or anti-HSC70 antibodies (sc-7298, Santa Cruz Biotechnology). After incubation with HRP-conjugated secondary antibodies diluted in blocking buffer, membranes were incubated with chemiluminescence substrate for 1 min before being exposed to films. Densitometry was performed using ImageJ software on three independent western blots. Expression levels of ARPC3 were normalized to the expression level of HSC-70.

Cell motility assay

Cells were plated at a density of 50,000 cells per well in a 6-well plate. After 24 hours, the media was refreshed and the plates were transferred to the stage of an inverted Leica IX-70 time lapse microscope fitted within a chamber that was heated to 37°C with an atmosphere containing 5% CO_2. Images were captured through a 20X phase contrast objective every 30 mins for a total of 48 hours. In order to measure cell migration, random cells were tracked in x and y from time-lapse videos for 30 hours using the manual tracking plugin in ImageJ. For the purposes of quantification, 30 cells from each experimental group were analysed from across two independent experiments. Results were expressed in terms of cell velocity (μm / minute).

Cell proliferation assay

To assess the proliferation kinetics of cells, 2000 HT29 cells were seeded (in quadruplicate wells) on to four different 96-well plates (plates 1 to 4). Cell viability was measured from plates 1, 2, 3 and 4 at 24, 48, 72 and 96 hours, respectively, using the CellTitre-Glo reagent (Promega) according to the manufacturer's instructions. The quantity of viable cells was expressed relative to the signal at 24 hours from three independent experiments.

Preclinical model of advanced liver metastasis

The Institute of Cancer Research Animal Ethics Committee granted approval for animal work and procedures were performed in accordance with the United Kingdom Home Office regulations. We used female CB17 SCID mice (CB17/Icr-*Prkdc*^{scid}/IcrIcoCrl) at 12-16 weeks of age (obtained from Charles River UK). Parental HT29 cells, or HT29 cells stably transduced with shRNA constructs as appropriate, were resuspended in growth factor-reduced Matrigel (Invitrogen) at a concentration of $1x10^7$ cells/ml. Cells were introduced into the liver by laparotomy performed under general anesthesia (inhaled isofluorane). A midline incision was made through the peritoneum and the left main lobe of the liver was exteriorized. This lobe was injected with $4x10^5$ cells in a volume of 40 μL using a 29-gauge needle and then returned to the peritoneal cavity. The wound was closed with wound clips. In order to assess the effect of ARPC3 knockdown on the HGP (Fig. 4a,b and Fig. 4e) mice were culled 21 days post-injection of cancer cells. The tumor-bearing liver lobe was harvested, fixed in formalin and embedded in paraffin.

For experiments where treatment was administered (Fig 4f-h), we waited for 10 days post-surgery to allow for tumor establishment. At 10 days, mice were injected subcutaneously with 75 mg/kg D-luciferin (Caliper Life Sciences), anesthetized with isofluorane and then imaged in an Lumina II™ IVIS (*In Vivo* Imaging System) instrument (Caliper Life Sciences). Quantification of liver bioluminescence was performed using Living Image™ software (Caliper Life Sciences) according to manufacturer's instructions. The bioluminescence measurement was used to ensure that subjects of equivalent tumor burden were allocated to each experimental group.

Capecitabine powder (LC Laboratories) was dissolved in vehicle for oral administration (40 mM citrate buffer pH 6, 5% gum Arabic). B20-4.1.1 (Genentech), an antibody that blocks both mouse and human VEGF-A[9], was dissolved in sterile PBS for intraperitoneal administration. One cycle of therapy consisted of the following: mice

received 500 mg/kg capecitabine or vehicle by oral gavage every day for 5 days, followed 2 days treatment break, with intraperitoneal injection of 2.5 mg/kg B20-4.1.1 or vehicle on the first and fifth day of the cycle. Mice were administered two cycles of therapy and then culled at 24 days post-injection of tumor cells. The tumor-bearing liver lobe was harvested, fixed in formalin and embedded in paraffin.

For quantification of tumor burden, H&E stained sections were prepared. Sections were digitally scanned (Nanozoomer, Hamamatsu) and imported into NDPI viewer software (Hamamatsu). The marquee tool was used freehand to create regions of interest (ROIs) around areas of tumor in the section and tumor burden measurement was calculated in terms of area in mm^2. For quantification of vessel density, sections were co-stained for CD31 (detected with TMB) and CK20 (detected with DAB). Tumor vessels were manually counted and expressed in terms of vessels per mm^2 of tumor area. H&E-stained sections were scored for HGP according to the same criteria used for human samples of liver metastasis. The scoring of tumor burden, vessel density and HGPs was performed in a blinded fashion. The number of mice per group was selected based on prior experience regarding the minimum number of animals necessary to detect a statistically significant difference between experimental groups. No randomization method was used.

Validation of ARPC3 staining specificity and scoring of ARPC3 staining intensity

HT29 cells stably transfected with a control non-targeting shRNA (control shRNA) or an ARPC3-targeted shRNA (ARPC3-shRNA3) were grown to confluency on tissue culture flasks. Cells were washed in PBS, harvested by trypsinization and then pelleted by centrifugation. Pelleted cells (approximately 1x10^7 cells per pellet) were then resuspended in formalin and fixed for 15 mins followed by pelleting again and embedding of the fixed pelleted cells in parafin. Tissue sections were prepared and then stained using a mouse anti-ARPC3 antibody (MABT95, Millipore) as described above in the section entitled

'Immunohistochemistry.' Antigen retrieval was performed in pH 6 citrate buffer with heating in a microwave for 18 mins and the antibody was used at a dilution of 1:2500.

The same staining protocol was used to stain for ARPC3 in FFPE tissue sections of human liver metastasis specimens. Positive staining for ARPC3 was observed in cancer cells and in some stromal cell types (including immune cells and Kuppfer cells), but only cancer cell staining was scored. The scoring of ARPC3 staining intensity in cancer cells was performed semi-quantitatively by a pathologist. For each case examined, the percentage of cancer cells having 1+ (weak), 2+ (moderate) or 3+ (strong) staining intensity was scored. The result for each case was expressed as an H-score as calculated by the formula: (% area of weak staining) + (2 x % area of moderate staining) + (3 x % area of strong staining). This generates a score of between 0 – 300 for each case scored.

Statistical analysis

Clinical data were analyzed using two-tailed χ^2-test (Figure 1b,f and Figure 2g and Supplementary Figures S3, S4 and S5 and Supplementary Tables S2, S4, S7 and S8) or Log-Rank test (Figure 4b,c). A multivariate logistic regression model was employed to determine whether the association between the HGPs for each individual lesion and pathological response remained significant when controlling for the effect of other clinical variables. Given that some lesions came from the same patient, a generalized estimating equation (GEE) approach was used in the multivariate analysis to account for the within-patient covariance. A Cox proportional hazards regression model was used to determine whether the association between the HGPs and overall survival remained significant when controlling for the effect of other clinical variables. Clinical variables included in the multivariate analyses were: gender, age, site of primary tumor, baseline lesion size, chemotherapy backbone, cycles of preoperative therapy, interval between last bevacizumab dose and resection.

Where appropriate, the Kolmogorov-Smirnov normality test was used to determine the normality of the data and the F-test equality of variances test was used to determine whether the variance between groups was similar. For normally distributed data, we used two-tailed unpaired Student's *t*-test (with Welch's correction applied if the variance between groups was not similar) to compare experimental groups (Fig 6g, Fig 6h). For non-normally distributed data, where the variance between groups was either similar or dissimilar, we used the non-parametric two-tailed Mann-Whitney *U*-test to compare experimental groups (Fig 4a, Fig 6d, Fig 6e, Fig 6f). For data where the sample number was too small (n = 3 independent experiments) to determine normality, but where the variance between groups was similar, we used two-tailed unpaired Student's *t*-test to compare experimental groups (Fig 6c, Fig S10). For all analyses, *P*-values below 0.05 were considered statistically significant. Statistical analyses were performed using JMP Version 11.0 (SAS Institute, Inc., Cary, NC, USA) and GraphPad Prism version 6.0 (GraphPad Software, San Diego, CA).

References for Online Methods

1. Ribero, D.*, et al.* Bevacizumab improves pathologic response and protects against hepatic injury in patients treated with oxaliplatin-based chemotherapy for colorectal liver metastases. *Cancer* **110**, 2761-2767 (2007).
2. Chang, H.H., Leeper, W.R., Chan, G., Quan, D. & Driman, D.K. Infarct-like necrosis: a distinct form of necrosis seen in colorectal carcinoma liver metastases treated with perioperative chemotherapy. *The American journal of surgical pathology* **36**, 570-576 (2012).
3. Chun, Y.S.*, et al.* Association of computed tomography morphologic criteria with pathologic response and survival in patients treated with bevacizumab for colorectal liver metastases. *JAMA* **302**, 2338-2344 (2009).
4. Boonsirikamchai, P.*, et al.* CT findings of response and recurrence, independent of change in tumor size, in colorectal liver metastasis treated with bevacizumab. *AJR. American journal of roentgenology* **197**, W1060-1066 (2011).
5. Goldhirsch, A.*, et al.* Personalizing the treatment of women with early breast cancer: highlights of the St Gallen International Expert Consensus on the Primary Therapy of Early Breast Cancer 2013. *Ann Oncol* **24**, 2206-2223 (2013).
6. Hammond, M.E.*, et al.* American Society of Clinical Oncology/College of American Pathologists guideline recommendations for immunohistochemical testing of estrogen and progesterone receptors in breast cancer (unabridged version). *Arch Pathol Lab Med* **134**, e48-72 (2010).
7. Wolff, A.C.*, et al.* Recommendations for human epidermal growth factor receptor 2 testing in breast cancer: American Society of Clinical Oncology/College of American Pathologists clinical practice guideline update. *J Clin Oncol* **31**, 3997-4013 (2013).
8. Gourlaouen, M., Welti, J.C., Vasudev, N.S. & Reynolds, A.R. Essential role for endocytosis in the growth factor-stimulated activation of ERK1/2 in endothelial cells. *J Biol Chem* **288**, 7467-7480 (2013).
9. Liang, W.C.*, et al.* Cross-species vascular endothelial growth factor (VEGF)-blocking antibodies completely inhibit the growth of human tumor xenografts and measure the contribution of stromal VEGF. *J Biol Chem* **281**, 951-961 (2006).

XVIII. Transition to manuscript V

We demonstrated evidence of an association between resistance to neoadjuvant anti-angiogenic therapy in patients with colorectal liver metastasis. These findings highlight a dichotomous biological behavior of colorectal liver metastases, as replacement and desmoplastic patterns display distinct histological features, vascularization processes, responses to neoadjuvant therapy and overall survival.

Based on these results, we wanted to investigate if the patterns could also explain heterogenous behaviors in specific clinical contexts, such as after portal vein embolization. Moreover, as portal vein embolization can also be part of a staged resection procedure, in which two consecutive surgeries are performed on patients in order to remove all lesions. We wanted to look into the dstribution of the patterns in the first and second stage surgeries in order to correlate the histological patterns to clinical outcomes, such as disease progression or disease control after PVE or during a staged procedure.

It is known that the microenvironment surrounding liver metastasis after portal vein embolization undergo dynamic changes including vascular supply redistribution, such that the hepatic arterial system attempts to compensate for the portal venous flow blockade in the embolizaed lobe. Thus we hypothesized that replacement lesions may be in a more favorable milieu based on the fact that they utilize mature nearby vasculature (vessel co-option) and therefore the compensatory arterial response may make hese tumors more prone to progress after PVE. Moreover, as we had shown that progression after portal vein embolization is associated with response to neoadjuvant chemotherapy, we wanted to investigate if the patterns were actually the variable determinant with disease progression, as our results clearly showed difference responses being attributed to the patterns.

XIX. Thesis Manuscript V

Ready for submission

Colorectal liver metastasis progression after portal vein embolization is determined by the histological growth patterns

Eve Simoneau[1], Peter Vermeulen[3], Gert Van den Eynden[2], Andrew Reynolds[3], Anthoula Lazaris[4], Stephanie Petrillo[4], Ayat Salman[4], David Valenti[5], Mazen Hassanain[1,6], Peter Metrakos[1,4,7]

[1]Department of Surgery, McGill University, Montreal, Canada

[2]Translational Cancer Research Unit (TCRU), GZA Hospitals St. Augustinus, Antwerp, Belgium

[3]Tumour Biology Team, Breakthrough Breast Cancer Research Centre, The Institute of Cancer Research, London, United Kingdom

[4]McGill University Health Center (MUHC) Research Institute, McGill University, Montreal, Canada

[5]Department of Radiology, McGill University, Montreal, Canada

[6]Department of Surgery, King Saud University, Riyadh, Saudi Arabia

[7]Department of Pathology, McGill University, Montreal, Canada

Correspondance:

Peter Metrakos, MD

McGill University Health Center – Glen Site

Montreal, QC, Canada, H4A 3J1

Phone: (514) 843-1600. Fax: (514) 843-1503

Email: peter.metrakos@mcgill.ca

Abstract

Introduction: Colorectal cancer liver metastases grow in three different histological growth patterns (HGP), which are known to exhibit different tumor vascularization. Tumor progression after portal vein embolization (PVE), whether before an extended resection or as part of staged resection, can negatively impact resectability. The aim of this study was to investigate if the growth patterns are associated with disease progression in this context. Methods: Between 2008 and 2014, all patients who underwent PVE, who had complete preoperative radiological data and pathological data from resected specimen were included in the study. Tumor volumes were measured for all patients and individual lesions and HGP were scored for each lesion. Patients who underwent staged resections were also included. Results: 178 lesions from 46 patients were included. Most (93.1%) patients exhibited disease control on neoadjuvant chemotherapy before the PVE. Ninety-eight lesions were progressive (PD) and 80 were stable (SD) after PVE. The distribution of HGP was significantly different across the two groups: in the PD group, lesions were predominantly replacement (average 80.3% ± 30.9 vs. 13.9% ± 25.7 desmoplastic, $p<0.001$). Conversely, in the SD group, the lesions were predominantly desmoplastic (64.0% ± 43.3 vs. replacement 33.1% ± 41.5%, $p<0.001$). In patients with two-stage resections without clinical disease progression, the average HGP were 77.1% ± 37.2 (desmoplastic), 22.6% ± 37.0 (replacement) and 0.3% ± 0.8 (pushing) ($p<0.001$). In patients with disease progression between the first and second stage surgery, the predominant HGP was replacement, with an average of 78.9% ± 28.4, compared to 20.6% ± 28.7 desmoplastic and 0.6% ± 1.5 pushing ($p<0.001$). Conclusion: The HGP of liver metastases are associated with disease progression in the context of PVE and staged resections. Non-invasive methods of determining growth patterns are needed to optimize patient stratification.

INTRODUCTION

Resection of colorectal cancer liver metastasis (CRCLM) provides the best long-term outcomes for patients. In fact, large surgical series have demonstrated a clear survival advantage of resection over systemic chemotherapy only by reporting 5-year survivals of 28-58% (1-3). Since the majority (80%) of patients present with initially unresectable disease, clinicians aimed to develop strategies that could increase the number of patients eligible for surgery. One of these methods is the use of portal vein embolization (PVE). Portal vein embolization is a method that entails blocking the portal flow to the diseased lobe of the liver, consequently inducing hypertrophy of the contralateral liver lobe in preparation for major resection(4,5). Since PVE can convert initially unresectable patients to a resectable state (6,7), clinicians favored the use of this preoperative technique for CRCLM, when indicated for patients with small future liver remnant (FLR). On the other hand, it has been shown in multiple series that PVE might stimulate tumor progression, a process that may occur in 40-80% of patients undergoing PVE(6,8-10). Accordingly, tumor progression after portal vein embolization is becoming a growing concern in the literature(8,9,11-15). Thus, identifying early patients at higher risk of tumor progression is becoming critically important. Furthermore, it has been previously demonstrated that liver metastases grow in three different histological growth patterns: a desmoplastic, a replacement and a pushing pattern(16,17). Each of these growth patterns are known to be associated with different types of vascularization. In fact, desmoplastic and pushing tumors utilize predominantly angiogenesis while the replacement pattern utilize vessel co-option, a process by which tumors utilize pre-existing mature vasculature instead of forming new blood vessels(16-18).

Due to the vascular dynamic changes occurring after portal vein embolization and the presence of tumor progression observed in a proportion of patients, our aim was to

investigate if the histological growth patterns are associated with tumor progression after PVE and in staged resections.

METHODS

Patient selection

The study was approved by our institution review ethics board and under the Liver Disease Biobank protocol (SDR11-066). All patients with a diagnosis of CRCLM who underwent hepatectomy with a preoperative portal vein embolization between January 2008 and May 2014 inclusively were included. More precisely, we included patients who received a preoperative embolization prior to an extended hepatectomy (extended right or left hepatectomy), as well as part of a staged liver resection (consisting of two consecutive surgeries performed, with portal vein embolization after the first surgery, in order to remove all tumors), as shown in Figure 1. The clinical course of all patients included neoadjuvant chemotherapy (with triphasic CT scans before and after treatment), followed by the portal vein embolization and a follow-up triphasic CT scan 3 to 4 weeks after the PVE. Decision to undergo preoperative PVE was based on tumor board recommendations for all patients.

Clinical variables

The clinical data collected included disease characteristics (primary and metastatic disease), chemotherapy data (regimen, number of cycles, timing), chemotherapy response based on Response Evaluation Criteria in Solid Tumors (RECIST), disease-free survival and overall survival. As standard practice, every patient was reevaluated approximately 3 months following the first baseline CT scan at which point the response and disease status

were evaluated by a multidisciplinary team, to confirm that patients can undergo PVE and resection of the hepatic lesions, judged by the feasibility of achieving an R0 resection.
For the purpose of the study, chemotherapy response was objectively evaluated based on RECIST guidelines by a radiologist who was blinded to the clinical and pathological information of patients. The measurable target lesions were assessed by triphasic CT scans before and after systemic neoadjuvant chemotherapy; the response for each individual lesion, as well as the response per patient were both measured. Briefly, a complete response (CR) was defined as complete disappearance of all lesions on follow-up imaging, while partial response (PR) and progression of disease (PD) were defined as a ≥ 30% decrease and ≥ 20% increase in the total diameter of the target metastatic lesions respectively. Any differences falling in between those cut-offs were judged to represent stable disease (SD). PD also included patients who developed new lesions or extra-hepatic disease on chemotherapy regardless of changes in lesion diameter.

Portal vein embolization and hepatectomy

Following neoadjuvant chemotherapy, the decision to undergo preoperative PVE was made based on the predicted future liver remnant (FLR), defined by the amount of liver parenchyma predicted to be left after resection, and typically measured using 3-dimensional CT volumetry. (19) If patients had a predicted FLR (expressed in %, as a proportion of the total liver volume) of ≤20%, or ≤30% with suspected parenchymal damage due neoadjuvant chemotherapy, they were offered a preoperative PVE in order to be eligible for hepatic resection. (20,21) PVE was performed either before an extended hepatectomy, or as part of a staged liver resection, which typically consisted of a left lateral resection (resection of segment 2 and 3), followed by a PVE and subsequently a right hepatectomy.
All PVE were performed under ultra-sound guidance, by transhepatic approach using ipsilateral puncture. The embolization materials included polyvinyl alcohol (PVA) and/or

coils. In some occasions, the PVE was performed in two stages where the posterior segments were embolized first followed by the anterior segments embolization to finally occlude all portal venous branches of the side to be resected.

Disease evaluation after PVE

In order to categorize lesions with progression of disease after PVE (PD_{PVE}) or stable disease the PVE (SD_{PVE}), the differences in tumor volumes before and after PVE were measured using 3-dimensional CT volumetric analysis. The triphasic CT scans were imported on a GE Medical Systems Advantage Windows 4.3 workstation (GE Healthcare, Chalfont St Giles, UK). Measurements were performed on axial view, porto-venous phase on maximum 5 mm thick multiphasic CT images. The tumor volumes (TV) of the lesions were expressed in cm^3. Tumor growth was defined as a percentage change in tumor volume of more than 15% (($TV_{post} – TV_{pre}$) / TV_{pre} x100). (10) The cut-off was determined based on published series validating the correlation of a 15% cut-off (using volumes) to progression of disease by RECIST (using diameters). (22,23) The size of the future liver remnant (FLR) and the total liver volume (TLV) pre and post-PVE were also measured similarly using 3D CT volumetry. All volumes were measured manually by two radiologists and all nearby structures such as the stomach, gallbladder, major vessels and diaphragm were carefully excluded from the measurements.

Histological growth pattern assessment

The histological growth patterns (HGP) of all lesions found in the resected specimens were scored. Sections from formalin-fixed paraffin-embedded blocks were cut at 5 μm and stained with hematoxylin and eosin (H&E). The H&E sections were scanned at 20X

magnification using the Aperio ScanScope XT System. Images were then imported in a digital pathology-viewing platform, which was used to score and share the images. Two pathologists independently scored all images and were blinded to the clinical information (treatment, disease progression or stability, timing of PVE, and details of the lesion assessed). When available, multiple representative H&E slides from a single lesion were scored, and the results were combined to designate a single average HGP score for each lesion. Based on previous studies defining and validating the HGP(16,24), the liver-metastasis interface was scored and attributed a proportion (expressed in %) of each of the three growth patterns: desmoplastic, replacement and pushing. A desmoplastic growth pattern was defined as the absence of direct contact between hepatocytes and tumor cells and by the presence of a desmoplatic stroma. A replacement growth pattern was defined as a close contact between hepatocytes and tumor cells, where tumor cells infiltrate and replace the surrounding parenchyma with preserving the nearby vasculature. A pushing growth pattern was defined as tumor cells in close contact with hepatocytes with an appearance of compression of the liver plate, but without invading into the parenchyma as observed in the replacement pattern and without a desmosplatic rim.

Statistical analysis

Data were analyzed in JMP version 11.0 statistics software and GraphPad Prism version 6.0 (GraphPad Software, San Diego, CA). Mean and standard deviation (normally distributed data) and Median and interquartile range (non-normally distributed data) were calculated for the continuous variables and frequencies and proportions for categorical variables. Student t-test was used for the difference of continuous variables and the Chi-square test or its alternative Fisher's Exact test were used to measure the difference of categorical variables. A p-value of less than 0.05 was considered significant.

RESULTS

Patients

Out of 209 lesions (from 50 patients) resected from patients who received a preoperative portal vein embolization between 2008 and 2014, 178 lesions (from 46 patients) were included in the final analysis. (Figure 2) Baseline characteristics of all patients are detailed in Table 1. All patients except for two received neoadjuvant chemotherapy, most of which (93.1%, n=41) had adequate disease control with a partial response or stable disease on neoadjuvant chemotherapy before they received the PVE. From this cohort, 12 patients had a complete staged resection. Therefore an additional 24 lesions (the pre-PVE lesions resected in the first stage surgery) from these patients were also included for a second analysis. Finally, 22 lesions from 8 patients who had a first stage resection, followed by the embolization, but were never resected due to disease progression, were also included in the study.

Distribution of histological growth patterns in resected lesions with preoperative portal vein embolization

When looking at the individual lesions characteristics, 98 lesions (55.1%) were categorized as PD_{PVE} based on tumor volumetry changes or if they were newly appearing lesions on the follow-up CT scan; the remaining ones (n=80, 44.9%) were categorized as SD_{PVE}. The distribution of HGP within the two groups (SD vs. PD after PVE) was found to be significantly different, with a predominance of replacement pattern in the group with post-PVE disease progression, as opposed to a predominance of desmoplastic lesions in the group with stable disease post-PVE (Figure 3, $p<0.001$). From the 98 PD_{PVE} lesions, 81.6% (n=80) were scored as predominantly (>50% of the section) replacement growth pattern. On the other hand, 61.3% (n=49) lesions in the group with stable disease after PVE were

scored with a predominance of desmoplastic growth pattern. The average proportion of histological growth patterns in the progression group was predominantly of the replacement group pattern, compared to desmosplatic and pushing patterns (80.3 ± 30.9% vs. 13.9 ± 25.7% and 5.9 ± 15.8% respectively, $p<0.001$ in both cases). Conversely, the predominant histological growth pattern in the stable disease group after PVE was the desmoplastic pattern with an average of 64.0 ± 43.3%, compared to replacement (33.1 ± 41.5%, $p<0.001$) and pushing (3.0 ± 10.4%, $p<0.001$). These results illustrate clear histological growth pattern distribution differences based on tumor progression or stability after PVE.

Completed and failed staged resections

To investigate if the lesions before and after the embolization were similar or different, we aimed to analyze metastatic lesions resected from staged resections (the pre-PVE (first stage) surgical specimens compared to their paired post-PVE (second stage) specimens). Twelve patients from the cohort were part of a staged resection, and their corresponding pre-PVE lesions (from the first surgery) were analyzed and scored similarly. Four of these 12 patients exhibited stable disease after the PVE based on tumor volumetry, and the remaining 7 patients exhibited disease progression. The HGP distribution in the first 4 patients (paired pre and post-PVE lesions, stable disease after PVE) was composed of predominantly desmoplastic pattern and for the most part, homogenous between pre and post-PVE lesions (Figure 4A). The average patterns were 77.1% ± 37.2 (desmoplastic), 22.6% ± 37.0 (replacement) and 0.3% ± 0.8 (pushing) ($p<0.001$). Conversely for the 8 patients with radiological disease progression between the first and second stage surgery, the predominant HGP was replacement, with an average of 78.9% ± 28.4, compared to 20.6% ± 28.7 desmoplastic and 0.6% ± 1.5 pushing ($p<0.001$). Notably, in the group with disease progression the pre-PVE lesions were desmoplastic in 3 patients, and replacement

in the remaining 4 patients. (Figure 4B). When examining an additional cohort of 22 lesions (from 8 patients) who underwent a first stage surgery, exhibited post-PVE disease progression and were not resected thereafter ("failed" staged resections), the baseline HGP was found to be of predominantly replacement pattern in more cases (14 out of 22 lesions, average percentage of replacement pattern 54.6% ± 40.1 vs. 41.6% ± 42.5 for desmoplastic pattern, p=0.7210), as shown in Figure 5.

DISCUSSION

This study highlights the association between the histological growth patterns and tumor outcome after portal vein embolization. Since failure to achieve resectability in this patient population is mainly due to disease progression after the PVE,(7,10,15) stratifying patients at risk of progression could help in tailoring therapy and potentially reduce the drop-out to surgery. Our group has investigated the association between histological growth patterns and treatment resistance in patients with colorectal cancer liver metastasis undergoing neoadjuvant chemotherapy; we have found a strong correlation between the invasive replacement growth pattern and disease progression (resistance) during systemic treatment (Frentzas et al, unpublished data). In fact, the vascularization process by which the tumors harboring a replacement pattern obtain their blood supply is vessel co-option(16-18); this process seems to be mediating treatment resistance in the context of neoadjuvant chemotherapy in combination with anti-angiogenic therapy (Frentzas et al, unpublished data). Based on these findings, we wanted to investigate if the invasive replacement pattern would also be associated with disease progression in more specific clinical contexts, such as portal vein embolization. The results of the current study support the fact that replacement growth pattern is associated with disease progression in the context of portal

vein embolization, as the majority of tumors exhibiting disease progression were mostly composed of the replacement pattern. Furthermore, a peculiar patient population undergoing portal vein embolization are those undergoing a two-stage surgery. This allowed us to compare within the same individuals the distribution of the histological growth patterns before and after the embolization. Our analysis of the two-stage surgery patients also verified our hypothesis. Moreover, 3 out of 8 patients who had two-stage surgery with disease progression displayed pre-PVE HGP predominantly desmoplastic, while their paired post-PVE patterns were predominantly replacement. Although these observations constitute more indirect evidence, this may suggest the ability of the HGP to undergo a "switch" from desmoplastic to replacement as patients start to show clinical disease progression. Undoubtedly, the nature of the surgical resections would not allow an investigator to analyze the same individual lesion before and after PVE, which we acknowledge is an important limitation of our study. Although the HGP are relatively homogenous for each individual patient (Frentzas et al, unpublished data), the staged resection patients do exhibit some heterogeneity in terms of the HGP distribution within the same individuals and therefore prevent a robust interpretation of these findings. It is therefore important to clarify that although we found an association between replacement pattern and disease progression after PVE, the assessment of the HGP is from a surgical specimen ie, after the embolization. As it is not possible to characterize the HGP in a non-invasive way yet, it is not possible to know the proportion of lesions that were initially (pre-PVE) replacement or desmoplastic. Finally, our analysis of the pre-PVE lesions in patients with failed staged resections demonstrates a higher proportion of replacement lesions, although not statistically significant. Consistent with the data in completed staged resections however, it is not surprising to observe both desmoplastic and replacement lesions prior to the intervention. This also shows that the replacement pattern is not simply

reflecting a treatment-effect caused by the embolization, as both patterns are present in this cohort of patients.

Several mechanism have been suggested to explain tumor progression occurring in the context of a portal vein embolization, most of which are derived from experimental studies (25). One proposed mechanism is based on the hepatic arterial buffer response, an intrinsic regulatory mechanism defined as an increase in hepatic arterial flow to the liver when portal venous flow decreases(26). In fact, several clinical and experimental studies suggested that portal vein embolization is followed by an immediate increase in arterial blood supply. Since the liver metastases derive their blood supply from the arterial system, it has been hypothesized to be contributing to the tumor progression observed after portal vein embolization(27-29). Correspondingly, since the replacement pattern is known to utilize vessel co-option, a process by which tumor derive their blood supply from pre-existing mature vessels, it may be that the replacement pattern is favored in the milieu generated by the embolization, resulting in tumor progression.

The clinical impact of these results lies in the possibility that the pre-PVE pattern is predictive of the post-PVE pattern, the latter being associated with tumor progression post-PVE. There is currently no study that has reported a method to accurately identify the histological growth pattern in a non-invasive way, without relying on the surgical specimen; therefore finding an imaging or another modality that could identify reliably the HGP pre-intervention would be key in order to demonstrate this. Although there may prognostic significance of determining the histological growth patterns before the PVE, our data suggests that there may be a proportion of patients undergoing a switch from desmoplastic to replacement pattern therefore no recommendation can be made in terms of patient selection for the intervention based on the pre-PVE growth patter. Future studies integrating molecular biology, dynamic imaging and pathological validation would be needed in order to characterize and stratify patients before the intervention.

References

1. Scheele J, Stangl R, Altendorf-Hofmann A. Hepatic metastases from colorectal carcinoma: impact of surgical resection on the natural history. Br J Surg. 1990 Nov;77(11):1241–6.

2. Abdalla EK, Vauthey J-N, Ellis LM, Ellis V, Pollock R, Broglio KR, et al. Recurrence and outcomes following hepatic resection, radiofrequency ablation, and combined resection/ablation for colorectal liver metastases. Ann. Surg. 2004 Jun;239(6):818–25–discussion825–7.

3. Fernandez FG, Drebin JA, Linehan DC, Dehdashti F, Siegel BA, Strasberg SM. Five-year survival after resection of hepatic metastases from colorectal cancer in patients screened by positron emission tomography with F-18 fluorodeoxyglucose (FDG-PET). Ann. Surg. 2004 Sep;240(3):438–47–discussion447–50.

4. Madoff DC, Abdalla EK, Vauthey J-N. Portal vein embolization in preparation for major hepatic resection: evolution of a new standard of care. J Vasc Interv Radiol. 2005 Jun;16(6):779–90.

5. Abulkhir A, Limongelli P, Healey AJ, Damrah O, Tait P, Jackson J, et al. Preoperative Portal Vein Embolization for Major Liver Resection. Ann. Surg. 2008 Jan;247(1):49–57.

6. Abdalla EK. Portal vein embolization (prior to major hepatectomy) effects on regeneration, resectability, and outcome. J Surg Oncol. 2010 Dec 15;102(8):960–7.

7. Wicherts DA, de Haas RJ, Andreani P, Sotirov D, Salloum C, Castaing D, et al. Impact of portal vein embolization on long-term survival of patients with primarily unresectable colorectal liver metastases. Br J Surg. 2010 Feb;97(2):240–50.

8. Simoneau E, Aljiffry M, Salman A, Abualhassan N, Cabrera T, Valenti D, et al. Portal vein embolization stimulates tumour growth in patients with colorectal cancer liver metastases. HPB (Oxford). 2012 Jul;14(7):461–8.

9. Hoekstra LT, van Lienden KP, Doets A, Busch ORC, Gouma DJ, van Gulik TM. Tumor progression after preoperative portal vein embolization. Ann. Surg. 2012 Nov;256(5):812–7–discussion817–8.

10. Simoneau E, Hassanain M, Shaheen M, Aljiffry M, Molla N, Chaudhury P, et al. Portal vein embolization and its effect on tumour progression for colorectal cancer liver metastases. Br J Surg. 2015 Sep;102(10):1240–9.

11. Elias D, De Baere T, Roche A, Mducreux, Leclere J, Lasser P. During liver regeneration following right portal embolization the growth rate of liver metastases is more rapid than that of the liver parenchyma. Br J Surg. 1999 Jun;86(6):784–8.

12. Kokudo N, Tada K, Seki M, Ohta H, Azekura K, Ueno M, et al. Proliferative activity of intrahepatic colorectal metastases after preoperative hemihepatic portal vein embolization. Hepatology. 2001 Aug;34(2):267–72.

13. Ribero D, Abdalla EK, Madoff DC, Donadon M, Loyer EM, Vauthey J-N. Portal vein embolization before major hepatectomy and its effects on regeneration, resectability and outcome. Br J Surg. 2007 Nov;94(11):1386–94.

14. Barbaro B, Di Stasi C, Nuzzo G, Vellone M, Giuliante F, Marano P. Preoperative right portal vein embolization in patients with metastatic liver disease. Metastatic liver volumes after RPVE. Acta Radiol. 2003 Jan;44(1):98–102.

15. Mueller L, Hillert C, Möller L, Krupski-Berdien G, Rogiers X, Broering DC. Major hepatectomy for colorectal metastases: is preoperative portal occlusion an oncological risk factor? Ann. Surg. Oncol. 2008 Jul;15(7):1908–17.

16. Vermeulen PB, Colpaert C, Salgado R, Royers R, Hellemans H, Van Den Heuvel E, et al. Liver metastases from colorectal adenocarcinomas grow in three patterns with different angiogenesis and desmoplasia. J. Pathol. 2001 Oct;195(3):336–42.

17. Van den Eynden GG, Majeed AW, Illemann M, Vermeulen PB, Bird NC, Høyer-Hansen G, et al. The multifaceted role of the microenvironment in liver metastasis: biology and clinical implications. Cancer Res. 2013 Apr 1;73(7):2031–43.

18. Stessels F, Van den Eynden G, Van der Auwera I, Salgado R, Van Den Heuvel E, Harris AL, et al. Breast adenocarcinoma liver metastases, in contrast to colorectal cancer liver metastases, display a non-angiogenic growth pattern that preserves the stroma and lacks hypoxia. Br. J. Cancer. 2004 Apr 5;90(7):1429–36.

19. Abdalla EK, Adam R, Bilchik AJ, Jaeck D, Vauthey J-N, Mahvi D. Improving resectability of hepatic colorectal metastases: expert consensus statement. Ann. Surg. Oncol. 2006 Oct;13(10):1271–80.

20. Azoulay D, Castaing D, Smail A, Adam R, Cailliez V, Laurent A, et al. Resection of nonresectable liver metastases from colorectal cancer after percutaneous portal vein embolization. Ann. Surg. 2000 Apr;231(4):480–6.

21. Adam R, Delvart V, Pascal G, Valeanu A, Castaing D, Azoulay D, et al. Rescue surgery for unresectable colorectal liver metastases downstaged by chemotherapy: a model to predict long-term survival. Ann. Surg. 2004 Oct;240(4):644–57–discussion657–8.

22. Ak G, Metintas M, Metintas S, Yildirim H, Ozkan R, Ozden H. Three-dimensional evaluation of chemotherapy response in malignant pleural mesothelioma. Eur J Radiol. 2010 Apr;74(1):130–5.

23. Jeon D-G, Kong C-B, Cho WH, Song WS, Cho SH, Choi SW, et al. Examination of the cutoff value of postchemotherapy increase in tumor volume as a predictor of subsequent oncologic events in stage IIB osteosarcoma. J Surg Oncol. 2014 Mar;109(3):275–9.

24. Van den Eynden GG, Bird NC, Majeed AW, Van Laere S, Dirix LY, Vermeulen PB. The histological growth pattern of colorectal cancer liver metastases has prognostic value. Clin. Exp. Metastasis. 2012 Aug;29(6):541–9.

25. Lim C, Cauchy F, Azoulay D, Farges O, Ronot M, Pocard M. Tumour progression and liver regeneration-insights from animal models. Nat Rev Gastroenterol Hepatol.

2013 Apr 9.

26. Eipel C, Abshagen K, Vollmar B. Regulation of hepatic blood flow: the hepatic arterial buffer response revisited. World J. Gastroenterol. 2010 Dec 28;16(48):6046–57.

27. Kito Y, Nagino M, Nimura Y. Doppler sonography of hepatic arterial blood flow velocity after percutaneous transhepatic portal vein embolization. AJR Am J Roentgenol. 2001 Apr;176(4):909–12.

28. Nagino M, Nimura Y, Kamiya J, Kanai M, Hayakawa N, Yamamoto H. Immediate increase in arterial blood flow in embolized hepatic segments after portal vein embolization: CT demonstration. AJR Am J Roentgenol. 1998 Oct;171(4):1037–9.

29. de Graaf W, van den Esschert JW, van Lienden KP, van Gulik TM. Induction of tumor growth after preoperative portal vein embolization: is it a real problem? Ann. Surg. Oncol. 2009 Feb;16(2):423–30.

Table 1. Baseline clinical characteristics per patient undergoing resection with preoperative PVE (n=46)

Variable	Patients (n=46)
Gender, n (%)	
Male	33 (71.7)
Female	13 (28.3)
Age, median (IQ range)	60 (51-66)
Primary tumor, n(%)	
Colon	31 (67.4)
Rectum	15 (32.6)
T1-2[a]	1 (5.3)
T3-4	18 (94.7)
N0[a]	1 (5.3)
N1	9 (47.3)
N2	10 (52.6)
Synchronous, n (%)	38 (82.6)
Metachronous, n (%)	8 (17.4)
Number of lesions per patient, median (IQ range)	5 (3-6)
Tumor volume (cm^3) per lesion, median (IQ range)	3.95 (1.12-20.40)
Neoadjuvant chemotherapy, n (%)	
Oxaliplatin	33 (71.7)
Irinotecan	5 (10.9)
Bevacizumab	27 (58.7)
Chemonaive	2 (4.3)
Number of neoadjuvant chemotherapy cycles, mean ± SD	6 ± 2
Neoadjuvant chemotherapy response[b]**, n (%)**	
Partial response	17 (37.0)
Stable disease	24 (52.2)
Progression of disease	5 (10.9)
Embolization	
One stage	36 (78.3)
Two stage[c]	10 (21.7)
Part of planned staged resection	12 (26.1)
FLR (%)[d]**, median (IQ range)**	
Pre-PVE	23.37 (18.42-27.57)
Post-PVE	31.18 (27.90-41.48)

a: based on 16 available resected primary specimens. b: Based on RECIST classification, for n=34 patients who received neoadjuvant chemotherapy. c: anterior and posterior portal venous branches embolization performed in two consecutive sessions. d: Based on the absolute future liver remnant (cm^3) / total liver volume (cm^3) x 100

Figures – Titles and legends

Figure 1.

Title:

Clinical course of patients undergoing preoperative portal vein embolization for CRCLM

Legend:

A: PVE in the context of an extended hepatic resection

B: PVE in the context of a staged resection

Figure 2.

Title:

Flowchart of included patients and post-PVE metastatic lesions

Figure 3.

Title:

Distribution of histological growth patterns after portal vein embolization, with and without disease progression

Legend:

Total number of lesions analyzed: 178 lesions from 46 patients. SD (stable disease after portal vein embolization, n=80 lesions) vs. PD (progression of disease after portal vein embolization, n=98 lesions). $p<0.0001$ (Chi-Square)

Abbreviations: R: replacement growth pattern; D: desmoplastic growth pattern; P: pushing growth pattern.

Figure 4

Title:

Completed staged resections

Legend:

A: Patients who underwent staged resection (two-stages) without radiological disease progression (n=4 patients with individual lesions from pre and post-PVE represented)

B: Patients who underwent staged resection (two-stages) with radiological disease progression (n=8 patients with individual lesions from pre and post-PVE represented)

Figure 5.

Title:

Distribution of HGP in the pre-PVE lesions, failed staged resections

Legend:

Representation of n=22 lesions from 8 patients who failed the second stage surgery due to disease progression. R (replacement): 54.6 +/- 8.6 (standard error of the mean (SEM)) +/- 40.1 (SD). D (desmoplastic): 41.6 +/- 9.1 (SEM) +/- 42.5 (SD), p=0.7210.

Figure 1.

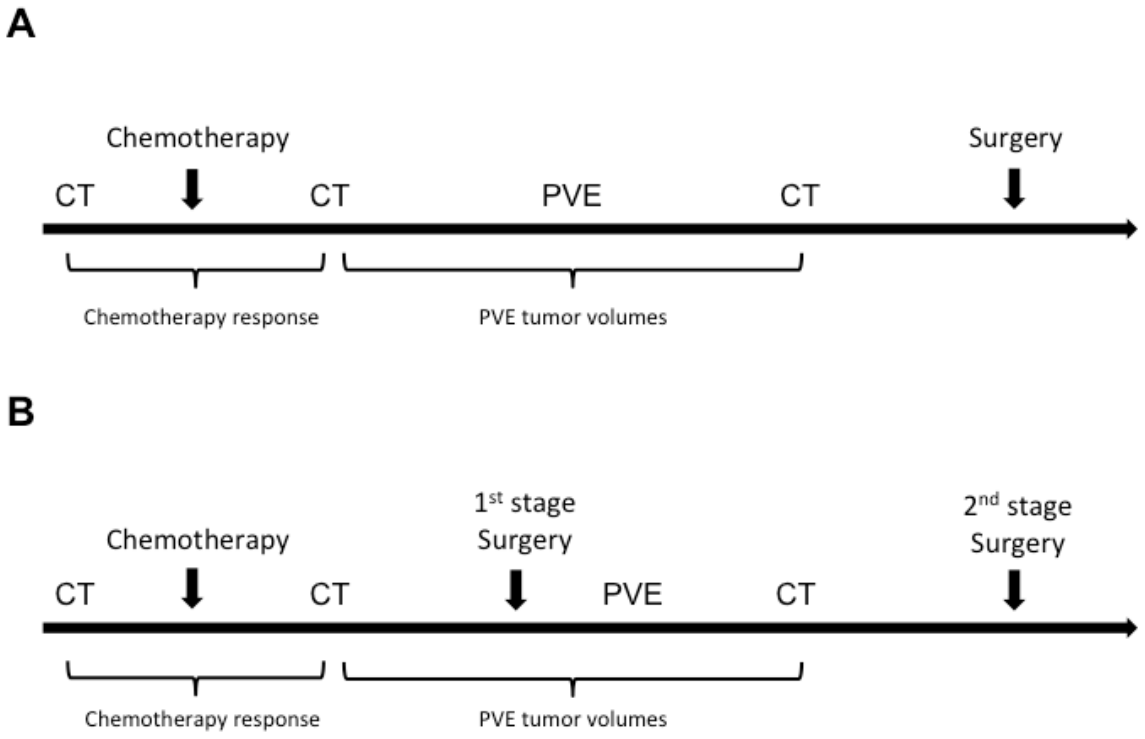
A
Chemotherapy
Surgery
CT
CT
PVE
CT
Chemotherapy response
PVE tumor volumes
B
1st stage
Surgery
2nd stage
Surgery
Chemotherapy
CT
CT
PVE
CT
Chemotherapy response
PVE tumor volumes

Figure 2.

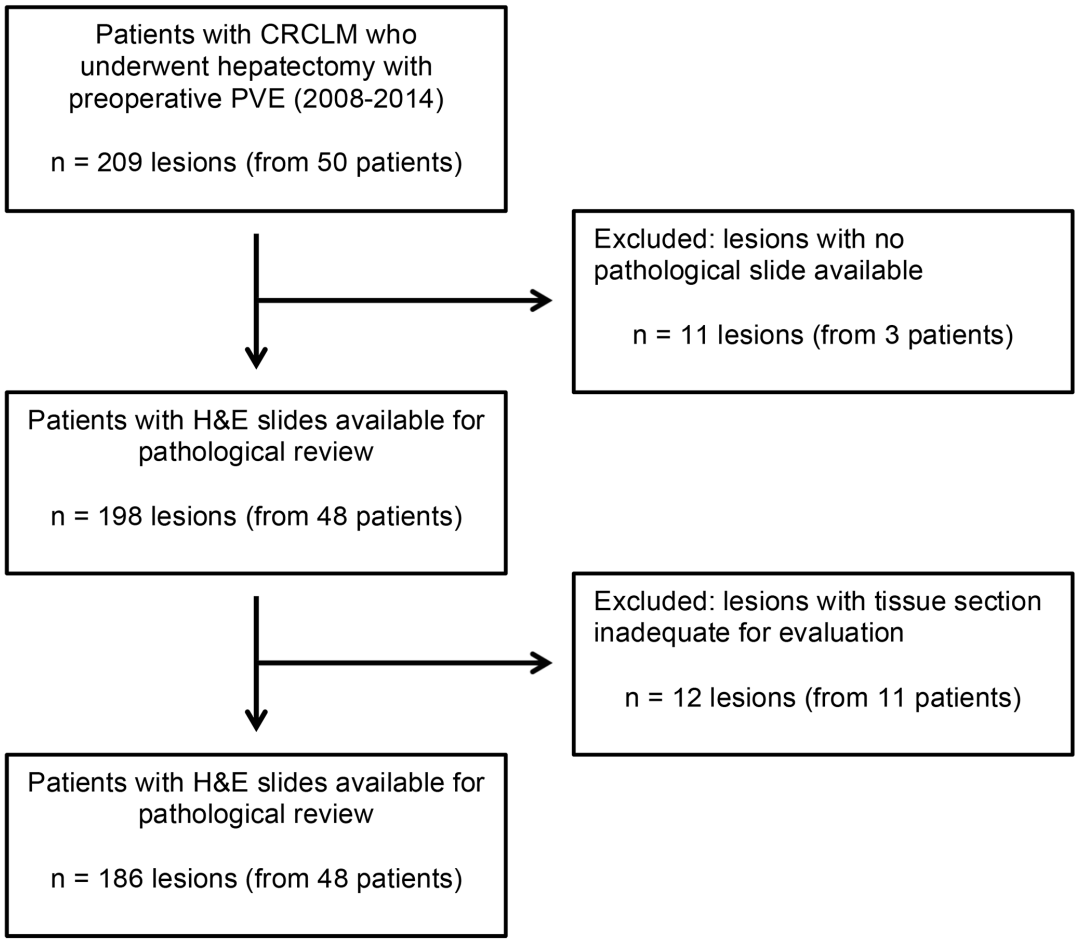
Patients with CRCLM who underwent hepatectomy with preoperative PVE (2008-2014)
n = 209 lesions (from 50 patients)
Excluded: lesions with no pathological slide available
n = 11 lesions (from 3 patients)
Patients with H&E slides available for pathological review
n = 198 lesions (from 48 patients)
Excluded: lesions with tissue section inadequate for evaluation
n = 12 lesions (from 11 patients)
Patients with H&E slides available for pathological review
n = 186 lesions (from 48 patients)

Figure 3.

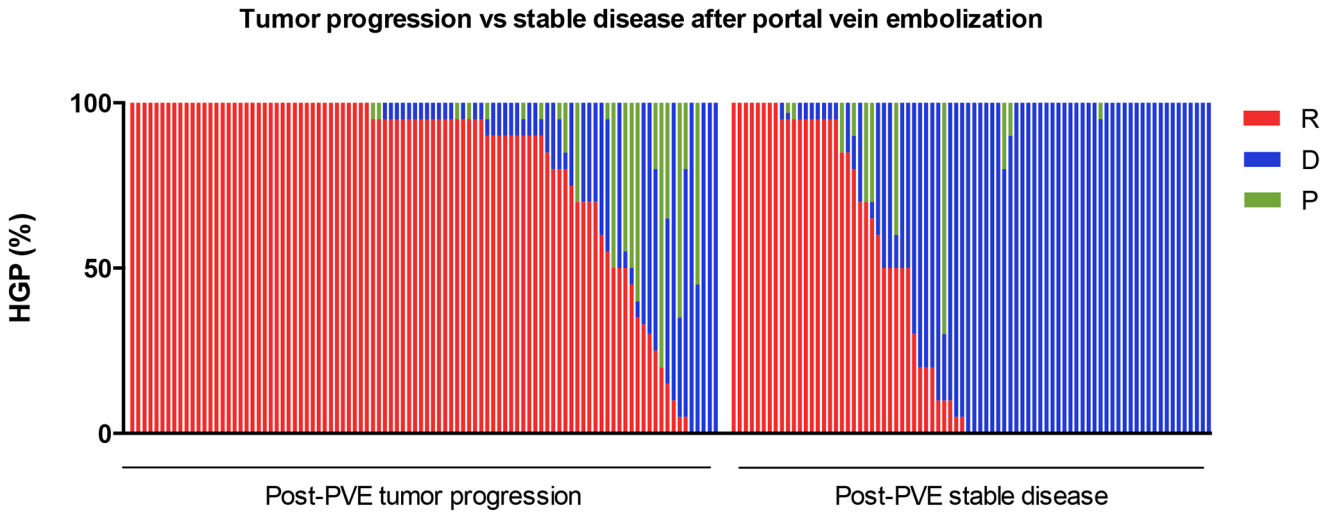
Tumor progression vs stable disease after portal vein embolization
HGP (%)
100
50
0
R
D
P
Post-PVE tumor progression
Post-PVE stable disease

Figure 4.

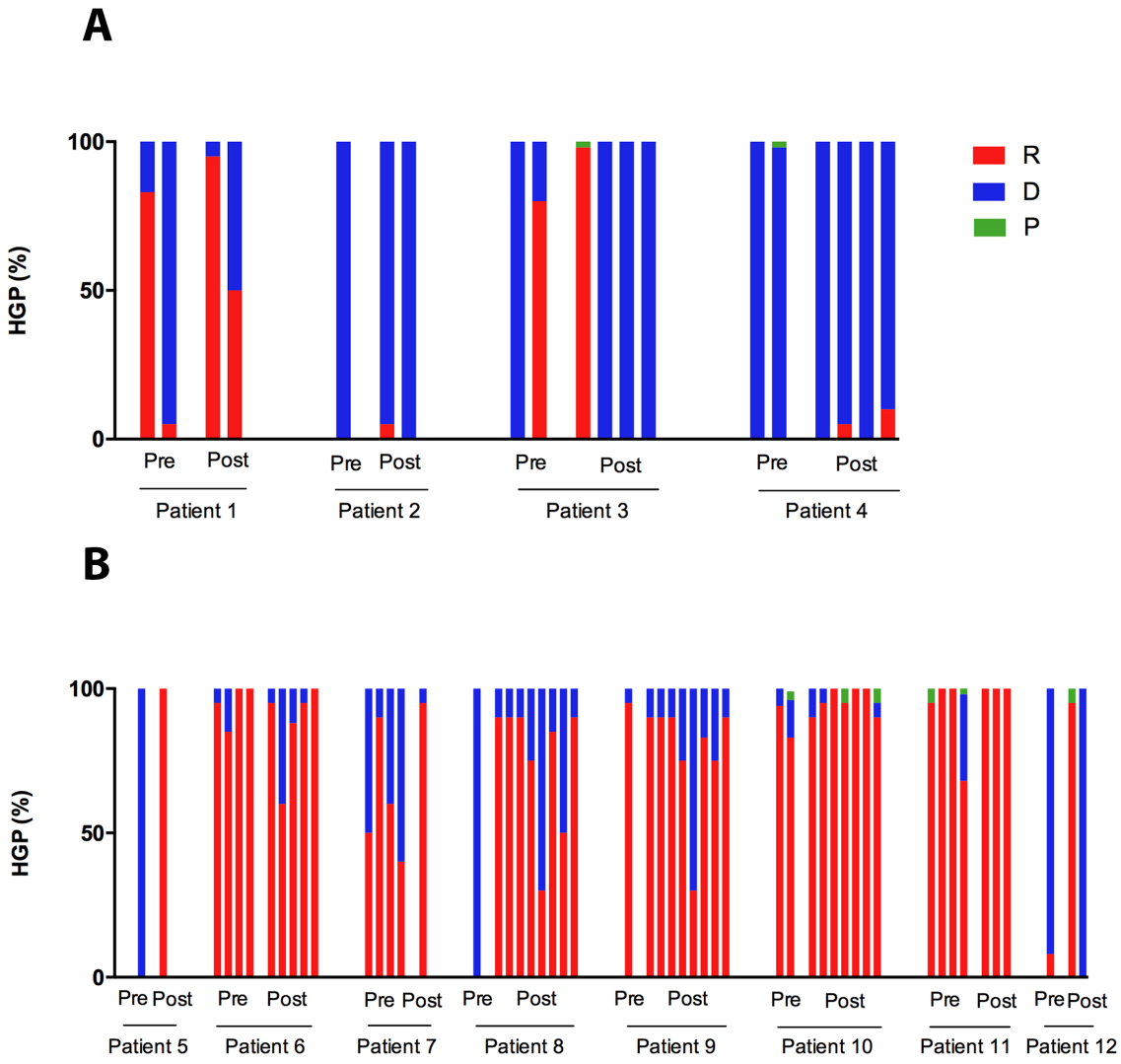
A
100
50
0
HGP (%)
R
D
P
Pre
Post
Patient 1
Patient 2
Patient 3
Patient 4
B
Patient 5
Patient 6
Patient 7
Patient 8
Patient 9
Patient 10
Patient 11
Patient 12

Figure 5.

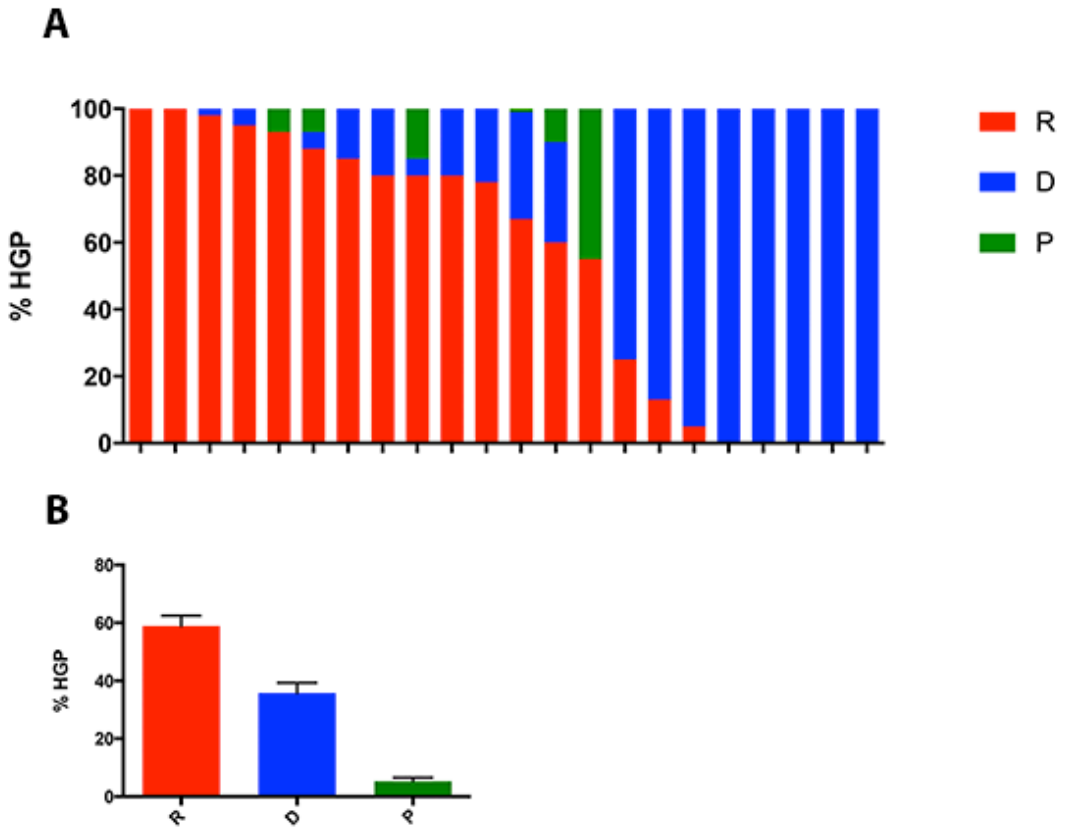

XX. Conclusion

Through this work, we demonstrated that colorectal liver metastasis is composed of distinct subtypes that are each associated with different tumor vascular supply pattern and harbor markedly different responses to therapy, which has an impact on the overall survival of these patients. The premise behind this work was intially based on clinical observation that tumors after portal vein embolization display different responses to this intervention: some tumors progress while others do not, as if they exhibit a prolonged response to the chemotherapy administered prior to the PVE and are essentially unresponsive to the stimulatory milieu surrounding them.

We first established the evidence of such an observation. Although some experimental and low-power clinical studies highlighted such observations(24-28,175), we demonstrated in a large patient cohort that a proportion of patients indeed show disease progression after portal vein embolization, while the other patients do not(165,176). Moreover, when we compared patients who did not undergo portal vein embolization but did receive neoadjuvant chemotherapy, we demonstrated that despite an interval of time off chemotherapy, these patients had continuous downsizing tumor response(165). In opposition to patients who developped tumor progression on close follow-up imaging after the PVE, these findings overall suggested an extremely heterogenous biological behavior of colorectal liver metastasis. As highlighted in our pilot study using RNA Seq, the unsupervised analysis which segragated tumor with progression apart from tumors with stable disease also highlighted intrinsic differences in tumor biology, despite them being all liver metastases from colorectal cancer subjected to the same interventions and neoadjuvant treatment.

Although the concept of tumor subtypes is not novel, it has not yet been supported by strong evidence in the field of liver metastasis. Primary colon cancer has been recently

described has being made of 5 different molecular subtypes(177) but the complex interaction of the host organ with tumor cells prevent the extrapolation of findings related to the primary tumor to liver metastases. We started from the hypothesis that liver metastasis growth patterns and their different tumor vascularization may represent different subtypes that would harbor a different biology and ultimately that these would be reflected in clinical outcomes. We demonstrated that desmoplastic is a favorable subtype which has a positive response to chemotherapy combined with antiangiogenic therapy and superior overall survival. On the other hand, the replacement pattern seems to be an unfavorable subtype which is associated with resistance to antiangiogenic therapy and ultimately poorer patient survival. This is the first study providing mechanistic evidence for Bevacizumab resistance and to our knowledge, the first report to show a significant survival benefit of adding antiangiogenic therapy, after stratifying patients accordingly by growth patterns. Finally we have demonstrated the validity of these findings in a specific clinical context, namely disease progression after portal vein embolization. Since we had shown that progression after PVE seemed to be associated with neodjuvant chemoerthapy response, we demonstrated that this may in fact have been indirect evidence for an association between the growth patterns and disease progression in this context. This work is thus concluded by the evidence that tumor progression after embolization is due to the tumor being prone to disease progression, namely those harboring the invasive replacement pattern.

This work opens the door to many future research venues. First the molecular pathways characterizing each of the patterns need to be elucidated, likely by integrating high-thouput technology to high-quality biobank tissue material and carefully selected tissue samples. Although our work has suggested a method of switching the patterns from a replacement to a desmoplastic by the inhibition of cell motility via ARPC3 blockade, deeper insights in the biology of the patterns are needed in order to understand the

distinct biological differences and provide potential therapeutic targets. The role of the surrounding liver parenchyma is also hypothesized to play a critical role in the histological growth patterns; the extent and nature of the interaction need to be investigated. In fact, unpublished preliminary data from our group resulting from next generation sequencing analyses of replacement and desmoplastic chemonaive metastatic lesions suggests different molecular signaling pathways expressed in the surrounding liver between the two patterns. These findings may also lead to further understanding on the nature and development of each pattern. Finally, this work has lead to initiatives in studying non-invasive methods (such as high resolution imaging) to identify the growth patterns, in order to use these findings clinically before patients undergo any type of intervention. By stratifying patients at presentation, based on the predominant patterns, a more personalized treatment approach could potentially change the course of treatment and have a positive impact on the survival of these patients.

XXI. Bibliography

1. Siegel R, Ma J, Zou Z, Jemal A. Cancer statistics, 2014. CA: A Cancer Journal for Clinicians. 2014 Jan;64(1):9–29.

2. Scheele J, Stangl R, Altendorf-Hofmann A. Hepatic metastases from colorectal carcinoma: impact of surgical resection on the natural history. Br J Surg. 1990 Nov;77(11):1241–6.

3. Seymour MT, Stenning SP, Cassidy J. Attitudes and practice in the management of metastatic colorectal cancer in Britain. Colorectal Cancer Working Party of the UK Medical Research Council. Clin Oncol (R Coll Radiol). 1997 Jan 1;9(4):248–51.

4. Goldberg RM, Sargent DJ, Morton RF, Fuchs CS, Ramanathan RK, Williamson SK, et al. A randomized controlled trial of fluorouracil plus leucovorin, irinotecan, and oxaliplatin combinations in patients with previously untreated metastatic colorectal cancer. J. Clin. Oncol. 2004 Jan 1;22(1):23–30.

5. Hochster HS, Hart LL, Ramanathan RK, Childs BH, Hainsworth JD, Cohn AL, et al. Safety and efficacy of oxaliplatin and fluoropyrimidine regimens with or without bevacizumab as first-line treatment of metastatic colorectal cancer: results of the TREE Study. J. Clin. Oncol. 2008 Jul 20;26(21):3523–9.

6. Saltz LB, Lenz H-J, Kindler HL, Hochster HS, Wadler S, Hoff PM, et al. Randomized phase II trial of cetuximab, bevacizumab, and irinotecan compared with cetuximab and bevacizumab alone in irinotecan-refractory colorectal cancer: the BOND-2 study. J. Clin. Oncol. 2007 Oct 10;25(29):4557–61.

7. Hughes KS, Simon R, Songhorabodi S, Adson MA, Ilstrup DM, Fortner JG, et al. Resection of the liver for colorectal carcinoma metastases: a multi-institutional study of patterns of recurrence. Surgery. 1986 Aug 1;100(2):278–84.

8. Nordlinger B, Sorbye H, Glimelius B, Poston GJ, Schlag PM, Rougier P, et al. Perioperative FOLFOX4 chemotherapy and surgery versus surgery alone for resectable liver metastases from colorectal cancer (EORTC 40983): long-term results of a randomised, controlled, phase 3 trial. Lancet Oncol. 2013 Nov;14(12):1208–15.

9. Nordlinger B, Guiguet M, Vaillant JC, Balladur P, Boudjema K, Bachellier P, et al. Surgical resection of colorectal carcinoma metastases to the liver. A prognostic scoring system to improve case selection, based on 1568 patients. Association Française de Chirurgie. Cancer. 1996 Apr 1;77(7):1254–62.

10. Jamison RL, Donohue JH, Nagorney DM, Rosen CB, Harmsen WS, Ilstrup DM. Hepatic resection for metastatic colorectal cancer results in cure for some patients. Arch Surg. 1997 May;132(5):505–10–discussion511.

11. Fong Y, Fortner J, Sun RL, Brennan MF, Blumgart LH. Clinical score for predicting recurrence after hepatic resection for metastatic colorectal cancer: analysis of 1001 consecutive cases. Ann. Surg. 1999 Sep 1;230(3):309–21.

12. Iwatsuki S, Dvorchik I, Madariaga JR, Marsh JW, Dodson F, Bonham AC, et al. Hepatic resection for metastatic colorectal adenocarcinoma: a proposal of a prognostic scoring system. J. Am. Coll. Surg. 1999 Sep;189(3):291–9.

13. Choti MA, Sitzmann JV, Tiburi MF, Sumetchotimetha W, Rangsin R, Schulick RD, et al. Trends in long-term survival following liver resection for hepatic colorectal metastases. Ann. Surg. 2002 Jun 1;235(6):759–66.

14. Abdalla EK, Vauthey J-N, Ellis LM, Ellis V, Pollock R, Broglio KR, et al. Recurrence and outcomes following hepatic resection, radiofrequency ablation, and combined resection/ablation for colorectal liver metastases. Ann. Surg. 2004 Jun;239(6):818–25–discussion825–7.

15. Fernandez FG, Drebin JA, Linehan DC, Dehdashti F, Siegel BA, Strasberg SM. Five-year survival after resection of hepatic metastases from colorectal cancer in patients screened by positron emission tomography with F-18 fluorodeoxyglucose (FDG-PET). Ann. Surg. 2004 Sep;240(3):438–47–discussion447–50.

16. Wei AC, Greig PD, Grant D, Taylor B, Langer B, Gallinger S. Survival after hepatic resection for colorectal metastases: a 10-year experience. Ann. Surg. Oncol. 2006 May;13(5):668–76.

17. Rees M, Tekkis PP, Welsh FKS, O'Rourke T, John TG. Evaluation of long-term survival after hepatic resection for metastatic colorectal cancer: a multifactorial model of 929 patients. Ann. Surg. 2008 Jan 1;247(1):125–35.

18. de Jong MC, Pulitano C, Ribero D, Strub J, Mentha G, Schulick RD, et al. Rates and patterns of recurrence following curative intent surgery for colorectal liver metastasis: an international multi-institutional analysis of 1669 patients. Ann. Surg. 2009 Sep;250(3):440–8.

19. Morris EJA, Forman D, Thomas JD, Quirke P, Taylor EF, Fairley L, et al. Surgical management and outcomes of colorectal cancer liver metastases. Br J Surg. 2010 Jul;97(7):1110–8.

20. Madoff DC, Abdalla EK, Vauthey J-N. Portal vein embolization in preparation for major hepatic resection: evolution of a new standard of care. J Vasc Interv Radiol. 2005 Jun;16(6):779–90.

21. Abulkhir A, Limongelli P, Healey AJ, Damrah O, Tait P, Jackson J, et al. Preoperative Portal Vein Embolization for Major Liver Resection. Ann. Surg. 2008 Jan;247(1):49–57.

22. Abdalla EK. Portal vein embolization (prior to major hepatectomy) effects on regeneration, resectability, and outcome. J Surg Oncol. 2010 Dec 15;102(8):960–7.

23. Wicherts DA, de Haas RJ, Andreani P, Sotirov D, Salloum C, Castaing D, et al. Impact of portal vein embolization on long-term survival of patients with primarily unresectable colorectal liver metastases. Br J Surg. 2010 Feb;97(2):240–50.

24. Elias D, De Baere T, Roche A, Mducreux, Leclere J, Lasser P. During liver regeneration following right portal embolization the growth rate of liver metastases is more rapid than that of the liver parenchyma. Br J Surg. 1999 Jun;86(6):784–8.

25. Barbaro B, Di Stasi C, Nuzzo G, Vellone M, Giuliante F, Marano P. Preoperative right portal vein embolization in patients with metastatic liver disease. Metastatic liver volumes after RPVE. Acta Radiol. 2003 Jan;44(1):98–102.

26. Kokudo N, Tada K, Seki M, Ohta H, Azekura K, Ueno M, et al. Proliferative activity of intrahepatic colorectal metastases after preoperative hemihepatic portal vein embolization. Hepatology. 2001 Aug;34(2):267–72.

27. Ribero D, Abdalla EK, Madoff DC, Donadon M, Loyer EM, Vauthey J-N. Portal vein embolization before major hepatectomy and its effects on regeneration, resectability and outcome. Br J Surg. 2007 Nov;94(11):1386–94.

28. Mueller L, Hillert C, Möller L, Krupski-Berdien G, Rogiers X, Broering DC. Major hepatectomy for colorectal metastases: is preoperative portal occlusion an oncological risk factor? Ann. Surg. Oncol. 2008 Jul;15(7):1908–17.

29. Charny CK, Jarnagin WR, Schwartz LH, Frommeyer HS, DeMatteo RP, Fong Y, et al. Management of 155 patients with benign liver tumours. Br J Surg. 2001 Jun;88(6):808–13.

30. Bonney GK, Gomez D, Al-Mukhtar A, Toogood GJ, Lodge JPA, Prasad R. Indication for treatment and long-term outcome of focal nodular hyperplasia. HPB (Oxford). 2007 Jan 1;9(5):368–72.

31. Cho SW, Marsh JW, Steel J, Holloway SE. Surgical management of hepatocellular adenoma: take it or leave it? Annals of surgical …. 2008.

32. Terkivatan T, de Wilt JH, de Man RA, van Rijn RR, Zondervan PE, Tilanus HW, et al. Indications and long-term outcome of treatment for benign hepatic tumors: a critical appraisal. Arch Surg. 2001 Sep 1;136(9):1033–8.

33. Hsieh HF, Chen TW, Yu CY, Wang NC, Chu HC. Aggressive hepatic resection for patients with pyogenic liver abscess and APACHE II score≥ 15. The American Journal of …. 2008.

34. Stanley SL. Amoebiasis. Lancet. 2003 Mar 22;361(9362):1025–34.

35. Moore FA, Moore EE, Seagraves A. Nonresectional management of major hepatic trauma. An evolving concept. Am J Surg. 1985 Dec 1;150(6):725–9.

36. Strong RW, Lynch SV, Wall DR, Liu CL. Anatomic resection for severe liver trauma. Surgery. 1998 Mar;123(3):251–7.

37. Clavien P-A, Petrowsky H, DeOliveira ML, Graf R. Strategies for safer liver surgery and partial liver transplantation. N. Engl. J. Med. 2007 Apr 12;356(15):1545–59.

38. Schwartz M, Roayaie S, Konstadoulakis M. Strategies for the management of hepatocellular carcinoma. Nat Clin Pract Oncol. 2007 Jul;4(7):424–32.

39. Balzan S, Belghiti J, Farges O, Ogata S, Sauvanet A, Delefosse D, et al. The “50-50 criteria” on postoperative day 5: an accurate predictor of liver failure and death after hepatectomy. Ann. Surg. 2005 Dec 1;242(6):824–9.

40. Adam R, Chiche L, Aloia T, Elias D, Salmon R, Rivoire M, et al. Hepatic resection for noncolorectal nonendocrine liver metastases: analysis of 1,452 patients and development of a prognostic model. Ann. Surg. 2006 Oct;244(4):524–35.

41. Reddy SK, Barbas AS, Marroquin CE, Morse MA, Kuo PC, Clary BM. Resection of Noncolorectal Nonneuroendocrine Liver Metastases: A Comparative Analysis. J. Am. Coll. Surg. 2007 Jan 1;204(3):372–82.

42. Simons JP, Ng SC, Hill JS, Shah SA, Bodnari A, Zhou Z, et al. In-Hospital Mortality for Liver Resection for Metastases: A Simple Risk Score. J. Surg. Res. 2009 Jan 1;156(1):21–5.

43. Simmonds PC, Primrose JN, Colquitt JL, Garden OJ, Poston GJ, Rees M. Surgical resection of hepatic metastases from colorectal cancer: a systematic review of published studies. Br. J. Cancer. 2006 Apr 10;94(7):982–99.

44. Frankel TL, D'Angelica MI. Hepatic resection for colorectal metastases. J Surg Oncol. 2014 Jan;109(1):2–7.

45. Liu DM, Kennedy A, Turner D, Rose SC, Kee ST, Whiting S, et al. Minimally invasive techniques in management of hepatic neuroendocrine metastatic disease. Am J Clin Oncol. 2009 Apr 1;32(2):200–15.

46. Andreou A, Brouquet A, Bharathy KGS, Perrier ND, Abdalla EK, Curley SA, et al. Liver resection for liver metastases from nondigestive endocrine cancer: Extrahepatic disease burden defines outcome. Surgery. 2012 Jun 1;151(6):851–9.

47. Groeschl RT, Nachmany I, Steel JL, Reddy SK, Glazer ES, de Jong MC, et al. Hepatectomy for Noncolorectal Non-Neuroendocrine Metastatic Cancer: A Multi-Institutional Analysis. J. Am. Coll. Surg. 2012 May 1;214(5):769–77.

48. Ryu SW, Saw R, Scolyer RA, Crawford M, Thompson JF, Sandroussi C. Liver resection for metastatic melanoma: equivalent survival for cutaneous and ocular primaries. J Surg Oncol. 2013 Aug 1;108(2):129–35.

49. Evrard S. [Colorectal liver metastases: history, sciences and clinical practices]. Bull Cancer. 2014 Apr;101(4):373–9.

50. de Haas RJ, Wicherts DA, Flores E, Azoulay D, Castaing D, Adam R. R1 resection by necessity for colorectal liver metastases: is it still a contraindication to surgery? Ann. Surg. 2008 Oct 1;248(4):626–37.

51. Scheithauer W, Rosen H, Kornek GV, Sebesta C, Depisch D. Randomised comparison of combination chemotherapy plus supportive care with supportive care alone in patients with metastatic colorectal cancer. BMJ. 1993 Mar 20;306(6880):752–5.

52. de Gramont A, Figer A, Seymour M, Homerin M, Hmissi A, Cassidy J, et al. Leucovorin and fluorouracil with or without oxaliplatin as first-line treatment in advanced colorectal cancer. J. Clin. Oncol. 2000 Aug;18(16):2938–47.

53. Douillard JY, Cunningham D, Roth AD, Navarro M. Irinotecan combined with fluorouracil compared with fluorouracil alone as first-line treatment for metastatic

colorectal cancer: a multicentre randomised trial. The Lancet. 2000.

54. Saltz LB, Cox JV, Blanke C, Rosen LS, Fehrenbacher L, Moore MJ, et al. Irinotecan plus fluorouracil and leucovorin for metastatic colorectal cancer. Irinotecan Study Group. N. Engl. J. Med. 2000 Sep 28;343(13):905–14.

55. Tournigand C, André T, Achille E, Lledo G, Flesh M, Mery-Mignard D, et al. FOLFIRI followed by FOLFOX6 or the reverse sequence in advanced colorectal cancer: a randomized GERCOR study. J. Clin. Oncol. 2004 Jan 15;22(2):229–37.

56. Fuchs CS, Marshall J, Mitchell E, Wierzbicki R, Ganju V, Jeffery M, et al. Randomized, controlled trial of irinotecan plus infusional, bolus, or oral fluoropyrimidines in first-line treatment of metastatic colorectal cancer: results from the BICC-C Study. J. Clin. Oncol. 2007 Oct 20;25(30):4779–86.

57. Hurwitz H, Fehrenbacher L, Novotny W, Cartwright T, Hainsworth J, Heim W, et al. Bevacizumab plus Irinotecan, Fluorouracil, and Leucovorin for Metastatic Colorectal Cancer. N. Engl. J. Med. 2004 Jun 3;350(23):2335–42.

58. Saltz LB, Clarke S, Díaz-Rubio E, Scheithauer W, Figer A, Wong R, et al. Bevacizumab in combination with oxaliplatin-based chemotherapy as first-line therapy in metastatic colorectal cancer: a randomized phase III study. J. Clin. Oncol. 2008 Apr 20;26(12):2013–9.

59. Adam R, Delvart V, Pascal G, Valeanu A, Castaing D, Azoulay D, et al. Rescue surgery for unresectable colorectal liver metastases downstaged by chemotherapy: a model to predict long-term survival. Ann. Surg. 2004 Oct;240(4):644–57–discussion657–8.

60. Adam R, Pascal G, Castaing D, Azoulay D, Delvart V, Paule B, et al. Tumor progression while on chemotherapy: a contraindication to liver resection for multiple colorectal metastases? Ann. Surg. 2004 Dec;240(6):1052–61–discussion1061–4.

61. Wong SL, Mangu PB, Choti MA, Crocenzi TS, Dodd GD, Dorfman GS, et al. American Society of Clinical Oncology 2009 clinical evidence review on radiofrequency ablation of hepatic metastases from colorectal cancer. J. Clin. Oncol. 2010 Jan 20;28(3):493–508.

62. Kornprat P, Jarnagin WR, DeMatteo RP, Fong Y, Blumgart LH, D'Angelica M. Role of intraoperative thermoablation combined with resection in the treatment of hepatic metastasis from colorectal cancer. Arch Surg. 2007 Nov;142(11):1087–92.

63. Pearson AS, Izzo F, Fleming RYD, Ellis LM, Delrio P, Roh MS, et al. Intraoperative radiofrequency ablation or cryoablation for hepatic malignancies. Am J Surg. 1999 Dec 1;178(6):592–8.

64. Elias D, Baton O, Sideris L, Boige V, Malka D, Liberale G, et al. Hepatectomy plus intraoperative radiofrequency ablation and chemotherapy to treat technically unresectable multiple colorectal liver metastases. J Surg Oncol. 2005 Apr 1;90(1):36–42.

65. Pawlik TM, Izzo F, Cohen DS, Morris JS, Curley SA. Combined resection and radiofrequency ablation for advanced hepatic malignancies: results in 172 patients.

Ann. Surg. Oncol. 2003 Nov 1;10(9):1059–69.

66. Shibata T, Niinobu T, Ogata N, Takami M. Microwave coagulation therapy for multiple hepatic metastases from colorectal carcinoma. Cancer. 2000 Jul 15;89(2):276–84.

67. Gold JS, Are C, Kornprat P, Jarnagin WR, Gonen M, Fong Y, et al. Increased use of parenchymal-sparing surgery for bilateral liver metastases from colorectal cancer is associated with improved mortality without change in oncologic outcome: trends in treatment over time in 440 patients. Ann. Surg. 2008 Jan 1;247(1):109–17.

68. Kokudo N, Tada K, Seki M, Ohta H, Azekura K, Ueno M, et al. Anatomical major resection versus nonanatomical limited resection for liver metastases from colorectal carcinoma. Am J Surg. 2001 Jan 1;181(2):153–9.

69. Lalmahomed ZS, Ayez N, van der Pool AEM, Verheij J, IJzermans JNM, Verhoef C. Anatomical versus nonanatomical resection of colorectal liver metastases: is there a difference in surgical and oncological outcome? World J Surg. 2011 Mar 1;35(3):656–61.

70. Gayowski TJ, Iwatsuki S, Madariaga JR, Selby R, Todo S, Irish W, et al. Experience in hepatic resection for metastatic colorectal cancer: analysis of clinical and pathologic risk factors. Surgery. 1994 Oct 1;116(4):703–701.

71. Jaeck D, Oussoultzoglou E, Rosso E, Greget M, Weber J-C, Bachellier P. A two-stage hepatectomy procedure combined with portal vein embolization to achieve curative resection for initially unresectable multiple and bilobar colorectal liver metastases. Ann. Surg. 2004 Dec;240(6):1037–49–discussion1049–51.

72. Jamal MH, Hassanain M, Chaudhury P, Tran TT, Wong S, Yousef Y, et al. Staged hepatectomy for bilobar colorectal hepatic metastases. HPB (Oxford). 2012 Nov;14(11):782–9.

73. Ferrero A, Viganò L, Polastri R, Muratore A, Eminefendic H, Regge D, et al. Postoperative liver dysfunction and future remnant liver: where is the limit? Results of a prospective study. World J Surg. 2007 Aug;31(8):1643–51.

74. van den Esschert JW, de Graaf W, van Lienden KP, Busch OR, Heger M, van Delden OM, et al. Volumetric and functional recovery of the remnant liver after major liver resection with prior portal vein embolization : recovery after PVE and liver resection. J. Gastrointest. Surg. 2009 Aug 1;13(8):1464–9.

75. Mailey B, Truong C, Artinyan A, Khalili J, Sanchez-Luege N, Denitz J, et al. Surgical resection of primary and metastatic hepatic malignancies following portal vein embolization. J Surg Oncol. 2009 Sep 1;100(3):184–90.

76. Shindoh J, Tzeng C-WD, Aloia TA, Curley SA, Zimmitti G, Wei SH, et al. Portal vein embolization improves rate of resection of extensive colorectal liver metastases without worsening survival. Br J Surg. 2013 Dec;100(13):1777–83.

77. Farges O, Belghiti J, Kianmanesh R, Regimbeau JM, Santoro R, Vilgrain V, et al. Portal vein embolization before right hepatectomy: prospective clinical trial. Ann. Surg. 2003 Feb;237(2):208–17.

78. Ganeshan DM, Szklaruk J. Portal vein embolization: cross-sectional imaging of normal features and complications. AJR Am J Roentgenol. 2012 Dec 1;199(6):1275–82.

79. Vauthey J-N, Chaoui A, Do KA, Bilimoria MM, Fenstermacher MJ, Charnsangavej C, et al. Standardized measurement of the future liver remnant prior to extended liver resection: methodology and clinical associations. Surgery. 2000 May 1;127(5):512–9.

80. Kooby DA, Fong Y, Suriawinata A, Gonen M, Allen PJ, Klimstra DS, et al. Impact of steatosis on perioperative outcome following hepatic resection. J. Gastrointest. Surg. 2003 Dec 1;7(8):1034–44.

81. Vauthey J-N, Pawlik TM, Ribero D, Wu T-T, Zorzi D, Hoff PM, et al. Chemotherapy regimen predicts steatohepatitis and an increase in 90-day mortality after surgery for hepatic colorectal metastases. J. Clin. Oncol. 2006 May 1;24(13):2065–72.

82. Pawlik TM, Olino K, Gleisner AL, Torbenson M, Schulick R, Choti MA. Preoperative chemotherapy for colorectal liver metastases: impact on hepatic histology and postoperative outcome. J. Gastrointest. Surg. 2007 Jul;11(7):860–8.

83. Robinson SM, Wilson CH, Burt AD, Manas DM, White SA. Chemotherapy-associated liver injury in patients with colorectal liver metastases: a systematic review and meta-analysis. Ann. Surg. Oncol. 2012 Dec 1;19(13):4287–99.

84. Rubbia-Brandt L, Audard V, Sartoretti P. Severe hepatic sinusoidal obstruction associated with oxaliplatin-based chemotherapy in patients with metastatic colorectal cancer. Annals of …. 2004.

85. Aloia T, Sebagh M, Plasse M, Karam V, Levi F, Giacchetti S, et al. Liver histology and surgical outcomes after preoperative chemotherapy with fluorouracil plus oxaliplatin in colorectal cancer liver metastases. J. Clin. Oncol. 2006 Nov 1;24(31):4983–90.

86. Ward J, Guthrie JA, Sheridan MB, Boyes S, Smith JT, Wilson D, et al. Sinusoidal obstructive syndrome diagnosed with superparamagnetic iron oxide-enhanced magnetic resonance imaging in patients with chemotherapy-treated colorectal liver metastases. J. Clin. Oncol. 2008 Sep 10;26(26):4304–10.

87. Hubert C, Fervaille C, Sempoux C, Horsmans Y, Humblet Y, Machiels J-P, et al. Prevalence and clinical relevance of pathological hepatic changes occurring after neoadjuvant chemotherapy for colorectal liver metastases. Surgery. 2010 Jan 1;147(2):185–94.

88. Karoui M, Penna C, Amin-Hashem M, Mitry E, Benoist S, Franc B, et al. Influence of preoperative chemotherapy on the risk of major hepatectomy for colorectal liver metastases. Ann. Surg. 2006 Jan 1;243(1):1–7.

89. Soubrane O, Brouquet A, Zalinski S, Terris B, Brézault C, Mallet V, et al. Predicting high grade lesions of sinusoidal obstruction syndrome related to oxaliplatin-based chemotherapy for colorectal liver metastases: correlation with post-hepatectomy outcome. Ann. Surg. 2010 Mar;251(3):454–60.

90. Welsh FKS, Tilney HS, Tekkis PP, John TG, Rees M. Safe liver resection following chemotherapy for colorectal metastases is a matter of timing. Br. J. Cancer. 2007 Apr 10;96(7):1037–42.

91. Kishi Y, Zorzi D, Contreras CM, Maru DM, Kopetz S, Ribero D, et al. Extended preoperative chemotherapy does not improve pathologic response and increases postoperative liver insufficiency after hepatic resection for colorectal liver metastases. Ann. Surg. Oncol. 2010 Nov 1;17(11):2870–6.

92. Hassanain M, Metrakos P, Fisette A, Doi SAR, Schricker T, Lattermann R, et al. Randomized clinical trial of the impact of insulin therapy on liver function in patients undergoing major liver resection. Br J Surg. 2013 Apr 1;100(5):610–8.

93. Fisette A, Hassanain M, Metrakos P, Doi SAR, Salman A, Schricker T, et al. High-dose insulin therapy reduces postoperative liver dysfunction and complications in liver resection patients through reduced apoptosis and altered inflammation. J. Clin. Endocrinol. Metab. 2012 Jan;97(1):217–26.

94. Michalopoulos GK. Liver regeneration. J. Cell. Physiol. 2007 Nov;213(2):286–300.

95. Fausto N, Campbell JS, Riehle KJ. Liver regeneration. Hepatology. 2006 Feb;43(2 Suppl 1):S45–53.

96. Taub R. Liver regeneration: from myth to mechanism. Nat. Rev. Mol. Cell Biol. 2004 Oct;5(10):836–47.

97. GRISHAM JW. A morphologic study of deoxyribonucleic acid synthesis and cell proliferation in regenerating rat liver; autoradiography with thymidine-H3. Cancer Res. 1962 Aug;22:842–9.

98. Cressman DE, Greenbaum LE, DeAngelis RA, Ciliberto G, Furth EE, Poli V, et al. Liver failure and defective hepatocyte regeneration in interleukin-6-deficient mice. Science. 1996 Nov 22;274(5291):1379–83.

99. Sakamoto T, Liu Z, Murase N, Ezure T, Yokomuro S, Poli V, et al. Mitosis and apoptosis in the liver of interleukin-6-deficient mice after partial hepatectomy. Hepatology. 1999 Feb 1;29(2):403–11.

100. Talarmin H, Rescan C, Cariou S, Glaise D, Zanninelli G, Bilodeau M, et al. The mitogen-activated protein kinase kinase/extracellular signal-regulated kinase cascade activation is a key signalling pathway involved in the regulation of G(1) phase progression in proliferating hepatocytes. Mol. Cell. Biol. 1999 Sep;19(9):6003–11.

101. Levy DE, Lee C-K. What does Stat3 do? J. Clin. Invest. 2002 May 1;109(9):1143–8.

102. Yamada Y, Kirillova I, Peschon JJ, Fausto N. Initiation of liver growth by tumor necrosis factor: deficient liver regeneration in mice lacking type I tumor necrosis factor receptor. Proc. Natl. Acad. Sci. U.S.A. 1997 Feb 18;94(4):1441–6.

103. Taub R, Greenbaum LE, Peng Y. Transcriptional regulatory signals define cytokine-dependent and -independent pathways in liver regeneration. Semin. Liver

Dis. 1999;19(2):117–27.

104. Koniaris LG, McKillop IH, Schwartz SI, Zimmers TA. Liver regeneration. J. Am. Coll. Surg. 2003 Oct;197(4):634–59.

105. Huh C-G, Factor VM, Sánchez A, Uchida K, Conner EA, Thorgeirsson SS. Hepatocyte growth factor/c-met signaling pathway is required for efficient liver regeneration and repair. Proc. Natl. Acad. Sci. U.S.A. 2004 Mar 30;101(13):4477–82.

106. Pediaditakis P, Lopez-Talavera JC, Petersen B, Monga SPS, Michalopoulos GK. The processing and utilization of hepatocyte growth factor/scatter factor following partial hepatectomy in the rat. Hepatology. 2001 Jan 1;34(4):688–93.

107. Burr AW, Toole K, Chapman C, Hines JE, Burt AD. Anti-hepatocyte growth factor antibody inhibits hepatocyte proliferation during liver regeneration. J. Pathol. 1998 Jul;185(3):298–302.

108. Okano J-I, Shiota G, Matsumoto K, Yasui S, Kurimasa A, Hisatome I, et al. Hepatocyte growth factor exerts a proliferative effect on oval cells through the PI3K/AKT signaling pathway. Biochem Biophys Res Commun. 2003 Sep 19;309(2):298–304.

109. Behrens A, Sibilia M, David J-P, Möhle-Steinlein U, Tronche F, Schütz G, et al. Impaired postnatal hepatocyte proliferation and liver regeneration in mice lacking c-jun in the liver. EMBO J. 2002 Apr 2;21(7):1782–90.

110. Leu JI, Crissey MA, Leu JP, Ciliberto G, Taub R. Interleukin-6-induced STAT3 and AP-1 amplify hepatocyte nuclear factor 1-mediated transactivation of hepatic genes, an adaptive response to liver injury. Mol. Cell. Biol. 2001 Jan 1;21(2):414–24.

111. Weir E, Chen Q, DeFrances MC, Bell A, Taub R, Zarnegar R. Rapid induction of mRNAs for liver regeneration factor and insulin-like growth factor binding protein-1 in primary cultures of rat hepatocytes by hepatocyte growth factor and epidermal growth factor. Hepatology. 1994 Oct;20(4 Pt 1):955–60.

112. Campbell JS, Prichard L, Schaper F, Schmitz J, Stephenson-Famy A, Rosenfeld ME, et al. Expression of suppressors of cytokine signaling during liver regeneration. J. Clin. Invest. 2001 May 1;107(10):1285–92.

113. Derynck R, Zhang YE. Smad-dependent and Smad-independent pathways in TGF-beta family signalling. Nature. 2003 Oct 9;425(6958):577–84.

114. Garborg K, Holme Ø, Løberg M, Kalager M, Adami HO, Bretthauer M. Current status of screening for colorectal cancer. Ann. Oncol. 2013 Aug;24(8):1963–72.

115. Slesser AAP, Georgiou P, Brown G, Mudan S, Goldin R, Tekkis P. The tumour biology of synchronous and metachronous colorectal liver metastases: a systematic review. Clin. Exp. Metastasis. 2013 Apr 1;30(4):457–70.

116. Jasperson KW, Tuohy TM, Neklason DW, Burt RW. Hereditary and familial colon cancer. Gastroenterology. 2010. pp. 2044–58.

117. Weisenberger DJ, Siegmund KD, Campan M, Young J, Long TI, Faasse MA, et al. CpG island methylator phenotype underlies sporadic microsatellite instability and is tightly associated with BRAF mutation in colorectal cancer. Nat Genet. 2006 Jul 1;38(7):787–93.

118. Pino MS, Chung DC. The chromosomal instability pathway in colon cancer. Gastroenterology. 2010. pp. 2059–72.

119. Armaghany T, Wilson JD, Chu Q, Mills G. Genetic alterations in colorectal cancer. Gastrointest Cancer Res. 2012 Jan;5(1):19–27.

120. Kumar S, Weaver VM. Mechanics, malignancy, and metastasis: the force journey of a tumor cell. Cancer Metastasis Rev. 2009 Jun 1;28(1-2):113–27.

121. Weinberg R. The biology of cancer. 2013.

122. Folkman J. The role of angiogenesis in tumor growth. Semin. Cancer Biol. 1992 Apr;3(2):65–71.

123. Woodhouse EC, Chuaqui RF, Liotta LA. General mechanisms of metastasis. Cancer. 1997.

124. Fidler IJ. Critical determinants of cancer metastasis: rationale for therapy. Cancer Chemother Pharmacol. 1999 Jan 1;43 Suppl:S3–10.

125. Chambers AF, Naumov GN, Varghese HJ, Nadkarni KV, MacDonald IC, Groom AC. Critical steps in hematogenous metastasis: an overview. Surg. Oncol. Clin. N. Am. 2001 Apr;10(2):243–55–vii.

126. Wyckoff JB, Jones JG, Condeelis JS, Segall JE. A critical step in metastasis: in vivo analysis of intravasation at the primary tumor. Cancer Res. 2000 May 1;60(9):2504–11.

127. Royston D, Jackson DG. Mechanisms of lymphatic metastasis in human colorectal adenocarcinoma. J. Pathol. 2009 Apr 1;217(5):608–19.

128. Owen JL, Mohamadzadeh M. Macrophages and chemokines as mediators of angiogenesis. Front Physiol. 2013;4:159.

129. Rejniak KA. Investigating dynamical deformations of tumor cells in circulation: predictions from a theoretical model. Front Oncol. 2012;2:111.

130. Shin MK, Kim SK, Jung H. Integration of intra- and extravasation in one cell-based microfluidic chip for the study of cancer metastasis. Lab Chip. 2011 Nov 21;11(22):3880–7.

131. Chambers AF, Groom AC, MacDonald IC. Dissemination and growth of cancer cells in metastatic sites. Nat. Rev. Cancer. 2002 Aug;2(8):563–72.

132. Hart IR. “Seed and soil” revisited: mechanisms of site-specific metastasis. Cancer Metastasis Rev. 1982 Jan 1;1(1):5–16.

133. Zetter BR. The cellular basis of site-specific tumor metastasis. N. Engl. J. Med.

1990 Mar 1;322(9):605–12.

134. Fidler IJ. Seed and soil revisited: contribution of the organ microenvironment to cancer metastasis. Surg. Oncol. Clin. N. Am. 2001 Apr;10(2):257–69–vii–viiii.

135. Radinsky R. Modulation of tumor cell gene expression and phenotype by the organ-specific metastatic environment. Cancer Metastasis Rev. 1995 Dec;14(4):323–38.

136. Fidler IJ. Modulation of the organ microenvironment for treatment of cancer metastasis. J. Natl. Cancer Inst. 1995 Nov 1;87(21):1588–92.

137. Radinsky R. Molecular mechanisms for organ-specific colon carcinoma metastasis. Eur. J. Cancer. 1995 Jan 1;31(7):1091–5.

138. Radinsky R, Ellis LM. Molecular determinants in the biology of liver metastasis. Surg. Oncol. Clin. N. Am. 1996 Apr 1;5(2):215–29.

139. Vekemans K, Braet F. Structural and functional aspects of the liver and liver sinusoidal cells in relation to colon carcinoma metastasis. World J. Gastroenterol. 2005 Sep 7;11(33):5095–102.

140. Smedsrød B, Le Couteur D, Ikejima K, Jaeschke H, Kawada N, Naito M, et al. Hepatic sinusoidal cells in health and disease: update from the 14th International Symposium. Liver Int. 2009 Apr 1;29(4):490–501.

141. Timmers M, Vekemans K, Vermijlen D, Asosingh K, Kuppen P, Bouwens L, et al. Interactions between rat colon carcinoma cells and Kupffer cells during the onset of hepatic metastasis. Int. J. Cancer. 2004 Dec 10;112(5):793–802.

142. Enns A, Gassmann P, Schlüter K, Korb T, Spiegel H-U, Senninger N, et al. Integrins can directly mediate metastatic tumor cell adhesion within the liver sinusoids. J. Gastrointest. Surg. 2004 Dec;8(8):1049–59–discussion1060.

143. Potter RF, Groom AC. Capillary diameter and geometry in cardiac and skeletal muscle studied by means of corrosion casts. Microvasc. Res. 1983 Jan 1;25(1):68–84.

144. Chambers AF, MacDonald IC, Schmidt EE, Morris VL, Groom AC. Preclinical assessment of anti-cancer therapeutic strategies using in vivo videomicroscopy. Cancer Metastasis Rev. 1998;17(3):263–9.

145. Chambers AF, MacDonald IC, Schmidt EE, Morris VL, Groom AC. Clinical targets for anti-metastasis therapy. Adv. Cancer Res. 2000;79:91–121.

146. Luzzi KJ, MacDonald IC, Schmidt EE, Kerkvliet N, Morris VL, Chambers AF, et al. Multistep nature of metastatic inefficiency: dormancy of solitary cells after successful extravasation and limited survival of early micrometastases. Am. J. Pathol. 1998 Sep;153(3):865–73.

147. Cameron MD, Schmidt EE, Kerkvliet N, Nadkarni KV, Morris VL, Groom AC, et al. Temporal progression of metastasis in lung: cell survival, dormancy, and location dependence of metastatic inefficiency. Cancer Res. 2000 May 1;60(9):2541–6.

148. Varghese HJ, Davidson MTM, MacDonald IC, Wilson SM, Nadkarni KV, Groom AC, et al. Activated ras regulates the proliferation/apoptosis balance and early survival of developing micrometastases. Cancer Res. 2002 Feb 1;62(3):887–91.

149. Homey B, Müller A, Zlotnik A. Chemokines: agents for the immunotherapy of cancer? Nat. Rev. Immunol. 2002 Mar;2(3):175–84.

150. Rak J, Filmus J, Finkenzeller G, Grugel S, Marmé D, Kerbel RS. Oncogenes as inducers of tumor angiogenesis. Cancer Metastasis Rev. 1995 Dec;14(4):263–77.

151. Joneson T, Bar-Sagi D. Ras effectors and their role in mitogenesis and oncogenesis. J. Mol. Med. 1997 Aug;75(8):587–93.

152. Katz ME, McCormick F. Signal transduction from multiple Ras effectors. Curr. Opin. Genet. Dev. 1997 Feb;7(1):75–9.

153. Campbell SL, Khosravi-Far R, Rossman KL, Clark GJ, Der CJ. Increasing complexity of Ras signaling. Oncogene. 1998 Sep 17;17(11 Reviews):1395–413.

154. Webb CP, Taylor GA, Jeffers M, Fiscella M, Oskarsson M, Resau JH, et al. Evidence for a role of Met-HGF/SF during Ras-mediated tumorigenesis/metastasis. Oncogene. 1998 Oct 22;17(16):2019–25.

155. Akhurst RJ, Derynck R. TGF-beta signaling in cancer--a double-edged sword. Trends Cell Biol. 2001 Nov 1;11(11):S44–S51.

156. Pruitt K, Der CJ. Ras and Rho regulation of the cell cycle and oncogenesis. Cancer Lett. 2001 Sep 28;171(1):1–10.

157. Thiery JP. Epithelial-mesenchymal transitions in tumour progression. Nat. Rev. Cancer. 2002 Jun;2(6):442–54.

158. Paschos KA, Majeed AW, Bird NC. Natural history of hepatic metastases from colorectal cancer--pathobiological pathways with clinical significance. World J. Gastroenterol. 2014 Apr 14;20(14):3719–37.

159. Vermeulen PB, Colpaert C, Salgado R, Royers R, Hellemans H, Van Den Heuvel E, et al. Liver metastases from colorectal adenocarcinomas grow in three patterns with different angiogenesis and desmoplasia. J. Pathol. 2001 Oct;195(3):336–42.

160. Van den Eynden GG, Bird NC, Majeed AW, Van Laere S, Dirix LY, Vermeulen PB. The histological growth pattern of colorectal cancer liver metastases has prognostic value. Clin. Exp. Metastasis. 2012 Aug;29(6):541–9.

161. Van den Eynden GG, Majeed AW, Illemann M, Vermeulen PB, Bird NC, Høyer-Hansen G, et al. The multifaceted role of the microenvironment in liver metastasis: biology and clinical implications. Cancer Res. 2013 Apr 1;73(7):2031–43.

162. Stessels F, Van den Eynden G, Van der Auwera I, Salgado R, Van Den Heuvel E, Harris AL, et al. Breast adenocarcinoma liver metastases, in contrast to colorectal cancer liver metastases, display a non-angiogenic growth pattern that preserves the stroma and lacks hypoxia. Br. J. Cancer. 2004 Apr 5;90(7):1429–36.

163. Scheele J, Stang R, Altendorf-Hofmann A, Paul M. Resection of colorectal liver metastases. World J Surg. 1995 Jan;19(1):59–71.

164. Hochster HS, Hart LL, Ramanathan RK, Childs BH, Hainsworth JD, Cohn AL, et al. Safety and Efficacy of Oxaliplatin and Fluoropyrimidine Regimens With or Without Bevacizumab As First-Line Treatment of Metastatic Colorectal Cancer: Results of the TREE Study. J. Clin. Oncol. 2008 Jul 20;26(21):3523–9.

165. Simoneau E, Aljiffry M, Salman A, Abualhassan N, Cabrera T, Valenti D, et al. Portal vein embolization stimulates tumour growth in patients with colorectal cancer liver metastases. HPB (Oxford). 2012 Jul;14(7):461–8.

166. Pamecha V, Glantzounis G, Davies N, Fusai G, Sharma D, Davidson B. Long-term survival and disease recurrence following portal vein embolisation prior to major hepatectomy for colorectal metastases. Ann. Surg. Oncol. 2009 May;16(5):1202–7.

167. Abdalla EK, Adam R, Bilchik AJ, Jaeck D, Vauthey J-N, Mahvi D. Improving resectability of hepatic colorectal metastases: expert consensus statement. Ann. Surg. Oncol. 2006 Oct;13(10):1271–80.

168. Pamecha V, Levene A, Grillo F, Woodward N, Dhillon A, Davidson BR. Effect of portal vein embolisation on the growth rate of colorectal liver metastases. Br. J. Cancer. 2009 Feb 24;100(4):617–22.

169. Oussoultzoglou E, Bachellier P, Rosso E, Scurtu R, Lucescu I, Greget M, et al. Right portal vein embolization before right hepatectomy for unilobar colorectal liver metastases reduces the intrahepatic recurrence rate. Ann. Surg. 2006 Jul;244(1):71–9.

170. Lim C, Cauchy F, Azoulay D, Farges O, Ronot M, Pocard M. Tumour progression and liver regeneration-insights from animal models. Nat Rev Gastroenterol Hepatol. 2013 Apr 9.

171. Otte JM, Schmitz F, Kiehne K, Stechele HU, Banasiewicz T, Krokowicz P, et al. Functional expression of HGF and its receptor in human colorectal cancer. Digestion. 2000;61(4):237–46.

172. Nabeshima K, Shimao Y, Inoue T, Itoh H, Kataoka H, Koono M. Hepatocyte growth factor/scatter factor induces not only scattering but also cohort migration of human colorectal-adenocarcinoma cells. Int. J. Cancer. 1998 Dec 9;78(6):750–9.

173. Byrne AM, Bouchier-Hayes DJ, Harmey JH. Angiogenic and cell survival functions of vascular endothelial growth factor (VEGF). J. Cell. Mol. Med. 2005 Oct;9(4):777–94.

174. Kollmar O, Corsten M, Scheuer C, Vollmar B, Schilling MK, Menger MD. Tumour growth following portal branch ligation in an experimental model of liver metastases. Br J Surg. 2010 Jun;97(6):917–26.

175. Hoekstra LT, van Lienden KP, Doets A, Busch ORC, Gouma DJ, van Gulik TM. Tumor progression after preoperative portal vein embolization. Ann. Surg. 2012 Nov;256(5):812–7–discussion817–8.

176. Simoneau E, Hassanain M, Shaheen M, Aljiffry M, Molla N, Chaudhury P, et al. Portal vein embolization and its effect on tumour progression for colorectal cancer liver metastases. Br J Surg. 2015 Sep;102(10):1240–9.

177. Sadanandam A, Lyssiotis CA, Homicsko K, Collisson EA, Gibb WJ, Wullschleger S, et al. A colorectal cancer classification system that associates cellular phenotype and responses to therapy. Nat. Med. 2013 May;19(5):619–25.